The biochemistry of algal bioactives: their role in modulation of digestive processes.

Mody Sweareh Albalawi

Thesis submitted for the Degree of Doctor of Philosophy

Institute for Cell and Molecular Biosciences
Medical School
Newcastle University

May 2020

Abstract

Obesity is a serious global threat to public health causing serious chronic metabolic diseases. The drug Orlistat has been used for obesity treatment; however, orlistat causes unpleasant gastrointestinal side-effects. Recent research has investigated bioactive compounds from seaweeds, like alginate, as pancreatic lipase inhibitors to modulate fat digestion and reduce caloric intake. Previous work has shown that certain alginates can inhibit pancreatic lipase activity *in vitro* by up to 72%.

The aim of this thesis is to investigate the effect of alginate on lipase activity *in vitro*, using three different approaches: turbidimetric assay, a kinetic assay and a synthetic model gut system.

The turbidimetric assay for pancreatic lipase showed alginates can inhibit pancreatic lipase, with the level of inhibition depending on alginate structure and concentration. Alginate with a high content of guluronate residues can inhibit pancreatic lipase activity more than alginate rich in mannuronate residues.

Kinetic analysis showed that alginates act as mixed inhibitors that can bind to both the free enzyme and the enzyme-substrate complex.

Alginate passed through the gastric phase of the synthetic model gut reduced glyceryl trioctanoate digestion, but not the digestion of olive or sunflower oil. However, alginate added at the small intestinal phase reduced olive oil digestion. The regulatory effect of alginate was affected by gastric pH resulting in gel formation and precipitation, reducing or preventing the release of free alginate and reducing lipase inhibition.

Alginate bread was digestible within the synthetic model with most alginate release occurring in the small intestinal phase. Alginate incorporated into bread did not reduce fat digestion, which may be due to alginate fragmentation resulting from high temperatures during the cooking process.

The capacity of unfragmented alginates to inhibit pancreatic lipase activity *in vitro* supports future investigations of alginate *in vivo* as a pancreatic lipase inhibitor to reduce fat digestion and absorption and hence, treat obesity.

Acknowledgements

Firstly, I would like to express my special thanks and gratitude to Professor Jeffery Pearson who gave me the great opportunity to finalise this project and without his constant support, guidance and direction over the past few years this project would not have been possible.

Secondly, I would also like to thank my second supervisor Dr. Chris Ward and lab group Dr Peter Chater, Dr Matt Wilcox, Dr Bernard Vernon, Dr Suraiami Mustar, and Muna Fallatah.

Most importantly I would like to thank my parents, my sisters Nahid and Mai, and my friends especially Nwayer and Shaden for their unwavering support, assistance, and encouragement to accomplish this project.

Finally, I would like to thank Tabuk University for its financial assistance, and Newcastle University for accepting my studentship.

Declaration

The research on which this thesis is based was carried out at the Institute for Cell and Molecular Biosciences, Newcastle University. I hereby declare that all laboratory work and analysis of the data presented in this thesis, with exception of NMR analysis to determine the chemical structure of the different alginates which was carried out by the Chemistry Department at Newcastle University, were performed by me. I have duly acknowledged all the sources of information which have been used in this thesis.

Contents

List of Abbreviations and Symbols

µl	Microlitre
µM	Micromolar
µmol	micromole
3-D	Three-dimensional
AB	Alginate bread
Al_2O_3	Aluminium oxide
BMI	Body mass index
$C_{29}H_{53}NO_5$	Tetrahydrolipstatin (Orlistat)
C_3H_6O	Acetone
$C_6H_8O_7$	Citric acid
Ca^{2+}	Calcium ion
$CaCl_2$	Calcium chloride
$CaCl_2.2H_2O$	Calcium chloride dihydrate
CB	Control bread
CCK	Cholecystokinin
CH_3COOH	Acetic acid
Cl^-	Chloride ion
DGGR	1,2-Di-o-lauryl-rac-glycero-3-(glutaric acid 6-methyl resorufin ester)
DH_2O	Deionised water
DIPF	Diiso-propylphosphofluoridate
DMMB	1,9-dimethyl methylene blue
EI complex	Enzyme-inhibitor complex
ES complex	Enzyme-substrate complex
Fe^{++}	Ferrous ion
g	Gravity
G	Guluronate
GG	Guluronate dimers
GGG	Guluronate trimers
GLUT5	glucose transporter five
GM	Guar gum

H^+	Hydrogen ion
H_2O_2	Hydrogen peroxide
H_3BO_3	Boric acid
H_3PO_4	Orthophosphoric acid
HCl	Hydrochloric acid
HDL	High-density lipoprotein
HIO_4	Periodic acid
HM pectin	High methylic esterification
IC_{50}	The half maximal inhibitory concentration
K^+	Potassium ion
K_2HPO_4	Potassium hydrogen phosphate
kcal	Kilocalorie
KCl	Potassium chloride
kg	Kilogram
KH_2PO_4	Potassium dihydrogen phosphate
K_m	Michaelis-Menten constant
KOH	Potassium hydroxide
L	Litre
LDL	Low-density lipoprotein
LM pectin	Low methyl ester pectin
M	Mannuronate dimers
m^2	Square meter
MG	Model gut solution
mg	Milligram
min	Minute
ml	Millilitre
mM	Millimolar
MM	Mannuronate dimers
Na^+	Sodium ion
Na^+/K^+-ATPase	Sodium-potassium adenosine triphosphatase
$Na_2S_2O_5$	Sodium metabisulphate

NaCl,	Sodium chloride
$NaCO_3$	Sodium carbonate
$NaHCO_3$	Sodium bicarbonate
NaOH	Sodium hydroxide
NCD-RisC	NCD Risk Factor Collaboration
NSP	Non-starch polysaccharide
OD	Optical density
OH^-	Hydroxyl group
PAS assay	Periodic Acid-Schiff assay
pH	Potential of Hydrogen
PHMBH	Polyhexamethylenebiguandinium chloride
pKa	Acid dissociation constant
ROS	reactive oxygen species
rpm	Revolutions per minute
SD	Standard deviation
SGLT1	Na^+-glucose transporter 1
S-O	Safranin-O
T-B	Toludine Blue
UK	United Kingdom
USA	United States of America
V_{max}	Maximal velocity of the reaction
α	Alpha
β	Beta
r_s	Spearman's rank correlation coefficient

List of Figures

List of Tables

List of Appendices

Chapter 1: General Introduction

1.1 Overview of obesity

Obesity can be defined as a body mass index (BMI) of greater than or equal to 30 kg/m^2, and it occurs due to an imbalance between the amounts of energy intake and output [1]. Excessive fat is stored in adipose tissue [2]; therefore, obesity can be indicated by an excess of triacylglyceride storage in adipose tissue[3]. Fat metabolism must be balanced to maintain homeostasis, and thus prevents the development of obesity [4]. The design and development of drugs for obesity treatment accounts for 2-6% of the total medical care costs in most developed countries, and it is expected that there will be a continuous increase in the market for anti-obesity drugs due to the global spread of obesity [4]. Moreover, the same study reported that more than one billion adults are overweight, and, according to the clinical diagnosis, more than 300 million of those are classified as obese [4]. In one study, it was estimated that by 2030, 86.3% of adults in the USA will be overweight, and more than half of these will be obese. Consequently, there will be a twofold increase in medical care costs every ten years until 2030, accounting for approximately 16-18% of the total costs of medical care in the USA [5]. It has been reported that obesity affects more than a third of people globally [6, 7]. It is has been estimated that by 2030, 38% of worldwide adults will be overweight and also another 20% of adults around the world will be obese [8]. According to data obtained from a pooled analysis of BMI from people in 200 countries, the worldwide obesity would exceed 6% in males and 9% in females by 2015 [9]. The health hazards of obesity include the development of serious chronic diseases such as type 2 diabetes, atherosclerosis, and hypertension. In addition, there is an increased risk of developing fatal coronary heart disease. Therefore, anti-obesity agents which control the process of gastrointestinal lipolysis have been used to protect against or treat obesity-related diseases [4, 10].

1.2 Overview of the digestive processes

The digestive system has four main functions: ingestion, digestion, absorption, and elimination. Ingestion is the process of food consumption. Digestion is a multi-step process of mechanical and chemical actions in which ingested macromolecules are broken down into smaller molecules that can be absorbed. Mechanical digestion begins in the mouth where the macromolecules are chewed,

torn and ground into smaller fragments referred to as boluses. After mastication, the food boluses move to the stomach via the esophagus where the ingested material is churned by stomach muscles and mixed with acidic gastric secretions that further breaks down the food matrix. This material, the chyme, in turn moves into the duodenum through the pyloric sphincter where the bile has an emulsifying effect, breaking large fat droplets to smaller droplets. Digestion also includes the hydrolytic effects of digestive enzymes (Table 1.1). Protein and carbohydrate macronutrients in consumed food largely consist of long chain polymers which are broken down by proteases and carbohydrases respectively for absorption in the small intestine. Ingested fat consists predominantly of triglyceride molecules which must be broken down to monoglycerides and fatty acids which are absorbed through micellar uptake. The absorption process includes the transport of digested food from the gut lumen into blood and lymphatic circulation. The elimination process involves removing waste and undigested foods such as some fibres (water-insoluble fibres) which are indigestible by bacteria in the colon [11-13]. Carbohydrate, protein, and fat macromolecules are digested by substrate specific digestive enzymes and there are more than a hundred enzymes involved in the digestive process [14].

	Enzyme	Enzyme function	Enzyme source
Carbohydrate	α- amylase	Breaks down α 1→4 glycosidic bonds in starch into smaller chains of glucose molecules	Produced by salivary glands (salivary amylase) and pancreas (pancreatic amylase).
	Sucrase	Separates the disaccharide sucrose into monosaccharides glucose and fructose.	Produced in the small intestine.
	Lactase	Splits the disaccharides lactose into glucose and galactose.	Produced in the small intestine.
	Maltase	Separates maltose into two molecules of glucose.	Produced in the small intestine.
Fat	Lipase	Breaks down fats into fatty acids and glycerol.	Produced in salivary glands (lingual lipase), the stomach (gastric lipase), and the pancreas (pancreatic lipase). The action of lipase is enhanced by bile.
Protein	Pepsin	Separates proteins into shorter chains of amino acids	Produced by the stomach.
	Trypsin	Separates short chains of amino acids into molecules containing one, two, or three amino acids	Produced by the pancreas

Table 1.1. Primary functions of selected digestive enzymes. Adapted from Brown, (2007) [14].

1.2.1 Carbohydrate digestion and absorption

Starch, maltose, sucrose, and lactose are the major constitutes of the digestible carbohydrates. Digestion of starch begins in the mouth by the action of salivary α-amylase produced from the salivary glands; however, starch undergoes only partial digestion in the mouth. In the stomach, α-amylase lacks hydrolytic activity due to the low pH environment [13]. However, it has been suggested that α-amylase can be protected within the bolus from gastric acid and pepsin inactivation by its substrate starch polymers, and therefore recover activity when the pH level rises in the small intestine [15]. Both salivary and pancreatic α-amylase are classified as endosaccharides which exclusively cleave the internal α-1,4 glyosidic bonds, however, α-1,6 and α-1,4 glyosidic bonds of glucose molecules at the branched points or at the terminus are not cleavable by these endosaccharides [16]. The digestion of starch restarts in the small intestine by the action of pancreatic amylase and the brush border enzymes. Pancreatic α-amylase continues the breakdown of starch molecules into glucose and maltose. The brush border enzymes complete the digestion of carbohydrates for absorption. The brush border enzymes include lactase, sucrase, maltase, maltose-glucoamylase and isomaltase (α-dextrinase), and they hydrolyse disaccharide molecules to simple sugars. Disaccharide maltose undergoes hydrolysis by maltase into two molecules of glucose, whereas isomaltase breaks down the α (1→ 6) bond in isomaltose, which is the product of amylopectin incomplete hydrolysis, into two molecules of glucose. Sucrase breaks the disaccharide sucrose into glucose and fructose, while lactase converts disaccharides lactose into the monosaccharides, glucose and galactose. The absorption of monosaccharides into the intestinal epithelial cell is achieved by either of two transport mechanisms: active transport or facilitated diffusion. Both glucose and galactose are absorbed by the enterocytes via the Na^+-coupled secondary active transport symporter, Na^+-glucose transporter 1 (SGLT1), which has a high affinity for Na^+ ions. The binding of two Na^+ ions to the SGLT 1 symporter, changes the symporter shape and allows the sugar molecule to bind to the symporter with high affinity. SGLT1 transports glucose (or galactose) and Na^+ ions from outside the cell to inside the cell. The movement of each molecule of D-glucose down its concentration gradient by SGLT1 is coupled with the transport of two Na^+ ions. The cell possesses internal ion concentrations which are low in Na^+ and high in K^+ due to the action of sodium potassium ATPase. The concentration of Na^+ outside of the cell is higher than the concentration of Na^+ ions inside the cell, in contrast, the concentration of K^+ ions outside the cell is lower than inside the cell. The Na^+ which arrives inside the cell through secondary active transport with glucose, dissociates from the SGLT1, subsequently, the glucose is released due to

the reduction in the affinity of the transporter for the glucose. The process of glucose transport to enterocytes requires energy because lipid bilayers have a low permeability to glucose, and this energy is provided through the Na^+ ion gradient produced by basolateral K^+/Na^+-ATPase. Then, the glucose moves from the cell on the basolateral side of enterocyte where the glucose concentration is high to a low concentration outside the cell through the facilitated diffusion transporter Glucose transporter 2 (GLUT2), which creates a central aqueous channel for the transport of monosaccharides (glucose, galactose or fructose) through the lipid bilayer to the bloodstream. However, unlike glucose and galactose which are absorbed by the enterocytes through the SGLT1 symporter, fructose is absorbed by enterocytes through a specific facilitated diffusion carrier called GLUT5. Inside the enterocyte cell, the fructose is converted to glucose and lactic acid which in turn reduces its intracellular concentration, helping in its continuous transport from the intestinal lumen through facilitated diffusion. Then, these mono-saccharides (glucose molecules) are moved to interstitial fluid via GLUT2 where they are released to the blood capillaries, then to the liver through the portal vein where they can be stored as glycogen [13, 16, 17]

1.2.2 Protein digestion and absorption

Digestion of dietary proteins is achieved through a range of proteolytic enzymes with each of the enzymes having different peptide bond specificity. Exopeptidases break down the protein chain one amino acid at a time from the carboxy or amino end of the protein or polypeptide while endopeptidases cleave specific internal bonds producing large polypeptides [16]. The majority of protein digestion starts in the stomach, where about 10-20 % of proteins are digested by the action of an endopeptidase pepsin [17]. Gastric hydrochloric acid has the ability to denature proteins, allowing the digestive enzymes to attack peptide bonds. Additionally, hydrochloric acid provides the appropriate acidic environment at which active pepsin is formed from its inactive proenzyme pepsinogen. The conformation of inactive pepsinogen is changed by the effect of HCl produced by the parietal cells. Pepsinogen is stable at pH between 6 and 9, but at pH equal to or less than 6, pepsinogen undergoes autocatalytic activation and is converted to the active pepsin in the stomach [16, 18, 19]. The optimum pH for pepsin activity is pH 2.0 [18]. In the stomach, pepsin is at its optimum pH, and acts effectively on the protein, converting large polypeptide chains into smaller

polypeptide chains. Pepsins possess a relatively wide specificity; however, they favour peptide bonds that attached to a sequence composed of large hydrophobic/aromatic amino acids such as phenylalanine, tyrosine, tryptophan, and leucine [16, 20]. Protein digestion continues in the lumen of the small intestine. The entry of partially digested proteins and polypeptides into the duodenum of the small intestine activates release of cholecystokinin (CCK) from duodenal I cells into the bloodstream which activates the pancreas to produce intestinal proteases (trypsin, chymotrypsin, proelastase and carboxypeptidase A and B) in their inactive forms (zymogens) trypsinogen, chymotrypsinogen, elastase and procarboxypeptidase A and B, respectively, along with pancreatic bicarbonate. Active trypsin is produced from the cleavage of trypsinogen by the action of a brush-border enzyme enterokinase. Then, this active trypsin stimulates the proteolytic enzyme cascade, with the cleavage of chymotrypsinogen, elastase and procarboxypeptidase A and B to produce their active forms. The bicarbonate starts to neutralise the gastric acid and produce an optimum pH at which the intestinal proteases can break down the polypeptide chains into chains of three or fewer of amino acids (tripeptides and dipeptides) as well as amino acids. Trypsin, chymotrypsin, and elastase are serine proteases which function as endopeptidases. Trypsin favours to attack the peptide bonds adjacent to lysine or arginine residue. Chymotrypsin tends to cleave the peptide bond attached to hydrophobic amino acids, whereas elastase cleaves elastin and peptide bonds attached to alanine, serine, and glycine [16].

The brush border peptidases cleave the tripeptides and dipeptides, releasing free amino acids. Additionally, the intracellular peptidases are responsible for the cleavage of some tripeptides and dipeptides which are absorbed via di- and tripeptide cotransporter 1 (PEPT 1), releasing free amino acids. The absorption process of the free amino acids into the epithelial cell in the small intestine is achieved by facilitated diffusion or secondary active transport via specific transport proteins mainly coupled to Na^+ uptake [13, 17, 18, 21]. The amino acid transporters are stereospecific transporters which transport L-isomer of amino acid rather than D-isomer. Also, many amino acid transporters have wide substrate specificity, hence, many amino acids can be carried by one transporter. Additionally, the specificity of amino acid transporter overlaps where the amino acids can access several transporters. Therefore, the amino acid transporters can be identified by the type of amino acid carried (acidic, basic, neutral, or zwitterionic) and the mechanism by which the amino acid is carried (facilitated diffusion or secondary active transport). Information about the common transporters for amino acids and oligosaccharides, the ions coupled with the transporters

if required, the kind of transport mechanism, and their positions in epithelial cells (apical or basolateral membrane) are summarised in Table 1.2. The neutral L-amino acids are transported across the apical side of enterocyte through the secondary active Na^+-dependent cotransporter (referred to as system B), and then they are transported across the basolateral side of enterocyte to the bloodstream via sodium ion-independent facilitated diffusion.

Transport System	Amino Acid Substrates	Cotransported Ions	Type of Transport	Location
B	Neutral	Na^+	Secondary active	Apical
B^{0+}	Neutral, basic, and cystine	Na^+	Secondary active	Apical
B^{0+}	Neutral, basic, and cystine	None	Exchanging	Apical
Y^+	Basic	None	Facilitated	Apical
Imino	Imino	Na^+ and Cl^-	Secondary active	Apical
X_{AG-}	Acidic	Na^+, H^+, and K^+		Apical
B	B	Na^+ and Cl^-	Secondary active	Apical
PAT1	Imino	H^+	Secondary active	Apical
A	Neutral and imino	Na^+	Secondary active	Basolateral
ASC	Neutral with 3-4 carbons	Na^+	Exchanging	Basolateral
Asc	Neutral with 3-4 carbons	None	Facilitated	Basolateral
L	Neutral, large, and hydrophobic	None	Facilitated	Basolateral
y^+	Basic	None	Facilitated	Basolateral
PEPT1	Oligopeptides	H^+	Secondary active	Apical

Table 1.2. Common transporters for amino acids and peptides in the epithelial cells of small intestine. Copied from Goodman, (2010) [16].

The free amino acids are moved from the basolateral side of the enterocyte into the bloodstream via three amino acid transporters independent of Na^+ ions (asc, L, and y transport systems). However, two amino acid transporters (A and ASC transport systems) which are dependent on Na^+ ions carry amino acids from the bloodstream into the enterocyte to supply the cell with nutrients [16].

The di- and tripeptides are transported through the apical membrane of the enterocyte by PEPT 1 coupled with H^+ ions. The pH of the unstirred water layer which bathes the brush border is around 6.0 while the intracellular pH of the enterocyte is about 7.4, indicating a difference in the concentrations of H^+ ion between the two regions. The H^+ electrochemical gradient is produced and powered by the Na^+/H^+ exchanger NHE3 in the brush-border membranes driven by Na^+/K^+

ATPases. The PEPT 1 transporter takes advantage of H^+ electrochemical gradient from the lumen to the cytoplasm of enterocyte [16, 22]. The di- and tripeptides which are carried to the enterocytes undergo further hydrolysis by intracellular peptidases inside the cells, producing free amino acids which are transported to the bloodstream through facilitated diffusion. However, not all the di- and tripeptides are broken down to amino acids and some are transported out via a basolateral peptide transporter [16].

1.2.3 Fat digestion and absorption

Dietary fats include triglycerides, phospholipids (e.g., phosphatidylcholine) and sterols (e.g., cholesterol). The majority of these dietary fats from either animal or plant sources are hydrolysed by digestive enzymes to their basic structures before being absorbed. Moreover, these dietary fats are hydrophobic macromolecules, and therefore they must undergo emulsification to allow their hydrolysis by the digestive enzymes into smaller molecules which can be absorbed easily by the body [23]. Triglycerides constitute the majority of ingested dietary fats where they form 90-95% of the whole energy obtained from dietary fats [16, 24]. Fat digestion starts in the mouth by the action of lingual lipase produced by lingual glands. Fat digestion continues in the stomach by the action of gastric lipase produced by Chief cells in the stomach where 10-30% of dietary fats (triglycerides) are digested [25]. However, the complete digestion of dietary triglycerides occurs in the small intestine by pancreatic lipase.

The arrival of fat into the intestinal duodenum activates the pancreas to produce lipases and esterases and triggers contraction of the gallbladder with the relaxation of the hepatopancreatic sphincter via the action of CCK to liberate bile. The bile contains bile salts which play a crucial role in fat digestion and absorption. Emulsification of dietary fats starts by cooking the food, continues with the action of crunching in the mouth, and mixing and peristalsis in the stomach [26]. The emulsion droplets which come from the stomach comprise triglycerides and diglycerides in their centre and are surrounded by polar lipids, phospholipids, fatty acids, triglycerides, cholesterol, denatured proteins, oligosaccharides, and bile salts are added in the intestinal duodenum. In the small intestine, large fat droplets undergo an emulsification process in which bile salts disperse them, leading to an increase in their surface area, thus allowing the digestive enzymes to hydrolyse them more effectively. Increasing the surface area of fat droplets enables the binding of higher

number of pancreatic lipase molecules at oil/water interface of the substrate.

Triglyceride hydrolysis by pancreatic lipase requires the presence of colipase. Pancreatic colipase is a protein coenzyme which is produced as an inactive procolipase which is then converted to the active colipase by the action of trypsin. The colipase has the ability to bind to both dietary triglyceride and to the lipase itself, enabling the access of the triglyceride to the active site of the lipase enzyme to undergo lipolysis. Also, the presence of colipase is necessary to avoid this inactivation. Pancreatic lipase attacks the ester bonds of triglyceride releasing two free fatty acids and a 2-mononacylglycerol molecule [16, 21, 27]. Dietary cholesterol esters undergo digestion by the action of pancreatic esterase releasing fatty acids and cholesterol. Dietary phospholipids are digested by phospholipase A_2, producing a lysophospholipid and a free fatty acid.

The lipid-soluble products produced from digestion of dietary fats undergo a solubilisation process by bile salts within the mixed micelles in the lumen of small intestine. Mixed micelles comprise bile and mixed lipids such as fatty acids, monoglycerides, cholesterol, lysophospholipids, and fat-soluble vitamins. The mixed micelles are transported through the unstirred water layer bathing the brush-border membrane of the enterocytes where the pH is low at this region due to Na^+/H^+ exchange at the apical membrane of the enterocyte. The fatty acids inside the mixed micelles are protonated and released from the mixed micelles to move across the lipid bilayer membranes through simple diffusion. Due to their solubility in water, medium-chain free fatty acids containing 4 to 12 carbon atoms can move through the unstirred water layer before being transported through the lipid bilayer to the enterocyte by simple diffusion [16]. They are then carried to the bloodstream where they are carried to the liver bound to albumin proteins. Other products resulting from lipid digestion are carried through the lipid bilayer and enter the enterocytes through simple diffusion. Once absorbed into the enterocytes, triglycerides are reformed in the cytoplasm of the enterocyte from monoglyceride molecules and fatty acids, and then the triglycerides are incorporated into chylomicrons which are then released to lymph and pass into the blood stream through the thoracic duct [16, 21].

1.3 Overview of the digestive enzymes

1.3.1 Alpha-amylase structure and activity

Alpha-amylase, which is also known as α-1, 4 glucan-4-glucanohydrolase (EC3.2.1.1), is a digestive enzyme found in mammals, micro-organisms and plants [28]. This enzyme cleaves α-D-(1, 4) glycosidic bonds of starch (plant), glycogen (animal) and different oligosaccharides. In mammals, there are two types of α-amylase, salivary amylase and pancreatic amylase [28]. In 1987, Buisson et al. studied the three-dimensional structure of porcine pancreatic α-amylase at 2.9 Å resolution using x-ray crystallography and divided the N-terminal domain, which consists of amino acids 1-410, into two domains A and B, suggesting that the porcine pancreatic α-amylase was composed of three domains (A, B, and C). Domain A is the largest domain composed of 330 amino acids (1 -100 and 169 -407) and located in the centre between domains B and C. Domain A possesses a structure of usual parallel-stranded alpha-beta barrel $(\alpha/\beta)_8$. Domain B, which is smaller than domain A, is composed of amino acids 101-168, and consists of two anti-parallel beta sheets as well as a long loop with less fixed inner structure. The domain B is located between the third beta-strand and the third alpha-helix of the central domain A and it links to domain A mostly through a disulfide bridge (Cys 70-Cys 115) and through Ca^{2+}, indicating that the enzyme is Ca^{2+} dependent. Domain C includes amino acids 408-496 and makes a spherical unit where the chain bends to eight anti-parallel β- strands. Domain C is linked to domain A via a single polypeptide chain which could provide some flexibility (Figure 1.1) [28].

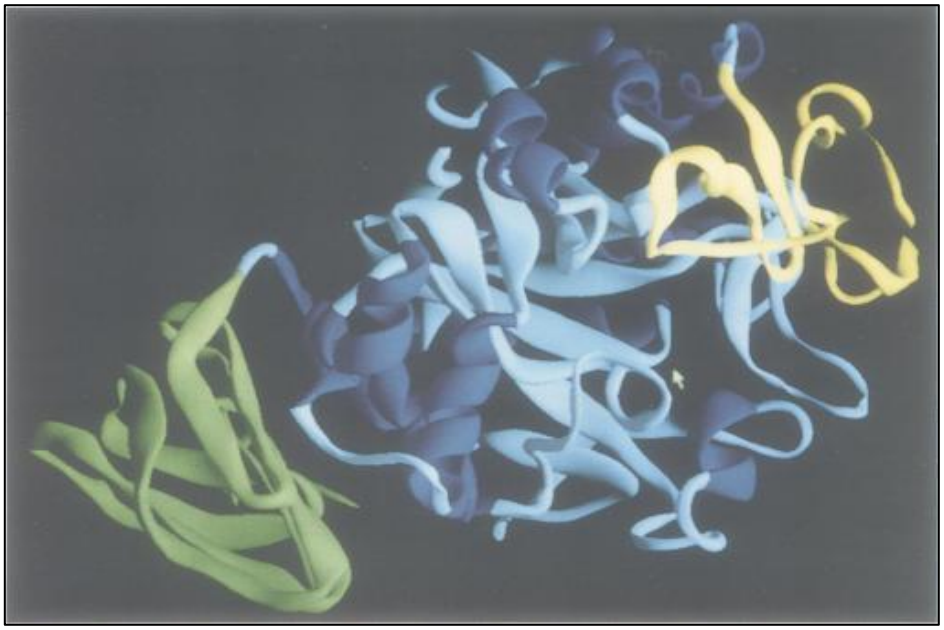

Figure 1.1. Solid ribbon representation of the alpha-carbon chain of porcine pancreatic amylase using the software developed by M. Carson (1987). Domain A with the (a/ β)$_8$ barrel structure is shown in dark blue (helices) and light blue (β-sheets and random coil), domain B in yellow and domain C in green. The arrow points to the active site cleft between domains A and B. Adapted from Buisson et al., (1987) [28].

According to Buisson (1987), the active site of pancreatic alpha-amylase is present in a cleft inside the central N-terminal domain, at the carboxy-end of the β-strands of the (α/β)$_8$ barrel. The same study reported that a pair of aspartic acid residues (Asp 197 and Asp 300) are involved in the catalytic mechanism of porcine pancreatic α-amylase [28]. Other amino acids bind to the substrate through hydrogen bonds and hydrophobic interactions. Alpha-amylase has specificity for interior α-D-(1, 4) glycosidic bonds of starch, glycogen and oligosaccharides converting them into smaller chains of glucose molecules. Salivary α-amylase hydrolyses 40% of ingested starch [29]. Salivary amylase is active at pH ranges from 6.6 to 6.8; however, it loses activity rapidly in the stomach due to the acidic environment [30]. When carbohydrates arrive into the small intestine, pancreatic amylase continues the carbohydrate digestion [31]. Human pancreatic amylase is stable at pH between 5.0 and 10.5, however, the optimum pH for pancreatic amylase is 7.1 [32]. Valle and his colleagues (1959) reported that calcium ions are crucial, and each α-amylase molecule needs at least one calcium ion to conserve the catalytic activity and tertiary structure of the enzyme [33]. Buisson, (1987) reported that the calcium ions are very important for conformational stability of pancreatic α-amylase since the ligand of these calcium ions belong to domains A and B, hence, the

calcium binding site produces an ionic bridge between the two domains [28]. As a result, the cleft of the catalytic site which exists between the domains A and B will be stabilised through this ionic bridge.

In porcine pancreatic amylase, four amino acids, Asn 100, His 201, Arg 158 and Asp 167, act to bind calcium ions [34]. The catalytic mechanism of glycoside hydrolases usually occurs at an anomeric carbon (C_1), the carbon forming the glycosidic bond, and this anomeric carbon possesses two conformations (α and β). The catalytic mechanism of theses enzymes is either an inverting or retaining mechanism. An inverting mechanism is where the primary conformation of the anomeric carbon is altered after cleavage of the glycosidic bond. In contrast, a retaining mechanism is where the initial conformation of the anomeric carbon remains unchanged after the cleavage of glycosidic bond.

Pinto et al. (2015) used computational techniques, quantum mechanic (QM) and molecular mechanic (MM) methods to define the catalytic mechanism of human pancreatic α-amylase (HPA) [35]. They reported that three residues, Asp 197, Glu233, and Asp300, are involved in the catalytic mechanism of HPA. This mechanism involves two steps: glycosylation and deglycosylation. During the glycosylation step, the glyosidic bond is cleaved, and this step is catalysed by carboxylic acids of Asp197 and Glu233 residues which act as nucleophilic and proton donor residues, respectively, to produce a covalent intermediate. The Asp197 nucleophilic residue attacks the anomeric carbon (C_1), breaking the glycosidic bond. Subsequently, a proton is transferred from Glu233 to the glycosidic oxygen forming a hydrogen bond between the Glu233 and the substrate, hence, the anomeric carbon atom attaches to Asp197 through a hydrogen bond. In the deglycosylation step, the covalent intermediate produced from the first step (glycosylation) undergoes a nucleophilic attack by the hydroxyl group of the water molecule located at the active site close to anomeric carbon (C_1), producing enzyme/substrate covalent intermediate, carrying out the sugar hydrolysis. The nucleophilic attack of the hydroxyl group of the water molecule activates deglycosylation through the breakdown of glycosidic bond and sequential transfer of a proton to the Glu233 residue through the glycosidic oxygen, hence, Glu233 will retain its protons that it had at the beginning of the catalytic reaction (Figure 1.2 and Figure 1.3). According to Pinto et al. (2015), the Asp 300 residue is essential for stability of the water molecule, which functions as a nucleophile for the second step, since the Asp300 enables the water molecule to be close enough to the C_1 of the sugar residue where this water molecule will occupy the same position which was

earlier occupied by the glycosidic oxygen, enabling the nucleophilic attack of the C_1 of the sugar residue by the water molecule [35].

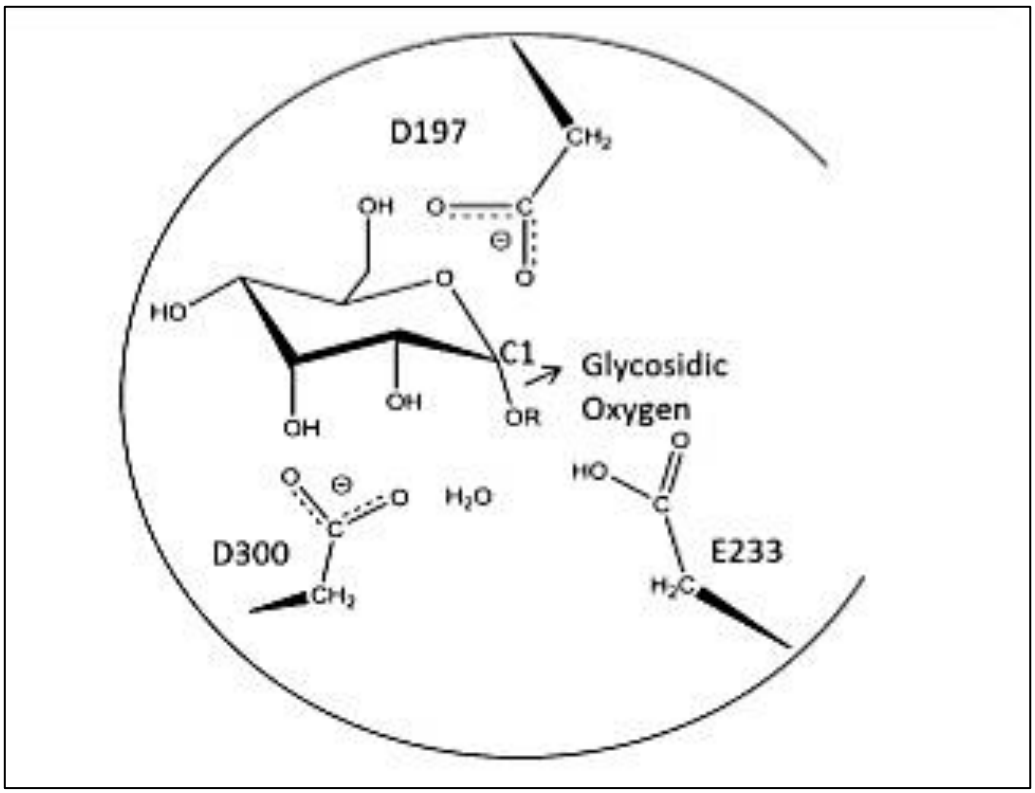

Figure 1.2. Conformation of α-amylase /substrate based on quantum mechanics (QM) layers. D197, D300, E233 represent aspartate 197, aspartate 300, and glutamate 233, respectively. C_1 represents an anomeric carbon, whereas the glycosidic oxygen is shown by the arrow. Taken from Pinto *et al.,* (2015)

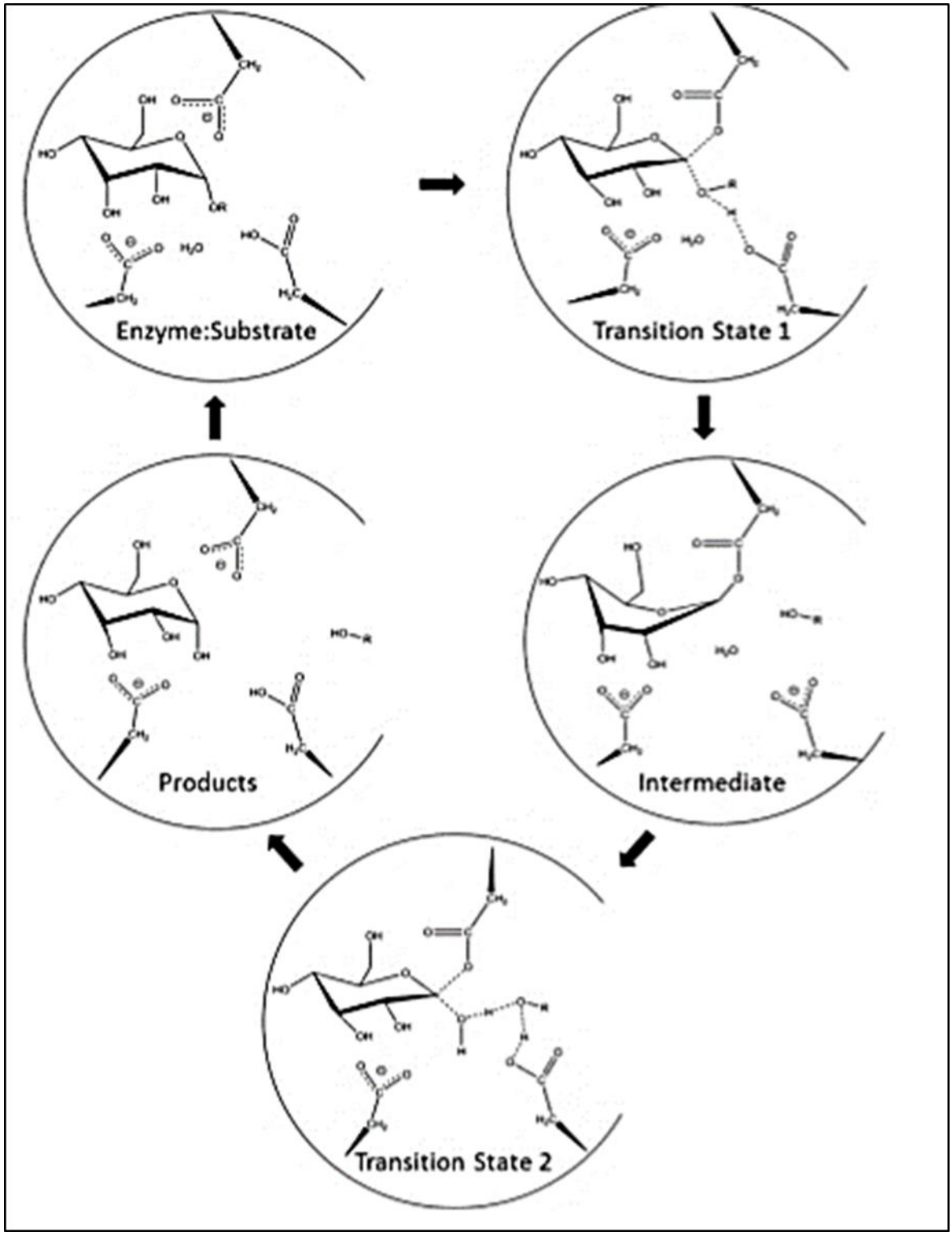

Figure 1.3. Catalytic mechanism for human pancreatic α-amylase (HPA). Residues and substrate are in the same position as shown in Figure 1.2. Taken from Pinto et al., (2015) [35].

1.3.2 Pepsin structure and activity

Pepsin is a member of a widespread aspartate super-family (EC 3.4.23.) which exists in different species including humans, plants, retroviruses, yeast and fungi. Pepsin is the main proteolytic enzyme in protein digestion. There are five types of pepsins, A, B, C, F, and Y, however, in humans, only pepsins A and C are present, and these pepsins are the active forms of the two immunological groups of pepsinogens PGI and PGII in human, respectively. PGI pepsinogen is minimally composed of pepsinogens 1-5, and it is produced by oxyntic glands of the fundus. PGII pepsinogen has only pepsinogens 6 and 7 and it is produced by the antrum pyloric glands, the fundus oxyntic glands, and the tissues of the proximal duodenum [19].

The first crystallisation for pepsin was achieved by John Northrop in 1930, and then the molecular and crystal structures of purified pepsin was determined in 1990 by Sielecki and his colleagues [36, 37]. The three-dimensional structure of pepsin (Figure 1.4) shows that it is made up of two lobes, N-terminal lobe and C-terminal lobe, which are almost identical in structure and size, producing a double symmetry composed mainly of β-sheets stablised by hydrogen bonds [38, 39]. In porcine pepsin, the N-terminal lobe includes amino acids 1 to 175, whereas the C-terminal lobe includes amino acids 176 to 326 [40]. The pepsin active site is made up of a pair of aspartate residues (Asp32 and Asp215) which exist in a deep cleft located between the two lobes. The cleft length is about 30Å (angstrom), and it is enclosed by a flexible flap, made up of 30-90 amino acids, bulging from the N-terminal section of the pepsin enzyme. The flap is made up of two antiparallel strands L71-G82 and it restricts the access of substrate to active site cleft [41]. Both Ser 35 and Thr 218 residues are involved in the hydrogen bonding network which links the Asp 32 and Asp 215 residues [19].

Seventeen water molecules are essential for supporting the shape, geometry and function of active sites and conserving the stability of the flexible flap during the binding of substrate to the active site cleft [42]. Eliminating these essential water molecules from pepsin by water miscible organic solvents such as ethanol results in its permanent inactivation [43]. The presence of water molecules within the hydrogen bonding network, which links the Asp32 and Asp215, enables nucleophilic attack by the hydroxyl group of the water molecule on the carbonyl carbon of the peptide bond to produce $–NH_2$ and COOH [19, 20]. Six stranded antiparallel beta sheets present between the N- and C terminal domains creates the active binding site of the substrate which is located at the reverse side of the aspartate diad. Peptides consisting of 7-9 amino acid residues can occupy the

active binding site for the substrate [19]. The catalytic diad Asp32 and Asp215 function as an acid and base, respectively, in the catalytic mechanism of pepsin. The carboxyl group of Asp215 protonates the oxygen atom on the scissile peptide bond, whereas the Asp32 carboxyl group as anion ($-COO^-$) acts as a nucleophile and attacks the carbonyl carbon of amide, which was protonated previously by Asp215, producing a tetrahedral intermediate complex. Then, the produced tetrahedral intermediate goes through a reversible four-center reaction to release the free acid as a product and the amino enzyme intermediate. This intermediate then undergoes a reaction with a water molecule producing the free amide as a product and regenerating the active pepsin enzyme [19, 44]. Asp32 has to have a low pKa at the highly acidic pH to maintain the negative charge on carbonyl group ($-COO^-$), and the extensive hydrogen bonding is responsible for maintaining the negative charge of the Asp32 carboxyl group, allowing the pepsin enzyme to act at this low pH [19].

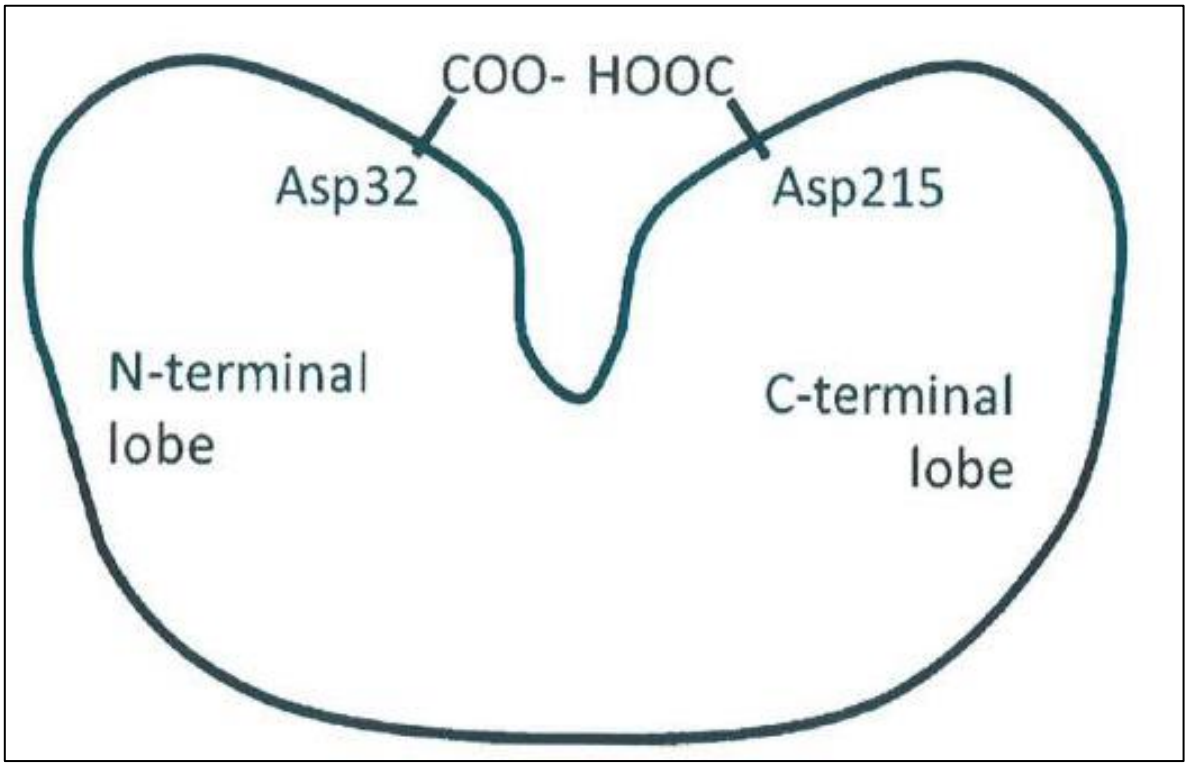

Figure 1.4. Schematic representation of structure of pepsin. Taken from Pearson *et al.,* (2010) [19].

Pepsin, which is an endopeptidase, cleaves interior peptide bonds of the protein, producing large polypeptides. Pepsin has a high affinity for peptides bound to aromatic amino acids such as Phe, Tryp, and Tyr. Pepsin is produced in the stomach as an inactive zymogen, pepsinogen, which is then converted to the active pepsin by an autocatalytic mechanism in the acidic pH environment caused by the secretion of gastric HCl. The primary structure of pepsinogen is similar to pepsin but in addition has 44 residues, the propeptide covalently linked to the N-terminus of the protein. Pepsinogen remains stable at pH ranged between 7 and 9, however, the pepsinogen undergoes irreversible denaturation at pH above 9 [19]. At low pH (<5.0), the carboxyl groups of pepsinogen are protonated spontaneously through an auto-catalytic mechanism which is controlled by the pH, leading to removal of the propeptides and producing pepsin. Pepsin has optimum pH 1.6 to 2.5. [36, 45]. Pepsin becomes permanently inactivated at pH above 7. However, it has been shown that the pH of inactivation relies on the concentration of pepsin as well as the environment where purified pepsin at concentrations between 0.1 and 1 mg/ml experienced a permanent inactivation at pH 7.0, whereas pepsin in gastric juice repelled permanent denaturation until pH ranged between the 7.5 and 7.7 [19, 46].

1.3.3 Pancreatic lipase structure and activity

Pancreatic lipase, which is also known as triacylglycerol acyl hydrolase (EC3.1.1.3), is present in the majority of adult vertebrates [47]. Human, pancreatic lipase is composed of 449 amino acid residues, and it contains two distinct domains linked together via a hinge region. The N-terminal domain, which is larger than C-terminal domain, is composed of amino acids 1 to 335 amino acids. The N-terminal domain has a usual alpha/beta structure which is controlled by a central parallel β-sheet. The N-domain contains the active site with a catalytic triad generated from the three amino acids Ser 152, Asp 176, and His 263. This catalytic triad is protected by a surface loop (lid) which does not allow access of solvent or substrate molecule.

The smaller C-domain is composed of amino acids 336 to 499, and it possesses a binding site for co-lipase. The C-domain consists of two β-sheet layers, giving a β-sandwich style. Each single beta sheet is composed of four anti-parallel strands (Figure 1.5) [48]. Lipase's catalytic triad site is surrounded by a short amphipathic lid between the disulphide-linked residues 237 and 261, preventing the entry of solvent or substrate molecule to the enzyme active site. The lid has a

hydrophilic external side, and internal hydrophobic side which is facing to the active site. Pancreatic lipase must undergo interfacial activation in which the lid covering the enzyme catalytic site is opened, allowing the entry of substrate into the active site of enzyme. The 3-D structures of lipase-procolipase complex and lipase-procolipase-bile salts-phospholipid shows that the procolipase binds to the C-terminal domain of lipase. However, in the case of mixed bile salts-phospholipid micelles, some alterations occur in the shape of the lid covering the lipase catalytic site where the hydrophobic side of the lid is exposed, whereas the hydrophilic side is buried, consequently the active site of lipase becomes accessible for the substrate. In its new open shape, the two lipase domains slightly turn around the hinge region, allowing binding of the N-terminal domain to procolipase through the open lid [48-51].

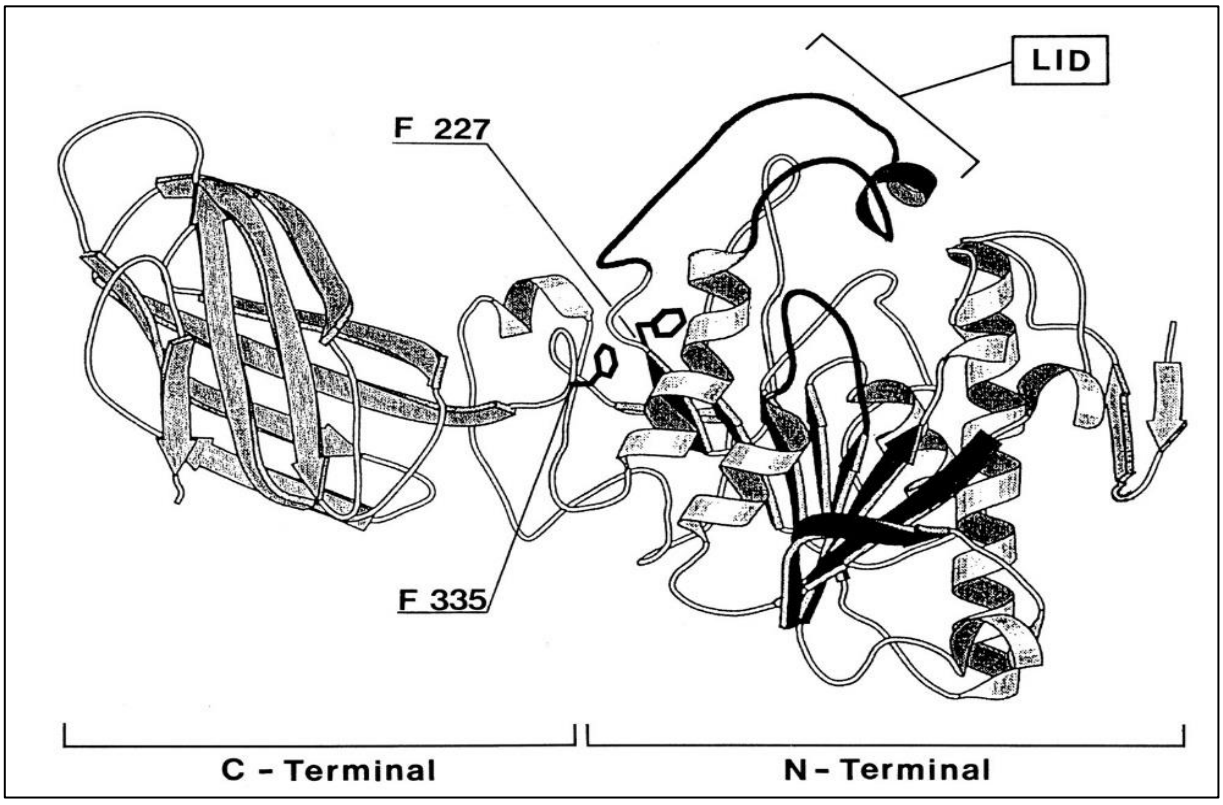

Figure 1.5. Schematic diagram of 3D-structure of the closed conformation of human pancreatic lipase. Arrows indicate β-strands, whereas coils indicate α-helix. The N- and C- terminal domains, the lid, and the side chains of Phe^{227} and Phe^{335}, which are the chymotryptic cleavage site, are indicated. Taken from Aoubala *et al*., (1995) [51].

The optimum pH for pancreatic lipase activity ranges from 7 to 9 [52]. It was reported that the

enzyme retains substantial activity at pH 6.5, however, the pancreatic lipase becomes irreversibly inactive (permanently denatured) at pH less than 4, therefore, gastric acid must be neutralised by bicarbonate in pancreatic juice to prevent enzyme permanent denaturation and maintain enzyme activity [47, 53].

There are many cofactors that affect pancreatic activity such as colipase, bile salts, and calcium ions. Colipase is a small non-enzymatic protein which has molecular weight about 10 kDa. Colipase is secreted as a procolipase which is converted by the action of trypsin to active colipase [47]. Binding of colipase to pancreatic lipase prevents enzyme inhibition by bile salts and protects the enzyme's surface from denaturation. Bile salts inhibit pancreatic lipase activity since the bile salts bind to the substrate interface, promoting surface tension and hindering the binding of lipase to substrate interface. Colipase remains at the substrate interaction site allowing the enzyme to interact with the substrate in the presence of the bile salts [45, 54]. Hydrolysis of intralipid usually involves two-phase kinetics: initially, the lag phase which is a slow phase followed by steady-state phase which is a highly hydrolytic activity phase.

Previous *in vivo* and *in vitro* studies showed that the presence of Ca^{2+} ions are essential for the activity of pancreatic lipase [54-60]. *In vitro* studies on the effect of calcium ions on the pancreatic lipase activity have shown that the activity of pancreatic lipase increased with increasing concentration of Ca^{2+} in the reaction mixture [55, 60]. It has been supposed that the bile salts bind to the substrate interface via the steroid nucleus giving the substrate a negative charge. The negative charge increases the electrostatic repulsion between the lipases and the interface of substrate. As a result, the penetration of lipases to the substrate interface may be reduced by the effect of electrostatic repulsion caused by this negative charge [61]. Armand et al. (1992) reported that the lag time of the reaction, which is the time required to approach the steady state maximum velocity, could be decreased by the addition of calcium ions, where these divalent ions reduce the electrostatic repulsion between the enzyme and the substrate [55]. Whickham et al (1998) showed that calcium ions could reduce the surface charge of emulsion droplets in the presence of bile salts, however, they did not find a relationship between the surface charge and the duration of lag phase, ruling out any important effect that electrostatic repulsion might have on the enzyme and the emulsion interface. It has been stated that the concentration of calcium in the fasted state is about 3-4 mM, however, in the fed state, the concentration of calcium increases significantly to about 15 mM. This significant increase in concentration of Ca^{2+} reduces the lag phase usually prior to

maximum lipase activity, subsequently, the lipolytic activity of pancreatic lipase *in vivo* increases [59]. Additionally, *in vitro* studies showed that the free fatty acids, which result from the hydrolytic action of the pancreatic lipase on triacylglycerides, accumulate at the substrate surface, preventing the further hydrolytic action of pancreatic lipase on the substrate. Therefore, during *in vitro* lipolysis, these free fatty acids are precipitated as soaps by the action of calcium ions forming insoluble Ca-soap [56, 59]. However, *in vivo*, these free fatty acids are removed by their absorption through the intestinal walls [59]. Moreover, it has been suggested that calcium ions mix with the bile salts forming liquid crystal. Then, free fatty acids are dissolved in this liquid crystal and absorbed through the epithelial cells of the small intestine. The absorption of the free fatty acids through epithelial cells aids in removing these free fatty acids from the substrate surface, preventing the inhibition of the pancreatic lipase *in vivo* [59].

Yang et al. (2000) reported that calcium binding sites are present in the tertiary structures of *Pseudomonas* lipases. The calcium ion ligands in the *Pseudomonas* lipase contains two molecules of water, two carbonyl groups of Gln 292 and Val 296, and two carboxyl groups Asp 242 and Asp 288. The same authors investigated the effect of EDTA at different temperature on lipase with calcium binding sites (wild type) and without calcium binding sites (mutant type). They found that the wild type of lipase, which contains the calcium binding sites, at temperature 37 °C was relatively stable where its activity was not affected, whereas the activity of mutant enzyme was low, showing that calcium is essential for the lipase stability and activation process in the presence of chelator EDTA. They found that replacing sp242 and Asp288 which are involved in the calcium binding sites of lipase decreased lipase activity but did not affect the activation process of lipase [62].

Pancreatic lipase specificity towards the fatty acids at positions sn-1 and sn-2, produces 2-monoacylglycerol and two free fatty acids. This enzyme initially attacks the fatty acid chain at sn-1, producing 2, 3-diacyglyceride and one free fatty acid. Secondarily, it attacks the fatty acid at sn-2, producing 2-monoacylgyceride and two fatty acid molecules. The complete hydrolysis of triacyglycerides by pancreatic lipase to free glycerols occurs, where 2-monoacyglyceride is rearranged to 1-monoacylglyceride which then undergoes enzymatic hydrolysis [63, 64].

The catalytic activity of lipase depends on the presence of an Asp-His-Ser catalytic triad at the active site of the enzyme which works as a charge-relay system where an alcohol group on the

serine residue of the catalytic triad site is linked via a hydrogen bond to nitrogen on histidine, and the nitrogen on histidine is linked via a hydrogen bond to the carboxylate group on aspartic acid.

The initial step in the mechanism of lipase is increasing the nucleophilicity of the serine alcohol by histidine which attracts the proton of the serine alcohol towards itself, producing an oxyanion (oxygen ion). Then, the resulting oxyanion attacks the carbonyl carbon of the substrate, producing the tetrahedral intermediate 1 (Figure 1.6). Both adjacent amino acids, histidine and aspartic acid, which are linked via hydrogen bonds to serine, stabilise the oxyanion of serine. The electrons present on the oxyanion are transferred to the carbon of carbonyl group, and the proton present on the histidine is moved to the diglyceride which is consequently liberated. The produced serine ester reacts with alcohol to complete the transesterification process. The hydrogen atom of alcohol molecules is removed by nitrogen atom of histidine, producing alkyl oxide onion. The carbon of the carbonyl group is attacked by hydroxide, the oxyanion of the intermediate is stabilised by hydrogen bonds (tetrahedral intermediate 2), and the electrons are moved back to the carbon carbonyl, hence, the free fatty acid is produced. Then, the oxygen atom on serine retrieves the hydrogen from the histidine, and subsequently, the serine becomes hydrogen-bonded to the histidine. During the catalytic mechanism of lipase, the function of aspartic acid is attracting the positive charge from the histidine when the histidine becomes fully protonated [65].

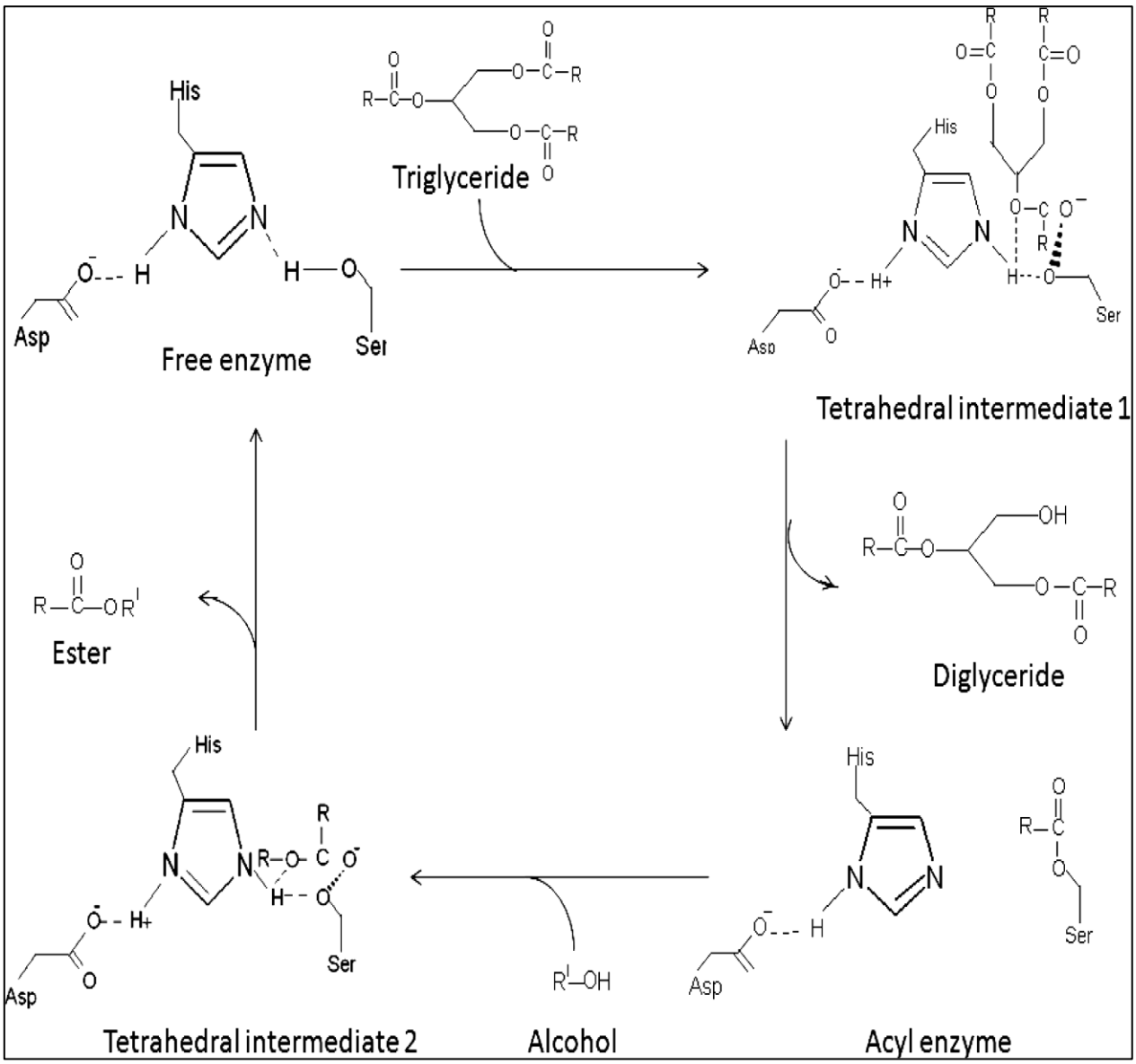

Figure 1.6. Mechanism of lipase-catalysed transesterification of triglycerides.Taken from Jegannathan & Abang, (2008) [65].

1.4 Treatment of obesity

1.4.1 Conventional obesity treatment

Methods such as diet, improved eating habits and physical activity can be used in obesity treatment. Obese individuals are advised to eat low-fat foods, and to eat a reduced-calorie diet to reduce energy by 500-1000 kcal per day resulting in a body weight loss of 0.5-1 kg per a week [66]. However, it was reported that dietary treatment succeeds in achieving average weight loss in only

15% of cases [67]. Daily physical exercise such as walking for 80-90 minutes or jogging for 35 minutes is suggested as an obesity treatment because it can promote weight loss [68]. However, physical activity without a calorie reduced diet minimally reduces body weight. Walking 40-60 minutes for four days every week managed only an energy deficiency of 1,000 kcal with reduction in body weight by 0.15 kg. Conversely, low calorie diets showed weekly energy deficiency of 3.500-7000 kcal with reduction in weight by 0.5-1 kg per week [66].

1.4.2 Surgical treatment for obesity

Surgical therapy such as gastric bypass, gastric banding, sleeve gastrectomy, and gastroplasty can be a reasonable option for obese individuals with a BMI >35 kg/m^2 [69]. Surgical treatment has produced considerable and well-documented results in weight loss, improving the patients' health and quality of life [66, 70]. However, due to the serious side effects of surgical treatments such as nutritional deficiency, gastrointestinal symptoms, vomiting, and shortness of breath, it is only recommended for morbidly obese people whose lives are in great danger because of their excess weight [69, 71].

1.5 New approaches to the treatment of obesity

1.5.1 Anti-obesity drugs targeting digestive enzymes:

Mu & Høy's 2004 study demonstrated that about 40% of all energy intake results from dietary fats, mainly from triacylglycerol. Therefore, the inhibition of pancreatic lipase activity has become the strategy most frequently used for the treatment of obesity. Different types of potential anti-obesity drugs from microbial and plant sources such as lipstatin and its derivative Alli/Orlistat have now been developed [4, 72], and it has been reported that obesity can be treated successfully by using anti-obesity drugs in combination with diet, revised eating habits and regular daily exercise [73].

1.5.2 Orlistat

Lipstatin is a highly selective drug which is isolated from Streptomyces *toxytincini.* This drug irreversibly inhibits pancreatic lipase with IC_{50} of 0.14 μM. However, due to its instability, it has been replaced by Orlistat [4, 74]. Orlistat, which is commercially available as Xenical and Alli, was approved in 1998, and it is considered the main clinically available drug for the long-term treatment of obesity [75]. In 2010, approximately 98% of all prescriptions for obesity treatment in the United Kingdom were for this drug. [72]. Orlistat is a saturated form of lipstatin, which is prepared by hydrogenation of lipstatin [76, 77]. Gastric and pancreatic lipases are inhibited by Orlistat through the nucleophilic attack of hydroxyl group of serine 152 residue at the active site of the lipase by the carbonyl carbon on the β-lactone ring of Orlistat, resulting in formation of long-lived acyl enzyme complex 1. The acyl enzyme complex 1 undergoes a spontaneous hydrolysis where the covalent bond between the –OH group on serine and the β-lactone ring of Orlistat is cleaved, releasing the active enzyme and producing the β-hydroxy carboxylic acid 2 (Figure 1.7) [78, 79]. It has been reported that Orlistat reduces the absorption of dietary fat by 30% [80]. However, this drug does produce some side effects such as diarrhoea, faecal incontinence, oily spotting, flatulence, nausea, and vomiting [77, 80, 81]. However, a 2001 study by Cavaliere et al suggested that avoiding a fat-rich diet and eating natural fibre such as Psyllium mucilloid can decrease the side effects of the drug [72].

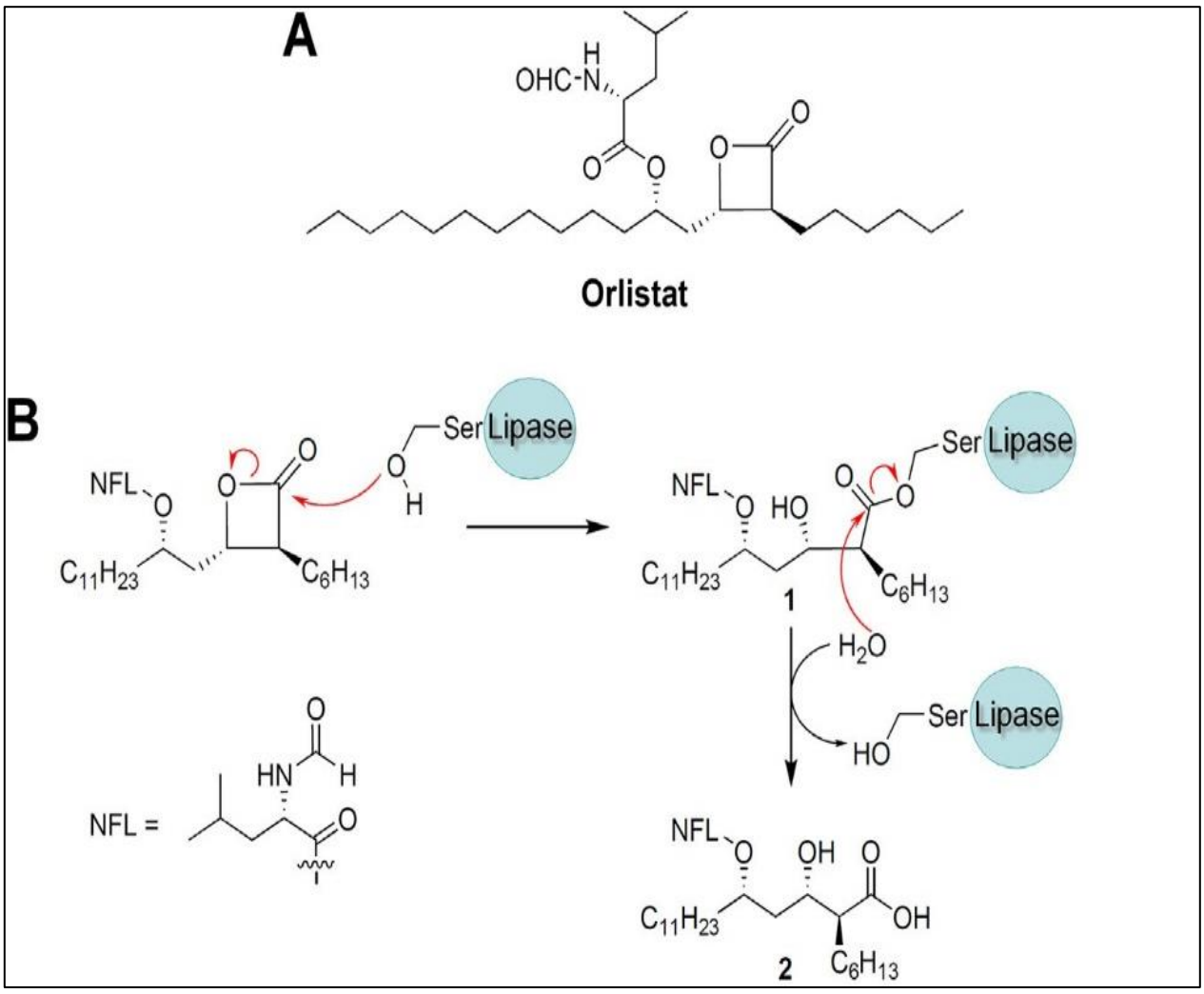

Figure 1.7. Schematic representation for the structure of Orlistat. **A** represents Orlistat structure, whereas **B** represents its mechanism in lipase inhibition. Adapted from Bénarouche et al., (2014).

Dietary fibre

Due to the limitation in the success of low-fat diets, calorie-restricted foods, and very low-calorie diets, and because the high cost and side effects of anti-obesity drugs as well as the negative effects arising from surgical treatment such as gastrointestinal symptoms and nutritional deficiencies [71], current treatments to combat obesity have been focused on using strategies such as satiety to control food consumption, and thus reduce energy intake [82]. The beneficial health effects of consuming high-fibre diets or fibre supplements as a method for weight loss have been confirmed by several international studies [83]. Dietary fibre can be defined as the edible parts of plants or analogues of non-starch polysaccharides and lignin which are indigestible and unabsorbed in the small intestine and are fermentable in the large intestine to short chain fatty acids which can be absorbed and used as energy source [84]. Dietary fibre is classified into water-soluble fibre such as storage polysaccharides, gum, pectin and mucilage, and water-insoluble fibre which includes cellulose, hemicellulose, and lignin. Both soluble and insoluble fibres have the ability to bind water and make a further reduction in the energy to weight ratio in diets [84-86]. However, in human, the amount of energy from short chain fatty acids of fermented fibre is low (5-10%) since only 40% of fibre undergoes the fermentation process, thus the consumption of fibrous food considerably reduces energy density [87, 88].

1.5.3.1 Beneficial health effects of dietary fibres

Most studies related to adult health have clearly shown that the consumption of dietary fibre possesses well-documented physiological effects such as the promotion of satiety, the reduction of hunger, the regulation of energy intake, and assistance in weight loss [85, 86, 88]. It was indicated that when energy intake is *ad libitum*, eating an additional 14 g/day of fibre for more than two days for 3.8 months decreased the energy intake and body weight by 10% and 1.9 kg, respectively [88]. Furthermore, obese and overweight individuals, who consumed high amounts of fibre showed greater decrease in energy intake by 18% and weight loss by 2.4 kg compared with normal individuals whose energy intake was reduced by 6% and body weight by 0.8 kg [88]. Chewing foods rich in fibre decreases the rate of ingestion and enhances satiation since the chewing requires more time and increased effort. This may also enhance the secretion of saliva and gastric acid in the stomach leading to gastric distention [88]. Moreover, the same study found that soluble fibre

has the ability to slow the transport of macronutrients from the stomach and reduce their digestion. In the small intestine, soluble fibre slows insulin and glycemic responses after eating and reduces hunger and energy intake [86, 88]. It has been reported that the reduction in energy density occurs due to the fibres capacity to provide bulk and weight to the diet which causes early signals of satiation and gastric fullness [88]. Also, Howarth et al (2001) reported that the addition of viscous dietary fibres, which tend to absorb enormous amounts of water, into foods promotes the signals of satiety by increasing the viscosity of gastrointestinal contents. The increase in viscosity of small intestinal contents delays stomach emptying and small bowel movement. As a result, the process of fat and carbohydrate absorption is delayed, thus the period in which the reaction between the nutritional substances and preabsorpative mechanisms of satiety lasts for a long time [86]. In addition, Burton-Freeman's study showed that healthy adult humans require consumption of 20 to 35g of dietary fibre every day. The same author noted that many epidemiologic studies have made a connection between the consumption of low fibre foods and obesity development [86].

1.5.3.2 The influence of dietary fibre on digestive enzymes

Previous studies have reported that dietary fibres can inhibit the activities of digestive enzymes. Ikeda and Kusano (1983) studied the effect of various indigestible polysaccharides on the activities of different digestive enzymes *in vitro*. They found that xylan, agar-agar and apple pectin could significantly reduce trypsin activity *in vitro* to 23, 52.4 and 38.3%, respectively [89]. The same authors reported that the activity of α-chymotrypsin was sharply decreased *in vitro* to 46.5, 54.4, and 56% by the action of xylan, sodium alginate and yeast mannan, respectively. Apple pectin and the carboxymethyl cellulose sodium salt considerably reduced α-amylase activity *in vitro* to 50.7 and 57.1%, whereas apple pectin could significantly reduce pepsin activity *in vitro* to 42.6%. Many studies reported that fibre-enriched foods considerably reduced the process of protein digestion in humans [89]. The activity of pancreatic lipase was inhibited *in vitro* by wheat germ and wheat bran. A subsequent decrease in the absorption rate of cholesterol by 10% and dietary triglycerides by 24% in the small intestine was observed in seven healthy adult men who consumed standardised coarse wheat bran (0.5 g/kg body weight) every day over four weeks [90]. Based on the previous findings, it has been proposed that the influence of dietary fibre on lipid metabolism involves inhibition of pancreatic lipase activity, preventing the breakdown of dietary fat in the small intestine. The

reduction in cholesterol and triglyceride absorption was assessed either by the decrease in the fat level in the plasma or the increased amount of fat present in the stool [91].

1.5.4 Bio-active algal polysaccharides

Marine-derived nutrients and some other marine bio-actives have been used as components in functional foods due to their physiological influence, with medical properties and numerous beneficial effects on health [92]. There are two types of dietary fibre involved in marine algae: water-soluble fibres including agars, alginic acid, furonan, laminarin and porphyran, and water-insoluble fibres cellulose, mannans and xylan [93]. In this literature review, marine bio-active compounds obtained from the macroalgae species, namely algal polysaccharide alginates, have been focused on due to their effects on health as soluble fibre, and their wide range of applications in medicine, pharmacology and industry. Algal polysaccharides are rich sources of carbohydrate, but they are indigestible and unabsorbed in the gastrointestinal tract, hence it cannot be deemed as high energy content food [92]. Edible seaweeds contain higher levels of fibres than the higher plants making up 33-50% of their dry weight [93]. The total content of polysaccharides in seaweeds is about 76% of dry weight [94].

Algal polysaccharides can be used as prebiotics, antibacterial agents, antiviral agent, non-toxic antioxidants, stabilisers, thickeners, and emulsifiers [94]. Furthermore, they can act as anti-coagulants, reduce low density lipid (LDL)-cholesterol in rats, provide protection against obesity and diabetes, decrease incidence of cancer of the large intestine, and decrease the absorption of after-meal glucose [93]. Eom et al's study (2013) on the effect of algal polyphenolic compounds, phlorotannins extracted from brown algae *Eisenia bicyclis* by methanol, showed that phlorotannins could reduce pancreatic lipase activity *in vitro*, and among the six tested derivatives (eckol, fucofuroeckol A , 7-phloroeckol , dioxindehydroeckol, phlorofucofuroeckol A, and dieckol), 7-phloroeckol had the most potent inhibitory effect (IC_{50}=12.7 μM), however, the anti-pancreatic lipase activity of 7-phloroeckol was lower than its positive control Orlistat (IC_{50}= 0.4 μM) [95]. Moreover, Matsumoto et al. (2010) reported that both algal bioactives fucoxanthin, which is extracted from edible brown algae, and its metabolite, fucoxanthinol, could reduce the lymphatic absorption of triglycerides as well as the concentration of triglycerides in the blood of rats, indicating that carotenoids could inhibit the activity of pancreatic lipase in the gastrointestinal tract

of rats [96]. Matsumoto and his colleagues (2010) found that the amounts of triglycerides liberated into the lymph after 4 h of administrating 1 ml of soybean oil containing 2 mg of fucoxanthin and fucoxanthinol to the lymph duct and the portal or the jugular vein were 53.1 and 59.4μmol, respectively, compared to 113.5 μmol of triglycerides released from the control group in which only 1 ml of soybean oil was administrated [96]. Additionally, Chater et al's study (2016) on the effect of three brown algal species *Ascophyllum nodosum, Fucus vesiculosus,* and *Pelvetia canaliculata,* used as whole seaweed homogenate, sodium carbonate extract, and supernatants and pellets of ethanol extract, on pancreatic lipase activity *in vitro* using a turbidimetric lipase activity assay or a synthetic model gut model mimicking the upper part of the gastrointestinal tract *in vivo,* found that all the algal extracts reduced the activity of pancreatic lipase, indicating that different algal bioactive compounds, namely alginate and polyphenols, are potent pancreatic lipase inhibitors [97].

Recently, considerable efforts have been made to study the role of fibrous polysaccharides from algae in modulation of digestive processes by using them in the food industry as food ingredients in an attempt to manage body weight and treat obesity [92, 93].

1.5.5 Chemical structure of alginate

Alginate is an ionic fibrous polysaccharide found in the cell walls of brown seaweed and some bacteria. Alginate is present in brown seaweed mainly as calcium salt of alginic acid, and sometimes as sodium, potassium and magnesium salts. Structurally, alginate is a linear unbranched biopolymer containing D-mannuronic (M) acid and L-guluronic (G) acid linked together by 1 →4 glycosidic bonds [59, 72, 98, 99] (Figure 1.8).

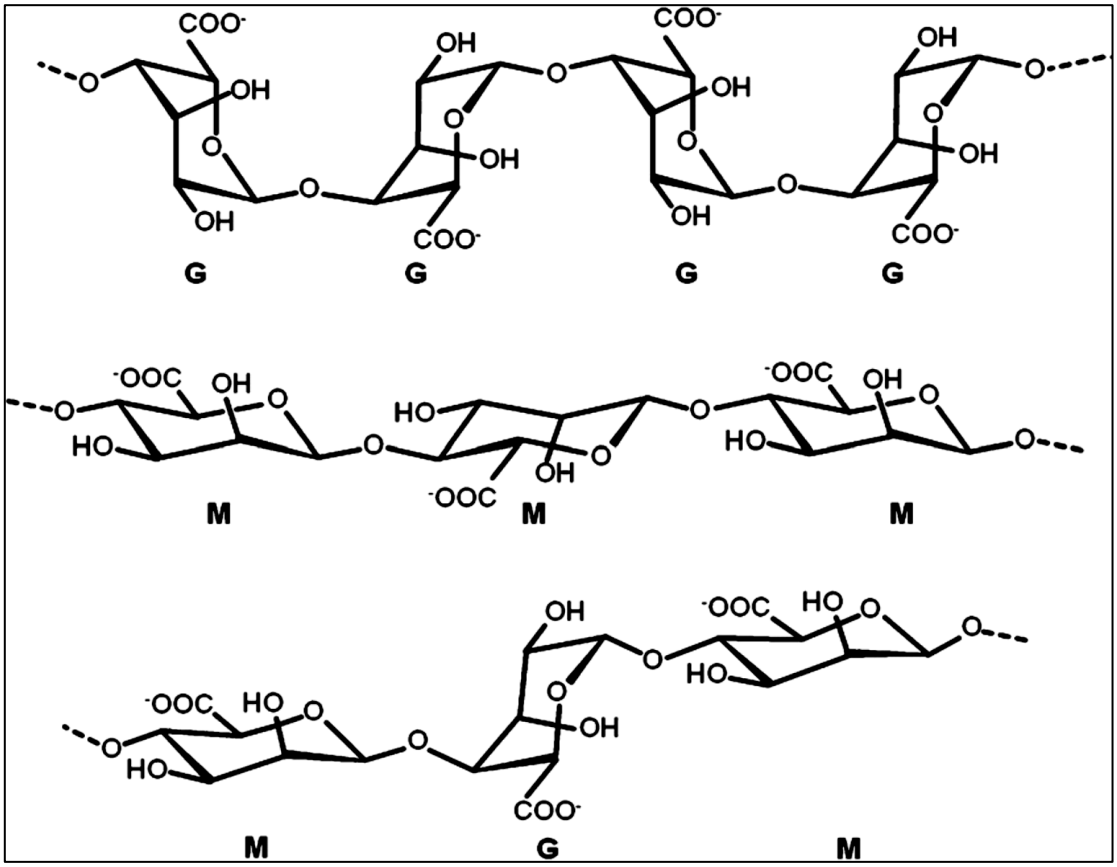

Figure 1.8. Chemical structures of G-block (G), M-block (M), and alternating M-G block in alginate.Adapted from Lee & Mooney, (2012) [100].

1.5.5.1 Alginate sources and production

Laminaria hyperborea, Macrocystis pyrifera and *Ascophyllum nodosum* are the most common kinds of brown seaweeds rich in alginate (Figure 1.9) [98].

The sodium and potassium salts of alginates are water-soluble, while calcium and magnesium salts are water-insoluble. Therefore, the first step in alginate extraction involves the conversion of insoluble calcium and magnesium alginates into soluble sodium alginate by treating them with an alkaline reagent: sodium carbonate pH 10 [101]. Alternatively, the same authors reported that alginate would extract efficiently by treating it with diluted mineral acid to convert the calcium alginate to alginic acid, and then alkali reagent is added to produce sodium alginate.

The crude sodium alginate solution can be purified by three methods: ethanol precipitation, calcium

chloride precipitation and hydrochloric acid precipitation. However, ethanol precipitation is the only method used to directly produce pure sodium alginate, whereas calcium chloride precipitation and hydrochloric acid precipitation produce calcium alginate and alginic acid, respectively, which can then be converted to sodium alginate. In the hydrochloric acid method, a solution of crude sodium alginate at pH 10 is mixed with hydrochloric acid (HCl) to produce alginic acid, then sodium carbonate (Na_2CO_3) is added and sodium alginate is formed. Next, the newly-formed sodium alginate is washed with ethanol, followed by exhaustive washing with ethanol using a soxhlet extractor to produce purified sodium alginate, which finally is dried (Figure 1.10). However, several comparative studies have indicated that purified sodium alginate can be made quickly, and in large amounts of high quality by the ethanol method which takes fewer steps compared to the HCl and $CaCl_2$ methods [101].

http://www.pearltrees.com/seine/phaeophyta/id8360227#l996

https://thewildcoastblog.com/2016/10/13/week-3-giant-kelp-macrocystis-pyrifera/

https://neomed-pharma.com/About-marine-algae/Ascophyllum-Nodosum

Figure 1.9. Brown seaweeds rich in alginate. (A) Laminaria hyperborea, (B) Macrocystis pyrifera and (C) Ascophyllum nodosum.

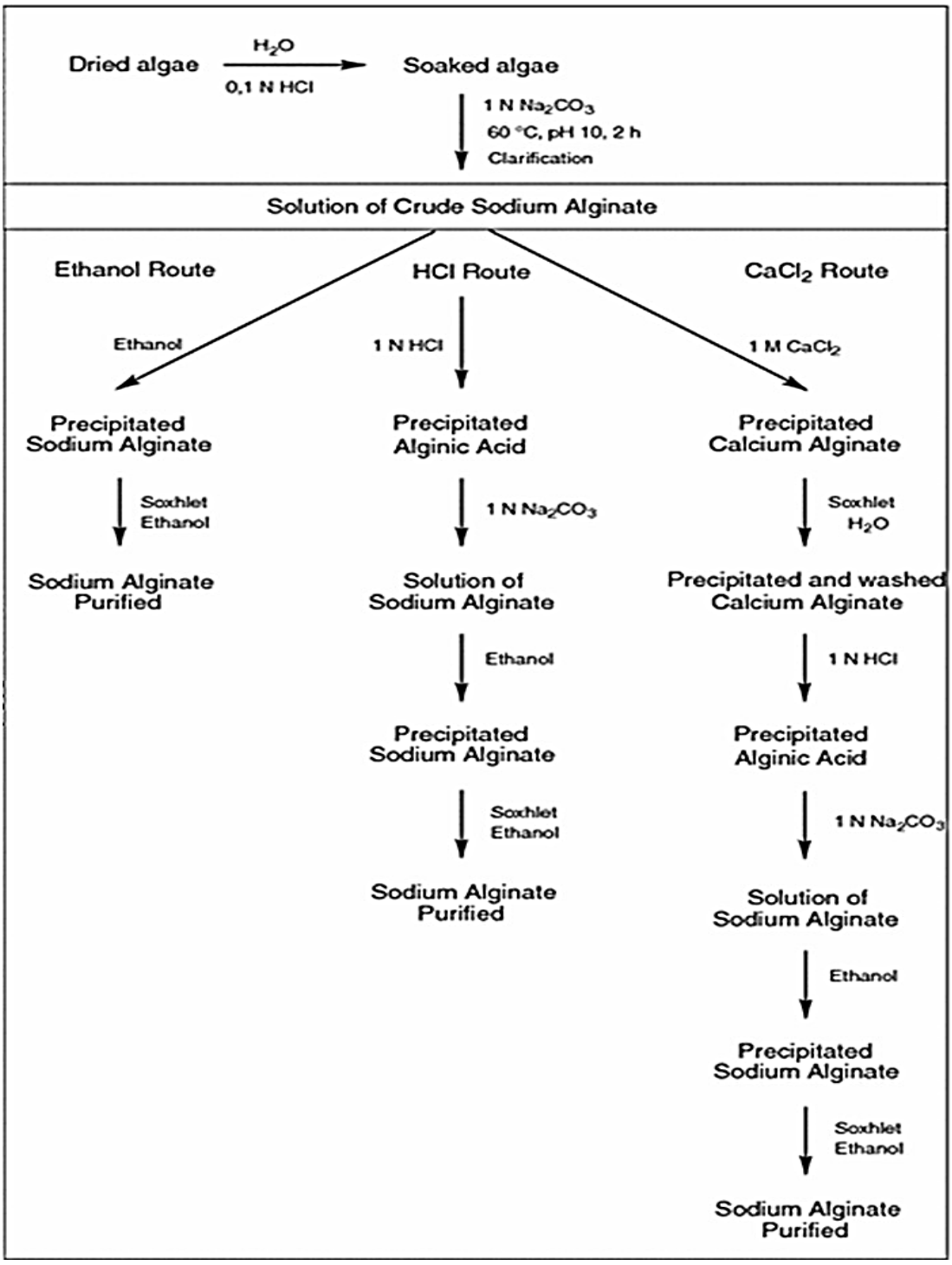

Figure 1.10. A schematic representation of the extraction-purification of sodium alginate from brown algae. Adapted from Thomas et al., (2012) [101].

1.5.5.2 Methods of gelling alginate

Alginate has a wide range of applications in biomedical, pharmacological and industrial fields due to its gelling properties. In this literature review, two methods of gelling alginate have been summarised.

1.5.5.3 Ionic cross-linking

Alginate gel can be simply produced by using divalent cations. When calcium ions are added to sodium alginate polymer, the sodium ions of guluronic acid residues in the polymer are replaced by calcium ions, which are bound strongly to α-L-guluronate blocks, and an egg-box shaped structure is formed between alginate chains resulting in the formation of "cross-linked networks (Figure 1.11). Gels produced by ionic cross-linking contain large amounts of calcium ions which may cause cell toxicity, leading to formation of giant foreign body cells [100].

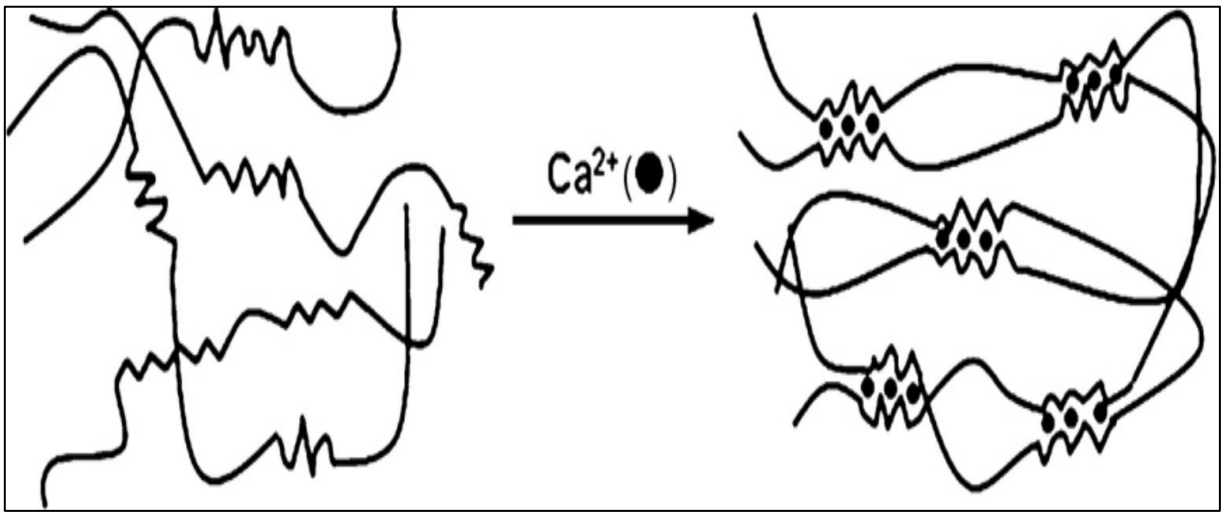

Figure 1.11. Alginate hydrogels prepared by ionic cross-linking (egg-box model)Adapted from Lee & Mooney, (2012) [100].

1.5.5.3.1 Alginic acid gels

Acid gels can be formed by reducing the pH of a sodium alginate solution slowly below the pK_a of the uronic residues, where pK_a for guluronic acid and mannuronic acids are 3.65 and 3.38, respectively. The direct addition of acid to the alginate solution results in alginic acid precipitation instead of acidic gel formation. Therefore, lowering the pH value of the alginate solution should be carried out by adding hydrolysing lactones such as D-glucono-δ-lactone (GLD) gradually, thus the electrostatic repulsion between the chains of alginate polymer will be decreased leading to the formation of hydrogen bonds, and thus a weak acid gel is formed. The addition of mineral acid to pre-formed ionically cross-linked gel results in the formation of alginic acid gel [102, 103].

1.5.5.3.2 Properties and applications of alginate

There are multiple applications for alginates in industry, medicine and pharmacy. In the food industry, alginates are used mainly as stabilisers, viscosifiers and gelling agents. Alginates are widely used as additives in jam, jellies, fruit fillings, onion rings and reconstituted meat [104]. Many studies have recently focused on using alginate hydrogel in the biomedical and pharmaceutical fields because it is biocompatible, low toxicity, fairly inexpensive and quickly forms gels [100]. The biomedical and pharmaceutical applications of alginates include using the hydrogel alginate as a dressing for moderate to severe wounds and also for dental impressions, in addition, the hydrogel alginate is used in formulations for protecting from gastric reflux, also in cell immobilisation for the production of antibiotics, steroids or ethanol from yeast cells [104] .

1.5.5.4 The valuable health benefits of alginates as a digestive enzyme inhibitor

Previous studies have shown that the addition of seaweed extracts of alginate to diets has potential positive health effects such as a decrease in blood glucose level in human [105], a promotion in fat discharge with stool [106], a decrease in energy consumption [10], and protection of the gastric and intestinal surface membranes from carcinogenic substances. The consumption of food containing sodium alginate modulates appetite since alginate gel formation in the stomach promotes early satiety through stretch receptors and delayed gastric emptying. Moreover, the

addition of alginate with calcium alters gelation and viscosity, and subsequently increased gastric distension, decreased nutrient absorption and delays postprandial insulin and glucose responses [83]. Furthermore, it has been demonstrated that about 52% [107]and 53.9% [108] of the digestive enzyme pepsin activity was inhibited by alginate, and the level of pepsin inhibition depended on the molecular weight of the alginate [109]. In the 2014 study by Wilcox et al. it was shown that alginates have an inhibitory effect on pancreatic lipase, and this can provide an explanation for the previous observation in the 1994 study by Sandberg et al., showing an increase in fatty acid discharge in the stool of ileostomy patients (Wilcox et al, 2014). The level of the inhibitory effect of the alginate relies on its structural content. Alginate containing a high proportion of guluronate (G) units inhibits pancreatic lipase more than alginate with high mannuronate (M) content [72].

1.5.5.5 Modification of alginate

Alginate biosynthesis studies have revealed that in both algae and bacteria the alginate is synthesised as a polymer of mannuronate, and the variety of structural and functional features of various alginates is produced by the modifying enzymes mannuronan C-5 epimerases, lyases, and acetylases. Alginate epimerases AlgE1, AlgE4, and AlgE6 have been isolated from the bacterium *a.vinelandii,* and can be used to modify chemical composition and the sequence of M and G residues in alginate *in vitro* to produce alginate polymer with the desired ratio of M and G residues and the arrangement of these residues for use in medical, pharmaceutical and industrial applications. AlgE4 converts M-blocks into a polymer consisting of MG sequences, while AlgE6 and AlgE1 form G-block homopolymers and bifunctional G-blocks + MG-blocks, respectively [103]. The M and G contents and their arrangement affects the properties of alginates such as viscosity, chain rigidity, gel formation and water binding capacity [103, 104].

Chapter 2: Lipase Regulation by Alginate

2.1 Introduction

Obesity has become a serious public health problem in all industrial countries. In western countries, 40% of energy from diets comes from fats, mainly triglycerides [110]. It had been reported that fats contain a large amount of carbon-hydrogen bonds which are rich in energy. Approximately 38 kJ is released from the consumption of one gram of oil or fat, and this is double the amount of energy released from the consumption of one gram of carbohydrates or proteins [111]. The daily average amounts of fats consumed by adults in the western world is 60 to 150 g, and about 90% of this fat intake is in the form of triglycerides, whereas the remaining 10% includes free fatty acids, cholesterol ester (CE), phospholipids, and plant sterols [23]. Triglyceride forms 90-95% of dietary fat, and their digestion occurs mainly in the small intestine by pancreatic lipase. Therefore, several studies have focused on reducing triglyceride digestion through inhibiting pancreatic lipase to reduce caloric intake and thus fight obesity [4, 112].

Orlistat, which is a derivative of lipstatin from *Streptomyces toxitricini*, has managed to decrease about 35% of fat absorption in humans by inhibiting gastric and pancreatic lipases as well as carboxyl esterase, thus reducing triglycerides and cholesterol ester hydrolysis [112]. Although Orlistat has become a very popular anti-obesity drug especially in the United Kingdom where it formed 98% of prescriptions for obesity treatment in 2010, some unpleasant gastrointestinal side effects were associated with using Orlistat. However, it has been reported that consuming natural fibres, such as *Psyllium mucilloid*, at the same time with Orlistat may decrease these [113]. Currently, many studies have suggested using dietary fibres, namely alginate as an obesity treatment. In 2015, Chater and his colleagues reported that alginate has the ability to reduce pepsin activity by 53.9% *in vitro* [108]. Additionally, it has been indicated that consumption of beverages or cereal bars containing alginate was linked to many health benefits including extended satiety, reduction in overall caloric intake, reduced levels of glucose and insulin in the blood, reduced fat digestion and weight loss. However, in these studies alginates caused some side effects such nausea, flatulence, burping, stomach-ache, and poor acceptability due to texture (reported as slimy in the mouth) and the individuals preferred the ordinary products which did not contain alginate [83, 105, 106, 114].

Alginate is an indigestible polysaccharide present in cell walls and intercellular spaces of brown seaweed (*Phyophyceae*). Furthermore, some bacteria such as *Azotobacter* and *Pseudomonas* have the ability to generate alginate as a component of their extracellular matrix. Alginate usually exists as a salt of alginic acid in brown seaweeds, mainly as calcium salt and sometimes as sodium, potassium or magnesium salts [108, 115-117]. Alginate is a linear biopolymer consisting of D-mannuronic (M) acid and L-guluronic (G) acids linked together by (1 →4) glycosidic bonds (Figure 1.8). Knowing the chemical structure and monomeric sequence of alginate is essential since it provides information about the functionality of alginate. For example, the content of guluronic acid residues (FG) and the average number of consecutive guluronate units in the alginate polymer determines the alginate gel strength. Alginate with high content of G blocks forms a rigid gel due to the restricted rotation around the glycosidic bond creating by diaxial linkage in G-block, whereas the alginate containing a high amount of M blocks forms a flexible gel since the diequatorial, axial/equatorial, equatorial/axial in M, MG, and MG blocks composition can freely rotate around the glycosidic bond [108, 118-121]. Alginate chemical composition and sequence can be characterised by using either ^{1}H or ^{13}C-nuclear magnetic resonance spectroscopy (NMR).

Alginate has been suggested as an inhibitor of pancreatic lipase, which is the main enzyme in triglyceride digestion, in an attempt to fight obesity. Therefore, the activity of pancreatic lipase must be assessed in the presence and absence of alginate to investigate alginate's effect on lipase activity. In this chapter, the activity of lipase was determined using an adapted version of Vogel & Zieve's (1963) assay [122]. This method is a turbidimetric assay which measures the reduction in triglyceride turbidity due to their hydrolysis to monoacylglycerol and free fatty acids by the action of pancreatic lipase. According to Vogel and Zeive (1963), the turbidimetric assay for determining lipase activity is one of the most effective titrimetric assays since it is rapid, sensitive, accurate, and repeatable. The same study reported that this method could be used in a routine clinically laboratory if the lipase substrate was carefully prepared as described in the paper.

2.2 Overview of triglycerides

Triglycerides are composed of glycerol and three fatty acids linked together by ester bonds (Figure 2.1). In infants, triglyceride digestion starts in the stomach by lingual lipase, which is a stable

enzyme under acidic conditions. This enzyme releases the short chain fatty acid from position 3 of triglycerides, producing a fatty acid and 1,2-diglyceride. Triglycerides which possess short-or medium chain fatty acids, such as milk triglycerides, are hydrolysed by gastric lipase [64]. Since the gastric lipase is inhibited by protonation of free fatty acids, only a trace amount of dietary fat is digested in the stomach compared with complete hydrolysis of these fats in the small intestine by the action of pancreatic lipase [123]. The lingual and gastric lipases are not able to hydrolyse cholesterol esters and phospholipids [124]. The majority of lipid digestion occurs in the small intestine where emulsified triglyceride molecules are hydrolysed by pancreatic lipase into monoglycerides, glycerol, and fatty acids [110].

Pancreatic lipase prefers to attack the ester bond at position sn-1 producing, 2, 3-diacylglycerol and free fatty acids, then the lipase attacks the ester bond at position sn-3, producing 2-monoacylglycerol and free acid [125, 126]. The digestion of triglycerides, cholesterol ester, and phospholipids in the small intestine by their digestive enzymes is controlled by two hormones: cholecystokinin (CCK) and secretin. Cholesterol ester is hydrolysed by the action of pancreatic enzyme cholesterol esterase into free cholesterol and free fatty acids which are absorbed in their free form. Phospholipids are hydrolysed by two pancreatic enzymes: phospholipase A_1 (PLA1) and phospholipase A_2 (PLA2). PLA2 is initially secreted as an inactive form (zymogen) and then activated by trypsin. It releases fatty acid at C_2 position of the phospholipid, producing a lysophospholipid. PLA 1 releases the fatty acid at C_1 position of lysophospholipid, producing a glycerophosphoryl base which may then be excreted in faeces or undergo further hydrolysis and absorption [23]. The products resulting from dietary fat hydrolysis are absorbed in the form of mixed micelles by the brush-border membrane of mucosal cells in the small intestine [23].

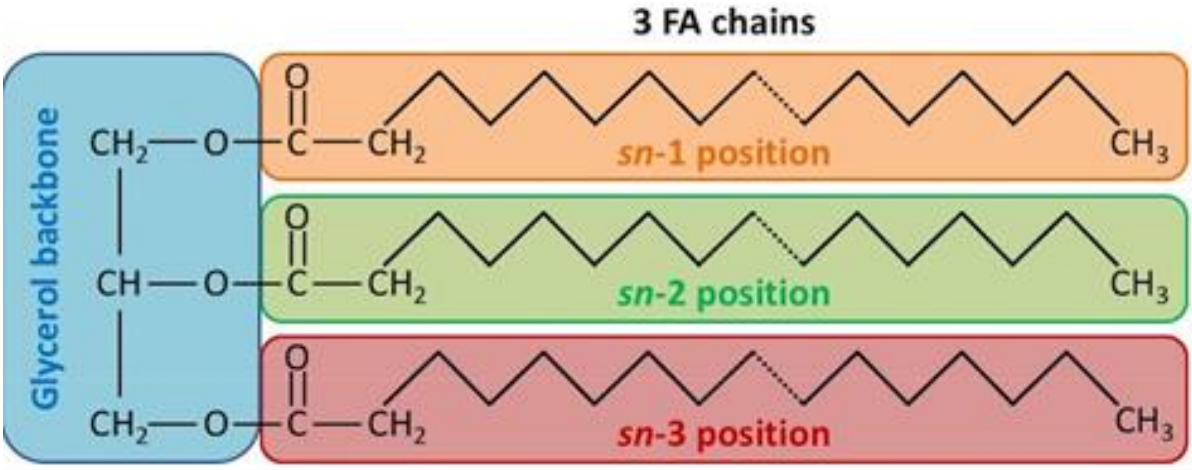

Figure 2.1. Schematic picture of a triglyceride molecule shows the glycerol backbone, fatty acid (FA) chains, and stereospecific numbering (*sn*) of carbon atoms. Adapted from Alfieri et al., (2018) [127].

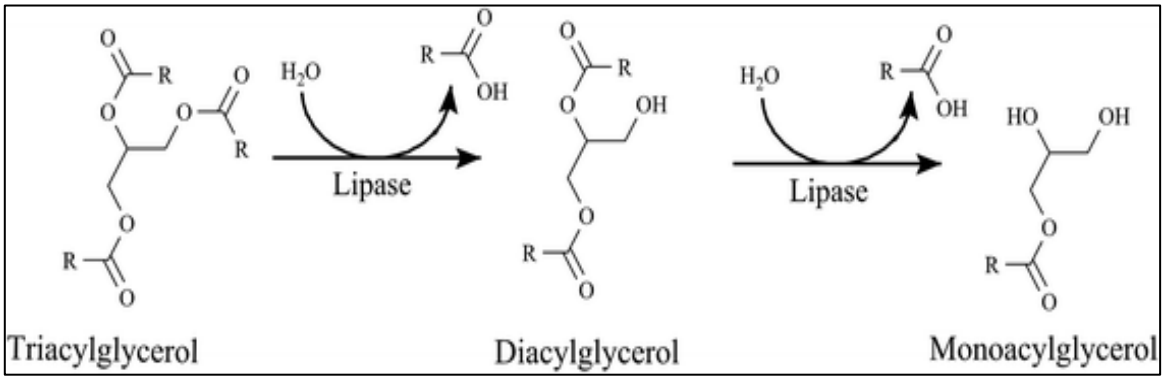

Figure 2.2. Schematic representation for mechanism of triacylglycerol hydrolysis by lipase. Taken from Kumar & Dubey, (2015) [125].

Fatty acids consist of a hydrocarbon chain, which is hydrophobic, and a terminal carboxyl group. Although, the chain length of fatty acids may range from 4 to 24 carbons long, fatty acids with 18 carbons long are the most predominant fatty acids in food [128]. Depending on the number of carbon atoms, fatty acids can be classified into short, medium and long chain fatty acids. Short chain fatty acids (SCFAs) contain 2-4 carbon atoms. Medium chain fatty acids (MCFAs) are composed of 6-10 carbon atoms, while long chain fatty acids (LCFAs) consist of 12-26 carbon atoms. Furthermore, fatty acids can be divided depending on the presence or absence of double bond into saturated and unsaturated fatty acids. Saturated fatty acids contain only single bonds in

their structure and can pack closely to each other, hence triglycerides with saturated fatty acids are solid at room temperature. Unsaturated fatty acids may have one double bond (monounsaturated) or more (polyunsaturated). These unsaturated fatty acids lack the ability to arrange closely to each other, thus triglycerides with this kind of fatty acids tend to be liquid at the room temperature [128-131]. LCFAs are the major form of fatty acids present in food [16, 26]. MCFAs are infrequently present in food. However, short-chain fatty acids are not present in food, but they are the main anionic components present in the faeces. SCFAs are produced from the breakdown of undigested lipids by the action of bacteria in the colon. Therefore, the synthesis and absorption of SCFAs occur solely in the colon [16]. Polyunsaturated linoleic acid (omega-6 fatty acid) and linolenic acids (omega-3 fatty acid) are not synthesised from other substances in the human body and must be taken in the diet and therefore are known as essential fatty acids [128].

Both chain length and degree of unsaturation of fatty acid affect fat absorption and digestion [132, 133]. Triglyceride digestion starts in the stomach by the action of lingual and gastric lipases and continues in the small intestine by the action of pancreatic lipase. Lipases have great affinity to hydrolyse triglycerides containing medium-chain fatty acids (MCFAs) more rapidly than triglyceride containing long-chain fatty acids (LCFAs), producing two free fatty acids and 2-monoacylglyceride for each triglyceride molecule acted on [134]. Additionally, the absorption rate of unsaturated fatty acids and MCFAs is quicker than the absorption rate of LCFAs [132]. MCFAs, which are released from the hydrolysis of medium-chain triglycerides (MCTs) in the stomach by the action of gastric lipase, can be absorbed in the stomach [135]. Also, due to the solubility of these MCFAs in the aqueous phase of small intestine, these fatty acids can be absorbed bound to albumin and transported to the liver via the portal vein [136].

Digestion of long-chain triglycerides (LCTs) requires stimulation of the pancreas to secrete the hormone cholecystokinin (CCK) and the pancreatic enzymes. CCK stimulates the gallbladder to release further bile in order to enable the emulsion process in which the triglyceride macromolecules are broken down to smaller fat droplets to increase their digestion by pancreatic lipase. Individual LCFAs released from the digestion of LCT combine to form micelles. Then, the micelles either cross the intestinal brush border through passive diffusion or are transported by fatty acid transporters to enter the enterocyte. After that, the free fatty acids are transported to the endoplasmic reticulum where they are converted to triglycerides and packaged with lipoprotein, cholesterol and other lipids into chylomicrons. The chylomicrons, which are released by the

enterocyte into the intercellular space through exocytosis, enter and transport along the lymphatic system and finally flow into the subclavian vein to arrive the bloodstream. LCFAs are transported to the mitochondria through the carnitine carrier for consequent β-oxidation [133, 137, 138].

Unlike LCT digestion, the digestion of MCT is simple and rapid and does not require CCK for its digestion. Also, MCT does not require packaging or modification and can be absorbed bound to albumin through passive diffusion along the gastrointestinal tract into the portal vein. Additionally, MCT does not need the carnitine carrier [133, 137, 138].

2.3 Aims

The aims of this chapter are to:

- Study the inhibitory effect of different concentrations of alginate on pancreatic lipase activity in vitro using an improved version of the turbidity assay (Vogel & Zeive, 1963).

- Characterise chemical structures of alginates using proton nuclear magnatic resonance (^{1}H NMR) to investigate whether their content of guluronic (G) and mannuronic acids (M) affects their inhibitory properties.

2.4 Methods

2.4.1 Materials

Seven alginate samples (1LF80, 1N80, BG3600, BG3610, BG3700, BG3800 and BG3900) were kindly supplied by Ruitenberg, (The Netherlands), whereas alginate CC01 was provided by Coca-Cola, the UK. Lipase, colipase, Orlistat (Tetrahydrolipstatin, Ro-18-06-47, $C_{29}H_{53}NO_5$) citric acid ($C_6H_8O_7$), potassium hydroxide (KOH), phosphoric acid (orthophosphoric acid, H_3PO_4), boric acid (H_3BO_3), acetone (C_3H_6O), hydrochloric acid (HCl), bile acids, and taurodeoxycholate sodium salt were purchased from Sigma Aldrich (Poole, UK). Aluminium oxide (Al_2O_3) was purchased from Fisher Scientific (Loughborough, UK), and olive oil was purchased from a local supermarket (Cooperative Food, UK).

2.4.2 Lipase activity assay

Lipase activity was determined using an improved version of Vogel & Zieve (1963) [122]. In this method, the activity of lipase was assessed by measuring the reduction in turbidity due to the hydrolysis of triacylglycerol to monoacylglycerol and free fatty acids by the action of lipase. In this study, a natural substrate, olive oil, was used as a lipase control (did not contain Orlistat or alginate) whereas Orlistat and alginates were used as an inhibition control and inhibitors, respectively.

2.4.2.1 Preparation of the olive oil substrate

Olive oil was passed through aluminum oxide (8 cm deep in a 2 x 32 cm glass chromatography column) to remove free fatty acids present in the oil. Then, purified olive oil stock was prepared by mixing 10 g of the olive oil with 100 ml of acetone. Next, 1 ml of the 10% solution was diluted with 10 ml of acetone to form 1% (v/v) olive oil stock solution. This stock solution was stored at 4 ˚C and this stock solution was used for all experiments.

2.4.2.2 Preparation of the buffer diluent containing 0.35% of sodium taurodeoxycholate

Buffer diluent consisted of 0.033M citric acid ($C_6H_8O_{7)}$, 0.343M potassium hydroxide (KOH), 0.033M orthophosphoric acid (H_3PO_4, has a specific gravity: 1L= 1.69 Kg, MW 98, 95%), 0.033M boric acid (H_3BO_3), and 0.35% taurodeoxycholate sodium salt. The buffer diluent was titrated to pH 7.3 using 6M HCl. For use in the assay, 100 ml of buffer diluent was heated to 70 ˚C, and then 4 ml of 1% stock olive oil solution was added, giving a 0.04% (vol/vol) substrate solution. Next, the substrate/ buffer solution was homogenised with heating at 70 ˚C for 10 min. Finally, the solution was allowed to cool at room temperature, and it must be used within 6 h from the preparation.

2.4.2.3 Preparation of lipase, Orlistat, and alginate solution

Lipase in buffer diluent at a concentration of 1 mg/ml was prepared. Then, 60 µl of colipase was added to the lipase/buffer diluent solution and the mixture vortexed. 0.025 mg/ml of Orlistat in substrate solution was prepared. For alginate preparation, 12 ml of substrate/ buffer diluent solution was added to 60 mg of alginate, giving a 5 mg/ml alginate solution. Then, this alginate solution was homogenised for 2 minutes. After that, lower concentrations of alginate (0.125. 0.25, 0.5, 1.25, and 2.5 mg/ml) were prepared by diluting 5 mg/ml alginate/substrate solution with the appropriate volumes of the substrate/ buffer solution. The dilutions were carried out in 96-well microplate (Table 2.1).

Alginate concentration (mg/ml)	Volume of 5 mg/ml alginate in substrate solution	Volume of 5 mg/ml substrate in buffer diluent solution
5	240 µl	0 µl
2.5	120 µl	120 µl
1.25	60 µl	180 µl
0.5	24 µl	216 µl
0.25	12 µl	228 µl
0.125	6 µl	234 µl

Table 2.1. Preparation of alginate solutions by addition of stock solution with diluent.

2.4.2.4 Sample preincubation

Two 96-well microplates (Bio Tek, USA) were used for lipase activity assays. In plate 1, 10 µl of lipase solution (1mg/ml) and 10 µl of the buffer diluent solution (blank) were placed separately in triplicate. In plate 2, 240 µl of each substrate solution alone (as lipase control), alginate/substrate at concentrations 5, 2.5, 1.25, 0.5, 0.25, and 0.125 mg/ml, and Orlistat/substrate solution (as inhibition control) were placed separately in six wells. Both plates were incubated at 37 ˚C for 10 minutes. Then, 200 µl of the three solutions present in plate 2 was transferred to plate 1 containing 10 µl of both lipase and blank solutions as shown in Figure 2.3. Finally, plate 1 was placed in the reader where the optical density was read every 5 minutes at 405 nm for 55 minutes. In the assay, 10 µl of lipase solution (1mg/ml) was added to 200 µl of samples (substrate/buffer diluent solution, Orlistat/substrate solution, or alginate/substrate solution), hence, the final concentration of lipase in the assay would be 0.048 mg/ml based on the equation:$C_1 \times V_1 = C_2 \times V_2$, where C_1 is initial concentration of solution, V_1 is the initial volume of solution, whereas C_2 is final concentration of solution, and V_2 is final volume of solution. The final concentration of 200 µl of 5, 2.5, 1.25, 0.5, 0.25, and 0.125 mg/ml of alginate solution added to 10 µl of either lipase or blank solution would be 4.8, 2.4, 1.2, 0.47, 0.24, and 0.12 mg/ml, respectively. The final concentration of 200 µl of either 0.04% substrate or 0.025 mg/ml Orlistat added to 10 µl of either lipase or blank solution would be

0.38 mg/ml and 0.024 mg/ml, respectively. The lipase inhibition was calculated as follows:

Percentage of pancreatic lipase inhibition= 1- ((Inhibition Control - Polymer Sample) / (Inhibition Control- Lipase Control)) x 100

5mg/ml alginate solution	2.5mg/ml alginate solution	1.25mg/ml alginate solution	0.5mg/ml alginate solution	0.25 mg/ml alginate solution	0.125 mg/ml alginate solution	5 mg/ml substrate solution (lipase control)	5mg/ml Orlistat solution
200µl alginate solution + 10µl lipase	200µl alginate solution + 10µl lipase	200µl alginate solution + 10µl lipase	200µl alginate solution + 10µl lipase	200µl alginate solution + 10µl lipase	200µl alginate solution + 10µl lipase	200µl substrate solution + 10µl lipase	200µl Orlistat solution + 10µl lipase
200µl alginate solution + 10µl lipase	200µl alginate solution + 10µl lipase	200µl alginate solution + 10µl lipase	200µl alginate solution + 10µl lipase	200µl alginate solution + 10µl lipase	200µl alginate solution + 10µl lipase	200µl substrate solution + 10µl lipase	200µl Orlistat solution + 10µl lipase
200µl alginate solution + 10µl lipase	200µl alginate solution + 10µl lipase	200µl alginate solution + 10µl lipase	200µl alginate solution + 10µl lipase	200µl alginate solution + 10µl lipase	200µl alginate solution + 10µl lipase	200µl substrate solution + 10µl lipase	200µl Orlistat solution + 10µl lipase
200µl alginate solution + 10µl blank	200µl alginate solution + 10µl blank	200µl alginate solution + 10µl blank	200µl alginate solution + 10µl blank	200µl alginate solution + 10µl blank	200µl alginate solution + 10µl blank	200µl substrate solution + 10µl blank	200µl Orlistat solution + 10µl blank
200µl alginate solution + 10µl blank	200µl alginate solution + 10µl blank	200µl alginate solution + 10µl blank	200µl alginate solution + 10µl blank	200µl alginate solution + 10µl blank	200µl alginate solution + 10µl blank	200µl substrate solution + 10µl blank	200µl Orlistat solution + 10µl blank
200µl alginate solution + 10µl blank	200µl alginate solution + 10µl blank	200µl alginate solution + 10µl blank	200µl alginate solution + 10µl blank	200µl alginate solution + 10µl blank	200µl alginate solution + 10µl blank	200µl substrate solution + 10µl blank	200µl Orlistat solution + 10µl blank

Figure 2.3. Plate layout for lipase activity microplate assay.

2.4.3 Preparation of alginate for ^{1}H NMR neighbour analysis

In this study, three alginates (CC01, 1LF80, and 1N80) inhibited pancreatic lipase activity, therefore the composition and monomer sequence of these alginates were determined using ^{1}H NMR. 10 mg/ml of alginate solution was prepared by dissolving powdered alginate in DH_2O under the vortex produced by a magnetic stirrer to allow complete dissolution of all alginate in the solution. Then, the alginate solution was titrated to pH 2 using 6 M HCl and incubated at 100 ^{o}C for 2-4 hours. Next, the alginate solution was neutralised to pH 7 using 1 M KOH. After that, aliquots of 1ml of the alginate solution were put in Eppendorf covered with plastic parafilm with holes to allow release of vapour, and frozen overnight at -20^{o}C. Finally, the frozen alginate samples were placed in the freeze dryer which enables them to be dried under a vacuum without passing through the liquid phase. The dried alginate samples were analysed using ^{1}H NMR to determine the chemical structure and sequence of the different alginates from the integrated intensities of the signals A (G, proton1), B1 (G<u>G</u>M, proton 5), B2 (M<u>G</u>M, proton 5), B3 (<u>M</u>G, proton 1), B4 (<u>M</u>M, proton 1) and C (<u>G</u>G, proton 5) (Figure 2.4 and Table 2.2).

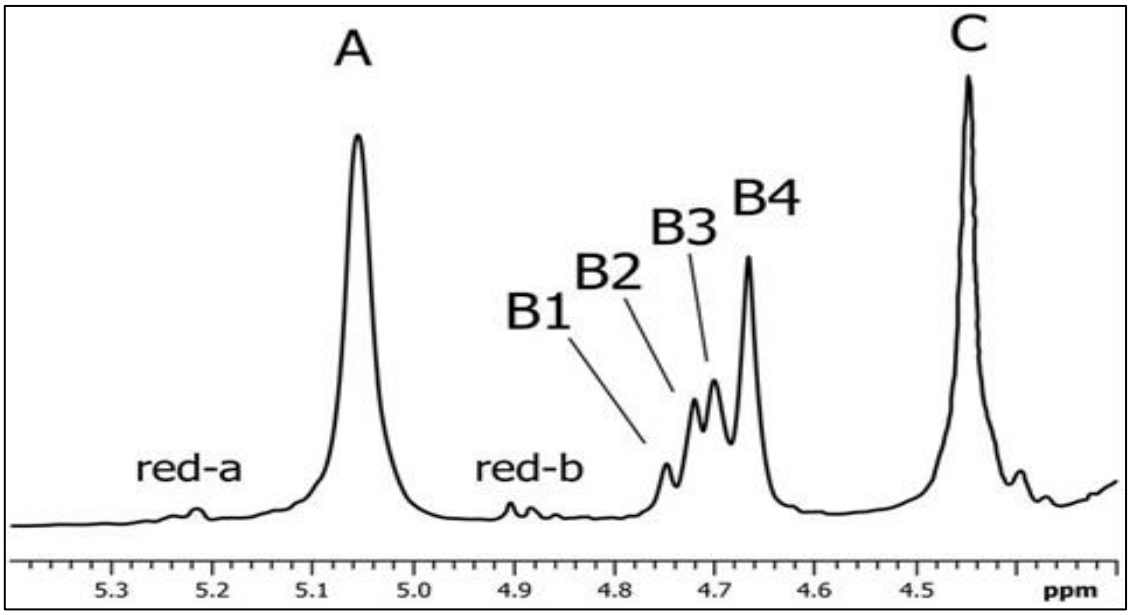

Figure 2.4. The Region of ^{1}H NMR Spectrum of Alginate used for Quantitative Analysis. Adapted from ASTM International Designation: F2259-10 (Reapproved 2012).

Alginate sequence	Equation
Guluronate (G)	G= 0.5 (A+ C+ 0.5(B1+ B2+ B3))
Mannuronate (M)	M= B4+ 0.5 (B1+ B2+ B3)
Guluronate dimers (GG)	GG= 0.5 (A+ C- 0.5 (B1+ B2+ B3))
Uronate dimer consisting of guluronate and mannuronate residues (GM)	GM= MG= 0.5 (B1+ B2+ B3)
Mannuronate (MM)	MM= B4
Uronate trimer consisting of two guluronates and mannuronate residues (GGM)	GGM= MGG= (B1) 0.5 (B1+ B2+ B3)/ (B1+B2)
Uronate trimer consisting of guluronate and two mannuronates residues (MGM)	MGM= (B2) 0.5 (B1+ B2+ B3)/ (B1+B2)
Guluronate trimers (GGG)	GGG= GG-GGM
Fraction of guluronate (F_G)	F_G = G/ (M+ G)
Fraction of mannuronate (F_M)	F_M = M/ (M+ G)
Fraction of guluronate dimers (F_{GG})	F_{GG} = GG/ (M+ G)
Fraction of mannuronate dimes (F_{MM})	F_{MM} = MM/ (M+ G)
Fraction of uronate dimer consisting of guluronate and mannuronate residues (F_{GM})	F_{GM} = F_{MG} = MG/ (M+ G)
Fraction of guluronate trimers (F_{GGG})	F_{GGG} = GGG/ (M+ G)
Fraction of uronate trimer consisting of two guluronates and one mannuronate residue (F_{GGM})	F_{GGM} = F_{MGG} = GGM/ (M+ G)
Fraction of uronate trimer consisting of one guluronate and two mannuronates residues (F_{GMM})	F_{GMM} = MGM/ (M+ G)
An average length of blocks of consecutive G monomers N (G> 1)	N (G> 1) = (F_G- F_{MGM})/ F_{GGM}

Table 2.2. Equations used for calculation of alginate content of guluronate (G), mannuronate (M), guluronate dimers (GG), uronate dimers consisting of guluronate and mannuronate residues (GM), mannuronate (MM), uronate trimer consisting of two guluronates and one mannuronate residues (GGM), uronate trimer consisting of one guluronate and two mannuronates residues (GMM), guluronate trimers (GGG), fraction of guluronate dimers (FG), fraction of mannuronate (FM), fraction of guluronate dimers (FGG), fraction of mannuronate dimers (FMM), fraction of uronate dimers consisting of guluronate and mannuronate residues (FGM), fraction of guluronate trimers (FGGG). Adapted from ASTM International Designation: F2259-10 (Reapproved 2012).

2.5 Statistical analysis

GraphPad Prism 7 statistical software was used to evaluate pancreatic lipase activity with olive oil (lipase control) versus the activity of pancreatic lipase with olive oil plus either Orlistat or different concentrations of alginates. One-way ANOVA (ordinary) followed by a post-hoc Dunnett's test was performed, and significance was taken at $P<0.05$. Two-way ANOVA followed by a post-hoc Bonferroni's test was used to compare inhibition level caused by different alginates at different concentrations. The data were analysed by calculating means, standard deviation (SD), and a Student's t-test (unpaired t- test) for the samples of the lipase assay. Each measurement used at least three replicates. The exact number of replicates is described in each figure legend.

2.6 Results

2.6.1 Orlistat inhibition of lipase activity

In control conditions, absorbance plotted against time had a negative slope and Spearman's rank correlation coefficient r_s= - 0.99 (P<0.0001), indicating an inverse relationship between time and absorbance (Figure 2.5). The significant decrease in absorbance of olive oil over time demonstrates that the triglycerides are being hydrolysed by lipase to monoacyglycerol and free fatty acids. However, an inhibition control (lipase plus olive oil plus Orlistat 0.025 mg/ml) showed a negligible decrease in absorbance over time where the absorbance changed from 0.42 to 0.40 over 50 minutes (r_s= - 0.98, P<0.0001).

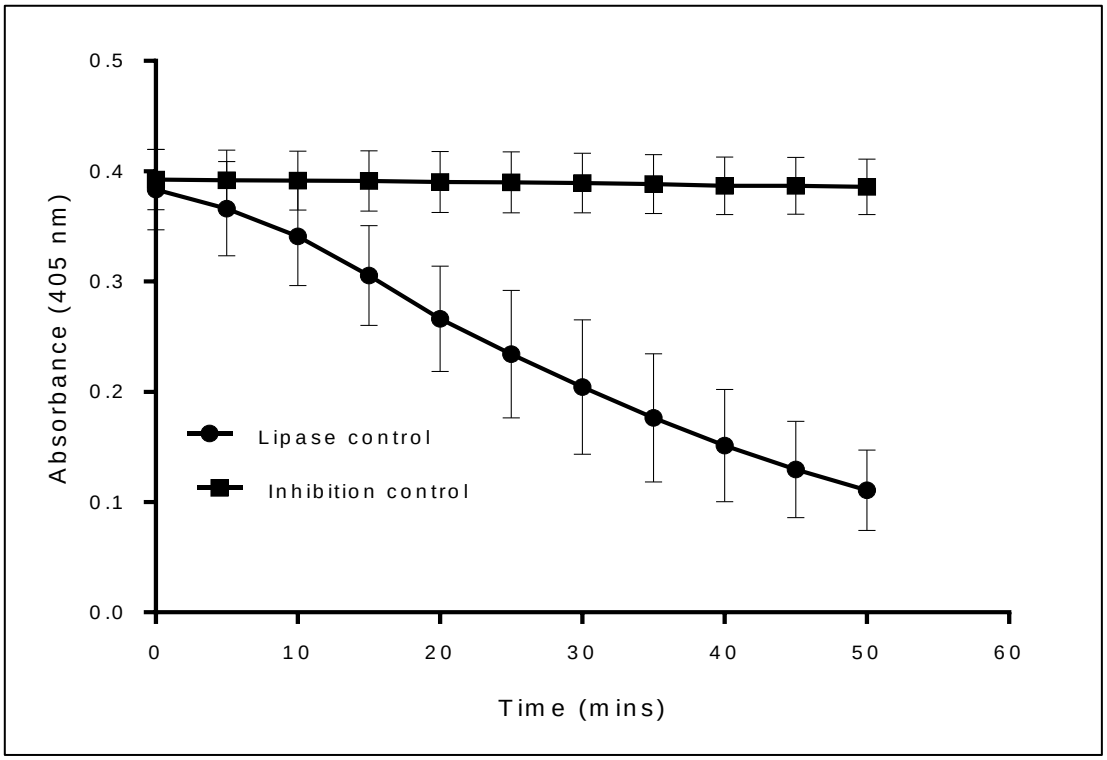

Figure 2.5. Change in absorbance over time in lipase activity assay. The change in absorbance at 405 nm over time (0-50 minutes) for lipase control (lipase plus olive oil) and an inhibition control (lipase plus olive oil plus 0.025 mg/ml Orlistat). Values are mean ± SD (n=6).

2.6.2 Alginate inhibition of lipase activity

Initially, the inhibitory effects of seven alginate samples at concentrations 4.8 and 1.2 mg/ml on lipase activity were investigated. The data presented in Table 2.3 showed that all alginate samples at 4.8 mg/ml could significantly inhibit pancreatic lipase activity ($p < 0.05$) with different levels of inhibition. However, among these alginates, CC01, 1N80 and 1LF80 had the highest inhibitory effects where they reduced lipase activity by 77.5 (±8.4), 73 (±3.02), and 68.9 (±0.92) %, respectively. Moreover, although all alginates at 1.2 mg/ml reduced lipase activity with different levels of inhibition, only CC01 and 1N80 had significant inhibitory effects on pancreatic lipase activity with P values less than 0.05.

Alginate	Lipase inhibition (%)					
	1.2 mg/ml			4.8 mg/ml		
	Inhibition (%)	P value	Significance	Inhibition (%)	P value	Significance
CC01	37.5 (±14.0)	0.002	**	77.5(±8.3)	0.0001	****
1N80	24.6 (±12.0)	0.002	**	73 (±3.0)	0.0001	****
1LF80	20.1 (±18.3)	0.227	ns	68.9 (±0.92)	0.0001	****
BG3600	11.4 (±13.0)	0.546	ns	56.3 (±13.6)	0.0001	***
BG3610	12.02 (±8.2)	0.058	ns	22.7 (±2.8)	0.0004	***
BG3700	14.3 (±7.4)	0.152	ns	43.5 (±6.96)	0.0001	****
BG3800	10.2 (±8.2)	0.188	ns	22.1 (±9.8)	0.0042	**
BG3900	17.6 (±13.8)	0.062	ns	58.9 (±4.5)	0.0001	****

Table 2.3. Concentration dependent inhibition of lipase by alginates.Values are mean % inhibition and the error bars are the standard deviation of three replicates (± SD, n=3), P values < 0.05 are represented by *, <0.005 are represented by **, <0.001 are represented by ***, and <0.0005 are represented by ****. Non-significant difference (P>0.05) is represented by ns. The substrate was prepared by diluting 1% (vol/vol) purified olive oil in acetone with buffer diluent to 0.04% (vol/vol).

2.6.3 Concentration dependence of lipase inhibition by alginate

Previous data of alginate's effects on pancreatic lipase activity showed that CC01, 1LF80 and 1N80 at 4.8 mg/ml had the greatest inhibitory effects. Therefore, the lipase activity assays in the presence of these three alginates at six different concentrations were repeated to investigate whether concentration influences the inhibitory effect and to determine concentration of alginate at which 50% of pancreatic lipase activity is inhibited (IC_{50}).

As seen in Figure 2.6 (graph A) CC01 alginate significantly inhibited pancreatic lipase activity ($P<0.05$) by 75.6 (± 10.6) %, 37.6 (± 11.5) % and 16.1 (± 9.4) %, at 4.8, 2.4, and 1.2 mg/ml, respectively, however, CC01 did not show a significant reduction in lipase activity at concentrations less than 1.2 mg/ml.

The activity of pancreatic lipase in the presence of 4.8 and 2.4 mg/ml of alginate 1N80 was significantly reduced by 62.7 (± 20) % and 22.7 (± 4.1) % with P values less than 0.05, respectively (Figure 2.6, graph B). 1LF80 significantly decreased lipase activity by 53.7 (± 8.5) % ($P<0.05$) at 4.8 mg/ml and by 20.3 (±1.1) % at 2.4 mg/ml (Figure 2.6, graph C). Also, no significant reduction in lipase activity was seen in the presence of either 1N80 or 1LF80 at concentrations below 2.4 mg/ml ($P>0.05$).

Figure 2.7 shows the correlation (Pearson's R) between inhibition level of lipase and CC01, 1N80 and 1LF80 alginates at different concentrations (0.12-2.4 mg/ml). Pearson's correlation coefficient values for CC01, 1LF80 and 1N80 were 0.99, 0.98 and 0.99 with P values of 0.0001, 0.0005, and 0.0001, respectively, indicating a robust positive relationship between inhibition level of lipase and alginate concentration. Inhibition of lipase by CC01 alginate was dose dependent as increasing alginate concentration twofold either from 1.2 to 2.4 mg/ml or from 2.4 to 4.8 mg/ml caused a significant increase in lipase inhibition level by 21.6% ($P<0.001$) and 38 % ($P<0.0001$), respectively. Also, a significant increase by 60% ($P<0.0001$) in inhibition level of lipase was observed when CC01concentration was increased by four times from 1.2 to 4.8 mg/ml (Figure 2.6, graph A). Moreover, although lipase inhibition by 1N80 looks to be dose dependent from 1.2 mg/ml, inhibition was only significant ($P< 0.05$) at concentrations 2.4 and 4.8 mg/ml. A significant increase in inhibition of lipase by 17.8 % ($P<0.03$) and 40.03% ($P<0.0001$) was seen upon doubling 1N80 concentration from 1.2 to 2.4 mg/ml or 2.4 to 4.8 mg/ml, respectively.

Additionally, increasing 1N80 concentration by fourfold from 1.2 to 4.8 mg/ml a significantly increased inhibition of lipase by 57.8% ($P<0.0001$) (Figure 2.6, graph B). Further, lipase inhibition by 1LF80 was dose dependent from 2.4 mg/ml where there was a significant increase in lipase inhibition by 19.7% ($P<0.009$) and 33.3% when the 1LF80 concentration was increased twofold from 1.2 to 2.4 mg/ml or from 2.4 to 4.8 mg/ml, respectively. Also, increasing 1LF80 concentration four times, from 1.2 to 4.8 mg/ml, caused a significant reduction by 53% ($P<0.0001$) in lipase activity (Figure 2.6, graph C).

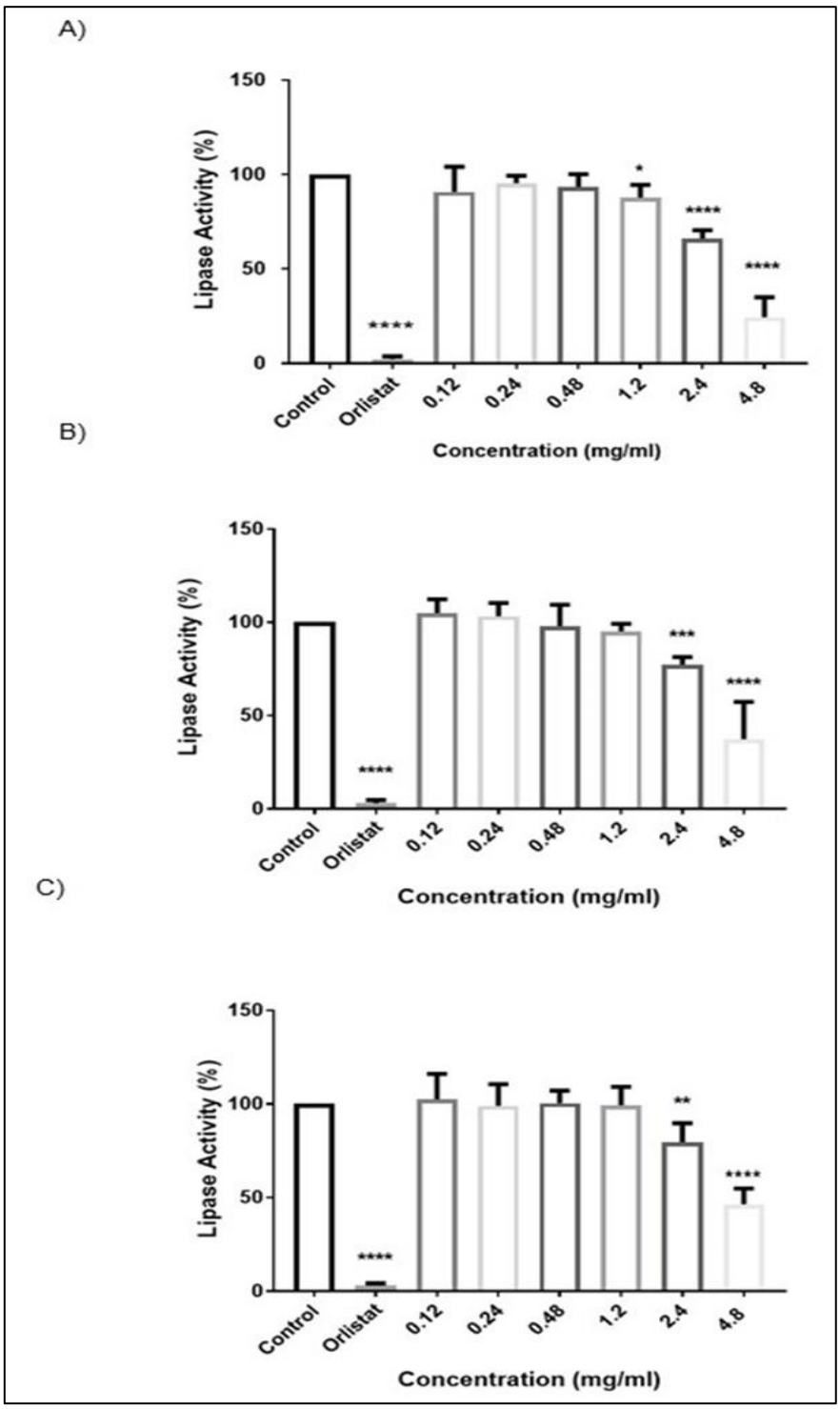

Figure 2.6. Concentration dependent inhibition of lipase by three alginates: (A) CC01, (B) 1N80 and (C) 1LF80. Lipase activity (%) for olive oil alone (control), olive oil with different concentrations of alginate, and olive oil with Orlistat were measured at 35 minutes where the reaction at this time point was still close to the linear phase. Values are percentage lipase activity and the error bars are the standard deviation of six replicates (± SD, n=6), P values < 0.05 are represented by *, <0.005 are represented by **, <0.001 are represented by ***, and <0.0005 are represented by ****. The absorbance was read at 405 nm every 5 min for 55 minutes.

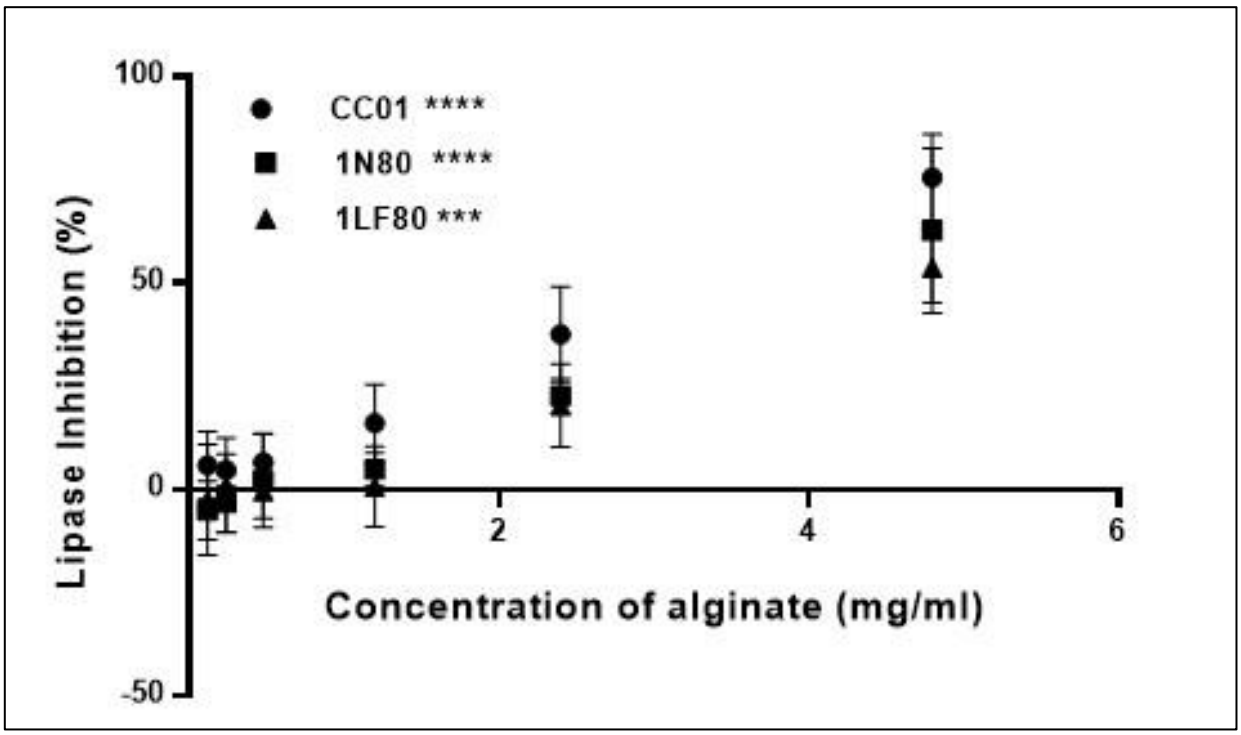

Figure 2.7. Correlation between inhibition of lipase and alginates concentrations. A significant positive correlation (P<0.05) existed between lipase inhibition level and alginate concentration with Pearson's R values of 0.99, 0.98 and 0.99 for CC01, 1LF8 and 1N80 alginates, respectively. Values are shown as mean ± SD (*n*=6). P values, <0.001 are represented by ***, and <0.0005 are represented by ****. Calculated from data presented in figure 2.6.

Two-way ANOVA analysis followed by a post-hoc Bonferroni's test indicated that CC01 reduced pancreatic lipase activity more than 1N80 and 1LF80 at all concentrations (0.12-4.8 mg/ml), however, the difference in inhibition in lipase activity was significant (P<0.05) between CC01 and 1LF80 at concentrations 1.2, 2.4, and 4.8 mg/ml, whereas the difference in inhibition level of lipase caused by either CC01 or 1N80 was significant only at 2.4 mg/ml (Figure 2.8).

Although there were significant differences in inhibition levels among different concentrations where all the three alginates (CC01, 1N80 and 1LF80) at concentrations 4.8 and 2.4 mg/ml reduced lipase activity more than the other concentrations with P<0.05, CC01 was the only alginate that significantly inhibited pancreatic lipase activity at 1.25 mg/ml and the inhibition of lipase by alginate was dose dependent. Orlistat significantly reduced lipase activities in all experiments with *P* equal to 0.0001.

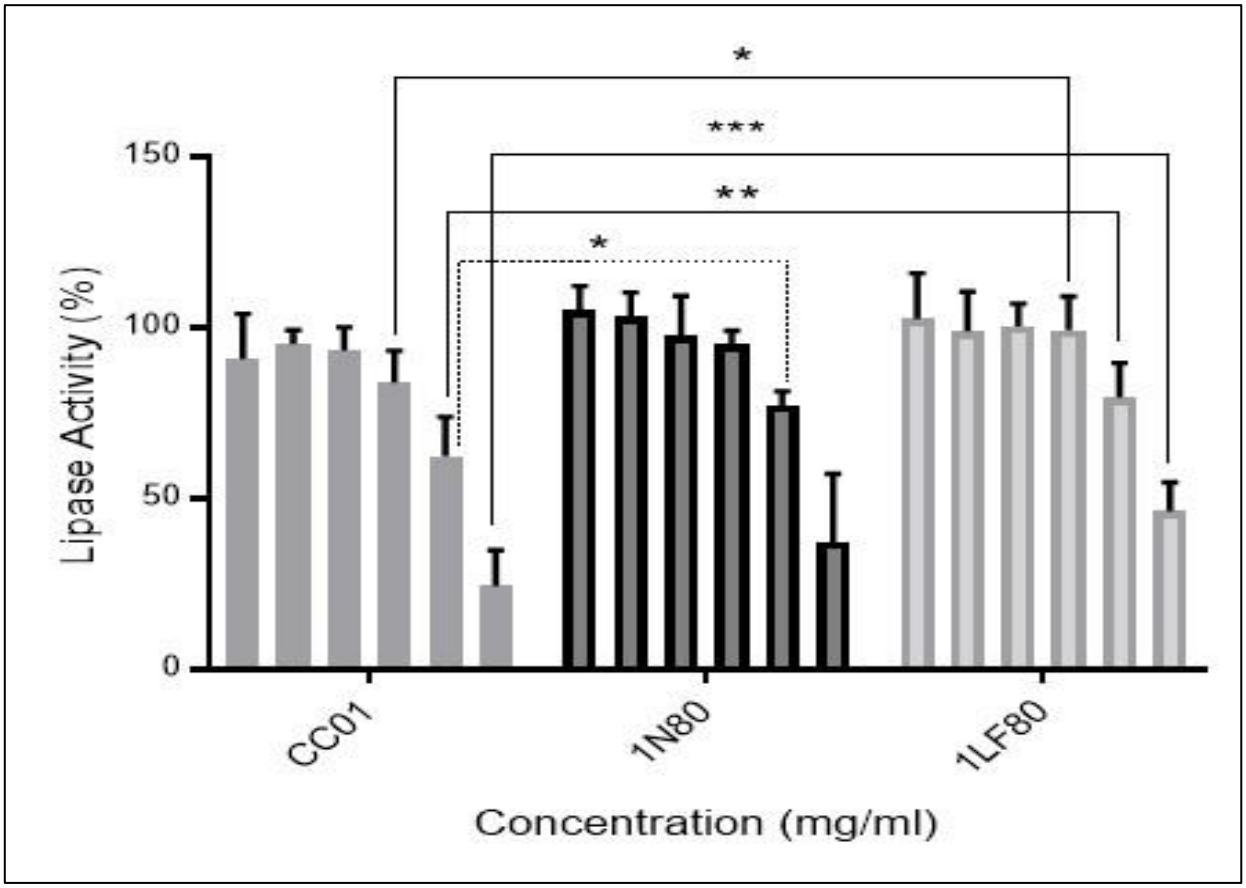

Figure 2.8. Concentration dependent inhibition of lipase caused by alginates. Three alginates CC01, 1N80 and 1LF80 at different concentrations (0.12-4.8 mg/ml)from left to right on the x-axis were used. The values are mean % inhibition and the error bars are the standard deviation of six replicates (± SD, *n*=6), P values < 0.05 are represented by *, <0.005 are represented by **, and <0.001 are represented by ***. In the assay, concentrations of lipase and substrate were 0.048 and 0.38 mg/ml, respectively. Combined data from figure 2.6 to compare inhibition level caused by different alginates at different concentrations.

Data from IC_{50} measurements shows that concentration of CC01 alginate required to reduce lipase activity by 50% was lower than those of 1N80 and 1LF80, suggesting that CC01 is a more potent inhibitor than either 1N80 or 1LF80. This variation in IC_{50} values could be due to alginate structure or source (Table 2.4).

Alginate	IC_{50} (mg/ml)	Standard deviation
CC01	3.02	(±0.25)
1N80	4.06	(±0.23)
1LF80	4.65	(±0.67)

Table 2.4. IC_{50} measurement for alginates CC01, 1N80 and 1LF80. Values are mean and standard deviation (± SD); *n*=6.

2.6.4 Characterisation of the alginates by ^{1}H NMR

CC01, 1LF80 and 1N80 alginates inhibited lipase activity with different levels of inhibition at the same tested concentrations, and the difference in inhibition levels may be associated with their chemical structure. Therefore, ^{1}H NMR neighbour analysis was used to analyse the alginate structure and determine their content of guluronate (G) and mannuronate (M) monomers.

Data shown in Table 2.5 demonstrated that among three alginates, CC01 has the highest content of guluronate F(G), guluronate dimers F(GG), and guluronate trimers F(GGG) and the lowest content of mannuronate F(M) and mannuronate dimers F(MM). 1N80 alginate contains more F(G), F(GG), and F(GGG) than 1LF80, while its content of mannuronate and mannuronate dimers is higher than CC01, but lower than 1LF80. Alginate 1LF80 has the lowest fractions of G, GG, and GGG, and the highest fractions of mannuronate and mannuronate dimers. Moreover, 1H NMR data showed that among the three alginates, CC01 has the highest average length of blocks of consecutive G monomers (N (G>1) =21.5), which is about three times higher than that in 1N80, and 20 times higher than the lowest one in 1LF80.

Both ^{1}H NMR spectrum of alginates (CC01, 1N80 and 1LF80) used for quantitative analysis, and the manual integrated intensities of the signals A (G, proton1), B1 (G<u>G</u>M, proton 5), B2 (M<u>G</u>M, proton 5), B3 (<u>M</u>G, proton 1), B4 (<u>M</u>M, proton 1) and C (<u>G</u>G, proton 5) are available in the appendix 2.

Alginate	F_G	F_M	F_{GG}	F_{MM}	F_{GM}	F_{GGG}	F_{GGM}	F_{GMM}	$N_{G>1}$	Ratio M/G
CC01	0.81	0.19	0.73	0.12	0.07	0.70	0.04	0.04	21.5	0.24
1LF80	0.43	0.57	0.21	0.34	0.23	0.13	0.10	0.13	1.05	1.30
1N80	0.56	0.45	0.40	0.29	0.16	0.33	0.07	0.095	6.6	0.80

Table 2.5. Codes and molecular characteristic for CC01, 1N80 and 1LF80 alginates used in this study. F(G) is the fraction of guluronate, F(GG) is the fraction of guluronate dimers, F(GGG) guluronate trimers. F(M) and F(MM) are the fractions of mannuronate and mannuronate dimers, respectively. F(GM) is the fraction of uronate dimer consisting of guluronate and mannuronate residues, and F(GGM) the fraction of uronate trimer consisting of two guluronates and one mannuronate residues. F(GMM) the fraction of uronate trimer consisting of one guluronate and two mannuronates residues. N (G>1) is the average length of blocks of consecutive G monomers.

Table 2.6 shows the correlation between IC_{50} of CC01, 1N80 and 1LF0 alginates and their contents and sequence of G, GG, GGG, M, MM, GM, GGM, and NG>1. Pearson's correlation coefficients showed a significant negative relationship ($P<0.05$) between alginate IC_{50} and content of G, GG, and GGG where the more G, GG, and GGG residues, the lower the IC_{50}, and the more potent inhibitor it is. Furthermore, Pearson's correlation coefficients showed a positive relationship between alginate fraction of M block and IC_{50} where the higher amount of M blocks, the greater the IC_{50}, and the weaker inhibitor it is. However, there was no significant correlation between alginate content of MM, GM, and GGM residues. Also, N (G>1), which is the average length of blocks of consecutive G monomers, had no effect on IC_{50} values.

Alginate Characteristic	IC_{50}			Pearson coefficient	P value	Significant
	CC01	1N80	1LF80			
F(G)	3.02(±0.25)	4.06(±0.23)	4.65(±0.67)	-0.99	0.014	*
F(GG)	3.02(±0.25)	4.06(±0.23)	4.65(±0.67)	-1	0.002	**
F(GGG)	3.02(±0.25)	4.06(±0.23)	4.65(±0.67)	-0.99	0.014	*
F(M)	3.02(±0.25)	4.06(±0.23)	4.65(±0.67)	0.99	0.032	*
F(MM)	3.02(±0.25)	4.06(±0.23)	4.65(±0.67)	0.78	0.434	ns
F(GM)	3.02(±0.25)	4.06(±0.23)	4.65(±0.67)	0.99	0.054	ns
F(GGM)	3.02(±0.25)	4.06(±0.23)	4.65(±0.67)	0.98	0.100	ns
NG>1	3.02(±0.25)	4.06(±0.23)	4.65(±0.67)	-0.99	0.063	ns

Table 2.6. The chemical features and mean IC_{50} vlaues of CC01, 1N80 and 1LF80 alginates. Pearson's correlation coefficients, P value, and whether the correlation is significant ($P<0.05$) or not significant (ns). FG is the fraction of guluronate, F(GG) is the fraction of guluronate dimers, F(GGG) guluronate trimers. F(M) and F(MM) are the fractions of mannuronate and mannuronate dimers, respectively. F(GM) is the fraction of uronate dimer consisting of guluronate and mannuronate residues, and F(GGM) the fraction of uronate trimer consisting of two guluronates and one mannuronate residues. F(GMM) the fraction of uronate trimer consisting of one guluronate and two mannuronates residues. N (G>1) is the average length of blocks of consecutive G monomers. P values < 0.05 are represented by *, <0.005 are represented by **, whereas P values >0.05 are represented by ns (Non-significant difference). IC_{50} values are mean ± SD, n=6.

2.7 Discussion

Data from the pancreatic lipase activity assay showed a strong reduction in the turbidity of lipase control (olive oil plus lipase) over time in contrast to olive oil treated with Orlistat (an inhibition control) which showed only a slight decrease in turbidity of over time, indicating that Orlistat is a potent inhibitor for lipase.

Also, the data available here indicated that all the alginates used reduced pancreatic lipase activity *in vitro*, showing that alginates could be used as pancreatic lipase inhibitors. This finding is supported by previous findings from Wilcox et al. (2014) in which the activity of pancreatic lipase with a synthetic substrate, DGGR, and natural substrate, olive oil, in the presence of alginate was assessed using colourimetric and turbidimeteric assays. Wilcox and his colleagues found that alginate reduced pancreatic lipase activity *in vitro* by 72.2% and 58% with DGGR and olive oil as substrates, respectively [72].

Furthermore, the data presented here showed that at the same concentration different alginates inhibited pancreatic lipase activity with varying degrees of inhibition. CC01, 1N80, and 1LF80 alginates had the most potent inhibitory effects compared with other alginates. This variation in reduction of the level of lipase activity could be attributed to alginate source or structure. Wilcox et al. (2014) reported that alginate isolated from *Laminaria hyperborea* caused a greater reduction in pancreatic lipase activity *in vitro* than alginate isolated from *Lessonia nigrescence* seaweed, showing that the type of seaweed from which alginate is extracted might influence inhibition properties of alginate [72]. However, in this work, the impact of alginate source on alginate inhibitory effect could not be assessed since no data are available about the source of alginates used here.

^{1}HNMR analysis for CC01, 1N80 and 1LF80 alginates showed that CC01 had the highest fractions of guluronate, guluronate dimers, guluronate trimers (F[GGG=0.70], and the lowest fractions of mannuronate, suggesting that the highest inhibitory effect of CC01 on lipase activity compared with other alginates could be explained by its high content of G, GG, and GGG residues. Previous studies by Taylor et al (2005) indicated that alginate rich in G units was able to bind to the protein part of mucin, whereas alginate containing high amounts of M units was unable to bind with the protein part of mucin, showing that the G blocks were essential for alginate-protein binding [139].1LF80 alginate had the lowest fraction of guluronate, guluronate dimers, and guluronate

trimers, and the highest fraction of mannuronate residues, hence, its content of M residues could account for its low inhibitory effect compared with CC01 and 1N80.

The high content of G, GG, and GGG residues in CC01 could also provide a reasonable explanation for relative lower IC_{50} value compared with those of 1N80 and 1LF80 especially that Pearson's coefficients indicated a significant negative correlation ($P<0.05$) between IC_{50} values and alginate content of G, GG, and GGG units, however, there was a significant positive correlation ($P<0.05$) between IC_{50} values and alginate content of M block, providing a reasonable explanation for the highest IC_{50} value of 1LF80 which has the greatest content of M residues compared with CC01 and 1N80. This finding is consistent with Wilcox et al's study (2014) which showed that alginate rich in G, GG, GGG residues inhibited pancreatic lipase activity *in vitro* more than alginate rich in M, MM residues, demonstrating a positive correlation between alginate content of G block and inhibition level. Hence, the activity of pancreatic lipase can be modulated to a varying level based on the alginate used.

Furthermore, the data presented here showed a significant positive correlation ($P<0.05$) between alginate concentration and inhibition level of lipase. This finding is also in agreement with Wilcox et al's study (2014) which showed that increasing lipase inhibition by alginate was concentration dependent [72]. In the study, Wilcox and his colleagues studied the impact of alginate concentration on lipase activity using a modified version of a turbidimetric assay (Vogel & Zeive, 1963) and olive oil as a substrate, the same as used in this study. They found that increasing concentration of LFR5/60 alginate from 0.21 to 0.86 mg/ml and from 0.86 mg/ml to 3.43 mg/ml increased inhibition level of lipase by 1.7-fold and 2.3-fold, respectively. They also found the same effect where inhibition level of lipase increased by100.0%, 76.4%, and 85% when the concentration of SF120, SF/LF, and SF200 alginates was increased four-fold in concentration from 0.21 to 0.86 mg/ml, respectively [72].

Inhibitory capacity of alginate is not limited to pancreatic lipase activity since earlier *in vitro* studies found that some alginates could reduce pepsin activity by 52% [107] and by 53.9% [108]. Also, alginates are not the only dietary fibres which reduce pancreatic lipase activity, as *in vitro* data from a microplate assay conducted by Wilcox, (2010) showed that pectin also had the ability to diminish pancreatic lipase activity by 24.7 (±6.3) %, and the inhibition level of lipase by pectin was based on the esterification degree of pectin [140]. The findings of Wilcox (2010) are consistent with those

of Isaksson et al [141]. Isaksson and his colleagues investigated the activity of pancreatic lipase in a synthetic buffer solution and human pancreatic juice following *in vitro* incubation with pectin of low methyl ester (LM pectin) and pectin with high methyl ester (HM pectin). They found that both LM pectin and HM pectin had the ability to reduce pancreatic lipase activity in a synthetic buffer solution and human duodenal juice *in vitro*, however, pectin inhibitory effect was greater in the human pancreatic juice. The same authors stated that the capacity of pectin to inhibit pancreatic lipase activity is related to its level of esterification. Moreover, Isaksson et al. (1983) stated that feeding rats with diet containing 5% pectin raised fat content in ileostomy effluent samples, proposing that pectin might reduce fat digestion [142].

Several mechanisms for lipase inhibition by alginate have been proposed. Alginates have the affinity to bind to both the substrate and the enzyme. In 2005, Taylor and her colleagues reported that rheological studies on various mixtures of mucin: alginate showed an intermolecular interaction between mucin (glycoprotein) and alginate [139]. Mucin is an amphoteric polymer, whereas alginate is negatively charged polymer, therefore, some charge-charge interactions may occur between mucin and alginate, also, hydrogen bonding may be involved in mucin-alginate interaction [143]. Taylor and her colleagues reported that alginate rich in G units has the ability to bind to mucin at particular positions along the protein backbone of the mucin, linking several mucin molecules together and producing a gel.

Kumar and Chauhan (2010) stated that pectin (pectin: lipase, 2:1) with a high degree of esterification (approximately 53%) reduced lipase activity by 82%, and this level of inhibition is rather similar to that produced by Orlistat (Orlistat: lipase, 1:1 ratio) which was 88%. Additionally, Kumar & Chauhan (2010) reported that pectin does not only bind to the substrate, but it can form a complex with the enzyme, resulting in protonation of serine and histidine residues in the active site [144]. However, there was limited information available about the substrate concentration and the units used for lipase activity in that study. In contrast, Wilcox et al. (personal communication) showed that when olive oil was used as a substrate to assess the activity of pancreatic lipase (3.4 U/ml) in the presence of 3.8 mg/ml of a commercial pectin with a level of esterification equal to 60%, the pectin reduced pancreatic lipase activity only by 11% [72]. It has been suggested that pectin inhibits pancreatic lipase activity through protonation of –OH groups of a serine residue in the active site of lipase by the carboxyl groups [144]. Since the carboxyl groups in the guluonate residues of alginate are located at a similar position to the carboxyl groups in pectin, these carboxyl

groups may interact with the pancreatic lipase, forming an alginate-lipase complex, and protonate the serine residues at the enzyme active site, subsequently, pancreatic lipase activity will be reduced (Figure 2.9) [72].

Both α-D-(1→4) polygalacturonate chains in low-methoxy (LM) pectin and α-L-(1→4) polyguluronate chains in alginate show specific binding ability for calcium ions due to the electrostatic interaction between Ca^{2+} and galacturonate and guluronate blocks of pectin and alginate, respectively, resulting in a gel formation. Both alginate and pectin show the same mechanism for binding Ca^{2+} due to the similarity in their structures, and the resulting structure from the interaction between the Ca^{2+} and pectin or alginate can be described as "egg-box" model (Figure 2.10). These α-(1→4) polyuronates in pectin (polygalactouronate) and alginate (polyguluronate) offer tetradentate binding sites (cavities) for Ca^{2+}. These cavities are produced from intermolecular interaction between chains of two uronate residues due to an electrostatic and ionic bonding of their carboxyl groups, producing a structure similar to the "egg box". The calcium ions then will fit in the cavities through the electrostatic interaction between calcium ions and oxygen of carboxylate, the ring, in glyosidic bond, and the -OH group of the subsequent residue [145-147]. These similarities in calcium binding further demonstrate the close agreement in -COO□ group orientation between alginate and pectin.

In pectin, the carboxyl groups are present at the site where the methyl groups are added by ester bonds though an esterification process. Increasing the degree of esterification where the methyl groups substitute for carboxyl groups, will reduce the number of carboxyl groups. This provides a reasonable explanation for the reduction observed in lipase inhibition caused by the pectin with a higher degree of esterification [141].

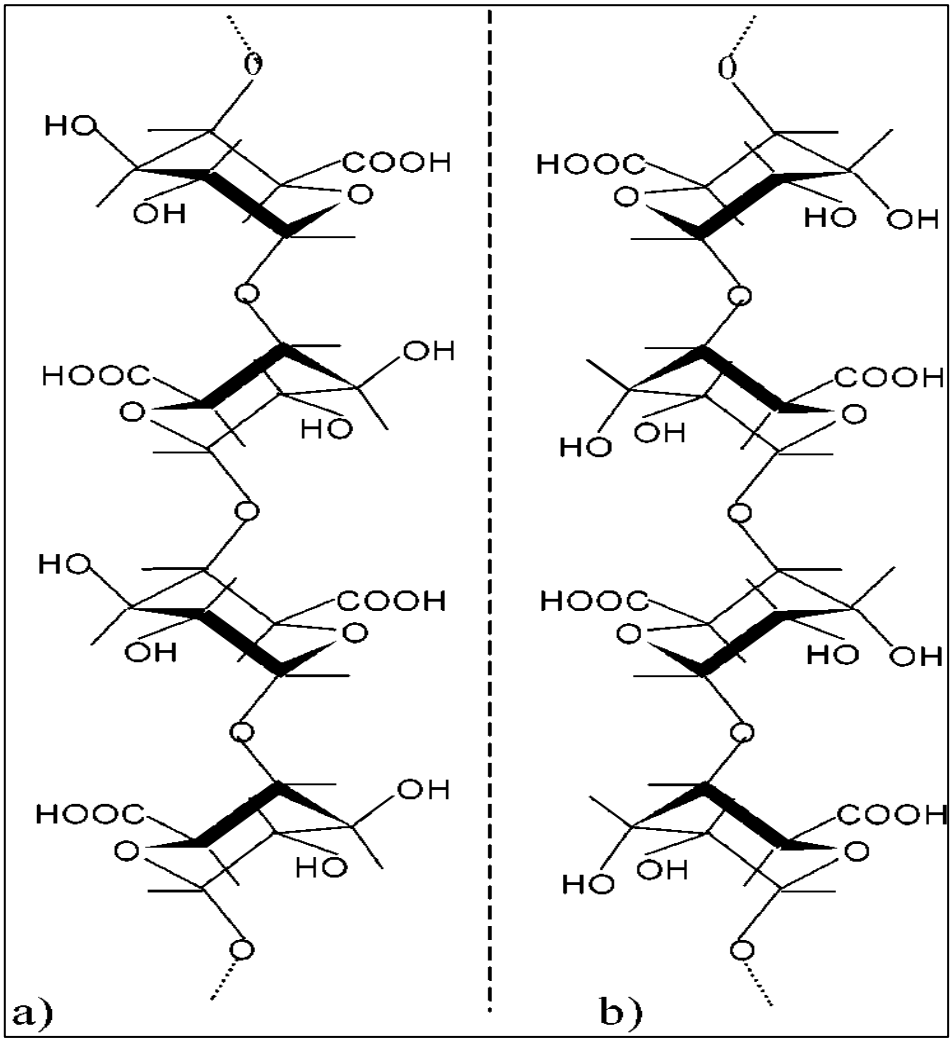

Figure 2.9. Schematic representation of (a) galacturonate and (b) guluronate chains of pectin and alginate, respectively, sharing structural similarities. Taken from Braccini and Perez, (2001) [145].

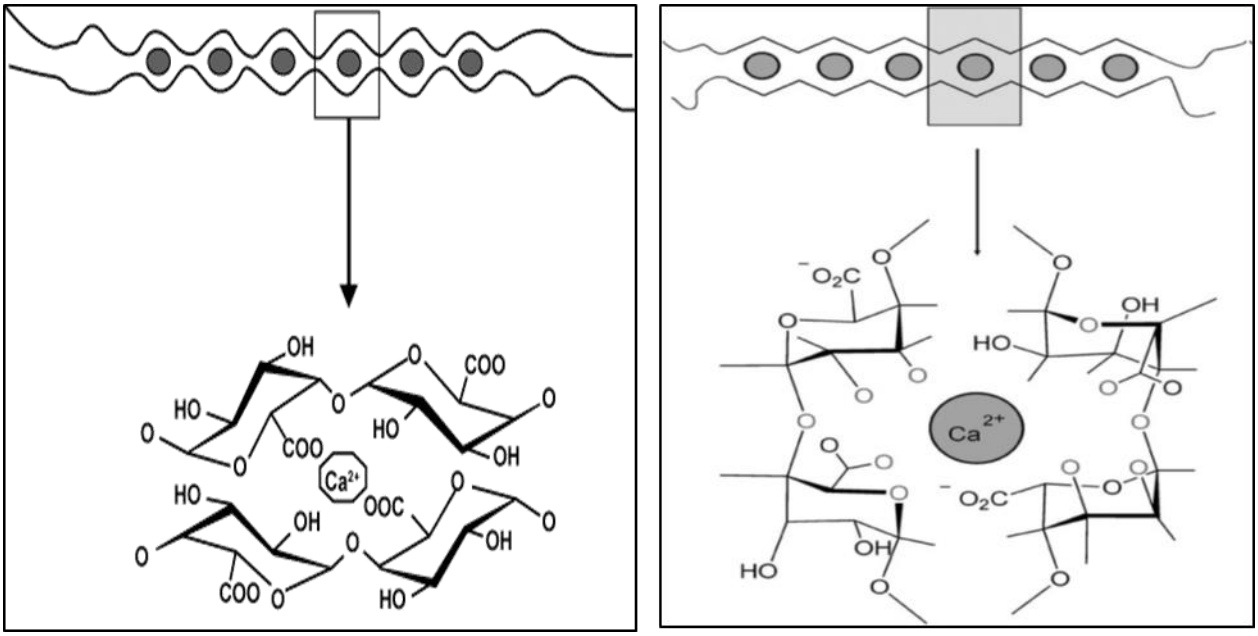

Figure 2.10. Schematic diagrams of the egg-box model for pectin and alginate. The left diagram represents the egg-box model for pectin taken from Axelos and Thibault, 1999 [148], whereas the right diagram represents the egg-box model for alginate taken from Leick e al., (2010) [149] gel formation.

Alginates may bind strongly to the substrate surface (oil/water interface), reducing opportunity for the enzyme to interact with the oil/water interface. Pancreatic lipase is water- soluble whereas triglyceride substrate is water-insoluble, hence, for the lipolytic reaction to occur, the lipase enzyme initially has to adsorb to the water/oil interface of substrate. Enzyme adsorption to the substrate surface enhances the activity of the lipase and increases the binding affinity of the enzyme to the substrate, producing the enzyme-substrate complex based on Michaelis-Menten Kinetics [91]. This is thought to be the mechanism by which other potent inhibitors such as chitosan, DEAE-Sephadex and DEAE polydextrose inhibit pancreatic lipase activity; however, chitosan, DEAE-Sephadex and DEAE polydextrose are positively charged polysaccharides whereas alginate is a negatively charged polysaccharide [91, 150]. Both DEAE-Sephadex and DEAE polydextrose contain many diethylaminoethyl (DEAE) groups in their structure, and can inhibit lipase activity *in vitro,* and the inhibition level relies on the substitution level of DEAE groups. When the substitution level of DEAE-polydextrose is high, only low concentration of DEAE polydextrose is required to reduce lipase activity by 50%. The same study reported that DEAE polydextrose at concentrations 1.44, 16.9, 61 and > 1000 μg/ml with a level of substitution equal to 1.09, 0.18, 0.079 and 0.048, respectively, managed to inhibit lipase activity by 50% [91, 150].

2.8 Conclusion

Alginate polymers caused a significant reduction in pancreatic lipase activity *in vitro*, suggesting alginates as potential lipase inhibitors which can reduce digestion of dietary triglycerides, hence, decreasing the amount of triglycerides absorbed by the body, and suggesting alginate may be used in weight management. However, the efficiency of alginates as lipase inhibitors depends on alginate concentration and their contents of guluronate and mannuronate blocks. Alginate inhibition of lipase is concentration dependent. Also, alginates that are rich in G blocks are more effective in inhibiting lipase activity than alginates rich in M blocks. Alginate could undergo enzymatic modification to easily produce the alginates with the preferred the properties. Therefore, alginates may be recommended in obesity treatment instead of conventional anti-obesity drugs such as Orlistat because the fibres present in alginates have the ability to decrease or prevent the unpleasant gastrointestinal side effects associated with Orlistat [113].

Chapter 3: Kinetic Studies of Lipase Activity

3.1 Introduction

Enzymes are biological catalysts which are produced by living cells and accelerate the rate of biochemical reactions in organisms, however, these molecules are not consumed throughout the reaction they catalyze [151, 152]. Enzymes can be isolated from living cells and applied commercially in speeding up rates of many essential processes such as production of sweetening agents, washing powders and different cleaning products [152]. However, the rates of enzyme-catalysed reactions are affected by factors such as substrate concentration, enzyme concentration, temperature, and concentration of free hydrogen ions (pH). Additionally, compounds called inhibitors affect enzyme activity [151, 152].

Enzyme kinetic studies are usually carried out to determine rates of enzyme-catalysed reactions, to understand the catalytic action of enzyme, to identify mechanisms of enzyme inhibition, and to determine how the variations in experimental circumstances impact reaction rates. The kinetics of an enzyme-substrate interaction usually depends on substrate concentration (or enzyme: substrate ratio) and the way by which inhibitors affect the interaction between enzyme and substrate can display useful information about their mode of action.

A Michaelis-Menten plot is usually used to express the interaction between enzyme and substrate in term of reaction initial velocity (V_0) and substrate concentration [S]. A Michaelis-Menten plot was used here to assess the rate of lipase-catalysed reactions in the presence and absence of alginates as inhibitors. On a Michaelis-Menten graph, the reaction velocity (V), which was measured from the alteration in absorbance over 35 minutes, was plotted on the y-axis versus substrate concentration on the x-axis in an attempt to determine the regulatory effect of alginates on lipase-catalysed reaction via comparing the kinetic parameters obtained from Michaelis-Menten plots of inhibited and uninhibited reactions. The non-linear data from Michaelis-Menten curves were then transformed into straight line Lineweaver-Burk plots in an attempt to identify the type of inhibition caused by alginate.

3.1.1 Michaelis-Menten plot

In enzymology, a single-enzyme, single-substrate reaction usually consists of two stages. Firstly, the substrate [S] binds to an enzyme [E], producing enzyme-substrate [ES] complex. Secondly, the [ES] complex converts to a product through a unimolecular reaction. This type of reaction usually follows the Michaelis-Menten equation which was obtained in 1913 by Leonor Michaelis and Maud Menten. It defines the initial rate of product formation for an enzyme-catalysed reaction with regard to two kinetic parameters V_{max} (maximal velocity of the reaction) and K_m (Michaelis-Menten constant) [153].

The Michaelis-Menten equation describing the initial rate of reaction involving a single substrate and single enzyme can be shown as the following:

$$V_{\circ} = \frac{V_m[S]}{K_m + [S]}$$

Equation 3.1. Michaelis-Menten equation for an-enzyme catalysed reaction.

Briggs and Haldane (1925) studied the theoretical foundation of Michaelis-Menten equation taking into consideration that the reaction is an irreversible unimolecular reaction (A→B) which is catalysed by an enzyme (*E*). They assumed that one molecule of substrate A (represented currently as *S*) binds reversibly with one molecule of enzyme (*E*), giving *EA* complex which is then converted to free enzyme (*E*) and product *B* (represented currently as P), where *B* may denote numerous molecules. They characterised this equation by the following reaction:

$$A + E \underset{K_3}{\overset{K_1}{\leftarrow\!\rightarrow}} AE \underset{K_4}{\overset{K_2}{\leftarrow\!\rightarrow}} B + E$$

Equation 3.2. An enzyme-catalysed reaction.

For an enzyme-catalysed reaction which obeys Michaelis-Menten kinetics, enzyme kinetic data are

fitted to the Michaelis-Menten equation using non-linear regression in which the initial velocity of reaction [V_0] is plotted versus the substrate concentration [S], producing a hyperbolic curve (Figure 3.1). Two essential kinetic parameters: maximal initial velocity (V_{max}) and Michaelis-Menten constant (K_m) can be determined from Michaelis-Menten curve in which the reaction velocity is measured at various substrate concentrations. V_{max} can be defined as the reaction velocity when all the enzyme active sites become completely occupied by the substrate molecules, and it can be determined graphically from the point where the Michaelis-Menten curve becomes a plateau. K_m is the concentration of substrate required to produce half maximum velocity ($V_{max}/2$). K_m measures the affinity of enzyme for the substrate where a small K_m value indicates a strong affinity between the enzyme and substrate, thus, the reaction requires a relatively low concentration of substrate to reach its maximum velocity, and vice versa [152, 154]. The Michaelis-Menten constant equation can be expressed as the sum of dissociation rate of enzyme-substrate complex into product and enzyme (K_2) and the reverse dissociation rate of enzyme-substrate complex into the substrate and enzyme (K_3) divided by the formation rate of enzyme-substrate complex (K_1). However, at the beginning of an enzyme-catalysed reaction, the concentration of product [P] is negligible compared to [S], hence, the K_4 constant which represents the reverse dissociation rate of product into ES complex was not included in the Michaelis-Menten constant equation (Equation 3.3).

$$\boldsymbol{K_m = \frac{K_2 + K_3}{K_1}}$$

Equation 3.3. Michaelis-Menten constant.

3.1.2 Lineweaver-Burk plot

Before the availability of non-linear regression, the non-linear curved data from Michaelis-Menten equation had to be transformed into a straight-line equation such as the Lineweaver-Burk equation to analyse the data using linear regression analysis. The Lineweaver-Burk equation is a transformation of Michalis-Menten equation (Equation 3.4), and it produces a straight line with X- and Y- intercepts known as Lineweaver-Burk plot (a double reciprocal plot). The x-intercept of Lineweaver-Burk plot is equivalent to $-1/k_m$, whereas the y-axis is equal to $1/V_{max}$, and the slope is

equal to K_m/V_{max} (Figure 3.1). However, the development of computer programmes able to perform non-linear regression analysis enables the direct fitting of data to the Michaelis-Menten equation [154].

In the current work, the Lineweaver-Burk plots for lipase reactions in the presence and absence of alginates were produced in an attempt to identify type of inhibition and assess the potency of regulatory effect of the biopolymer through calculating the dissociation constant of inhibitor (K_i).

$$\frac{\mathbf{1}}{\boldsymbol{V_0}} = \frac{\boldsymbol{K_m}}{\boldsymbol{V_{max}[S]}} \times \frac{\mathbf{1}}{\boldsymbol{V_{max}}}$$

Equation 3.4. Lineweaver-Burk equation produced by linear transformation of Michaelis-Menten equation.

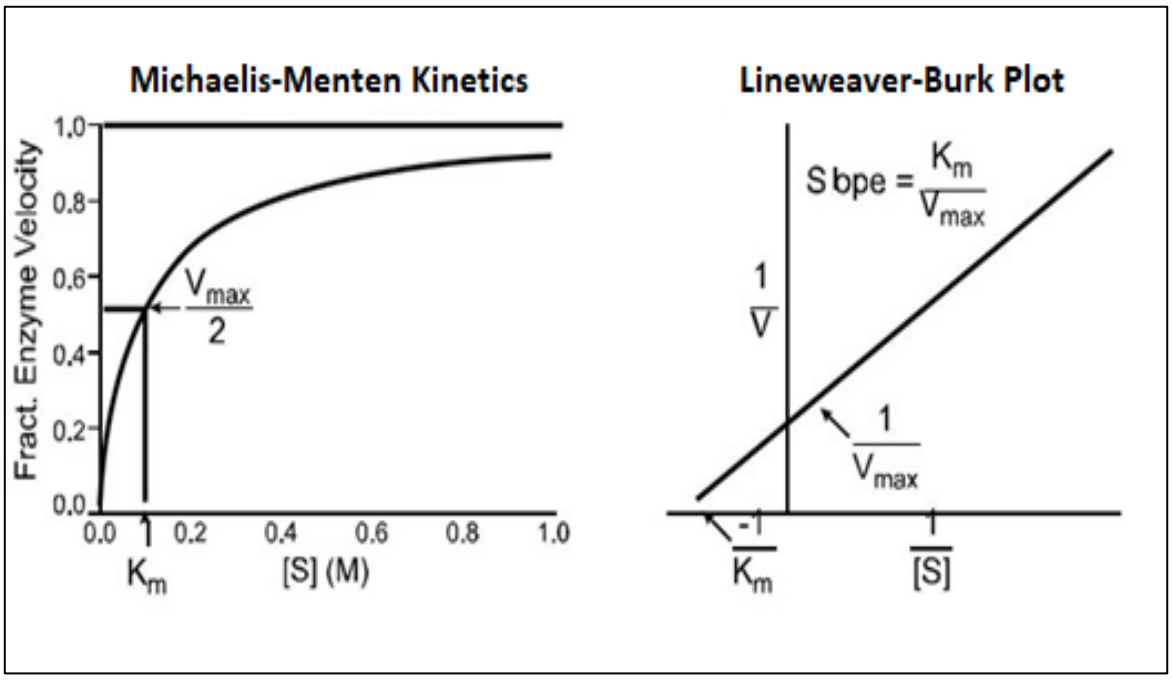

Figure 3.1. General example of Michaelis-Menten plot (left) and Lineweaver-Burk plot (right). Lineweaver-Burk plot is produced by linear transformation of Michaelis-Menten equation. Adapted from Kenakin, (2012) [154].

3.1.3 Regulation of enzyme-catalysed reaction

As mentioned in the introduction section of this chapter, the rates of enzyme-catalysed reactions can be affected by various factors, and one of these factors is the presence of an inhibitor which results in alteration in either V_{max} or K_m or both. The alteration in kinetic parameters caused by inhibitors can be observed by comparing Michaelis-Menten and Lineweaver-Burk plots for inhibited and uninhibited reactions. The way by which the presence of inhibitor alters V_{max} and K_m can offer useful information about the type and potency of the inhibitor.

3.1.4 Enzyme inhibition

Inhibitors are molecules which reduce the catalytic activity of enzymes. Enzyme inhibitors can be either reversible or irreversible. Irreversible inhibitors bind covalently to the enzyme, causing permeant loss of enzyme catalytic action. Conversely, reversible inhibitors bind to enzyme non-covalently, resulting in a temporary loss of enzyme catalytic activity. However, the enzyme has the ability to return to its full activity once the inhibitors are eliminated via separation techniques such as dialysis, gel filtration, and chromatography [152, 155]. Reversible inhibition can be competitive, non-competitive, uncompetitive, or mixed, and they can be distinguished by the kinetics of inhibition.

3.1.4.1 Competitive inhibition

In this model of inhibition, the inhibitor [I] has chemical structure similar to the substrate, therefore, it competes with the substrate for the active site of enzyme. The competitive inhibitor binds reversibly to the active site of the enzyme, preventing the formation of enzyme-substrate complex. The competitive inhibitor binds only to the free enzyme and does not have any affinity to ES complex. However, the inhibitory effect of the competitive inhibitor is temporary where this effect can be removed by increasing substrate concentration. This type of inhibition apparently increases the K_m of its substrate, but the V_{max} remains unchanged (Figure 3.2) [152, 154].

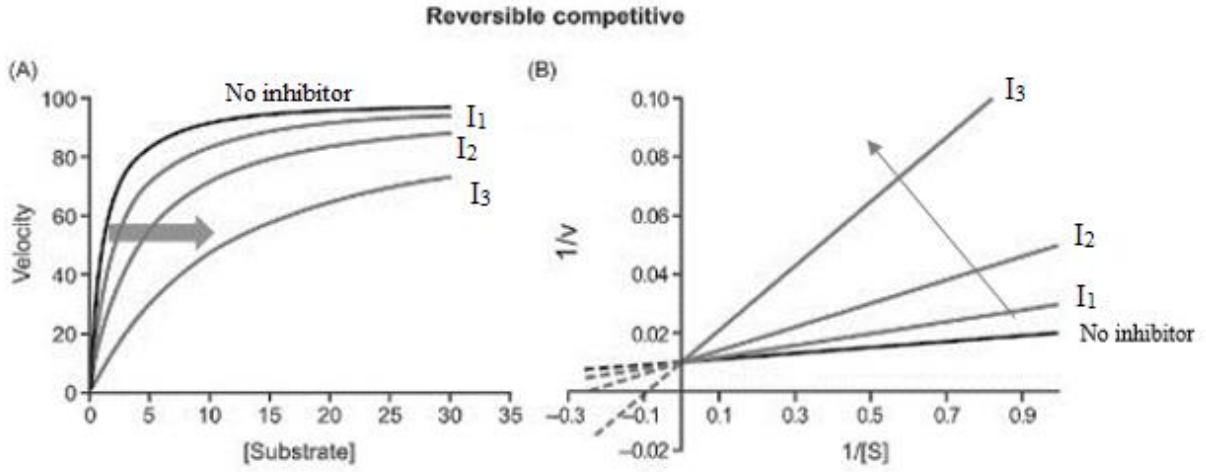

Figure 3.2. Michaelis-Menten (A) and Lineweaver-Burk (B) plots for a reversible competitive inhibitor.I_1, I_2 and I_3 are inhibitors. The black line in each plot indicates the kinetic behaviour in the absence of an inhibitor, and the grey lines in each plot indicate the change in kinetic behaviour for increasing concentration of inhibitor. In each plot, the inhibitor concentration increases in the direction of the grey arrow. The competitive inhibition is distinguished by a rise in the V_{max} of the reaction with no change in K_m. The Lineweaver-Burk plots are of increasing slope (showing increasing K_m values) with increasing concentrations of inhibitor, and the lines of uninhibited and inhibited reactions cross at the ordinate axis at the same point. A modified version taken from Kenakin, (20120 [154]

3.1.4.2 Non-competitive inhibition

This type of inhibitor binds equally to enzyme at a site different from the active site or the ES complex, reducing catalytic action of the enzyme. Unlike a competitive inhibitor, the effect of non-competitive inhibitor cannot be stopped by increasing substrate concentration. This type of inhibitor is structurally distinct from the substrate. In the presence of non-competitive inhibition, V_{max} of the reaction is reduced due to diminution in concentration of active enzyme in the solution which in turn hinders formation of product. However, since the substrate cannot bind when the inhibitor is bound, also, the ES complex cannot breakdown to E and P when the inhibitor is bound, so both rates of formation and dissociation of [ES] complex are reduced equally, therefore, the K_m remains unchanged (Figure 3.3) [152, 154].

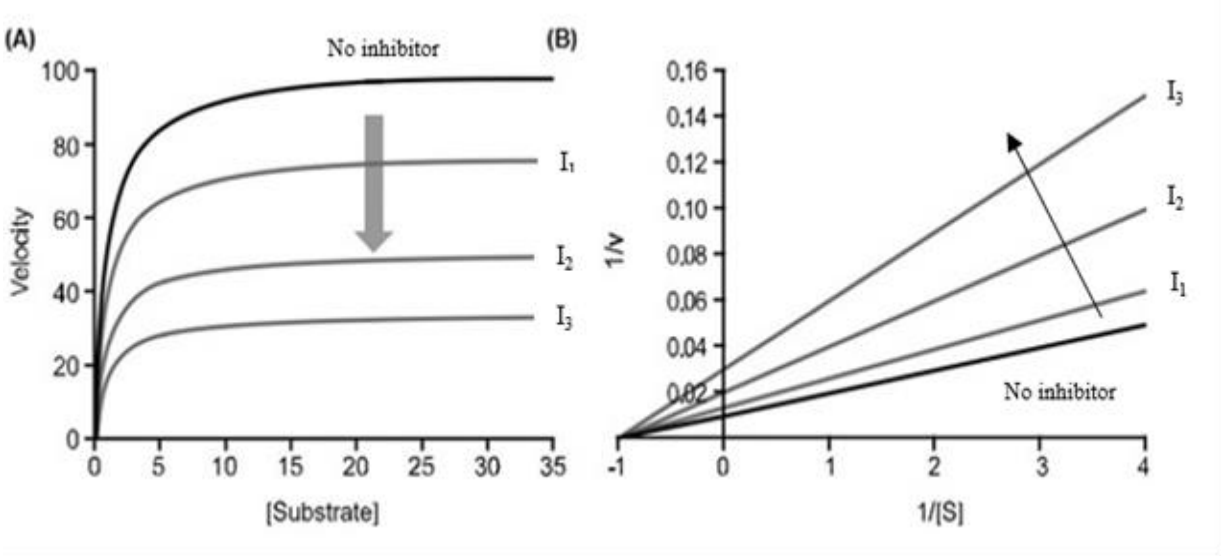

Figure 3.3. Michaelis-Menten (A) and Lineweaver-Burk (B) plots for reversible non-competitive inhibition.The non-competitive inhibition is distinguished by a diminution in the V_{max} of the reaction with no change in the K_m for its substrate. On Lineweaver-Burk plot, both inhibited and uninhibited lines of best-fit cross the x-axis at the same point. I_1, I_2 and I_3 are inhibitors. The black line in each plot indicates the kinetic behaviour in the absence of an inhibitor, and the grey lines in each plot indicate the change in kinetic behaviour for increasing concentration of inhibitor. In each plot, the inhibitor concentration increases in the direction of the grey arrow. A modified version adapted from Kenakin, (2012) [154].

3.1.4.3 Uncompetitive inhibition

In this type of inhibition, the inhibitor [I] binds selectively to the [ES] complex and not to the free enzyme since the substrate binding modifies the enzyme structure to produce a binding site for the inhibitor. Therefore, this type of inhibition only occurs when the ES complex is formed by the presence of substrate bound to the enzyme. Uncompetitive inhibition reduces V_{max} due to hindrance of the product formation, also, the K_m is reduced in the presence of uncompetitive inhibitor due to binding of inhibitor to [ES] complex which in turn diminishes the dissociation rate of [ES] to the product and enzyme (Figure 3.4) [152, 154].

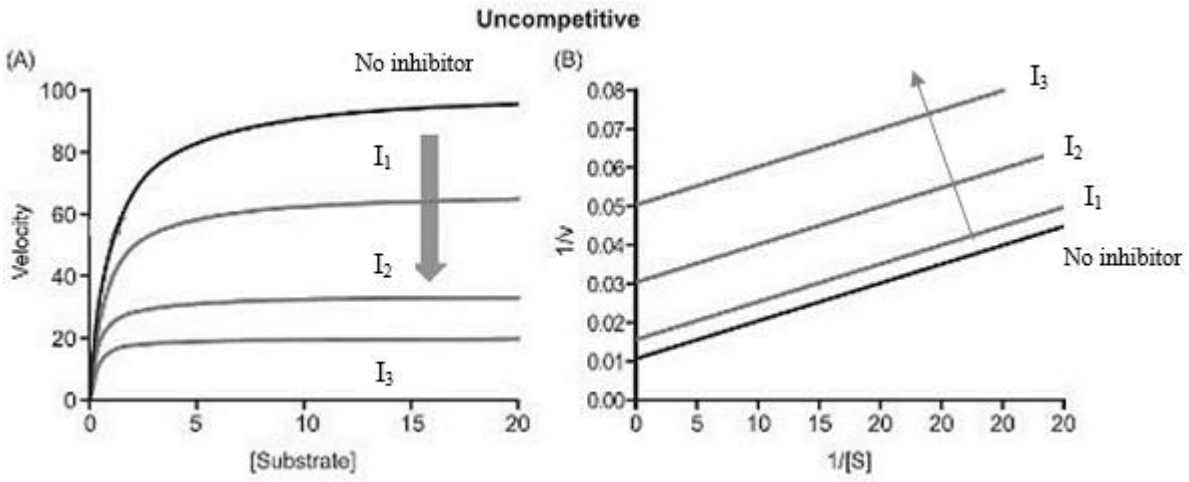

Figure 3.4. Michaelis-Menten (A) and Lineweaver-Burk (B) plots for reversible uncompetitive inhibition. Uncompetitive inhibition is characterised by a reduction in the apparent K_m and V_{max} values. The Lineweaver-Burk plots are parallel and do not cross.I_1, I_2 and I_3 are inhibitors. The black line in each plot indicates the behaviour of kinetic reaction in the absence of inhibitor, and the grey lines in each plot indicate the change in kinetic behaviour for increasing concentration of inhibitor. In each plot, the inhibitor concentration increases in the direction of the grey arrow. A modified version taken from Kenakin, (2012) [154]**.**

3.1.4.4 Mixed inhibition

In this type of inhibition, the inhibitor has the affinity to bind to both the free enzyme [E] and the enzyme-substrate [ES] complex, however, the binding affinity of inhibitor for the [E] and [ES] - complex are not equal. The inhibitor can bind to the free enzyme at a site different from the active site, allowing the enzyme-substrate binding. Mixed inhibition apparently reduces the V_{max} and apparently increases the K_m value (Figure 3.5). However, when the mixed inhibitor has an equal binding affinity for both the [E] and [ES] complex, the K_m will not be altered, and the inhibitor in this case is considered to be a non-competitive inhibitor [154].

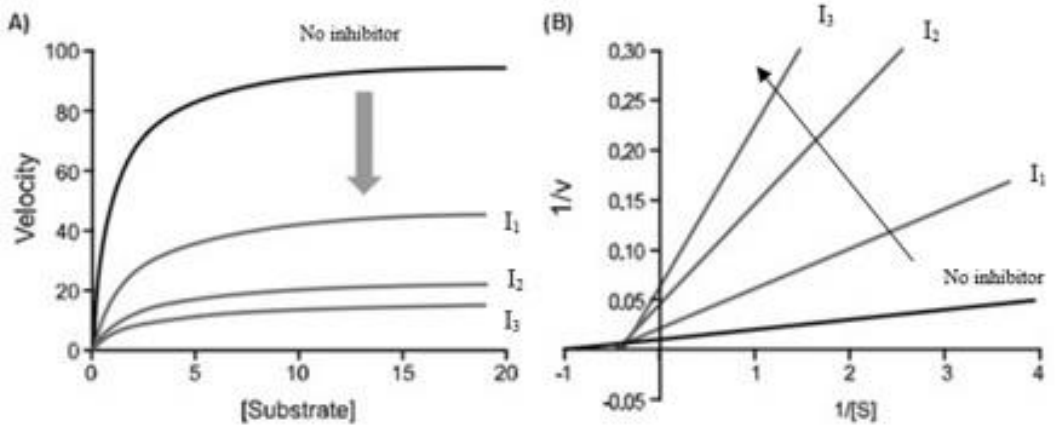

Figure 3.5. Michaelis-Menten (A) and Lineweaver-Burk (B) plots for reversible mixed inhibition. The mixed inhibition is characterised by an apparent reduction in the V_{max} value and an apparent increase in K_m value. The Lineweaver-Burk plots where the best-fit lines of inhibited and uninhibited reactions do not cross any of the axis at the same point.The inhibitor has unequal affinity for E and ES. I_1, I_2 and I_3 are inhibitors. The black line in each plot indicates the behaviour of kinetic reaction in the absence of inhibitor, and the grey lines in each plot indicate the change in kinetic behaviour for increasing concentration of inhibitor. In each plot, the inhibitor concentration increases in the direction of the grey arrow a modified version taken from Kenakin, (2012) [154].

3.1.4.5 Irreversible inhibition

In this type of inhibition, the inhibitor binds permanently to the enzyme, altering the structural conformation of enzyme to create a highly stabilised [EI] complex. The inhibitor usually binds covalently to an amino acid residue at the enzyme active site or a site close to the active site, causing a permeant inactivation of the enzyme. For example, diiso-propylphosphofluoridate (DIPF), which is a constituent of nerve gases, causes irreversible inhibition of the enzyme acetylcholinesterase via the formation of a covalent bond with a serine residue in the active site of the enzyme, stopping transmission of nerve impulses. Also, glycopeptide transpeptidase, which creates cross-links in the cell wall of bacteria, can be irreversibly inhibited by the antibiotic penicillin which binds covalently to a serine residue in the active site of the enzyme, inhibiting the synthesis of the cell wall [154, 156].

3.1.5 Quantification of alginate's regulatory effect

The mechanism by which the enzyme is inhibited can be essential to know because it may assist in identifying the association between the inhibition level required to yield a significant effect. For example, the effect of a competitive inhibitor can be decreased by high concentrations of substrate, whereas the efficiency of uncompetitive inhibition can be promoted by high concentrations of substrate because the maximum amount of ES complex will be present. Lineweaver-Burk plots can be used to define the influence of an inhibitor of the enzyme and provide information about the mechanism of inhibition [154]. The inhibition dissociation constant (K_I) can be defined as the concentration of inhibitor needed to yield half maximum inhibition and is usually used to identify the type of inhibition. The inhibition dissociation constant is a measure of the potency of inhibitor through measuring the binding affinity of the inhibitor to the enzyme. The smaller the inhibition constant, the stronger the inhibitor, and vice versa [157]. The inhibitor may bind either to the free enzyme (E) or enzyme-substrate complex (ES), or both depending on the type of inhibition. The inhibition dissociation constants K_I and $K_{\acute{I}}$ represent the binding of inhibitor to E and ES-complex, respectively [158] (Equation 3.5).

$$\begin{array}{ccc} E + S & \rightleftarrows & ES \rightleftarrows E + P \\ + & & + \\ I & & I \\ K_I \downarrow\uparrow & & \downarrow\uparrow K_{\acute{I}} \\ EI & & ESI \end{array}$$

Equation 3.5. General equation for the inhibitor binding to two forms of the enzyme with K_I and $K_{\acute{I}}$ representing the binding of inhibitor to E and ES-complex, respectively.

The V_{max} and K_m for an uninhibited reaction, and the apparent Maximum Velocity ($V_{max\ app}$) and Michaelis Constant ($K_{m\ app}$) for inhibited reactions are obtained from the y- and x- intercepts of their Lineweaver-Burk plots where the y-intercept is equivalent to inverse of V_{max} while x-intercept is equal to inverse of a negative K_m [154, 158]. The K_I and $K_{\acute{I}}$ can be determined from the concentration of inhibitor (I), the $V_{max\ app}$ and $K_{m\ app}$ constants of the inhibited reaction, as well as the V_{max} and K_m of uninhibited reaction using the appropriate form of equation depending on the type of inhibition (Table 3.1) [158].

Inhibition Type	Rate of Equation	$K_{m\ app}$	$V_{max\ app}$
None	$v = V_{max}[S]/(K_m + [S])$	K_m	V_{max}
Competitive	$v = V_{max}[S]/([S] + K_m\ (1 + [I]/K_I)$	$K_m(\ 1 + [I]/K_I)$	V_{max}
Mixed	$v = V_{max}[S]/((1 + [I]/K_I)K_m + (1 + [I]/K_{\acute{I}}\ [S]))$	$K_m(1 + [I]/K_I)\ /(1 + [I]/K_{\acute{I}})$	$V_{max}/(1 + [I]/K_{\acute{I}})$
Non-competitive	$v = (V_{max}[S]/\ (1 + [I]/K_I))/K_m + [S])$	K_m	$V_{max}/(1 + [I]/K_I)$
Uncompetitive	$v = V_{max}[S](K_m + [S](1 + [I]/\ K_{\acute{I}}))$	$K_m\ /(1 + [I]/\ K_{\acute{I}})$	$V_{max}/(1 + [I]/K_{\acute{I}})$

Table 3.1. General equations used for determining the Michaelis-Menten rate equation, the apparent Maximum Velocity ($V_{max\ app}$) and the apparent Michaelis ($K_{m\ app}$) constants. K_I and $K_{\acute{I}}$ represent the binding of inhibitor to E and ES-complex, respectively. Adapted from Garrett and Grisham, (2008) [158]

3.2 Aims

Data presented in Chapter 2 of this thesis showed that all tested alginates succeeded in reducing pancreatic lipase activity *in vitro*, however, CC01, 1N80 and 1LF80 possessed the most potent inhibition effects, suggesting that these three alginates could be used as potent inhibitors of pancreatic lipase *in vivo*. In the current chapter, the kinetics of both lipase/substrate interactions in the absence and presence of CC01, 1N80 and 1LF80 alginates as inhibitors were studied, and both Micheales-Menten and Lineweaver-Burk analysis were used to evaluate the strength of regulatory effects of alginates and to identify type and mechanism of inhibition.

3.3 Method

3.3.1 Materials and equipment

All chemicals and equipment used for the lipase kinetic assay were identical to those used in the turbidity assay of lipase activity in Chapter 2.

3.3.2 Kinetic assay of lipase activity

Olive oil was passed through a glass chromatography column (2x 32 cm) containing 8 cm of aluminium oxide to remove the free fatty acids. Unlike lipase activity assay (section 2.4.2.1, p. 48), 10 g of this purified olive oil was made up to 50 ml using acetone, producing a 20% (w/v) solution of purified olive oil in acetone which was stored as a stock solution at 4 °C for use in all experiments. A higher concentration of substrate was used here to ensure that the saturation concentration is reached where all the active sites of lipase become occupied and any competitive inhibitor will be out competed.

Buffer diluent containing 0.35% (w/v) sodium taurodeoxycholate was prepared and titrated to pH 7.3 as previously described in section 2.4.2.2 of Chapter 2. For lipase kinetic assay, 40.5 ml of the buffer diluent was heated to 70 °C, then 4.5 ml of 20% purified olive oil solution was added to the heated diluent buffer, giving a 2% olive oil solution. The 2% olive oil solution (as a substrate solution) was homoginsed for 10 minutes with continuous heating at 70 °C. After that, it was diluted further with an appropriate volume (µl) of the buffer diluent to prepare different concentrations of substrate (0.063, 0.125, 0.25. 0.5 and 1 % (v/v)). 1 mg/ml of lipase in buffer diluent was prepared. Then, 60 µl of colipase was added to the lipase solution, and the mixture vortexed. Orlistat in substrate solution at concentration 0.025 mg/ml was prepared. 5 mg/ml solution of alginate in substrate was prepared.

For sample preincubation, two 96-well microplates (Bio Tek, USA) were used. For the kinetic assay of lipase control (in the absence of alginate), 10 µl of lipase solution (1mg/ml) and buffer diluent solution were placed separately in triplicate in plate 1. In plate 2, 240 µl of substrate (olive oil) solution at different concentrations (0.063, 0.125, 0.25. 0.5, 1 and 2 % (v/v)) was placed separately in sex wells.

For kinetic assay of lipase in the presence of alginate, 10 µl of lipase solution (1 mg/ml) and buffer diluent solution were placed separately in triplicate in plate 1. In plate 2, 240 µl of a mixture consisting of 5 mg/ml alginate in different concentrations of substrate solutions (used as an inhibition control) was placed in six wells. Also, 240µl Orlistat solution (used as a positive inhibition control) was placed separately in six wells of plate 2. Both plates 1 and 2 were incubated at 37 ˚C for 10 minutes. Then, 200 µl of the samples present in Plate 2 was transferred to Plate 1 containing 10 µl of both lipase and blank solutions. Finally, Plate 1 was placed in the reader where the optical density was read every 5 minutes at 405 nm for 55 minutes. In the assay, 200 µl of the substrate solutions at 2, 1, 0.5, 0.25, 0.125, 0.063% (vol/vol) were added to 10 µl of lipase solution, giving final substrate concentrations of 19.05, 9.52, 4.76, 2.38, 1.19, and 0.59 mg/ml in the reaction mixture, respectively. Also, 10 µl of lipase solution (1 mg/ml), and 200 µl of alginate solution (5 mg/ml) were used in the assay, hence, the final concentrations of lipase and alginate in the reaction mixture were 0.048 and 4.8 mg/ml, respectively. Measurements of kinetics of lipase/substrate in the presence and absence of alginate were carried out four times for the control and each biopolymer (CC01, 1N80, and 1LF80).

3.4 Statistical analysis

Kinetic parameters (K_m and V_{max}) were calculated using GraphPad Prism 7 statistical software using substrate-velocity data and non-liner regression to produce Michaelis-Menten plot. Lineweaver-Burk plot was created using linear regression from GraphPad Prism 7 statistical software to identify type of inhibition and display inhibition kinetics. Each sample was examined four times, and the kinetic constants were analysed by calculating means and standard deviation (±SD).

3.5 Results

Figure 3.6 shows Michaelis-Menten curves for lipase control reactions in the absence and presence of CC01 alginate at 4.8 mg/ml. For the lipase control reaction, the reaction velocity increased as the substrate concentration increased from 0 to 9.5 mg/ml. However, at substrate concentrations greater than 9.5 mg/ml, the reaction-rate curve started to level off, and the reaction reached its maximum velocity at V_{max} = 0.328 (Δ absorbance/35 min), indicating that all the enzyme active sites became completely occupied by substrate molecules. Subsequently, the reaction velocity became independent of the substrate concentration, and any further increase in the substrate concentration did not change the reaction velocity. However, when CC01 alginate was added to the reaction mixture at concentration equal to 4.8 mg/ml, the reaction velocity increased with the increase in substrate concentration, however, the increase in velocity was lower than that of the lipase control at all substrate concentrations, and the biopolymer allowed the reaction to reach a plateau at a lower point where the V_{max} was equal to 0.08 (Δ absorbance/35 min) compared with that of lipase control, indicating that CC01 reduced the velocity of reaction.

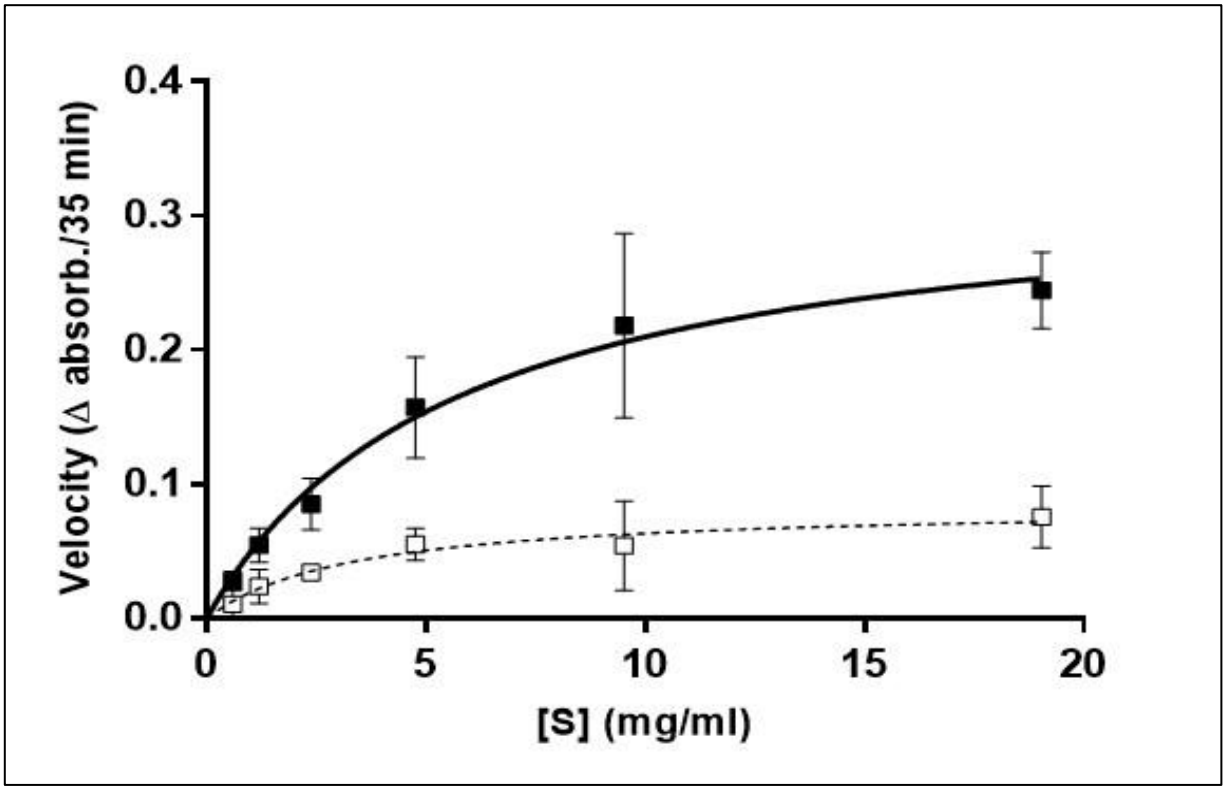

Figure 3.6. Michaelis-Menten plot for lipase control (■) and lipase with CC01 alginate (□) solutions.The lipase control solution consists of 0.048 mg/ml lipase and substrate at different concentrations (19.05-0.59 mg/ml), whereas the lipase treated with CC01consists of 0.048 mg/ml lipase with different concentrations of substrate (19.05-0.59 mg/ml) and 4.8 mg/ml of CC01 alginate.Velocity is expressed as the change in absorbance over 35 minutes where the reaction at this time point was still close to the linear phase. Values are mean ± SD., *n*=4.

The non-linear data from the Michaelis-Menten plot for lipase reactions both in the absence and presence of 4.8 mg/ml of alginate were transformed into linear Lineweaver-Burk plots using GraphPad Prism 7 to display inhibition kinetics and identify the type of inhibition (Figure 3.7).

As shown in Figure 3.7 the y-intercept of Lineweaver-Burk plot for lipase reaction in the presence of CC01 (8.93 Δ absorbance/35 min) was higher than that in the absence of CC01 (2.71 Δ absorbance/35 min), showing that the CC01 reduced V_{max} of lipase reaction.

However, both best-fit lines for lipase in the presence and absence of CC01 crossed the x-axis at different points where the x-intercept for lipase in the presence of CC01 (-0.180 mg/ml) was lower than that of lipase in the absence of the biopolymer (-0.138 mg/ml), subsequently, the K_m of lipase in the presence of CC01 biopolymer became lower than that in the absence of the biopolymer (Table 3.3). Therefore, it is clear that adding the CC01 into the reaction mixture caused a mixed

inhibition.

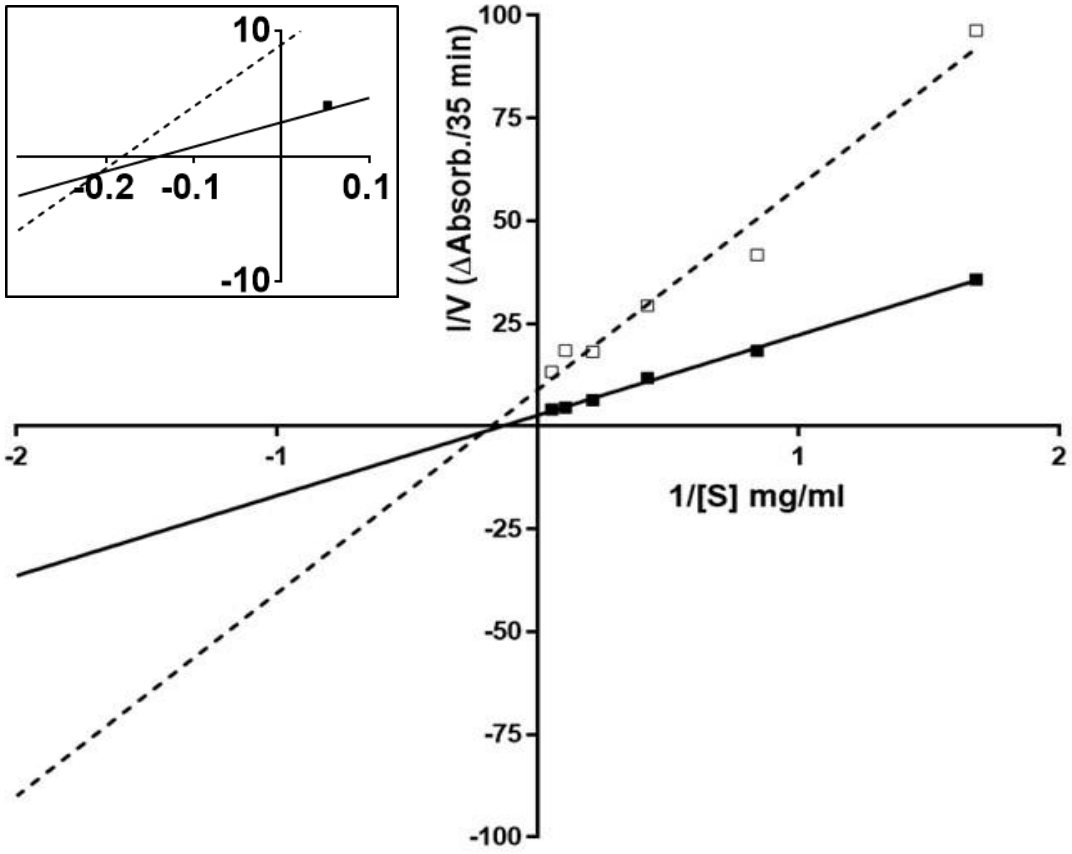

Figure 3.7. Lineweaver-Burk plot for lipase control (■) and lipase with CC01 alginate (□) solutions.The lipase control solution consists of 0.048 mg/ml lipase with different concentrations of substrate (19.05-0.59 mg/ml), whereas the lipase treated with alginate consists of 4.8 mg/ml of CC01 and 0.048 mg/ml lipase with different concentrations of substrate (19.05-0.59 mg/ml). Velocity is expressed as the change in absorbance over 35 minutes where the reaction at this time point was still close to the linear phase. Values are mean ± SD., *n*=4. The absorbance was read at 405 nm every 5 min for 55 minutes. The insert shows a magnified view of the x- and y-intercepts of the Lineweaver-Burk plot.

Figure 3.8 demonstrates a typical non-linear Michaelis-Menten curve for the lipase enzyme reaction in the absence (lipase control) and presence of 4.8 mg/ml 1N80 alginate. The lipase control is the same data as shown in Figure 3.6.

When 1N80 alginate was added to the reaction, the velocity decreased at all substrate concentrations compared with velocity of the control reaction, and the presence of the biopolymer allowed the reaction to reach its maximum velocity at 0.145 (Δ absorbance/35 min) which was

lower than the V_{max} of lipase control reaction, demonstrating that the 1N80 reduced the velocity of lipase reaction.

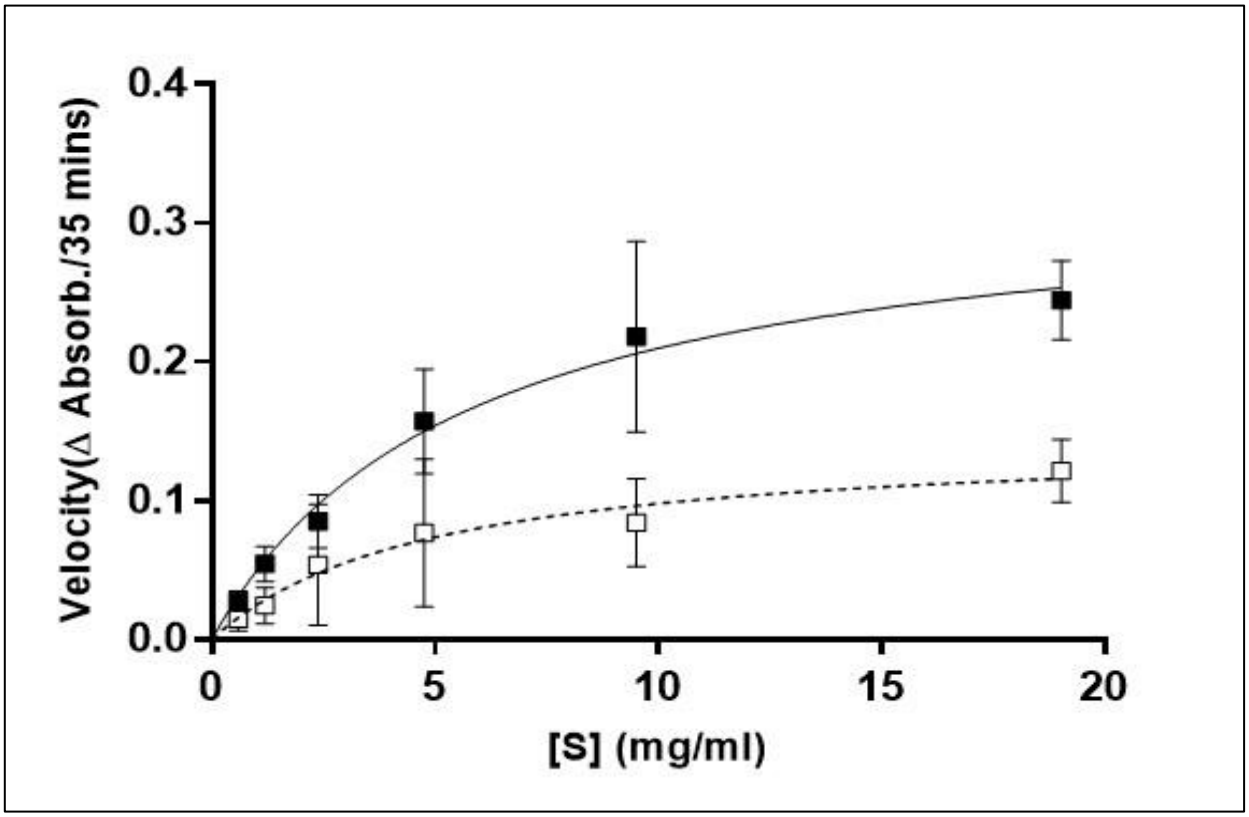

Figure 3.8. Michaelis-Menten plot for lipase control (■) and lipase with 1N80 alginate (□) solutions.The lipase control solution consists of 0.048 mg/ml lipase with different concentrations of substrate (19.05-0.59 mg/ml), whereas the lipase with alginate consists of 4.8 mg/ml of 1N80 and 0.048 mg/ml lipase with substrate at different concentrations (19.05-0.59 mg/ml). Velocity is expressed as the change in absorbance over 35 minutes where the reaction at this time point was still close to the linear phase. Values are mean ± SD., *n*=4. The absorbance was read at 405 nm every 5 min for 55 minutes.

The Lineweaver-Burk plot for the lipase reaction in the presence and absence of 4.8 mg/ml 1N80 alginate is shown in Figure 3.9. It is obvious from the figure that the y-intercept of Lineweaver-Burk plot of lipase in the presence of 1N80 (6.27 Δ absorbance/35 min) was higher than that in the absence of 1N80 (2.71 Δ absorbance/35 min), hence, the apparent V_{max} of lipase in the presence of 1N80 decreased compared with that in the absence of the biopolymer. However, the best-fit lines for lipase reaction in the presence and absence of the biopolymer crossed the x-axis at different points where the x-intercept for the reaction in the presence of 1N80 was lower than that in the absence of 1N80, indicating that the apparent K_m of the inhibited reaction was lower than the K_m

of uninhibited reaction (Table 3.3). Therefore, the changes in both the apparent K_m and V_{max} show that adding 1N80 to the reaction mixture caused a mixed inhibition.

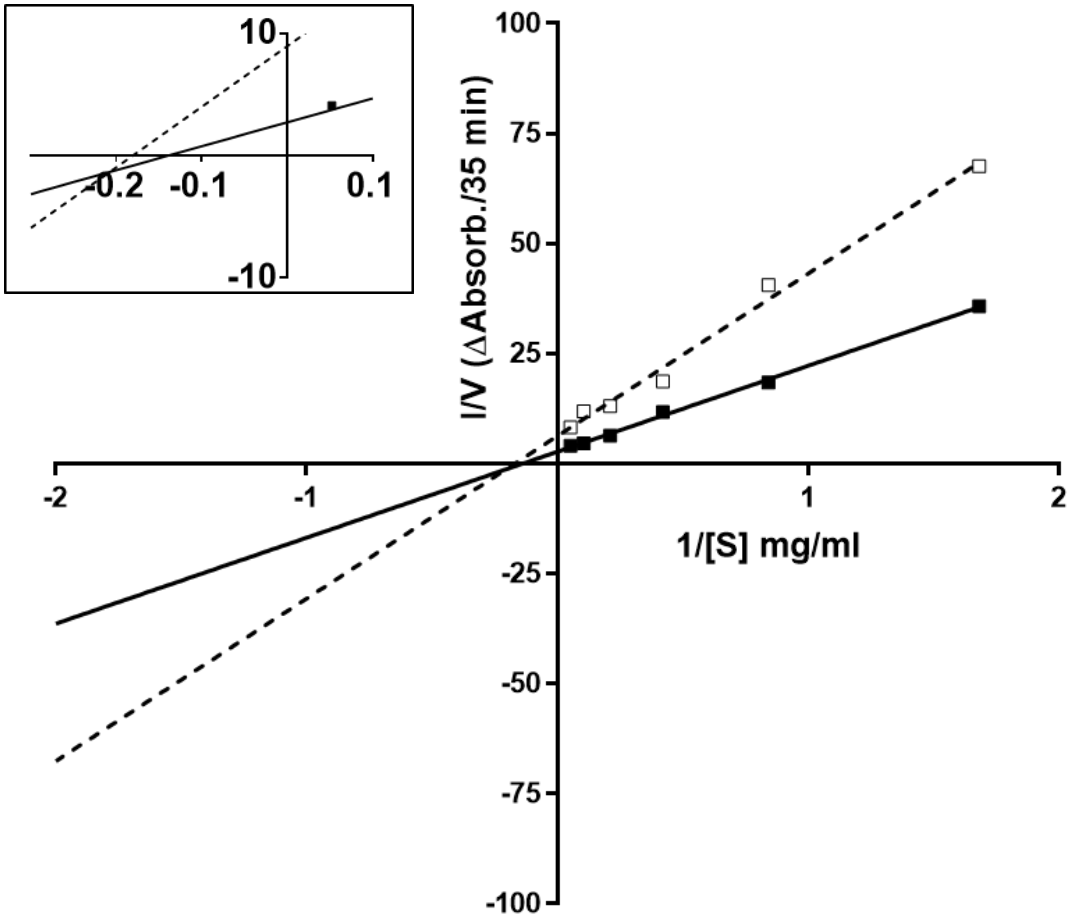

Figure 3.9. Lineweaver-Burk plot for lipase control (■) and lipase with 1N80 alginate (□) solutions.The lipase control solution consists of 0.048 mg/ml lipase with different concentrations of substrate (19.05-0.59 mg/ml), whereas the lipase treated with alginate consists of 4.8 mg/ml of 1N80 and 0.048 mg/ml lipase and substrate at different concentrations (19.05-0.59 mg/ml). Velocity is expressed as the change in absorbance over 35 minutes where the reaction at this time point was still close to the linear phase. Values are mean ± SD., *n*=4. The absorbance was read at 405 nm every 5 min for 55 minutes. The insert shows a magnified view of the x- and y-intercepts of the Lineweaver-Burk plot.

A non-linear Michaelis-Menten curve for lipase/substrate in the presence and absence of 4.8 mg/ml 1LF80 alginate is shown in Figure 3.10. For the lipase reaction in the presence of 1LF80, the reaction velocity increased with the increase in substrate concentration, but this increase in velocity at all substrate concentrations was lower than that of lipase control reaction in the absence of 1LF80. Also, the reaction in the presence of 1LF80 reached its maximum velocity at 0.178 (Δ absorbance/

35 min) which was lower than that of lipase control reaction, indicating that adding the 1LF80 to the reaction mixture reduced the reaction velocity.

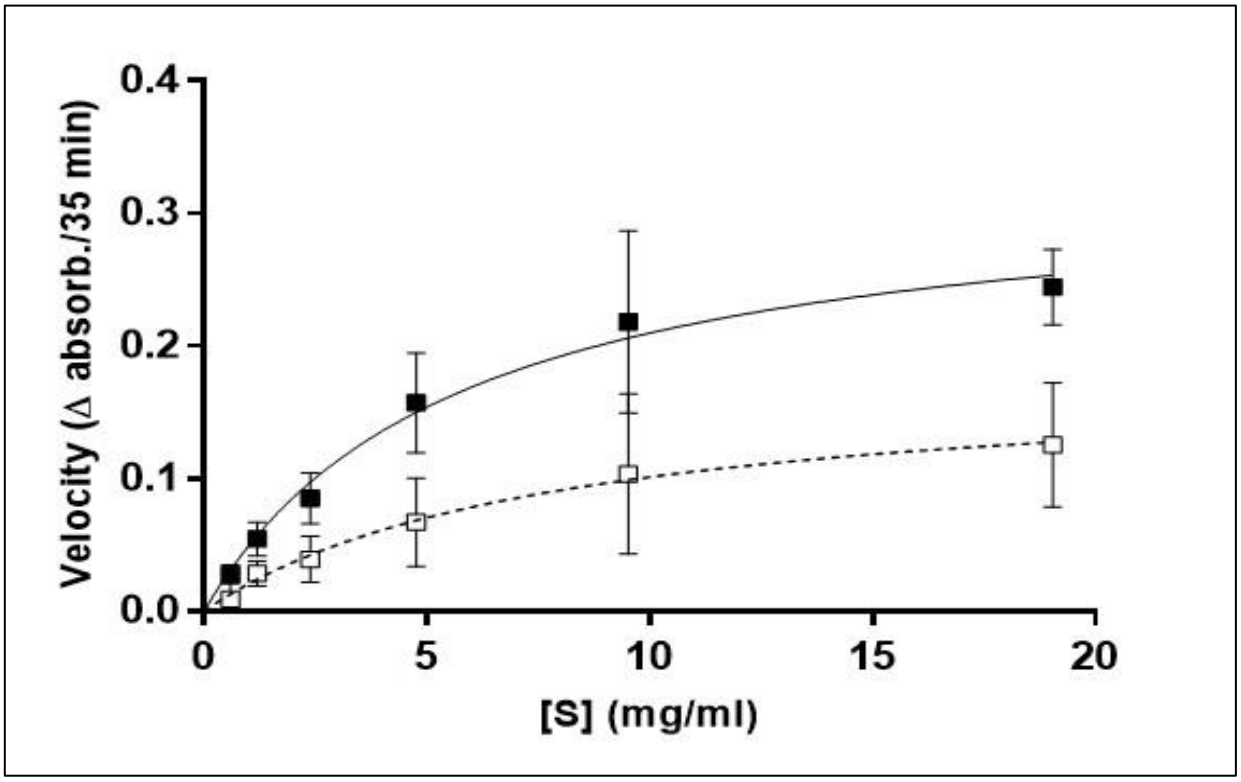

Figure 3.10. Michaelis-Menten plot for lipase control (■) and lipase with 1LF80 alginate (□) solutions. The lipase control solution consists of 0.048 mg/ml lipase with different concentrations of substrate (19.05-0.59 mg/ml), whereas the lipase treated with alginate consists of 4.8 mg/ml of 1LF80 and 0.048 mg/ml lipase with substrate at different concentrations (19.05-0.59 mg/ml). Velocity is expressed as the change in absorbance over 35 minutes where the reaction at this time point was still close to the linear phase. Values are mean and ± SD., *n*=4. The absorbance was read at 405 nm every 5 min for 55 minutes.

It is clear from the Lineweaver-Burk plot (Figure 3.11) that both best-fit lines of lipase reactions in the presence and absence of 1LF80 crossed at a point close to the origin. However, in the presence of 4.8 mg/ml 1LF80, the best-fit values for the y-intercept was a negative value (-0.565 Δ absorbance/35 min) and the x-intercept was positive (0.009 mg/ml), giving unexpected negative values for V_{max} and K_m (Table 3.3). Consequently, the type of inhibition caused by 1LF80 biopolymer could not be determined directly from the V_{max} and K_m of Lineweaver-Burk plot. Therefore, type of inhibition caused by this biopolymer was assessed from the V_{max} and K_m calculated previously from the Michaelis-Menten curve of the biopolymer (Figure 3.10, Table 3.2).

Based on the kinetic information provided by Michaelis-Menten curve (Table 3.2), there was a

reduction in both V_{max} and K_m of the lipase reaction following addition of 1LF80, indicating that the biopolymer might cause a mixed inhibition.

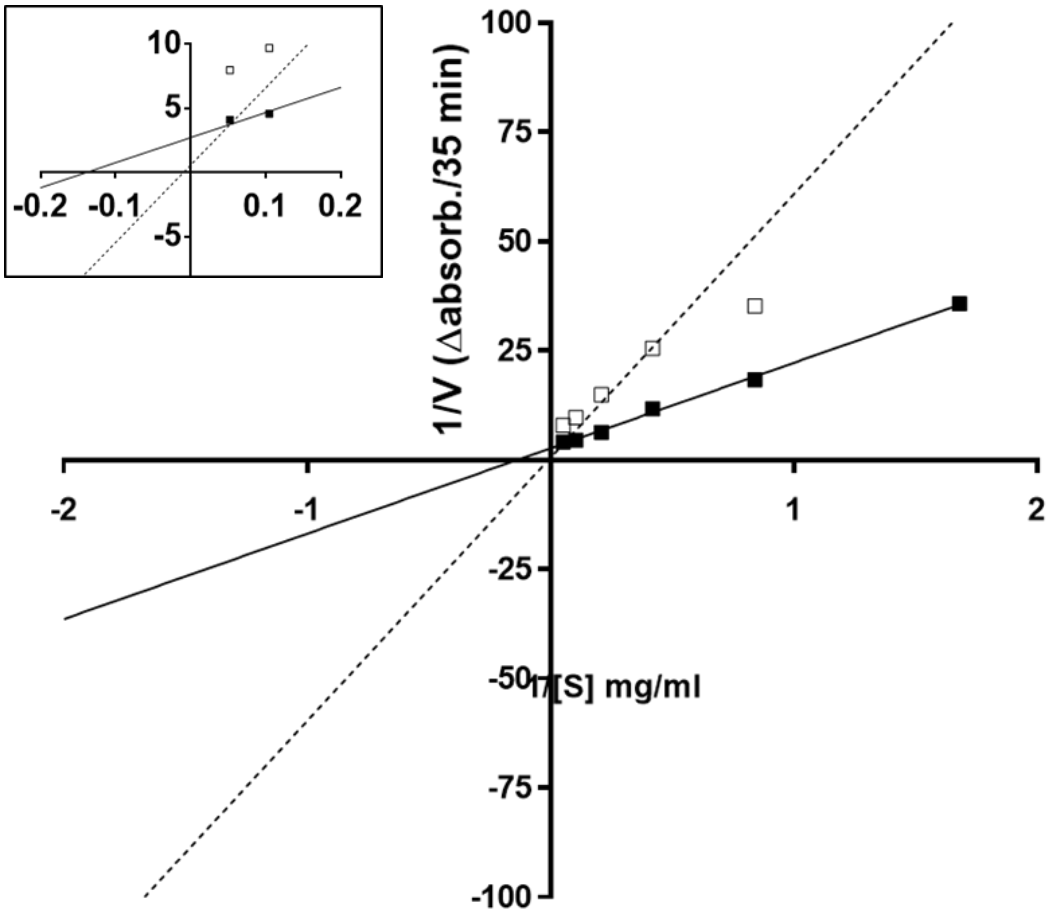

Figure 3.11. Lineweaver-Burk plot for lipase control (■) and lipase with 1LF80 alginate (□) solutions. The lipase control consists of 0.048 mg/ml lipase with different concentrations of substrate (19.05-0.59 mg/ml), whereas the lipase treated with alginate consists of 4.8 mg/ml of 1LF80 and 0.048 mg/ml lipase with substrate at different concentrations (19.05-0.59 mg/ml). Velocity is expressed as the change in absorbance over 35 minutes where the reaction at this time point was still close to the linear phase. Values are mean ± SD., n=4. The absorbance was read at 405 nm every 5 min for 55 minutes. The insert shows a magnified view of the x- and y-intercepts of the Lineweaver-Burk plot.

The Maximum velocity (V_{max}) and Michaelis constant (K_m) calculated from the Michaelis-Menten plots for all three alginates are shown in Table 3.2. The apparent V_{max} and K_m values for each biopolymer obtained from the Michaelis-Menten plot were compared to the V_{max} and K_m values of lipase control where no alginate was added to the reaction mixture.

Adding CC01, 1N80, or 1LF08 alginate to the reaction mixture reduced lipase activity and allowed the reaction to approach the apparent V_{max} at lower point compared with the V_{max} of control (Table 3.2). Moreover, there was a subsequent reduction in the apparent K_m value following the addition of CC01 or 1N80 alginate to the reaction mixture, indicating that the presence of CC01and 1N80

increased the enzyme binding affinity for substrate to form ES-complex. The K_m constant is derived from rate of breakdown of ES complex divided by the rate of formation of ES complex, so alteration of this will change K_m.

In contrast, the presence of 1LF80 in the reaction mixture increased the apparent K_m; the larger K_m suggests less ES complex will be formed, and there is a high possibility for the substrate to dissociate from the active site of the enzyme to free enzyme and free substrate.

Sample	Apparent Kinetic Constants		95% Confidence Intervals	
	V_{max} (Δ OD/ 35 min)	K_m (mg/ml)	V_{max} (Δ OD/ 35 min)	K_m (mg/ml)
Lipase control	0.328	5.674	0.242 to 0.433	3.163 to 10.61
CC01	0.084	3.334	0.059 to 0.131	1.129 to 10.36
1N80	0.145	4.865	0.095 to 0.289	1.427 to 21.08
1LF80	0.178	7.67	0.109 to 0.468	2.231 to 41.45

Table 3.2. Michaelis Menten kinetic parameters for lipase control and lipase inhibited by 4.8 mg/ml of alginates.

The type of inhibition caused by alginate based on the V_{max} and K_m constants calculated from Lineweaver-Burk plots are shown in Table 3.3. Obviously, there was an apparent reduction in the V_{max} and K_m values for CC01 or 1N80 compared with the V_{max} and K_m values of lipase control, also, the best-fit lines of these two biopolymers (Figure 3.7 and Figure 3.9) from Lineweaver-Burk plot crossed the x-axis at different points, showing that adding either CC01 or 1N80 caused a mixed inhibition.

The type of inhibition caused by 1LF80 could not be defined directly from the Lineweaver-Burk plot due to negative values for V_{max} and K_m. Therefore, the type of inhibition caused by this biopolymer was assessed from the V_{max} and K_m values of Michaelis-Menten plot based on the fact that the kinetic constants V_{max} and K_m for the alginates CC01 and 1LF80 obtained from Michaelis-Menten and Lineweaver-Burk plots showed similar values. The Michaelis-Menten kinetic data for the 1LF80 biopolymer (Table 3.2) showed an apparent decrease in V_{max} and an increase in K_m in

the presence of biopolymer compared with those values for lipase control which was free of 1LF80. In addition, the best-fit lines from Lineweaver-Burk plots (Figure 3.11) crossed close to the origin of x-y axis, suggesting that the 1LF80 may act as a mixed inhibitor in this reaction.

Sample	Lineweaver-Burk Plot Intercepts		Apparent Kinetic Parameters		Type of inhibition
	y-intercept (ΔAbsorb./ 35 mins)	x-intercept (mg/ml)	V_{max} (ΔAbsorb./ 35 mins)	K_m (mg/ml)	
Lipase control	2.711	- 0.138	0.369	7.194	No inhibitor was added
CC01	8.930	- 0.180	0.112	5.524	Mixed inhibition
1N80	6.272	- 0.169	0.159	5.917	Mixed inhibition
1LF80	-0.565	0.009	- 1.770	- 111.11	Unknown from the Lineweaver-Burk plot.

Table 3.3. Lineweaver-Burk Kinetic parameters for lipase control and lipase inhibited by 4.8 mg/ml of alginates.

The obtained kinetic information from Michaelis-Menten and Lineweaver-Burk plots showed that CC01, 1N80, and 1LF80 alginates were acting as mixed inhibitors where each biopolymer has the ability to bind to the free E (with dissociation constant K_I) and ES complex (with dissociation constant K_{I}). However, the enzyme binding affinity for the free E and ES complex is unequal (Equation 3.6).

$$
\begin{array}{ccc}
E + S & \rightleftarrows & ES \rightleftarrows E + P \\
+ & & + \\
I & & I \\
K_I \downarrow\uparrow & & \downarrow\uparrow K_{\acute{\imath}} \\
EI & & ESI
\end{array}
$$

Equation 3.6. Enzyme-catalysed reaction in the presence of a mixed inhibitor.

The inhibition constant (K_I or K) is usually calculated to evaluate the potency of an inhibitor where the higher the inhibition constant value, the weaker the inhibitor and higher concentration is required to yield 50% of maximum inhibition. The CC01, 1N80 and 1LF80 biopolymers were classified as mixed inhibitors, and this type of inhibition usually shows the characteristics of two types of inhibition (uncompetitive and non-competitive inhibition), therefore, the K_I and $K_{\acute{\imath}}$ constants for each biopolymer were calculated to determine the predominant characteristic of inhibition by comparing binding affinity to the free E and ES complex through the values of their inhibition constants. The K_I and $K_{\acute{\imath}}$ are usually calculated from the V_{max} and K_m of Lineweaver-Burk plot. However, the V_{max} and K_m obtained from the Lineweaver-Burk plot gave invalid negative values for 1LF80, so the K_I and $K_{\acute{\imath}}$ were calculated from the V_{max} and K_m of the Michaelis-Menten plot. Both K_I and $K_{\acute{\imath}}$ were calculated from the V_{max} and K_m values of lipase control and the apparent V_{max} and K_m values of the alginate using the mixed inhibition equation presented in Table 3.1.

The kinetic inhibition constants K_I and $K_{\acute{\imath}}$ calculated from Michaelis-Menten or Lineweaver-Burk plots for the different alginates were similar (Table 3.4). The mixed inhibition caused by CC01 and 1N80 showed more uncompetitive-like characteristics by their greater binding affinity to the ES complex than the free enzyme. The greater binding affinity of inhibitor toward the ES complex was shown by the smaller K_{ib} compared to the K_{ia}.

However, the K_I of 1LF80 was less than the $K_{\acute{\imath}}$, indicating that the inhibitor had a higher binding affinity to the free enzyme. The smaller the inhibition constant (K_I or $K_{\acute{\imath}}$), the higher the affinity.

Sample	K_I (mg/ml)	$K_{í}$ (mg/ml)	Type of lipase inhibition
CC01	3.71 [3.14]	1.65 [2.09]	Mixed inhibition which showed more uncompetitive-like characteristics
1N80	5.11 [5.28]	3.80 [3.63]	Mixed inhibition which showed more uncompetitive-like characteristics
1LF80	3.22 [unknown]	5.59 [unknown]	Mixed inhibition which showed a higher affinity for the free enzyme.

Table 3.4. Kinetic inhibition constants (K_I and $K_{í}$) calculated from the V_{max} and K_m of both Michaelis-Menten and Lineweaver-Burk plots. The values in brackets represent K_I and $K_{í}$ values calculated from Lineweaver-Burk plot. The K_I and $K_{í}$ represent the binding affinity of inhibitor for the free enzyme and enzyme-substrate complex, respectively.

The correlation between the apparent V_{max} or K_m of biopolymers obtained from the Michaelis-Menten plots and their fraction of fraction of guluronate residues (F[G]) was investigated. There was a significant negative correlation ($P<0.005$) between the Vmax and F(G) where the maximal reaction velocity is lower in the presence of alginates with increased fraction of guluronate residues (Figure 3.12). Data from ^{1}HNMR analysis of alginates in Chapter 2 of this thesis (Table 2.5 in results section) showed that CC01 had the highest content of G blocks and this could explain its capability to reduce the V_{max} of reaction to level much greater than the 1N80 and 1LF80. There was a negative correlation between K_m and F(G) alginate with high fraction of guluronate residue, however, this correlation was not significant ($P>0.05$) (Figure 3.13).

For mixed inhibition, the apparent $K_{m,}$ which is represented by $K_{m\,app}$, is calculated as the following:

$$K_{m_{app}} = \frac{1 + \left[\frac{[I]}{K_I}\right]}{1 + \left[\frac{[I]}{K_{í}}\right]}$$

As the concentration of inhibitor [I] is constant, then for the $K_{m\,app}$ to decrease, the K_I must be larger than the $K_{í}$ as with CC01 and 1N80 alginates. However, if the $K_{í}$ is greater than the K_I, then the K_m will apparently increase as with 1LF80 alginate.

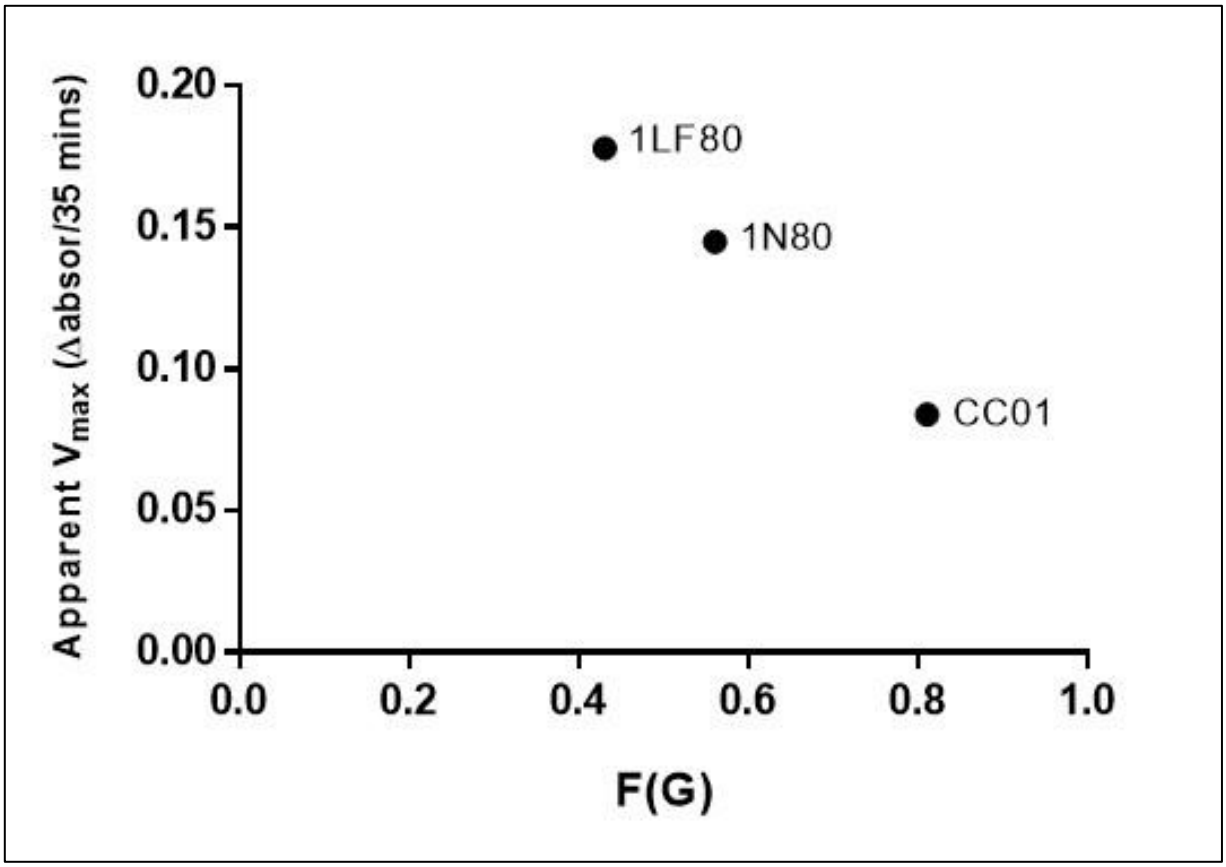

Figure 3.12. Correlation between apparent V_{max} of alginates and their fraction of guluronate residues (F[G]). V_{max} was calculated from Michaelis-Menten plots. A negative correlation between V_{max} and F[G] was seen with a Pearson coefficient r of -0.99 and a $P<0.05$.

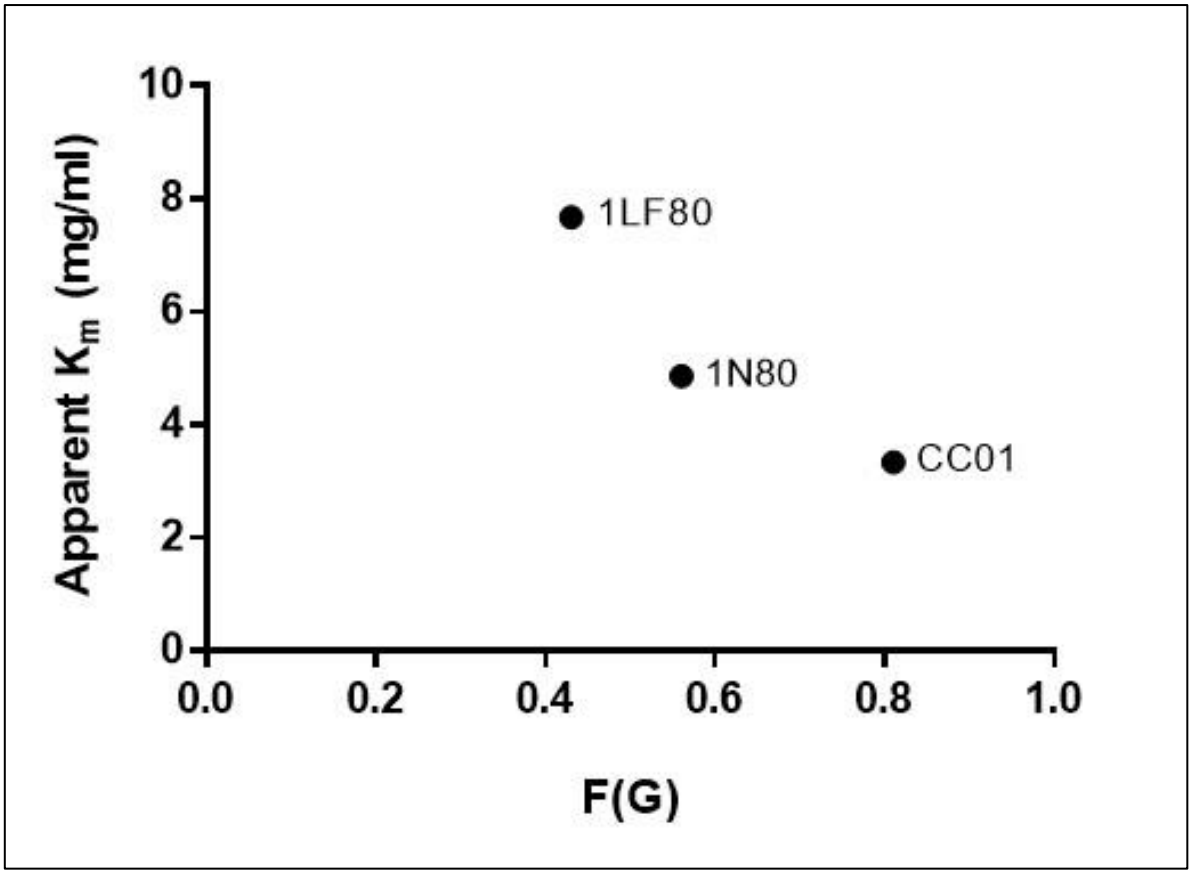

Figure 3.13. Correlation between apparent K_m of alginates and their fraction of guluronate residues (F[G]). K_m was calculated from Michaelis-Menten plots. A negative correlation between K_m and F[G] was seen with a Pearson coefficient r of -0.93 and a p->0.05, indicating that the correlation was insignificant.

3.6 Discussion

The investigations of enzyme kinetics aimed to define the regulatory effect of alginate on enzyme-substrate affinity (K_m) and the maximum velocity (V_{max}) of reaction by comparing their kinetic parameters with those of the lipase control.

Kinetic data showed that adding CC01, 1N80, or 1LF80 alginates into the reaction mixture decreased the velocity of reaction at all substrate concentrations compared to the reaction velocity in the absence of alginate at the same substrate concentrations. Also, the presence of alginate allowed the reaction to reach the V_{max} at a lower point compared to the V_{max} of lipase control, indicating that the algal bioactive could inhibit lipase activity. This result is in agreement with the Wilcox et al. study (2014) which reported that alginate can reduce pancreatic lipase activity *in vitro*. The inhibitory effect of alginate on pancreatic lipase is not limited only to alginate bioactives, other studies have shown that other algal bioactive compounds such as fucoxanthins and its metabolite fucoxanthinols [96], phlorotannins [95], alginates, polyphenols and fucoidans [97] can reduce the activity of pancreatic lipase *in vitro*.

There was a significant negative correlation between the apparent V_{max} and alginate's frequency of gluconate residues where CC01 reduced the maximum velocity of lipase more than 1N80 and 1LF80 biopolymers. ^{1}H NMR data presented in Chapter 2 of this thesis showed that CC01 has the highest content of G, GG, and GGG residues compared with 1N80 and 1LF80. In addition, the data from the lipase activity assay in Chapter 2 of this thesis showed that CC01 had the ability to reduce pancreatic lipase activity to a much greater extent than the other two biopolymers. This finding is consistent with the Wilcox et al. study (2014) which showed that alginate rich in G, GG, and GGG residue inhibited pancreatic lipase activity *in vitro* more than alginate rich in M and MM residues, demonstrating a positive correlation between alginate content of G block and inhibition level. Therefore, the highest inhibitory effect of CC01 on lipase velocity could be due to its greatest content of G blocks.

Alginates rich in G blocks produce strong and stiff gels compared to alginate rich in M blocks which produce softer and more flexible gels [159, 160]. It has been stated that alginate has the ability to bind to the enzyme itself and this binding is limited on alginate rich in G block. Alginate with high content of G residue exhibits binding affinity to the protein part of mucin, however, alginate rich in M blocks will not bind to the protein [139]. Additionally, it has been suggested that

hydroxyl groups of G block in alginate can protonate serine and histidine residues at the active site of pancreatic lipase, reducing proton shuttle mechanism which is an essential mechanism for activation of pancreatic lipase; this is supposed to be the mechanism by which pectin inhibits the pancreatic lipase [72, 144]. This could explain the highest level of lipase inhibition achieved by CC01 alginate.

According to the V_{max} and K_m constants obtained from Lineweaver-Burk plots of CC01 and 1N80 biopolymers, both biopolymers were classified as mixed inhibitors since their presence in the reaction mixture caused an apparent reduction in the V_{max} and K_m values compared to the V_{max} and K_m of lipase control. However, the type of inhibition produced by the 1LF80 alginate could not be identified from the Lineweaver-Burk plot since both V_{max} and K_m constants calculated from the Lineweaver-Burk plot showed negative values which cannot be interpreted. These unexpected negative values may appear due to the effect of experimental error in this type of plots where the lowest concentrations of substrate usually have the largest experimental error. Therefore, the type of inhibition caused by the 1LF80 was determined using the V_{max} and K_m constants calculated from Michaelis-Menten plot and according to theses calculated constants, 1LF80 was classified as a mixed inhibitor. The K_I and $K_{I'}$ of mixed inhibition were determined here in an attempt to determine the predominant form of inhibition through evaluation of inhibitor binding affinity to the free enzyme and the ES-complex.

Both K_I and $K_{I'}$ data showed that there was no difference between the inhibition constants of CC01 or 1N80 obtained either from the Michaelis-Menten or Lineweaver-Burk plots. Additionally, the data showed that all the three biopolymers had the ability to bind the free enzyme and the ES-complex unequally. However, CC01 and 1N80 alginates showed more uncompetitive-like characteristics by their greater binding affinity to the ES-complex than the free enzyme where the $K_{I'}$ (the inhibitor binding affinity to the ES-complex) values were less than the K_I (the inhibitor binding affinity to the free enzyme). Therefore, these lower $K_{I'}$ values of CC01 and 1N80 suggested that the two biopolymers bound tightly to the enzyme-substrate complex, and their probability to dissociate is low.

In contrast, the K_I and $K_{I'}$ data for 1LF80 showed that the biopolymer had the ability to bind the free enzyme as well as the ES-complex with a greater binding affinity for the free enzyme than the ES-complex which hindered the transformation of substrate and reduced the rate of product

formation, showing that 1LF80 caused a mixed inhibition.

In mixed inhibition shown here, there are many possible mechanisms by which the inhibitor (biopolymer) can bind to the free enzyme (E) and the enzyme-substrate (ES) complex. The inhibitor can bind the free enzyme at a site different from the active site (allosteric site) forming enzyme-inhibitor (EI) complex preventing the substrate binding to the enzyme active site (Figure 3.14A). The inhibitor binding to a site different to the active site induces some conformational changes in the enzyme shape which in turn reduces the effectiveness of active site. Binding of the inhibitor to the free enzyme reduces the turnover number (K_{cat}) and $V_{max.}$ The turnover number can be defined as the number of substrate molecules that can be converted to the product molecules by a single enzyme over a period of time.

The inhibitor can also bind to the ES-complex where the substrate first binds to the active site of enzyme, forming the ES complex, and inducing some alterations in the structure of enzyme and that could either expose the inhibitor binding site which already exists, hence the inhibitor can bind to this site (Figure 3.14B), or creates a new binding site which did not exist previously (Figure 3.14C). This is the only mechanism by which an uncompetitive inhibitor works.

In uncompetitive inhibition, the inhibitor binds only to the ES-complex since the binding of substrate to enzyme creates a new binding site for inhibitor, allowing the inhibitor to bind, and form the ESI complex. However, binding the inhibitor to ES complex reduces concentration of an active ES complex in the reaction mixture and increases the concentration of inactive ESI complex. In uncompetitive inhibition, the V_{max} is decreased due to the binding of inhibitor to the ES complex which causes a reduction in the concentration of an activated ES complex available in the mixture, also, the reduction in ES complex decreases the $K_{m.}$ Both CC01 and 1LF80 are mixed inhibitors, however, they showed more uncompetitive inhibition like characteristic by greater binding affinity to the ES complex, as well as the reduction in their V_{max} and K_m values.

Many mechanisms have been suggested for pancreatic lipase inhibition by alginate, however, the exact mechanism by which the alginate inhibits the activity of pancreatic lipase is still unknown. It has been assumed that alginate can bind to both the free enzyme and the substrate. Alginate can interact with glycoproteins, such as mucin, and this binding has been detected using rheological measurements over a range of mucin: alginate ratios [139]. Alginate with high content of G residues

has the ability to bind to mucin at particular positions within the protein core, linking many mucin molecules together and producing a gel. However, alginate with high content of M units did not interact and link mucin molecules together, indicating that the G blocks are very important for mucin-alginate binding [139].

Alginate also may bind to the lipid/water interface of substrate, decreasing the access of the enzyme to substrate interface. This is assumed to be the mechanism by which other effective inhibitors such as chitosan, DEAE sephadex and DEAE polydextrose inhibit pancreatic lipase activity. However, these inhibitors are cationic molecules while alginate is anionic [91, 150].

Pectin inhibits lipase by binding to the free enzyme, causing serine and histidine residues present in the active site to become protonated, resulting in reduced enzyme activity [144]. It is supposed that the carboxyl groups of pectin are responsible for protonation of serine and histidine in the lipase active site [141]. The same authors reported that increasing esterification of pectin reduced its inhibitory effect on pancreatic lipase activity since pectin esterification involves replacing the carboxyl groups with methyl groups which in turn reduces the number of carboxyl groups responsible for protonation of serine and histidine in the active site of enzyme [141]. It was assumed that alginate may also inhibit pancreatic lipase activity in the same way where the carboxyl groups in G block of alginate are in identical sites to that of carboxyl groups of pectin which explains how both can bind calcium ions [72].

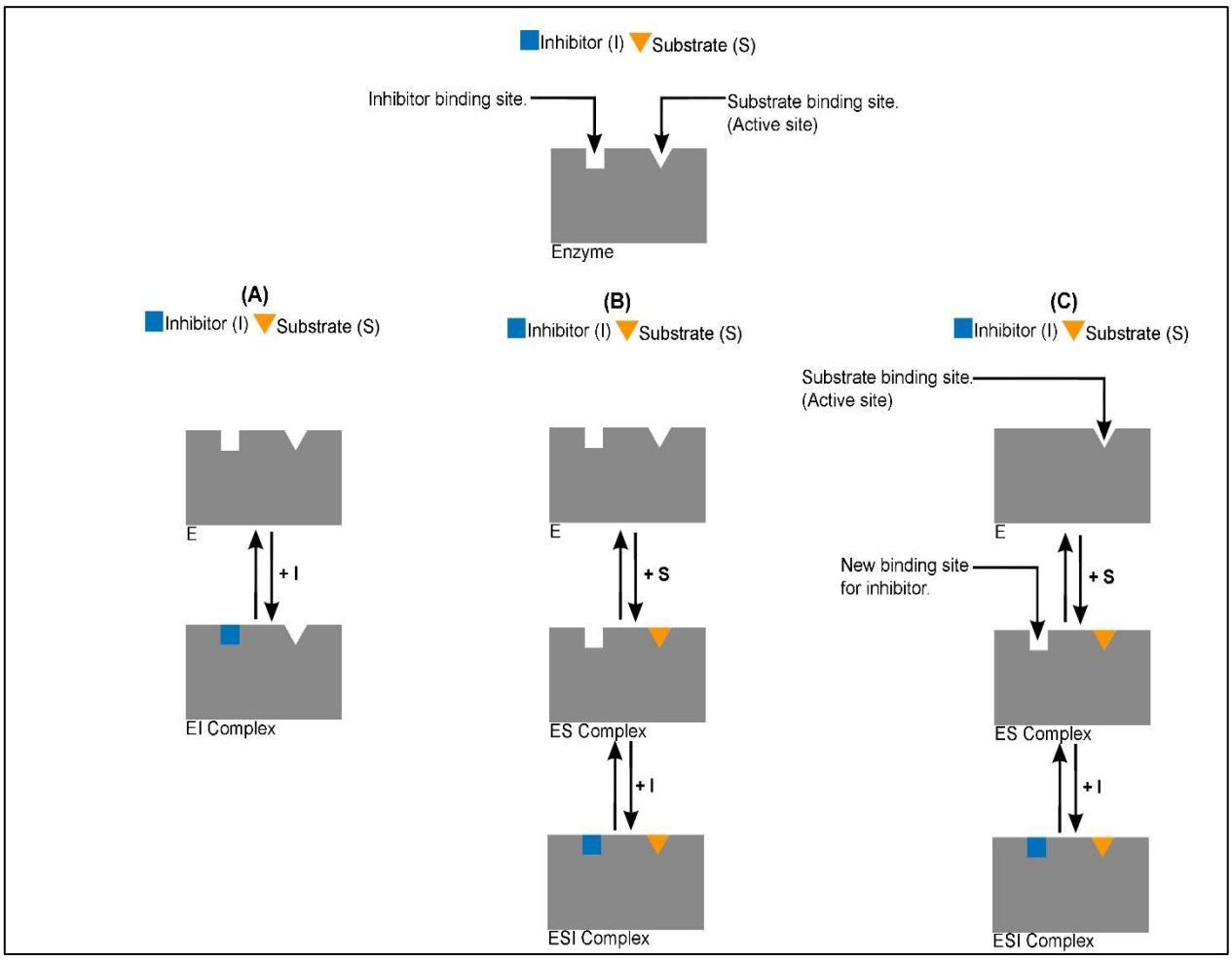

Figure 3.14. Schematic diagram showing mechanisms of mixed inhibition.(A) The inhibitor can bind to the free enzyme at a site different from the active site, forming enzyme-inhibitor complex (EI) and inducing some changes in enzyme structure. Consequently, the effectiveness of active site is reduced. (B) The enzyme has two sites: substrate binding site and an inhibitor binding site. The substrate can bind at the active site of enzyme, forming ES complex, causing some conformational changes in the structure of enzyme, and exposing the inhibitor binding site; hence, the inhibitor can bind to this site producing ESI complex. (C) The substrate binds to an enzyme active site, forming an enzyme-substrate (ES) complex, inducing some conformational changes in the enzyme shape. Subsequently, a new binding site is created, and the inhibitor can bind to this site forming ESI complex.

3.7 Conclusion

The kinetic information obtained here showed that CC01, 1N80, and 1LF80 reduced reaction velocity, allowing the reaction to reach a V_{max} at lower substrate concentration. Alginate content of G blocks positively correlated with the inhibitory effect on lipase activity. Additionally, all three biopolymers used here acted as mixed inhibitors where they had the ability to bind the free enzyme and ES-complex with different binding affinities. Moreover, both CC01 and 1N80 biopolymers showed more uncompetitive-like characteristics by their greater binding affinity to the ES complex. However, the 1LF80 biopolymer showed a trend of inhibition with greater binding affinity to the free enzyme than the ES complex.

Chapter 4: Fat Digestion within the Synthetic Model Gut System

4.1 Overview of the synthetic model gut

The digestion and absorption of dietary lipids are associated with health and the development of metabolic diseases such as obesity. Several previous studies have confirmed that alginates can inhibit pancreatic lipase activity *in vitro* by 72.2 (±4.1) %, thus reducing the energy derived from high calorie foods and potentially preventing the development of obesity [72, 161]. Furthermore, experimental data from previous investigations of the inhibitory effects of alginate on pancreatic lipase activity (Chapter 2), using a modified version of Vogel and Zieve (1963), showed that all the tested alginate samples inhibited the activity of pancreatic lipase with different levels of inhibition [122]. Alginates CC01, 1N80 and 1LF-80 possessed the highest inhibitory effects where they significantly inhibited lipase activity by 75.6 (± 10.6), 62.7 (± 20), and 53.7 (± 8.5) %, respectively. Therefore, further investigation was carried out to study the inhibitory effects of these alginates on lipase activity *in vitro* using a synthetic model gut system developed at Newcastle University. The model gut system aims to imitate *in vivo* digestive processes from mouth to terminal small intestine in a physiologically relevant manner, and thus the enzymatic and chemical digestive processes of these macromolecules can be studied.

The developed model gut system consists of three synthetic gastrointestinal fluids (saliva, gastric juice and pancreatic juice) and porcine bile. The synthetic gastrointestinal fluids are not buffered, and are prepared at different pH to mimic the pH and ionic content of the relevant section of the gastrointestinal tract *in vivo* [162]. In the present study, three fat substrates (glyceryl trioctanoate, olive oil and sunflower oil) were used alone as controls for fat digestion, whereas the model gut (MG) solution without substrate, which consists of synthetic saliva in deionised water (DH_2O), was used as a background control. The values measured for the background control were subtracted from those for the digestion of the fat substrate to account for any interference from digestive fluids. The effect of three alginate samples CC01, 1N80, and 1LF80, which were supplied by the Coca-Cola and Ruitenberg companies, on the activity of pancreatic lipase have been studied because the two companies are interested in producing products containing alginates in an attempt to reduce caloric intake. In this chapter, the effects of these alginates, which could inhibit lipase activity in the turbidity assay as shown previously in Chapter 2 of this study, were analysed in the synthetic model gut system.

4.2 Aims

The data from the turbidity assay which were presented in Chapter 2 show that CC01, 1N80 and 1LF80 alginates reduce pancreatic lipase activity at different rates depending on their source and content of G- and M-blocks. Therefore, the aims of this chapter were:

- To study the overall effects of different amounts of the alginates (CC01, 1N80 and 1LF80) on fat digestion *in vitro* using a synthetic model gut system to determine whether the alginates can inhibit pancreatic lipase activity and slow the subsequent digestion of fat. The model gut system allows samples to be collected at different time points, thus enabling measurement of the amount of glycerol liberated to assess whether the fat substrates undergo digestion and to evaluate whether there is any significant difference between the amount of glycerol liberated from the digestion of fat substrate alone (as a control) and those released from the digestion of fat substrate treated with alginate

- As many studies have suggested that fats are digested at different rates depending on fatty acid chain length, the digestion rates of three fat substrates with different level of fatty acid chain length: glyceryl trioctanoate (medium-chain triglycerides), olive oil (a mixture of long-medium chain triglycerides), and sunflower oil (long-chain triglycerides) were assessed here using the model gut to determine which fat substrates have the highest digestion rate, and whether there is a link between fatty acid chain length and digestion rate.

- To investigate the impact of pH on the capacity of alginate to inhibit pancreatic lipase where the pH of alginate solutions within the synthetic model gut was measured at different time points of the gastric and small intestinal phases.

- To assess the regulatory effect of different amounts of CC01 alginate on olive oil digestion in vitro using a buffered salivary diluent containing 372mM $NaHCO_3$ instead of 62mM $NaHCO_3$ in an attempt to avoid acidic pH found in the stomach and subsequent gelling of alginate.

4.3 Methods

4.3.1 Materials

All chemicals and enzymes used in the synthetic model gut experiments were purchased from Sigma-Aldrich. Pig bile was obtained fresh from a local slaughterhouse. Olive oil and sunflower oil were purchased from a local supermarket (Cooperative Food, UK). The alginate sample CC01 was provided by Coca-Cola, whereas 1LF80 and 1N80 alginates were supplied by Ruitenberg, based in the Netherlands.

4.3.2 Preparation of synthetic gastrointestinal fluids

The fluids of the synthetic model gut were prepared prior to use as stock solutions, and the enzymes were added immediately before passing the sample in the model gut.

- Synthetic Salivary diluent (pH 7.4): Salivary diluent was composed of 62mM $NaHCO_3$, 6mM K_2HPO_4, 15mM NaCl, 6.4mM KCl and 3mM $CaCl_2.2H_2O$. For experiments, 1µl/ml α-amylase salivary diluent was prepared. Then, DH_2O was added to the salivary diluent containing α-amylase in 1:1 ratio to prepare the synthetic saliva.

- Synthetic Gastric diluent (pH 1-2): Gastric diluent consisted of 49.6mM NaCl, 9.4mM KCl, 2mM KH_2PO_4 and 5mM Urea in DH_2O. The gastric enzymes included 400 U/L gastric like lipase from bacteria – (Amano Enzyme Inc AP12), which is active at pH 2, and porcine pepsin (0.5 mg/ml).

- Synthetic Pancreatic Diluent (pH 8.0): Pancreatic Diluent was composed of 110mM $NaHCO_3$, 2.5mM K_2HPO_4, 54.9mM NaCl, 1mM $CaCl_2.2H_2O$ and 1.67mM Urea dissolved in DH_2O. For the pancreatic enzyme preparation, pancreatin was added fresh into the pancreatic diluent (70 mg/ml). However, because triglycerides of glyceryl trioctanoate produce fatty acids with low pKa (i.e. octanoic acids which have pKa 4.9), the pancreatic diluent used with this substrate (glyceryl trioctanoate) was made with a higher amount of $NaHCO_3$, 322.8 mM, to avoid the low pH which can result from liberation of these fatty acids (Table 4.1).

- Fresh porcine bile (pooled): Bile was collected from 10 – 20 porcine gall bladders. The bile was stored in 75 ml containers at –20 ˚C until required.

Triglyceride	Fatty Acid	Fatty Acid pK_a
Glyceryl Trioctanoate	Octanoic Acid (Caprylic Acid)	4.9
Olive Oil	Oleic Acid	9.85
Sunflower Oil	Linoleic Acid	9.24

Table 4.1. Characteristics of triglyceride substrates processed in the synthetic model gut system.

4.3.2.1 Synthetic model gut sample preparation

- Fat substrate alone as a control: Three different triglycerides (glyceryl trioctanoate, olive oil, and sunflower oil) with different fatty acid chain lengths were tested in a synthetic model gut. Each fat substrate sample was prepared by adding 5 ml of DH_2O into 5 ml of synthetic saliva and 5 ml of the substrate (glyceryl trioctanoate, olive oil or sunflower oil), giving a total volume of 15 ml.

- Fat substrate solution: Contained 5 ml fat substrate, 5 ml saliva, and 5 ml DH_2O.

- Model gut solution (MG) as a background control: Prepared by adding 5 ml of synthetic saliva into 10 ml of DH_2O. MG solution absorbance was subtracted from substrate absorbance to correct any interference in the model gut system.

- Alginate with fat substrate**:** Prepared by adding 250, 500 or 1000 mg of alginate (CC01, 1N80 or 1LF80) into a beaker containing 5 ml fat substrate, 5 ml DH_2O, and 5 ml synthetic saliva.

- Alginate in MG solution: Prepared by adding the alginates into a mixture consisting of 10 ml DH_2O and 5 ml of synthetic saliva. This was used as a background for alginate. The absorbance of alginate in the MG was subtracted from alginate/fat substrate absorbance to correct any alginate interference in the synthetic model gut.

4.3.3 Synthetic Model Gut System Procedure

The synthetic model gut system consists of two water baths (Figure 4.1). Artificial gastrointestinal fluids (gastric and pancreatic juices) as well as porcine bile were pre-incubated in water bath 1 at 37 °C. Four beakers (each 600 ml volume) containing fat substrate alone, MG solution, fat substrate with alginate, or alginate in MG solution were placed in water bath **2** at 37 °C. A Watson Marlow Peristaltic pump was adjusted to a rate of 0.5 ml/min to pump artificial gastric and pancreatic juices into the beakers containing samples. Four lab-egg overhead compact stirrers were used for mixing the samples and artificial fluids.

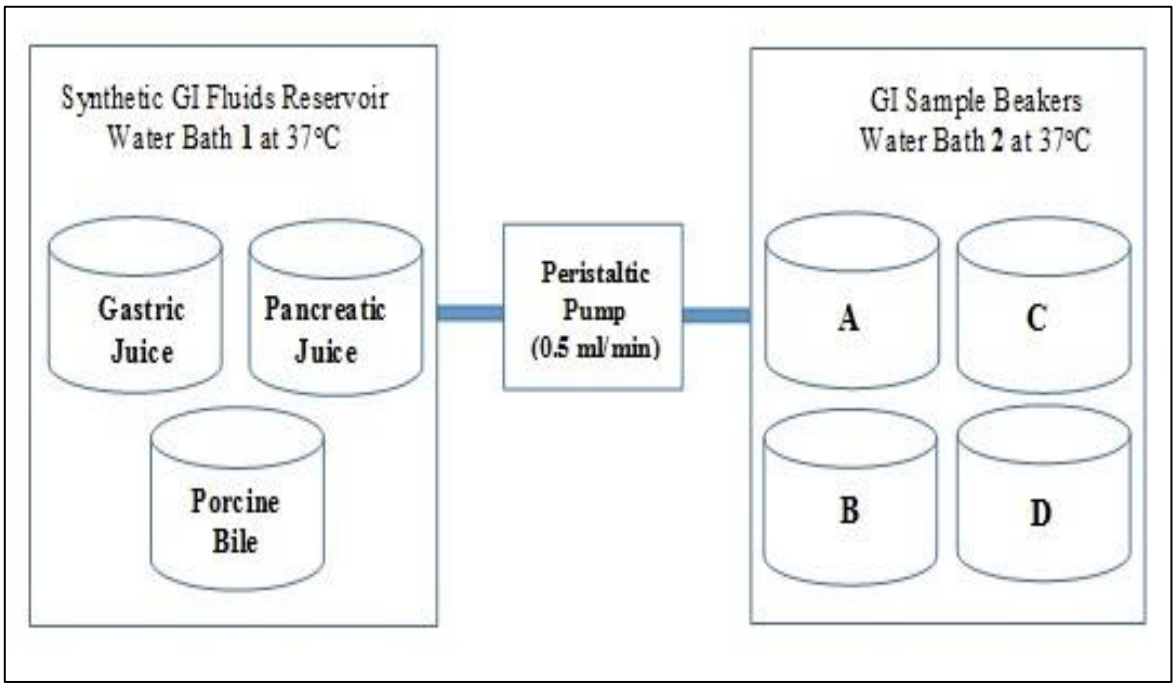

Figure 4.1. Schematic diagram for model gut system set up. Water bath 1 contains the gastrointestinal fluids. Water bath 2 contains the sample solutions. A represents fat substrate alone, B represents model gut (MG) solution alone, C represents fat substrate with alginate, and D represents alginate in MG solution.

The samples digestion process within the synthetic model gut system involved three stages: salivary phase (mouth), gastric phase (stomach) and small intestinal phase (small intestine). For the salivary phase preparation, 5µl of α-amylase was added fresh to 5ml of salivary diluent and 5 ml of DH_2O. For the gastric phase preparation, 150 mg and 12 mg of pepsin and gastric lipase, respectively, were added fresh into 300 ml of gastric diluent. For the pancreatic phase preparation,

21 g pancreatin was added fresh into 300 ml of pancreatic diluent, then the mixture was mixed using a magnetic stirrer. After that, the pancreatic juice was filtered using glass wool to remove insoluble proteins and lipids present in the pancreatin.

The salivary phase lasted for 10 minutes. The gastric phase started after adding 50 ml of gastric juice into the glass beakers containing samples, and the remaining synthetic gastric juice was pumped in at a rate of 0.5 ml/min for one hour. At 60 minutes, the gastric phase ended, and the pancreatic phase started when 25 ml of fresh porcine bile was added into the beakers. Finally, synthetic pancreatic juice was pumped in at a rate of 0.5 ml/min for two hours.

4.3.3.1 Model gut sample collection

500 µl samples were taken separately at time points T_0, T_{15}, T_{30}, T_{60}, T_{60T}, T_{75}, T_{90}, T_{120}, T_{150}, and T_{180} minutes. T_{60} represents the last sample taken from the gastric phase, whereas T_{60T} represents the first sample taken from the small intestinal phase. The samples were added immediately into 500 µl of 10% (w/v) trichloroacetic acid in DH_2O to stop enzymatic reactions and precipitate out the undigested substrate. Samples were stored at 4 ^{o}C overnight. After that, the samples were centrifuged at 10,000 rpm (9,300 g) for 10 minutes, and 5 µl of each supernatant was placed in duplicate in a 96-well microplate (Bio Tek, USA) for quantification of glycerol release. Then, the colourimetric glycerol assay was carried out by adding 80 µl of free glycerol reagent (Sigma-Aldrich) into the supernatants. After that, the plate was shaken and left at room temperature for 20 minutes to allow colour development. Finally, the absorbance was read at 550 nm and the amount of glycerol released from digestion of triglycerides was calculated as described below.

4.3.4 Quantification of glycerol

The colourimetric glycerol assay was used to quantify the glycerol released from fat (triglyceride) digestion. Free Glycerol Reagent (Sigma-Aldrich) uses coupled enzymatic reactions to produce a quinoneimine dye which absorbs at 550 nm. There was a positive correlation between the concentration of free glycerol in the sample and the absorbance. The amount of glycerol in the model gut samples was calculated from a standard curve for glycerol in DH_2O. At room

temperature, DH_2O was added to the free glycerol reagent in the ratio 4:1, respectively. Then, 2 mM glycerol in DH_2O was prepared as a glycerol standard and diluted to lower concentrations (1, 0.5, 0.25, 0.125. 0.062, and 0.031 mM). Next, 5 µl of each glycerol standard solution was placed in duplicate in the same 96-well microplate (Bio Tek, USA) as the sample supernatants. After that, 80 µl of the free glycerol reagent was added to each sample and standard, mixed and left for 20 minutes at room temperature until a pink colour developed. Finally, the plate was read at 550 nm and the concentration of glycerol in each sample determined from the standard curve. To correct any interference, the absorbance of the MG solution alone was subtracted from the absorbance of the control (fat substrate alone), whereas the absorbance of alginate in the MG solution was subtracted from the absorbance of fat substrate with alginate. The total amount of released glycerol at each time point was determined by multiplying by the total volume present in the model gut system at that time point. The glycerol released from digestion of each substrate was calculated as a mean of the total number of replicates.

4.3.5 pH measurements

All pH measurements were carried out at room temperature using a Martini Mi150 pH meter. The pH meter was calibrated using buffer solutions of pH 4 and 7. Then, the pH of fat substrate alone and in combination with alginate were measured at different time points of the gastric and small intestinal phases of the synthetic model gut.

4.4 Statistical analysis

Statistical calculations to evaluate the effectiveness of different amounts of three alginate samples (CC01, 1N80, and1LF80) in reducing fat digestion were carried out using Two-way Repeated ANOVA followed by a Post-Hoc Bonferroni test at a significance level (α) below 0.05 to compare between the amount of glycerol released from the digestion of fat substrates alone and the glycerol amount released from fat substrates in combination with alginates. Data have been displayed as mean and standard deviation (SD), and the number of replicates is demonstrated in each figure legend.

4.5 Results

4.5.1 Glycerol standard curve

Figure 4.2 illustrates the standard curve for glycerol in DH_2O using the free glycerol reagent. The data shows that there was an increase in the absorbance (0-0.21 OD) at 550 nm which was directly proportional to the increase in glycerol concentration (0.031-2 mM) with good linearity (R^2=0.99).

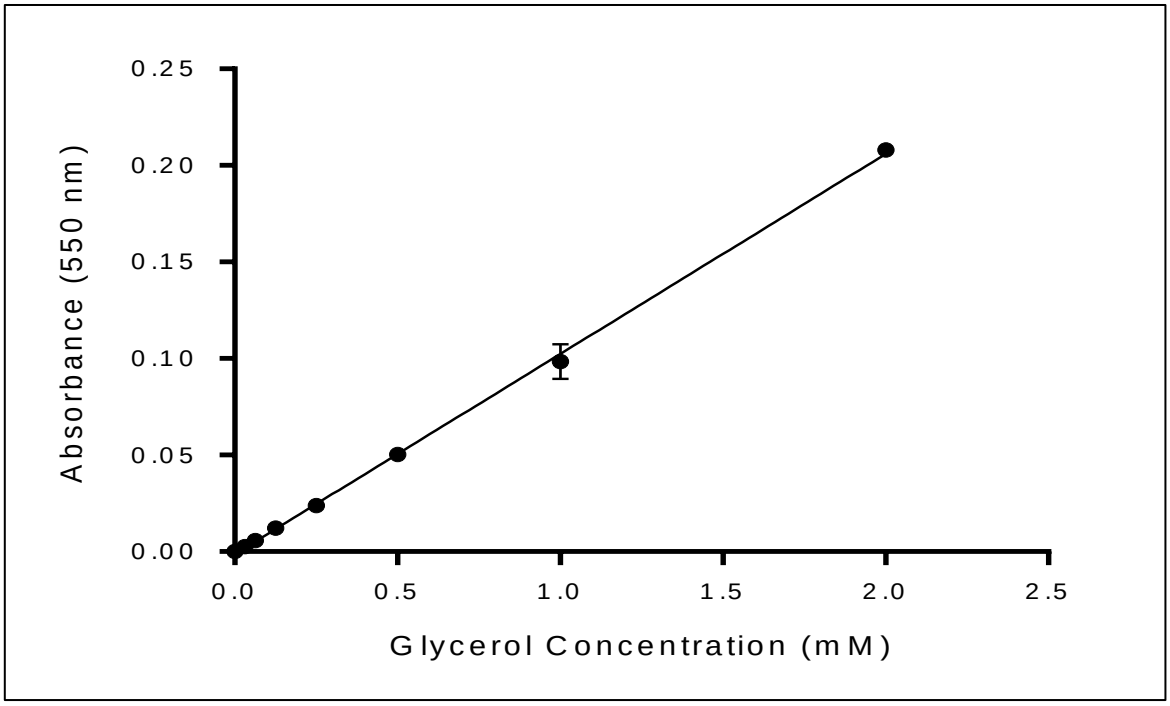

Figure 4.2. Standard curve of absorbance at 550nm against glycerol concentration in DH_2O. Values are mean, and the error bars are the standard deviation of six replicates (± SD, n=6).

4.5.2 Digestion of fat substrates within the synthetic model gut system

Figure 4.3 shows the gastrointestinal digestion of 5 ml glyceryl trioctanoate, olive oil and sunflower oil individually within the synthetic model gut system.

During the gastric phase (0-60 minutes), small amounts of glyceryl trioctanoate and olive oil were digested, where only 2.4 (±2.2) and 1(±0.9) mg of glycerol were released from glyceryl trioctanoate and olive oil digestion, respectively, at the end of the gastric phase. However, no glycerol was released from sunflower oil digestion during the gastric phase.

After 60 minutes, the small intestinal phase started when porcine bile was added, and the synthetic pancreatic juice was pumped into the samples. During the first 15 minutes of the intestinal phase, there was a significant increase in the digestion rate of glyceryl trioctanoate and 25.1 (±7.2), 51.3 (±6.8), 55.9 (5.3), and 61.3 (±7.7) mg of glycerol were released from glyceryl trioctanoate digestion at 90, 120, 150, and 180 minutes, respectively.

Also, the digestion rates of olive oil and sunflower oil began to increase after 15 minutes of the small intestinal phase reaching 5.4 (±3.9), 12.3 (±3.8), 22.1 (±7.7), and 35.4 (±8) mg glycerol from olive oil digestion and 2.8 (±0.33), 8.5 (±0.68), 16 (±0.02) and 24.9 ((±4.5) mg from sunflower oil digestion at 90, 120, 150, and 180 minutes, respectively.

There was a significant increase in the amount of glycerol released at the end of the small intestinal phase (at 180-minute) compared to the end of the gastric phase (at 60-minute), demonstrating that the majority of sunflower oil digestion occurred in the small intestinal phase.

Although the amount of glycerol released from glyceryl trioctanoate digestion was higher than that released from olive oil or sunflower oil digestion at all time points of the model gut procedure (Figure 4.3), a Post-Hoc Bonferroni test showed a significant difference ($P<0.05$) at 75, 90, 120, 150, and 180 minutes between the amounts of glycerol released from the digestion of glyceryl triocatonate and that released from olive oil or sunflower oil digestion at 75, 90, 120, 150, and 180 minutes of the model gut procedure. Also, although the amount of glycerol released from olive oil was higher than that released from sunflower oil digestion, this difference was statically significant ($P<0.05$) only at the end of the model gut system (at 180-minute).

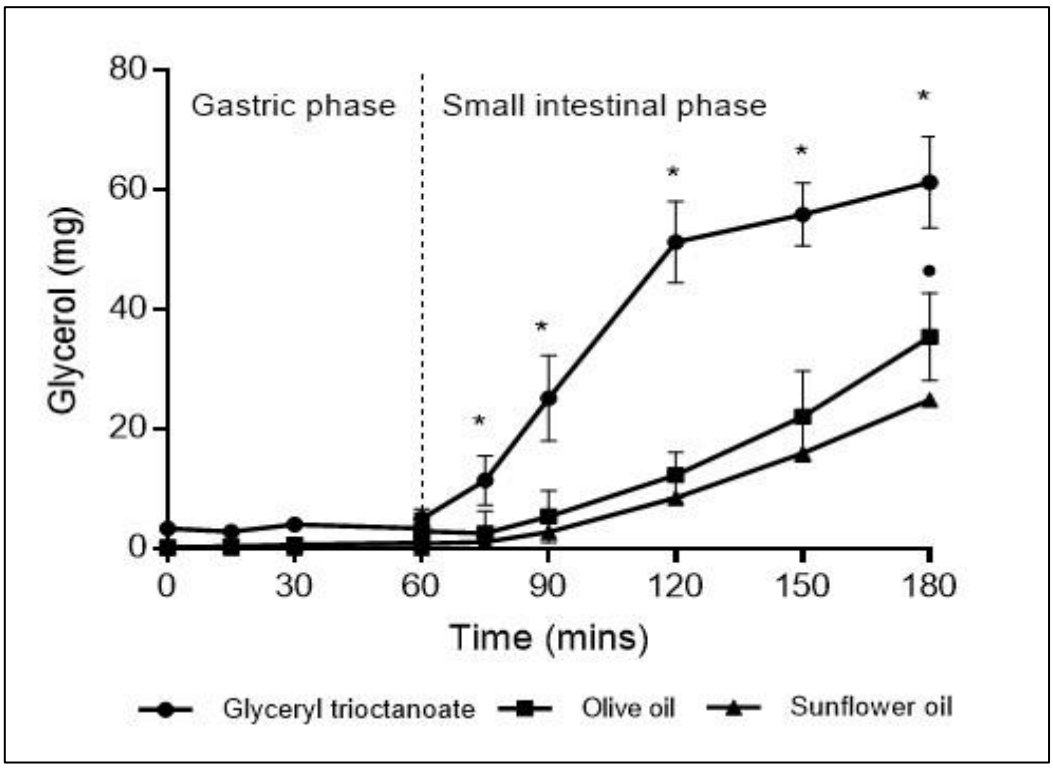

Figure 4.3. Release of glycerol over time from digestion of glyceryl trioctanoate, olive oil and sunflower oil within the synthetic model gut system. A significant difference ($P<0.05$) between the glycerol released from digestion of glyceryl trioctanoate and that released from olive oil and sunflower oil digestion, whereas • indicates a significant difference ($P<0.05$) between the glycerol released from digestion of olive oil and that released from sunflower oil digestion.

4.5.3 Evaluation of the variability of control fat substrates digestion in the model gut system

Table 4.2, Table 4.3 and Table 4.4 show the mean amounts of glycerol released from the simulated digestion within the synthetic model gut system for different repeats of 5 ml of glyceryl trioctanoate alone, olive oil alone or sunflower oil alone.

As can be shown from the Table 4.2, there was a variation between the amounts of mean glycerol released from the digestion of the several glyceryl trioctanoate controls at all time points of the gastric phase. The amounts of glycerol released from the digestion of different controls ranged between 0.16-4.97 mg at the end of the gastric phase (at 60-minute). During the small intestinal phase, there was also a variation between the amounts of glycerol released from the digestion of glyceryl trioctanoate controls at all time points. At 180 minutes the range of mean glycerol released from 5ml glycerol trioctanoate in the control digestions in the model gut system was 48.82-

66.15mg, this represents a 1 to 1.35 ratio between the lower and higher mean value.

The data presented in Table 4.3 shows that there was a variation between the amounts of mean glycerol released from the digestion of different olive oil controls during the gastric phase. During the small intestinal phase, there was also a difference between the amounts of glycerol released from the digestion of different olive oil controls at all time points, and the amounts of glycerol released for the different controls ranged between 24.95 and 46.90mg at the end of the small intestinal phase (at-180 minute), indicating a relatively high variation with a ratio of 1 to 1.88 between the lower and higher value.

The data in Table 4.4 demonstrate that there was a variation between the amounts of glycerol released from the sunflower oil controls during the gastric phase, and the amount of glycerol released ranged between 0.02-1.31mg. Also, varying amounts of glycerol were liberated from the digestion of different sunflower oil controls during the small intestinal phase, at the end of the small intestinal phase there was a range of 17.45-27.99 mg again indicating a relatively high variation with a ratio of 1 to 1.60 between the lower and higher value.

The variation between the amounts of glycerol released from the digestion of different samples of the same fat substrate (glyceryl trioctanoate, olive oil or sunflower oil) might be because of the use of different porcine bile samples in this set of experiments. The bile is composed of different substances such as bile salts, mucus, phospholipids, cholesterol, and bilirubin, and different bile samples contain different contents of these substances which may affect the digestion rate of fat substrate. Also, the variation between the amounts of glycerol released by the digestion of the same fat substrate may occur due to the difference in the synthetic gastrointestinal fluids (saliva, gastric and pancreatic juices). New synthetic gastrointestinal fluids were prepared for each set of experiments. Therefore, each experiment performed here has its internal control, which was carried out at the same conditions, to account for the differences in all these variables.

Time (mins)	Mean glycerol released from glyceryl trioctanoate digestion (mg)												
	Control 1	Control 2	Control 3	Control 4	Control 5	Control 6	Control 7	Control 8	Control 9	Control 10	Control 11	Control 12	Glycerol range (mg)
0	0.290	0.873	0.646	1.695	0.212	0.341	0.794	0.525	0.449	0.217	0.171	0.194	(0.17-1.69)
15	4.662	1.758	3.520	1.769	0.180	0.678	4.011	5.000	4.447	0.369	0.537	0.792	(0.18-5)
30	5.609	1.919	0.531	2.248	0.086	0.229	2.782	2.677	2.499	0.120	0.262	0.063	(0.06-5.6)
60	4.006	4.973	3.725	3.675	0.248	0.163	2.992	4.190	3.182	0.063	0.568	0.453	(0.16-4.97)
60	3.686	4.723	5.885	2.409	1.419	0.488	6.177	6.550	8.352	1.316	0.469	1.484	(0.46-8.35)
75	7.957	10.922	5.571	6.608	4.782	0.890	18.207	11.345	14.823	4.845	1.402	2.657	(0.89-18.20)
90	25.499	31.712	19.789	17.705	23.992	9.066	35.854	22.840	34.205	7.551	6.141	9.305	(6.14-35.85)
120	37.995	54.279	41.713	25.532	31.849	25.450	53.469	35.021	46.901	28.694	21.591	26.140	(21.59-54.27)
150	39.073	63.450	58.917	32.699	44.096	38.183	46.619	36.225	45.977	45.902	38.364	42.383	(32.69-63.45)
180	48.826	63.856	64.792	53.544	54.005	56.314	58.234	60.326	57.721	66.153	55.358	61.203	(48.82-66.15)

Table 4.2. Glycerol release during the digestion of different glyceryl trioctanoate controls within the model gut system. Each glyceryl trioctanoate control sample consists of 5ml glyceryl trioctanoate, 5ml of synthetic saliva and 5ml of DH_2O. The glycerol released from glyceryl trioctanoate digestion is measured at different time points of during the gastric (0-60 minute) and small intestinal (60T-180 minute) phases of the model gut. Data for each control are shown as mean of three replicates.

Time (mins)	Mean glycerol released from olive oil digestion (mg)												
	Control 1	Control 2	Control 3	Control 4	Control 5	Control 6	Control 7	Control 8	Control 9	Control 10	Control 11	Control 12	Glycerol range (mg)
0	0.75	0.05	0.25	0.05	0.41	0.07	0.12	0.13	0.42	0.47	0.25	0.75	(0.04-0.75)
15	0.83	0.07	0.05	0.91	0.92	0.46	0.19	0.02	0.18	0.28	0.66	0.30	(0.02-0.92)
30	1.11	0.05	0.36	0.99	1.23	1.28	0.09	0.53	0.07	0.49	0.47	1.17	(0.05-1.23)
60	0.72	0.01	0.11	2.33	2.21	1.79	0.45	0.41	0.40	0.67	0.73	1.37	(0.01-2.33)
60	2.59	0.59	0.41	5.75	5.78	7.50	0.60	1.58	1.38	0.17	1.20	0.85	(0.17-7.50)
75	1.78	0.04	0.77	6.45	7.99	5.88	0.51	1.32	0.07	1.96	2.98	1.38	(0.04-7.99)
90	2.69	3.98	2.58	11.70	10.95	8.43	2.46	3.35	2.28	2.30	10.29	7.14	(2.28-11.70)
120	13.66	12.54	7.73	18.20	17.34	14.02	8.81	11.93	6.63	9.05	24.10	10.48	(6.63-24.10)
150	30.23	18.59	18.59	31.02	30.98	26.60	13.43	17.87	11.53	15.77	28.21	14.15	(11.53-31.02)
180	36.59	38.39	28.50	46.90	46.32	36.36	24.95	35.34	25.64	29.05	42.18	26.24	(24.95-46.90)

Table 4.3. Glycerol release during the digestion of different olive oil as controls within the synthetic model gut system. Each olive oil control sample consists of 5ml olive oil, 5ml synthetic saliva and 5ml DH_2O. The glycerol released from olive oil digestion is measured at different time points of the gastric (0-60 minute) and small intestinal (60T-180 minute) phases of the model gut. Data for each control are shown as mean of three replicates.

Time (mins)	Mean glycerol released from sunflower oil digestion (mg)									
	Control 1	Control 2	Control 3	Control 4	Control 5	Control 6	Control 7	Control 8	Control 9	Glycerol range(mg)
0	0.03	0.13	0.01	0.26	0.01	0.16	0.35	0.09	0.01	(0.01-0.35)
15	0.05	0.16	0.05	0.04	0.05	0.33	0.49	0.17	0.06	(0.04-0.49)
30	0.19	0.25	0.10	0.07	0.10	0.26	0.49	0.04	0.03	(0.03-0.49)
60	1.31	0.17	0.12	0.02	0.07	0.11	0.65	0.12	0.06	(0.02-1.31)
60	1.15	1.34	1.33	0.53	1.55	0.54	2.18	0.36	0.21	(0.21-2.18)
75	1.99	1.68	1.95	1.10	0.54	1.61	2.30	0.74	0.27	(0.27-2.30)
90	2.01	1.91	4.22	2.54	1.56	3.57	5.57	3.22	0.63	(0.63-5.57)
120	4.57	5.85	6.67	9.84	5.24	9.30	12.79	8.44	6.70	(4.57-12.79)
150	9.31	10.54	12.05	16.71	15.37	15.87	20.79	18.06	9.01	(9.01-20.79)
180	26.06	17.45	19.60	20.90	25.28	27.99	23.05	24.74	18.00	(17.45-27.99)

Table 4.4. Glycerol release during the digestion of different sunflower oil controls within the synthetic model gut system. Each sunflower oil control sample consists of 5ml sunflower oil, 5ml synthetic saliva and 5ml DH_2O. The glycerol released from sunflower oil digestion is measured at different time points of the gastric (0-60 minute) and small intestinal (60T-180 minute) phases of the synthetic model gut system. Data for each control are shown as mean of three replicates.

4.5.4 Digestion of fat substrates in combination with 500 mg alginate added at the salivary phase

4.5.4.1 Glyceryl trioctanoate

Figure 4.4 shows the digestion of 5 ml glyceryl trioctanoate alone and in combination with 500mg of alginates CC01, 1N80, and 1LF80 added at the salivary phase of the synthetic model gut, respectively.

As shown in Figure 4.4 (graph A), during the gastric phase, only 3.5 (±0.5) mg and 2.3 (±0.7) mg glycerol were released from digestion of glyceryl trioctanoate alone and with 500 mg of CC01, respectively. However, during the first 15 minutes of the small intestinal phase, there was a gradual increase in the amounts of glycerol released from the digestion of glyceryl trioctanoate alone and in combination with CC01. After 75 minutes, there was significant difference ($P<0.05$) between the amount of glycerol released from digestion of glyceryl trioctanoate alone and that released from digestion of glyceryl trioctanoate treated with 500 mg CC01, where 30.9 (±7.1), 45.1 (±9.4), 43 (±5.8), and 58.8 (±1.4) mg glycerol was liberated from digestion of glyceryl trioctanoate alone compared with 17.2 (±4.2), 29.8 (±4.3), 23.4 (±8.9), and 31,8 (±3.2) mg glycerol produced from glyceryl trioctanoate in combination with CC01 at 90, 120, 150, and 180 minutes, respectively (Figure 4.4, graph A)

In addition, during the gastric phase, the amount of glycerol produced from the digestion of glyceryl trioctanoate alone was 1.4 (±2) mg compared to 0.3 (±0.78) mg glycerol released from the digestion of glyceryl trioctanotate with 500 mg 1N80 (Figure 4.4, graph B). During the first hour of the small intestinal phase (60T-120 minutes), the digestion rates of both glyceryl trioctanoate alone and glyceryl trioctanoate treated with 500 mg 1N80 increased gradually. However, there were significant differences ($P<0.05$) between their rates of digestion at 150 and 180 minutes, where the amounts of glycerol released from digestion of glyceryl trioctanoate treated with 1N80 were 22.3 (±2.3) mg and 39.8 (±6.6) mg compared to 38 (±5.6) mg, and 54.6 (±1.5) mg of glycerol liberated from the digestion of glyceryl trioctanoate alone at 150 and180 minutes, respectively, indicating a significant effect of treatment.

Although both CC01 and 1N80 alginates could reduce glyceryl trioctanoate digestion, the amount of glycerol released from digestion of glyceryl trioctanoate with CC01 at 180-minute was lower

than that released from the digestion of glyceryl trioctanoate with 1N80, showing that CC01alginate can reduce the digestion rate of glyceryl trioctanoate more than 1N80 alginate.

However, no significant difference ($P>0.05$) was seen between digestion of glyceryl trioctanoate alone and glyceryl trioctanoate treated with 500 mg of 1LF80 alginate, indicating that 1LF80 did not reduce the glyceryl trioctanoate digestion (Figure 4.4, graph C).

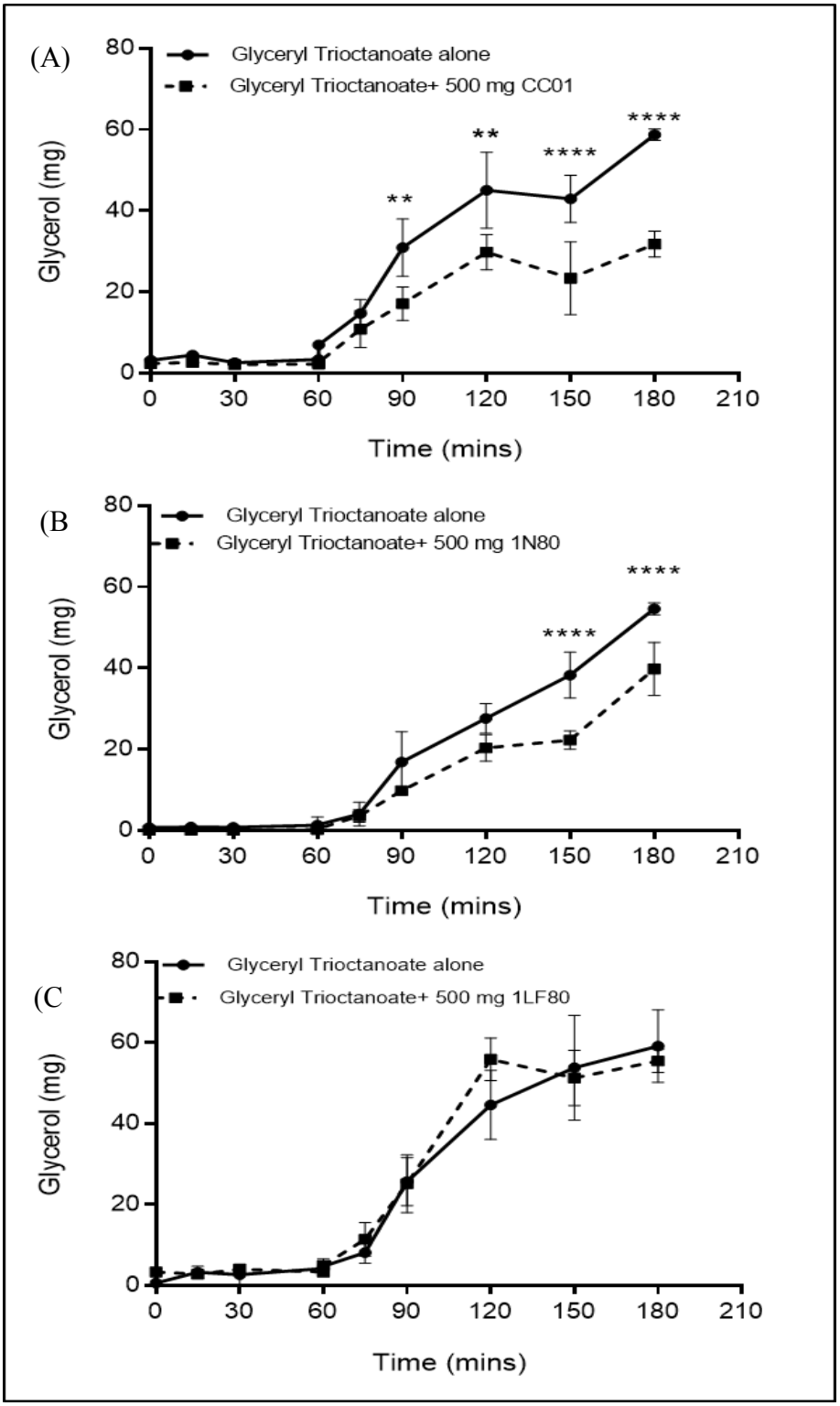

Figure 4.4. Glycerol liberation during the digestion of glyceryl trioctanoate alone or in combination with 500 mg of alginates in the synthetic model gut. Three alginates: (A) CC01, (B) 1N80, and (C) 1LF80 were added separately into samples of 5ml of glyceryl trioctanoate at the salivary phase of the model gut. Data are shown as mean ± SD, (n=3). P values <0.005 are represented by ** and <0.0005 are represented by ****.

4.5.4.2 Olive oil

Graphs A, B, and C of Figure 4.5 demonstrate *in vitro* digestion of 5ml of olive oil alone and olive oil treated with 500 mg of alginates CC01, 1N80, and 1LF80, respectively. During the gastric phase, negligible amounts (≤ 2.5 mg) of glycerol were released from the digestion of olive oil alone or in combination with any alginate. However, Bonferroni's test showed that the amounts of glycerol released from the digestion of either olive oil alone or olive oil treated with alginate increased significantly ($P<0.05$) during the small intestinal phase compared to those liberated from their digestion in the gastric phase.

At the end of the small intestinal phase, the amount of glycerol released from the digestion of olive oil treated with CC01 was 41.4 (±4.6) mg, compared with 36.2 (±2) mg glycerol released from the digestion of olive oil alone, but this difference was not significant ($P<0.05$) (Figure 4.5, graph A).

At the end of the small intestinal phase, 27 (±2.4) mg of glycerol was released from the digestion of olive oil in combination with 500 mg 1N80, compared to 27.1 (±2.4) mg of glycerol released from the digestion of olive oil treated with 500 mg 1N80 compared to 26.4 (±5.8) mg of glycerol released from the digestion of olive oil alone, and the P value was greater than 0.05, indicating a non-significant effect of 1N80 on the olive oil digestion (Figure 4.5, graph B).

Olive oil in combination with 500 mg of 1LF80 released 25.4 (±5.4) mg glycerol, compared with 23 (±8.3) mg glycerol released from the digestion of olive oil alone at the small intestinal phase suggesting a non-significant effect of the alginate on olive oil digestion (Figure 4.5, graph C).

Some gel and precipitate were formed during the simulated gastric phase in the alginate samples. This gel was still present in the beaker of the olive oil treated with alginate for all the samples during the small intestinal phase, suggesting that the alginate was not completely dissolved and released into the reaction mixture. This could explain why the digestion rate of olive oil was not reduced by the alginate.

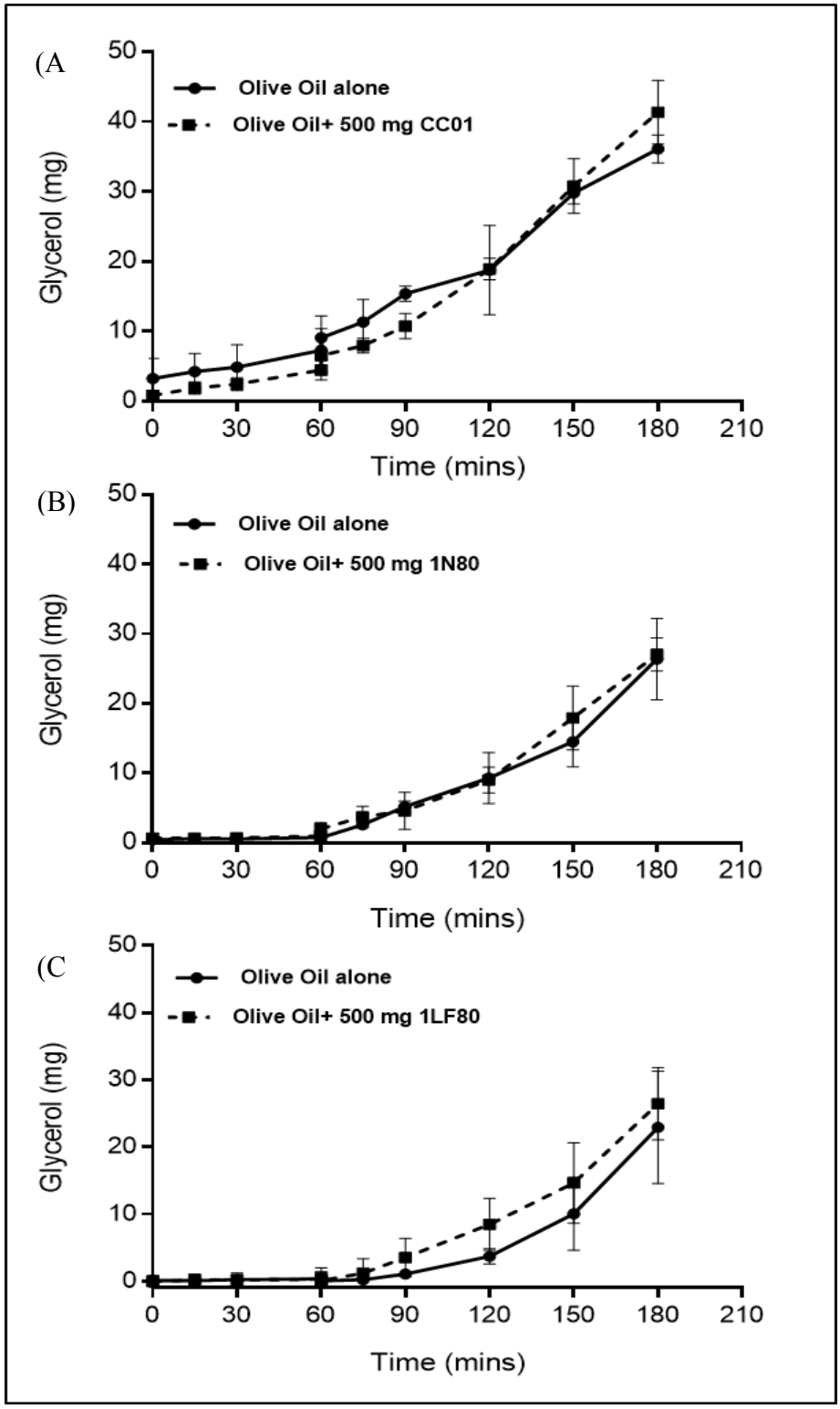

Figure 4.5. Glycerol liberation during the digestion of olive oil alone or in combination with 500 mg of alginates in the synthetic model gut. Three alginates: (A) CC01, (B) 1N80, and (C) 1LF80 were added separately into samples of 5ml olive oil at the salivary phase of the model gut. Data are shown as mean ± SD, (n=3).

4.5.4.3 Sunflower oil

Sunflower oil is rich in free fatty acids which are products of fat digestion because if the reaction solution is saturated with a reaction product, the rate of reaction will be slower. Therefore, sunflower oil must be passed through aluminum oxide (8 cm deep in glass chromatography column with 1.5-2 cm diameter) to remove the free fatty acids.

Figures 4.6A, 4.6B, and 4.6C show the digestion of 5 ml of sunflower oil without free fatty acids alone as a control and in combination with 500 mg of CC01, 1N80 and 1LF80, respectively.

During the gastric phase, the amounts of glycerol released from the digestion of sunflower oil alone and the oil with alginates (CC01, 1N80 or 1LF80) were very small (≤1 mg). However, after 15 minutes of the small intestinal phase, there was a gradual increase in the amount of glycerol produced from the digestion of oil alone and in combination with CC01, 1LF80 or 1N80. At the end of the pancreatic small intestinal phase, the amounts of glycerol released from the digestion of sunflower oil treated with CC01 (Figure 4.6, graph A) or 1N80 (Figure 4.6, graph B) were 24.4 (±4.5) and 24.7(±4.1) mg compared with 21 (±4.4) and 25.3 (±7.5) mg from their control digestions, respectively. On the other hand, sunflower oil treated with 500 mg 1LF80 produced 29.7 (±5.2) mg of glycerol compared with 25 (±3.6) mg from oil digestion alone (Figure 4.6, graph C). However, considering $P>0.05$ at all time points, there was no significant difference between the digestion of sunflower oil alone or in combination with 500 mg of CC01, 1N80 or 1LF80.

Furthermore, gel and lumps were observed in the samples treated with alginates at the end of the gastric phase and they remained present at the end of the model gut procedure. Gelling of alginate could have been responsible for the lack of inhibition in the digestion rate of sunflower oil if the alginate was not completely released in the reaction mixture.

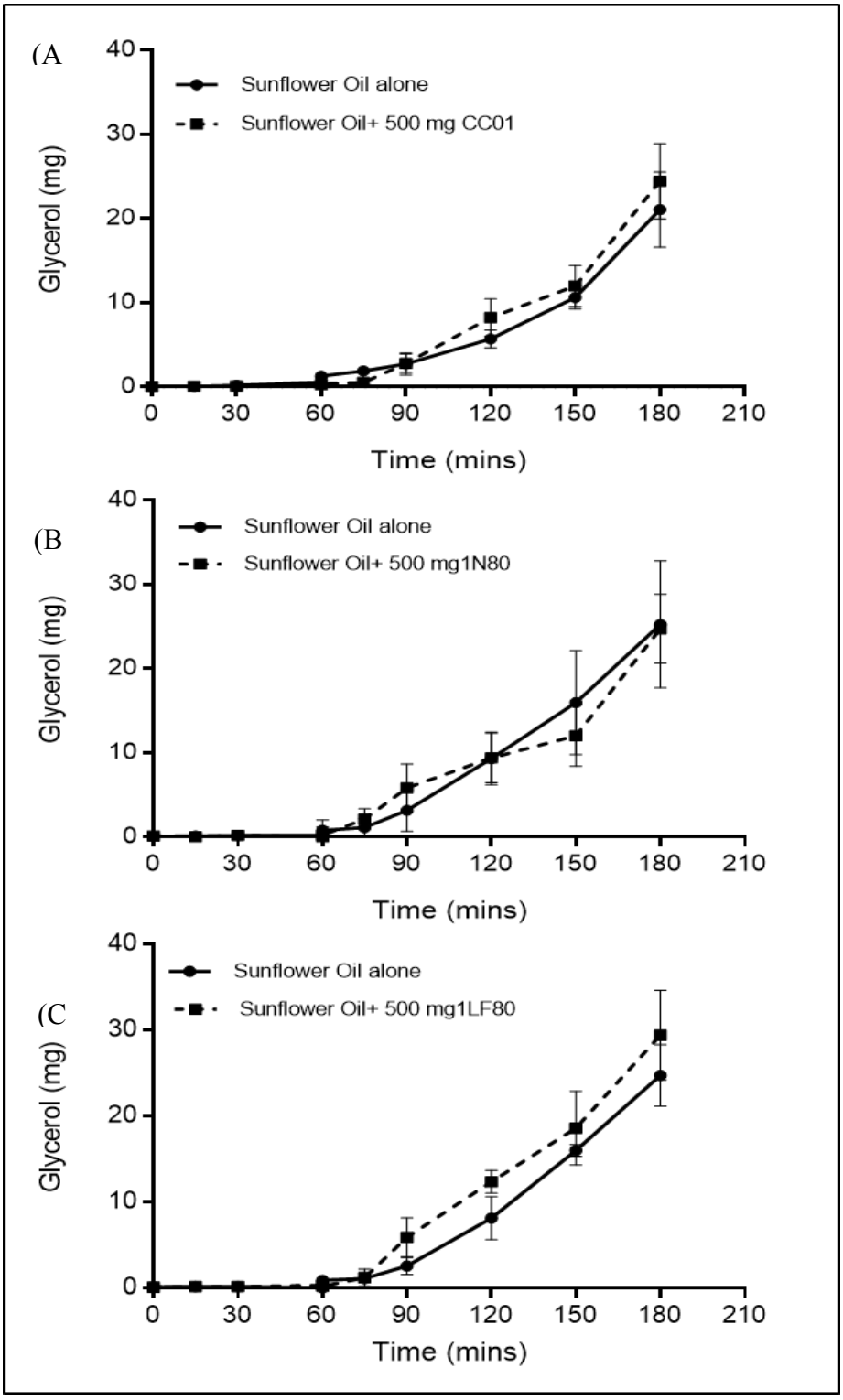

Figure 4.6. Glycerol liberation during the digestion of a sample of sunflower oil alone or in combination with 500 mg of alginates in the synthetic model gut. Three alginates: (A) CC01, (B) 1N80, and (C) 1LF80 were added separately into samples of 5ml sunflower oil free from free fatty acids at the salivary phase of the model gut. Data are shown as mean ± SD, (n=3).

4.5.5 Digestion of olive oil in combination with 1000 mg CC01

Data from the digestion of olive oil in combination with 500 mg of alginate (CC01, 1N80, or 1LF80) presented in this chapter showed that the alginate had no significant effect on olive oil digestion. Therefore, a higher amount (1000 mg) of CC01 alginate, which has the highest content of G blocks, was used in an attempt to inhibit olive oil digestion. This alginate was chosen as the inhibition level of pancreatic lipase by alginate was dependent on the concentration and the content of G blocks as shown in Chapter 2 of this study as well as in earlier research conducted by Wilcox et al. (2014).

The data in Figure 4.7 demonstrates the gastrointestinal digestion of 5 ml olive oil containing free fatty acids alone and olive oil treated with 1000 mg of CC01 in the model gut. It is obvious that during the gastric phase (0-60 minutes), no glycerol was released from the digestion of olive oil alone and olive oil with alginate. However, during the gastric phase, CC01 alginate precipitated and formed a gel which was still observed in the bottom of the beaker at the end of the procedure.

During the first 30 minutes of the intestinal phase, there was a gradual increase in the digestion rate of olive oil alone and the digestion rate of olive oil in combination with CC01 alginate, but no significant difference was detected between the two digestion rates. After 90 minutes, there was a significant increase in the amounts of glycerol produced from the digestion of both olive oil alone and olive oil with CC01, with no significant difference between the amounts of glycerol released from their digestion. However, at the end of the small intestinal phase, the amount of glycerol released from the digestion of olive oil treated with CC01 (43 (±3) mg) was significantly higher ($P<0.005$) than that released from the digestion of olive oil alone (35 (±2.8) mg). This suggests that 1000 mg CC01 may have activated pancreatic lipase digestion of olive oil. Another possibility is that the high levels of alginate were interfering with the glycerol assay. However, additional experiments (data are not shown here) showed this was not the case (see discussion in section 4.6).

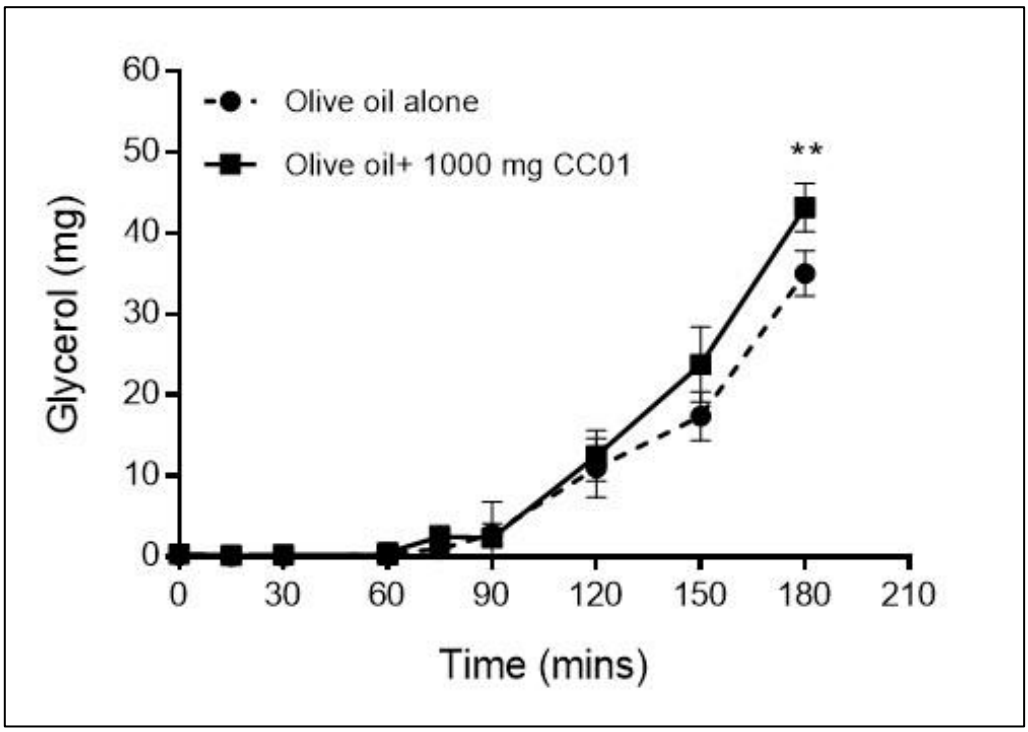

Figure 4.7. Glycerol liberation during the digestion of olive oil containing free fatty acids alone or in combination with 1000 mg CC01 in the synthetic model gut. Data are shown as mean ± SD, (n=3). P values < 0.005 are represented by**.

4.5.6 Digestion of olive oil free from free fatty acids in combination with 1000 mg CC01

Previous data demonstrated that 1000 mg of CC01 may have activated olive oil digestion, leading to the hypothesis that this occurs because olive oil contains large amounts of free fatty acids, which are the product of triglyceride breakdown. Therefore, if the reaction solution is saturated with reaction product, it will slow down the rate of reaction. However, if the alginate binds these free fatty acids, it effectively removes them from the reaction mixture and the reaction is able to proceed at a faster rate. Therefore, the effect of CC01 alginate was studied using free fatty acid-free olive oil to investigate whether removing free fatty acids from the olive oil accelerates its reaction rate. The oil was passed through aluminum oxide (8 cm deep in glass chromatography column 1.5-2 cm diameter) to remove free fatty acids.

The data in Figure 4.8 show the digestion of 5 ml free fatty acid-free olive oil alone and in combination with 1000 mg of CC01 in the model gut. During the gastric phase, no glycerol was

released from the digestion of the olive oil alone or olive oil treated with 1000 mg CC01. In addition, CC01 alginate showed some gel and precipitations. However, data from the pancreatic small intestinal phase suggested that alginate activated olive oil digestion where the amounts of glycerol liberated from olive oil treated with CC01 alginate were higher than those liberated from the olive oil alone. At the end of the pancreatic small intestinal phase, the amounts of glycerol released from olive oil treated with 1000 mg of CC01 was 45 (±10.6) mg, while the glycerol released from the olive oil alone was 26.6 (±3.8) mg. The differences in the amounts of glycerol released at 90, 150, and 180 minutes of the pancreatic phase from the olive oil alone and the olive oil treated with alginate were statistically significant ($p \leq 0.05$), providing evidence that alginate binding of free fatty acids was not the reason for the apparent increase in digestion of olive oil treated with alginate.

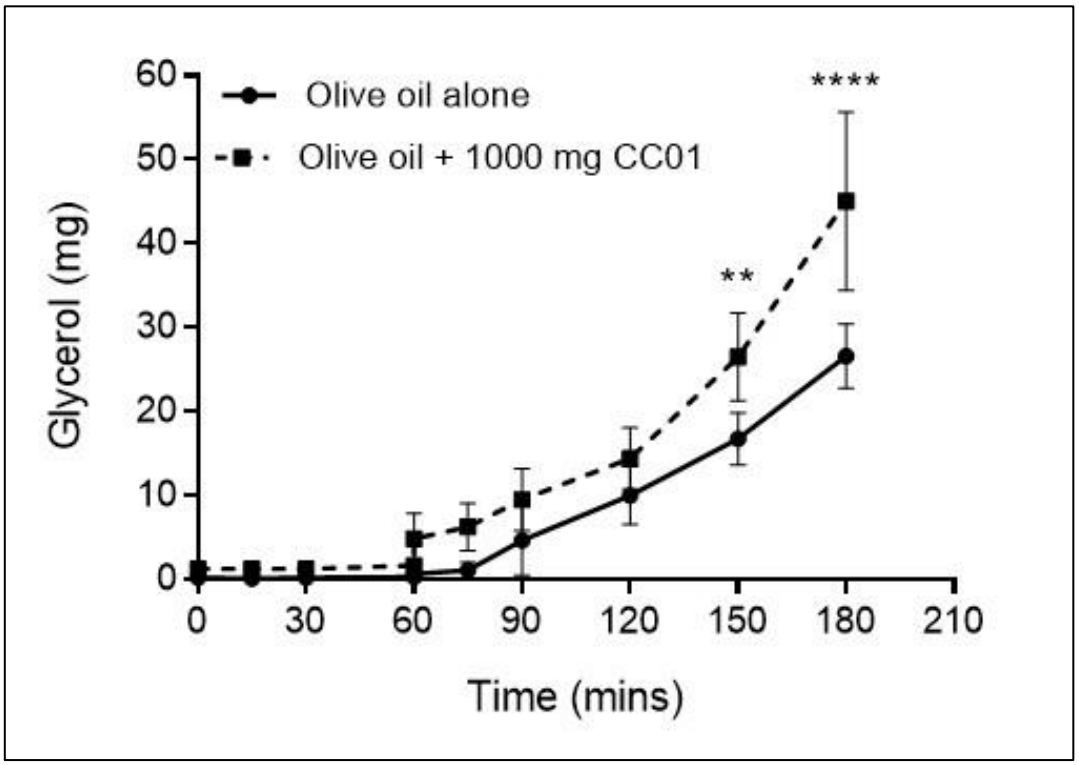

Figure 4.8. Glycerol liberation during the digestion of olive oil without free fatty acids alone or in combination with 1000 mg CC01 in the synthetic model gut. Data are shown as mean ± SD, (n=3). P values < 0.005 are represented by** and <0.0005 are represented by ****.

4.5.7 Gelling of alginate added at the salivary phase

The data just described above showed that alginate did not inhibit the digestion of fat. However, gels, some lumps, and precipitation were seen in the sample beaker containing alginate when the

sample passed through the gastric phase, indicating that the alginate underwent gelation in the gastric phase (Figure 4.9). The gels and lumps were still seen at the bottom of the beaker at the end of model gut, showing that the gel did not dissolve, and the alginate was not released in the reaction mixture, which could explain the ineffectiveness of alginate in reducing the fat digestion. Furthermore, it was noticed that 1000 mg of alginate produced a large amount of gel, double (by observation) that formed from the 500 mg of alginate, suggesting a correlation between the amount of gel formed and the amount of alginate added to the solution.

On the other hand, when the samples containing alginate in combination with glyceryl trioctanoate were passed through the gastric phase, gels, lumps, and precipitation were formed and still seen at the end of the gastric phase. However, no gels, lumps or precipitation were seen at the end of the small intestinal phase (at-180 minute), suggesting that the gel was dissolved, and the alginate was released in the reaction mixture to reduce the triglycerides hydrolysis. This was supported by the previous data obtained from digestion of glyceryl trioctanoate in combination with alginate which showed that alginate could inhibit glyceryl trioctanoate digestion (Figure 4.4, graphs A and B).

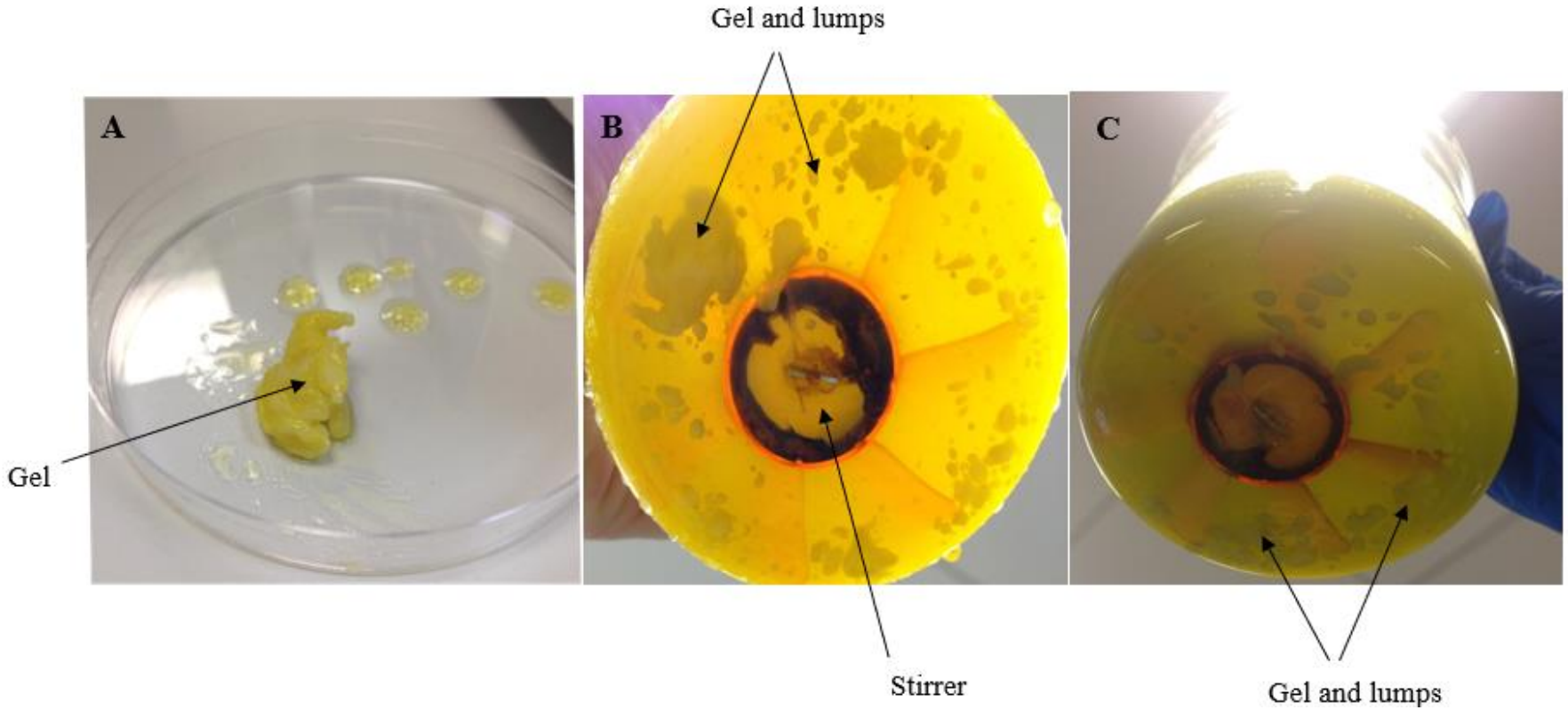

Figure 4.9. Gel formed during alginate passage through the gastric phase of the model gut system. A and B show the gel at the end of gastric phase (T_{60}) whereas C shows the gel and lumps at the end of the small intestinal phase (T_{180}).

4.5.8 Effect of alginate added during the small intestinal phase on fat digestion

Earlier results showed that there was no significant reduction in the digestion of olive oil treated with alginates, and this may occur because the $CaCl_2$ in saliva and acidic pH caused alginates to form gels which would affect their efficiency in reducing fat digestion. Therefore, the effect of alginates on olive oil digestion in the synthetic model gut was investigated as described previously, but the alginates (CC01, 1N80, and 1LF80) were added 10 minutes after the start of the pancreatic small intestinal phase (at 70-minute of the model gut procedure) to allow bile and pancreatic juice to provide a rather less acidic environment and avoid gel formation.

4.5.8.1 Olive oil alone and in combination with 500 mg of alginate

Graphs A, B, and C in Figure 4.10 illustrate the *in vitro* digestive processes of olive oil alone as a control and olive oil with 500 mg of CC0, 1N80 and 1LF80 in the synthetic model gut, respectively. During the gastric phase, the amount of glycerol released from the digestion of olive oil alone or in combination with CC01 were negligible (≤1 mg) (Figure 4.10, graph A). After 15 minutes of the pancreatic intestinal phase, there was a gradual increase in glycerol release from the digestion of olive oil alone and olive oil treated with 500 mg CC01. However, at 120, 150, and 180 minutes, there were significant differences ($P<0.05$) between the amounts of glycerol released from digestion of olive oil alone, 11(±3), 22.4 (±6.7), 35(±5.3) mg, respectively, and those released from digestion of olive oil with CC01, 3.12 (±3.9), 12.1 (±4.9), and 21 (±4.8) mg, at 120, 150, and 180 minutes, respectively (Figure 4.10, graph A).

The data shown in graph B of Figure 4.10 indicate that during the gastric phase, only small amounts of glycerol (≤ 1mg) were released from the digestion of olive oil alone and olive oil in combination with 500 mg 1N80. During the small intestinal phase, there was an increase in mean glycerol released from olive oil alone and olive oil in combination with 500 mg 1N80. At 150 and 180 minutes, the amounts of glycerol released from the digestion of olive oil alone were 22.8 (±2.4) and 37.2 (±5.4) mg, respectively, and these amounts of glycerol were significantly greater ($P<0.05$) than those released from the digestion of olive oil treated with 1N80, which were 14.3 (±3.3) and 28.6 (±5.8) mg, respectively, showing that 500 mg of 1N80 alginate added at the small intestinal phase (T_{70}) could reduce olive oil digestion.

There was no significant difference ($P>0.05$) between the amounts of glycerol released from the digestion of olive oil alone and olive oil treated with 500 mg of 1LF80 alginate, demonstrating that 500 mg of 1LF80 alginate introduced during the small intestinal phase did not affect olive oil digestion (Figure 4.10, graph C).

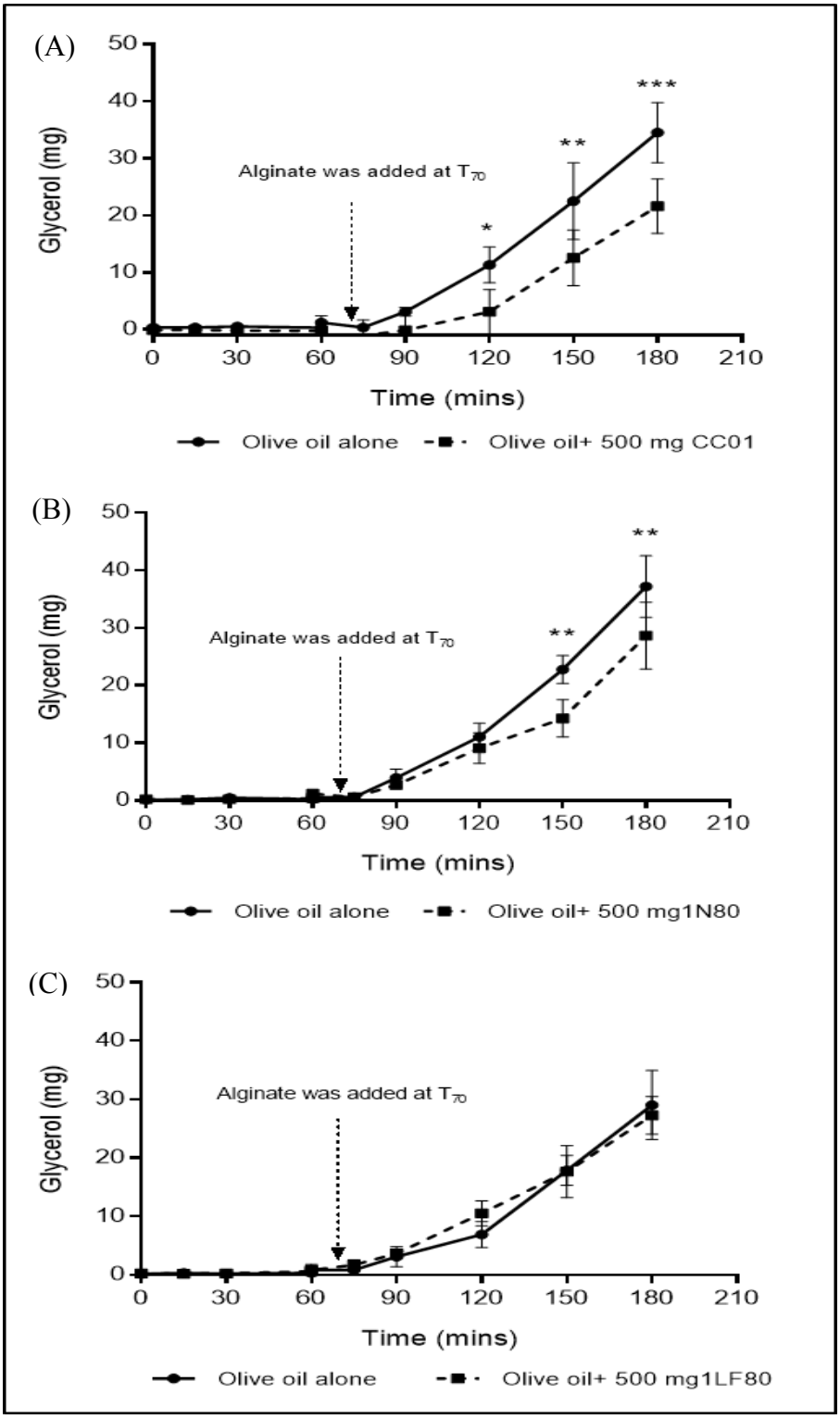

Figure 4.10. Glycerol liberation during the digestion of olive oil alone or in combination with 500mg alginates added during the small intestinal phase of the model gut. 500mg of alginates (A) CC01, (B) 1N80 and (C) 1LF80 were added separately into samples of 5ml olive oil. Data are shown as mean ± SD (n=3). P values < 0.05 are represented by *, < 0.01 are represented by **, and <0.001 are represented by ***. The dotted arrow indicates that alginate was added at T_{70} of the model gut procedure.

4.5.8.2 Olive oil alone and in combination with 1000 mg of alginate

The data in Figure 4.11 illustrate digestion of 5 ml of olive oil alone and with 1000 mg CC01, 1N80, and 1LF80 in the gastric and pancreatic small intestinal phases of the synthetic model gut, respectively.

The data in graph A of Figure 4.11 compare olive oil digestion in the presence and absence of 1000 mg CC01. During the gastric phase, small amounts of glycerol (≤1 mg) were released from digestion of the olive oils. During the first 10 minutes of the small intestinal phases, there was an increase in the digestion rate of the two samples (Figure 4.11, graph A), after which 1000 mg CC01 alginate was added to the olive oil. The digestion rates of olive oil alone and treated with CC01 increased, and at 90 and 180 minutes, there were significant differences ($P<0.05$) in mean glycerol released from the olive oil with CC01 (5.2 (±1.9) mg and 39 (±6) mg) and mean glycerol released from digestion of olive oil alone (1 (±1.3) mg and 28.1 (±1.7)) mg, respectively, demonstrating activation in olive oil digestion by 1000 mg CC01 alginate.

Data shown in Figure 4.11 (graph B) compare olive oil digestion in the presence and absence of 1000 mg 1N80 and this shows that only small amounts of glycerol (≤ 1mg) were released from digestion of the two samples during the gastric phase (0-60 minutes). However, during the small intestinal phase (60-180 minutes), the digestion rates for olive oil alone or in combination with 1000 mg 1N80 alginate increased with no significant difference during the first 60 minutes of the small intestinal phase (60-120 minutes). However, there was a significant difference ($P<0.05$) at 150 and 180 minutes between glycerol liberated from digestion of olive oil treated with 1000 mg 1N80 and digestion of olive oil alone, where the glycerol liberated from digestion of olive oil treated with 1000 mg 1N80 at 150 and 180 minutes was 27.2 (±1.4) and 42 (±7.2) mg, respectively, compared to 19.4 (±7.6) and 32.5 (±8.5) mg released from digestion of olive oil alone at 150 and 180 minutes, respectively, indicating that 1N80 could activate olive oil digestion.

The data in Figure 4.11 (graph C) compare digestion of olive oil in the presence and absence of 1000mg 1LF80. The amounts of glycerol released from digestion of olive oil during the gastric phase were negligible (<1 mg). Unlike the gastric phase, during the small intestinal phase higher amounts of glycerol were released from digestion of olive oil alone and olive oil in combination with 1000 mg 1LF80 alginate. However, although the digestion rate of olive oil treated with 1000

mg 1LF80 appeared higher than the digestion rate of olive oil alone at all time points of the small intestinal phase, Bonferroni's test indicated a significant difference ($P<0.05$) only at the end of the small intestinal phase where the mean glycerol released from digestion of olive oil treated with 1LF80 was 42.7 (±11.4) mg, compared to 29 (±5.8) mg of glycerol released from digestion of olive oil alone, showing that 1000 mg 1LF80 could activate olive oil digestion.

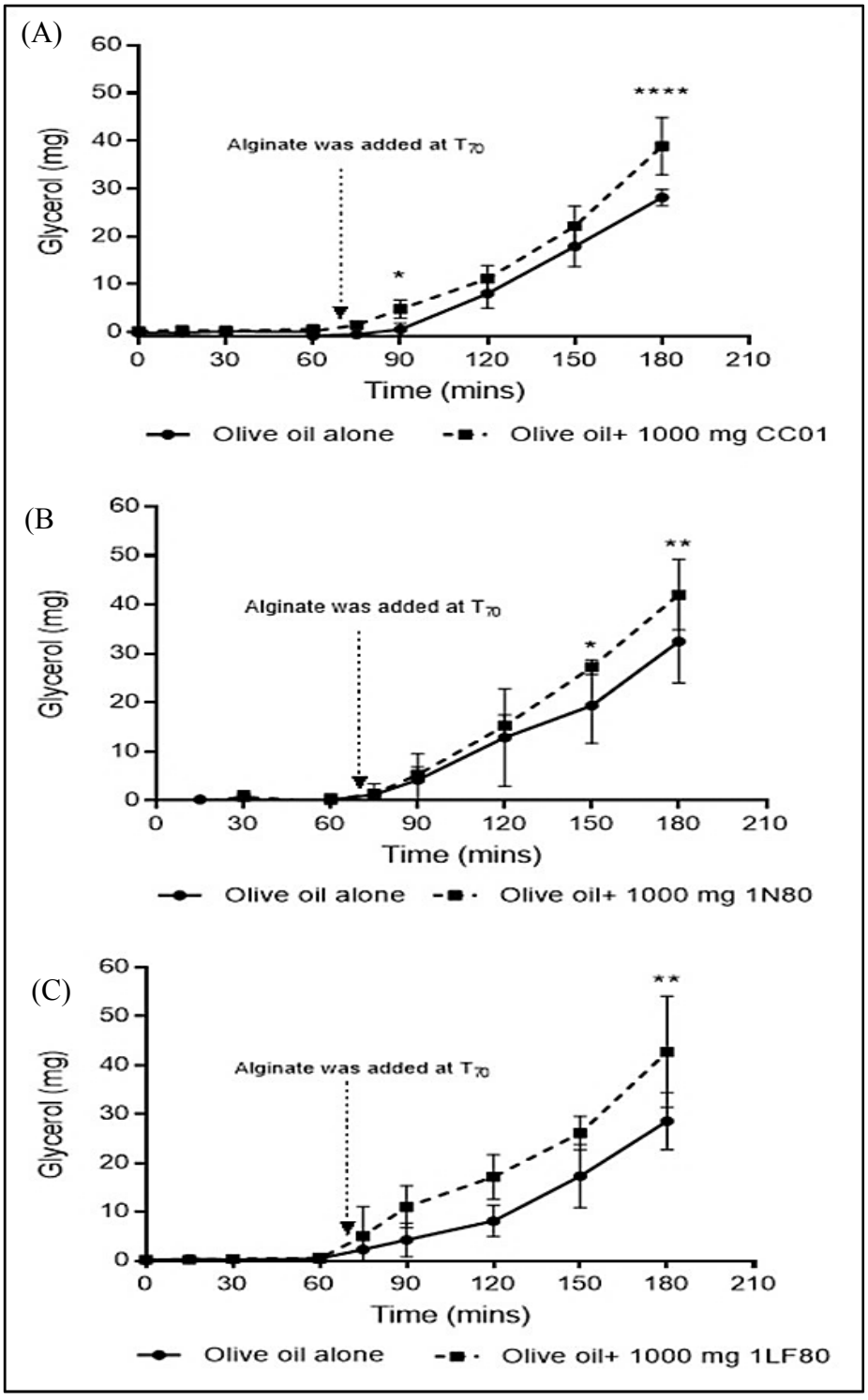

Figure 4.11. Glycerol liberation during the digestion of olive oil alone or in combination with 1000mg alginates added during the small intestinal phase of the model gut. 1000mg of alginates (A) CC01, (B) 1N80, and (C) 1LF80 were added separately into samples of 5ml olive oil. The dotted arrow indicates that alginate was added at T_{70} of the model gut procedure. Data are shown as mean ± SD (n=3). P values < 0.05 are represented by *, < 0.01 are represented by **, <0.001 are represented by ***, and <0.0005 are represented by ****.

4.5.8.3 Olive oil alone and in combination with 250 mg of CC01 alginate

Results from the turbidity assay discussed in Chapter 2 of this thesis showed that alginates could inhibit the activity of pancreatic lipase. The highest level of lipase inhibition was caused by CC01 alginate, which is rich in G block, and the level of inhibition of lipase by CC01 was dose-dependent. In addition, earlier results presented in this chapter showed that 500 mg of alginate added at the small intestinal phase could reduce the digestion of olive oil in the synthetic model gut whereas 1000 mg alginate appeared to increase it. Therefore, the effect of 250 mg of CC01 alginate on olive oil digestion was tested to investigate whether the level of lipase inhibition by alginate is concentration-dependent.

Figure 4.12 shows the *in vitro* gastrointestinal digestion of 5 ml of olive oil alone and in the presence of 250 mg CC01 alginate. During the gastric phase, glycerol production from digestion of olive oil was undetected. During the small intestinal phase (CC01 alginate added at 70-minute), the digestion rate of olive oil alone was greater than that of olive oil in combination with CC01. The glycerol release from digestion of olive oil alone at 150 and 180 minutes, 28 (±4.1) and 47.1 (±7.2) mg, was significantly ($P<0.05$) higher than the glycerol amounts produced from digestion of olive oil treated with CC01, 17.3 (±3.6) and 33.4 (±4) mg, respectively.

Moreover, at the end of the small intestinal phase, the amount of glycerol released from the digestion of olive oil treated with 250 mg of CC01 alginate (33.4 (±4) mg) (Figure 4.12) was significantly higher ($P<0.05$) than the amount of glycerol released from the digestion of olive oil treated with 500 mg of CC01 added at the small intestinal phase (21 (±4.8) mg) (Figure 4.10, graph A), demonstrating that inhibition of lipase by alginate is dependent on the concentration of alginate.

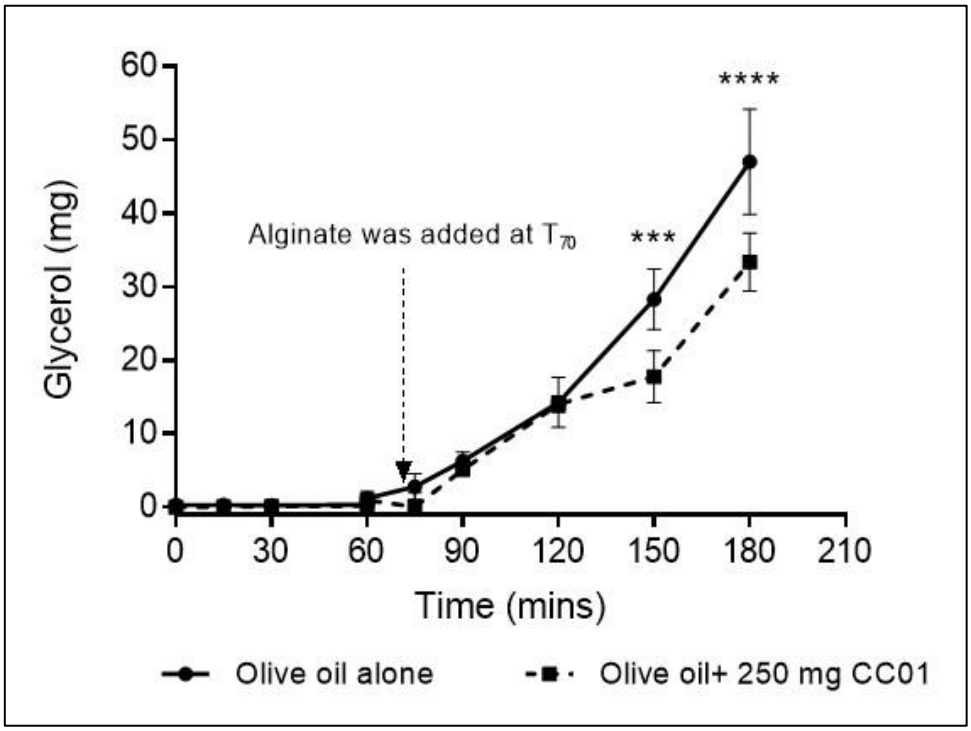

Figure 4.12. Glycerol liberation during the digestion of olive oil alone or in combination with 250 mg CC01 added during the small intestinal phase of the synthetic model gut. The dotted arrow indicates that alginate was added at T_{70} of the model gut procedure**.** Data are shown as ± SD, (n=3). P values <0.001 are represented by ***, and <0.0005 are represented by ****.

4.5.8.4 Olive oil alone and in combination with 250 mg of CC01 alginate added at the salivary phase

As the effect of 250 mg CC01 alginate added during the salivary phase was not tested previously due to 500 mg CC01 having no effect on olive oil digestion, it was now also tested.

As seen in Figure 4.13, during the gastric phase, only small amounts of glycerol were released from digestion of both olive oil alone and olive oil treated with 250 mg CC01 added at the salivary phase. During the small intestinal phase, the amount of glycerol released from the digestion of olive oil in combination with 250 mg of CC01 at the 180-minute was 38.1 (±4.7) mg compared to 34.5 (±2.5) mg of glycerol produced from the digestion of olive oil alone. No significant difference was detected between the intestinal digestion of olive oil alone and that of olive oil treated with 250 mg, demonstrating that unlike 250 mg CC01 added at the small intestinal phase, 250 mg of CC01 alginate added at the salivary phase did inhibit the digestion rate of olive oil.

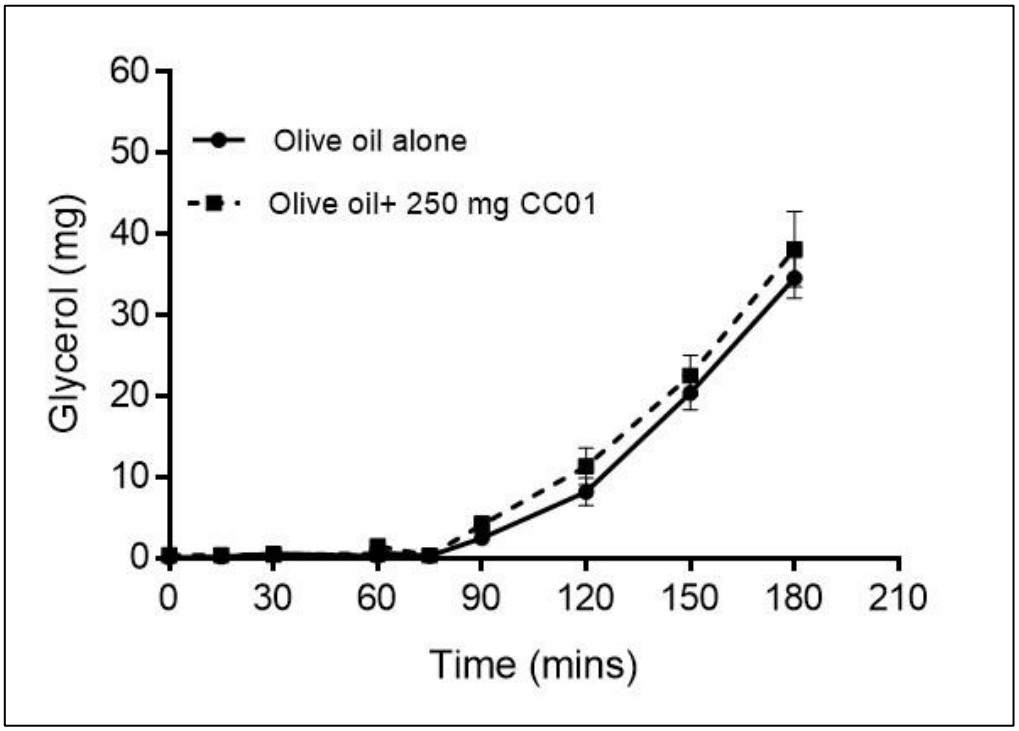

Figure 4.13. Glycerol liberation during the digestion of olive oil alone or in combination with 250 mg CC01 added at the salivary phase of the synthetic model gut. Data are shown as mean ± SD (n=3).

4.5.8.5 Glyceryl trioctanoate alone and in combination with 500 mg CC01 added at the small intestinal phase

Figure 4.14 demonstrates *in vitro* digestion of 5 ml glyceryl trioctanoate alone and in the presence of 500 mg CC01 alginate added after 10 minutes of the pancreatic small intestinal phase (T_{70}). As expected, insignificant amounts of glycerol (≤1 mg) were released from digestion of glyceryl trioctanoate during the gastric phase. However, during the pancreatic intestinal phase, the digestion rates of both glyceryl trioctanoate alone and glyceryl trioctanoate treated with CC01 rose sharply at the same level, and no significant difference ($P>0.05$) was seen between mean glycerol released from their digestion at all time points, showing that 500 mg CC01 added at the pancreatic phase had no effect in reducing glyceryl trioctanoate digestion.

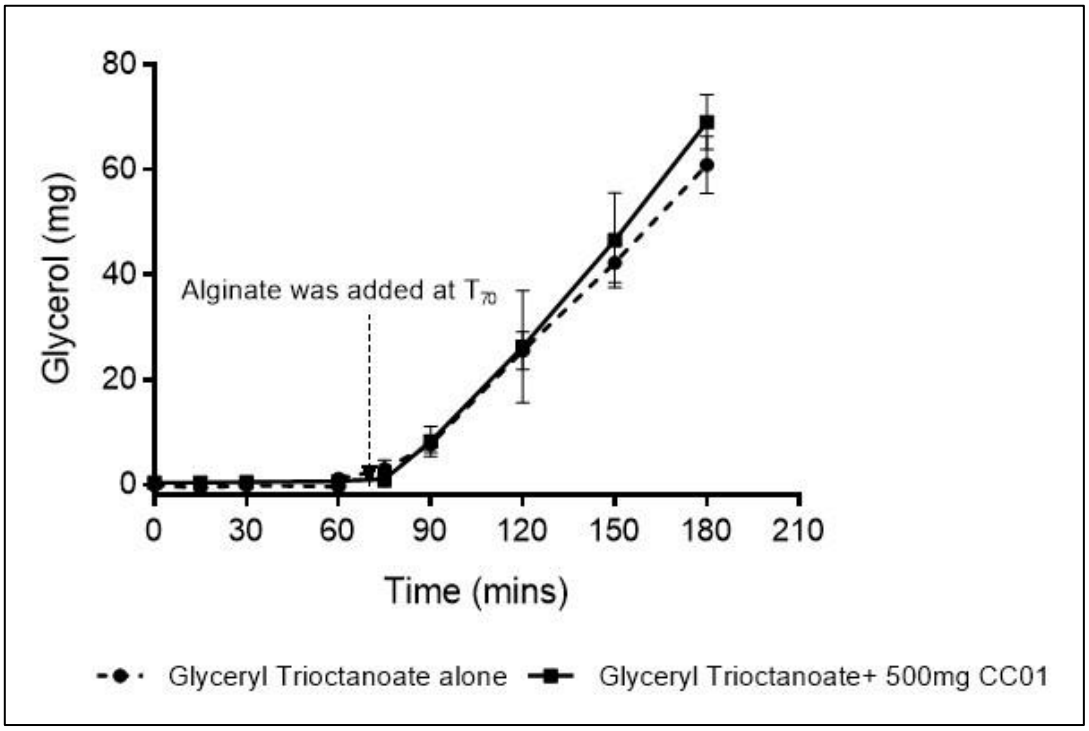

Figure 4.14. Glycerol liberation during the digestion of glyceryl trioctanoate alone or in combination with 500 mg CC01 added during the small intestinal phase of the synthetic model gut.Data are shown as mean ± SD (n=3). The dotted arrow indicates that alginate was added at T_{70} of the model gut procedure.

4.5.9 Digestion of olive oil alone and in combination with alginate added at salivary phase using a buffered synthetic salivary diluent

Results obtained from the model gut experiments for digestion of olive oil in combination with CC01 added at the salivary phase showed that CC01 did not inhibit olive oil digestion. Also, some precipitation and gel formation were observed in the bottom of the beakers containing alginate samples, which might be because the pH in the gastric phase ranged between 2 and 3, values which are below the pKa values for guluronate (3.65) and mannuronate (3.38) monomers of alginate polymer and this could lead to acid gel formation.

However, olive oil digestion was reduced when CC01 was added at the small intestinal phase (T_{70}) where the pH values were above 4.5, and no gels or precipitations were observed at the end of the small intestinal phase. Therefore, an attempt was made to avoid alginate precipitation and gelling during the gastric phase through buffering the synthetic salivary diluent.

Initial investigations carried out on synthetic salivary diluent showed that a salivary diluent

containing a higher amount of $NaHCO_3$, 372mM, could reduce gel formation and precipitation. Also, pH measurements showed that the buffered salivary diluent could provide pHs in the stomach phase higher than those for a normal salivary diluent. Consequently, the effect of alginate (CC01) on olive oil digestion within the model gut using the buffered salivary diluent was examined to ascertain whether producing less acidic pHs in the stomach enables alginate to reduce olive oil digestion.

The synthetic salivary diluent (pH 7.4) was prepared as described in the methods (section 4.3.1) of this chapter but using 372mM $NaHCO_3$ instead of 62mM $NaHCO_3$. The samples were passed through salivary, gastric and small intestinal phases of the model gut. The collected samples were treated as described earlier in section 4.3.3.1 of this chapter.

Figure 4.15 shows the digestion of olive oil alone using normal and buffered salivary diluents containing 62mM $NaHCO_3$ and 372mM $NaHCO_3$, respectively. It is obvious that during the gastric phase, the amounts of glycerol produced from olive oil digestion using either normal or buffered salivary diluent were small ($\leq$ 1 mg). During the first hour of the small intestinal phase, the amounts of glycerol produced from the digestion of olive oil treated with normal salivary diluent and that produced from olive oil treated with buffered salivary diluent increased with no significant difference between their digestion rates. However, at 150 and 180 minutes of the small intestinal phase, the amounts of glycerol produced from digestion of olive oil treated with normal salivary diluent were 22.1 (±7.7) mg and 35.4 (±8.0) mg, compared to 17.4 (±5.2) mg and 27.9 (±5.3) mg produced from the digestion of olive oil treated with buffered salivary diluent, with P values <0.0005, at 150 and 180 minutes, respectively, indicating that the digestion rate of olive oil treated with normal saliva was significantly higher than that of olive oil treated with buffered saliva, showing that buffering the salivary diluent could reduce the digestion rate of olive oil.

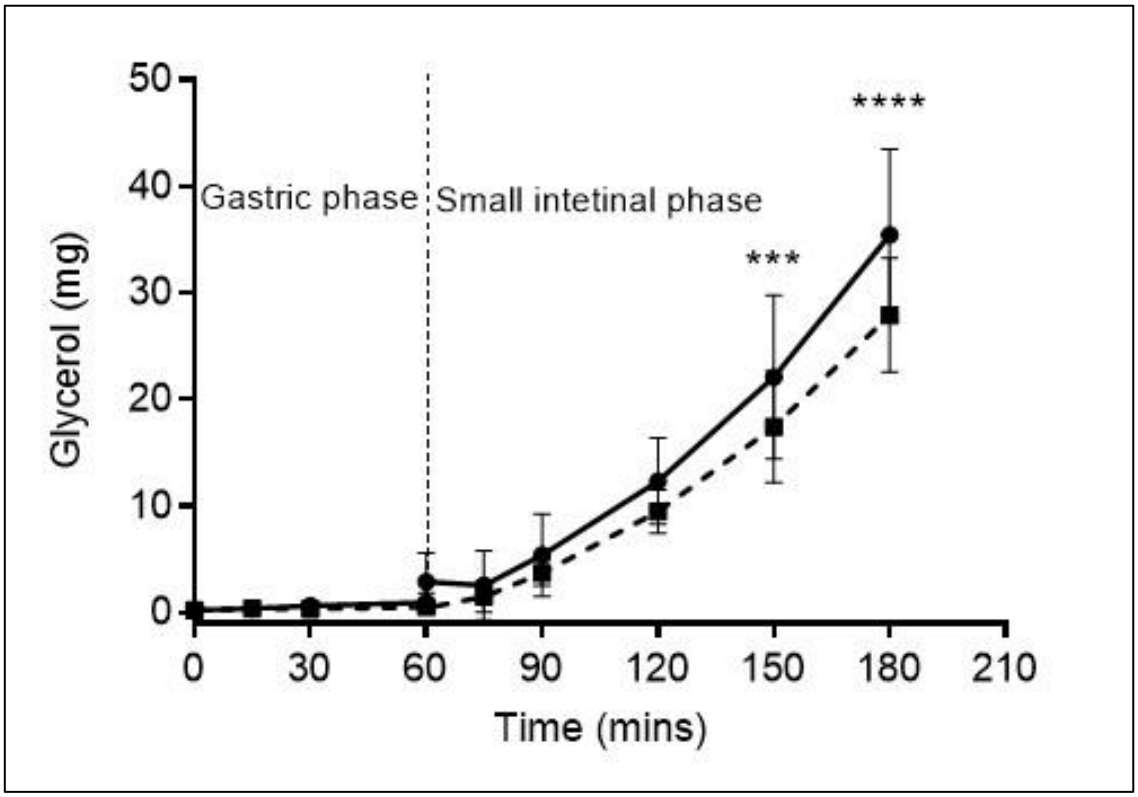

Figure 4.15. Glycerol liberation during the digestion of olive oil alone using normal salivary diluent (●) or buffered salivary diluent (■) in the synthetic model gut. Data are shown as mean ± SD, (n=9). P values <0.0005 are represented by *** and <0.0001 are represented by ****.

Graphs A, B, and C in Figure 4.16 show digestion of olive oil alone using a buffered salivary diluent and the digestion of olive oil in combination with 250, 500, and 1000 mg CC01 alginate added at the salivary phase using a normal synthetic salivary diluent containing 62mM $NaHCO_3$ or buffered salivary diluent containing 372mM $NaHCO_3$, respectively.

As shown in graph A of Figure 4.16, during the gastric phase, the amounts of glycerol released from the digestion of olive oil alone using buffered salivary diluent, the digestion of olive oil treated with 250 mg of CC01 alginate and normal salivary diluent or the digestion of olive oil treated with 250 mg CC01 and buffered salivary diluent were negligible (≤1 mg of glycerol). During the first hour of the small intestinal phase, the digestion rates of olive oil alone using buffered salivary diluent, olive oil treated with 250 mg CC01 in combination with normal salivary diluent, and olive oil treated with 250 mg CC01 in combination with buffered synthetic salivary diluent increased equally. However, at the end of the small intestinal phase (at 180-minute), the digestion rate of olive oil in combination with 250 mg CC01 and buffered salivary diluent was significantly higher

($P<0.001$) than that for olive oil alone using buffered diluent where the amount of glycerol released from the digestion of olive oil in combination with 250 mg CC01 was 29.41 (±3.4) mg compared to 25.1 (±2.4) mg released from olive oil alone. Additionally, a small amount of gel was observed at the end of the small intestinal phase in the samples containing 250 mg CC01 and buffered salivary diluent, but this was less than the gel produced from 250 mg CC01 in combination with normal salivary diluent containing 62mM $NaHCO_3$.

Data in Figure 4.16 (graph A) also shows that at 150 and 180 minutes, the digestion rate of olive oil treated with 250 mg CC01 and normal salivary diluent was significantly higher ($P<0.05$) than the digestion rate of olive oil treated with 250 mg CC01 and buffered diluent where the amounts of glycerol liberated from digestion of olive oil treated with 250 mg CC01 and normal salivary diluent were 25.2 (±4.9) mg and 41.5 (±5.8) mg, compared to 16.1 (±1.7) and 29.4 (±3.4) mg of glycerol released from digestion of olive oil treated with 250 mg CC01 and buffered salivary diluent, respectively, indicating that the 250 mg of CC01 alginate added at the salivary phase in combination with buffered salivary diluent containing 372mM $NaHCO_3$ could significantly reduce the digestion rate of olive oil, compared to 250 mg CC01 in combination with normal salivary diluent containing 62mM $NaHCO_3$.

Data in graph B of Figure 4.16 show that during the gastric phase, the amounts of glycerol released from the digestion of olive oil alone, the digestion of olive oil treated with 500 mg CC01 and normal salivary diluent, or the digestion of olive oil treated with 500 mg CC01 and buffered salivary diluent was small (<3 mg). During the small intestinal phase, no significant difference ($P>0.05$) was detected between the amount of glycerol released from digestion of olive oil alone and that released from the digestion of olive oil in combination with 500 mg CC01 and buffered salivary diluent, suggesting that the 500 mg CC01 in combination with buffered salivary diluent had no effect on olive oil digestion (Figure 4.16, graph B). Also, a small amount of gel was observed at the end of the small intestinal phase, which was less than (by observation) the gel produced from 500 mg of CC01 alginate treated with (62mM $NaHCO_3$) normal saliva.

Data in Figure 4.16 (graph B) also shows that during the small intestinal phase, there was a difference between the digestion rate of olive oil treated with 500 mg CC01 and buffered salivary diluent and the digestion rate of olive oil treated with 500 mg CC01 and normal salivary diluent at

all time points of the small intestinal phase. However, this difference was statistically significant ($P<0.05$) only at 150 and 180 minutes, where the amounts of glycerol released from digestion of olive oil treated with 500mg CC01 and buffered salivary diluent were 14.3 (±8.3) and 32 (±9.3) mg compared to 30.8 (±3.9) and 41.4 (±4.6) mg produced from the digestion of olive oil treated with 500mg CC01and normal salivary diluent at 150 and 180 minutes, respectively. This shows that 500 mg CC01 in combination with buffered synthetic salivary diluent could significantly reduce the digestion rate of olive oil compared to 500 mg of CC01 in combination with normal salivary diluent.

Data presented in Figure 4.16 (graph C) demonstrate that during the gastric phase, the amounts of glycerol released from the digestion of olive oil alone, the digestion of olive oil in combination with 1000 mg and normal salivary diluent, or the digestion of olive oil in combination with 1000 mg CC01 and buffered salivary diluent were small (≤3 mg). However, after 15 minutes from the start of the small intestinal phase, there was an increase in the digestion rate for both olive oil alone and olive oil in combination with 1000 mg CC01 and buffered salivary diluent, with a significant difference ($P<0.05$) between digestion rates at the end of the small intestinal phase (at 180-minute), where the amount of glycerol released from digestion of olive oil in combination with 1000 mg CC01 and buffered salivary diluent was 41.14 (±2.76) mg, compared to 27.59 (±2.89) mg from digestion of olive oil alone, showing that 1000 mg CC01in combination with a buffered salivary diluent may activate olive oil digestion. Moreover, some gels and lumps were observed at the end of the small intestinal phase, but these were half than (by observation) those observed upon the addition of 1000 mg CC01 alginate to olive oil at the salivary phase using the normal salivary diluent containing 62 mM $NaHCO_3$.

Additionally, as can be seen in Figure 4.16 (graph C), during the small intestinal phase, no significant difference was detected between the amount of glycerol liberated from digestion of olive oil treated with 1000 mg CC01 and buffered salivary diluent and that liberated from digestion of olive oil treated with 1000 mg CC01 and normal salivary diluent. This shows that unlike 250 and 500 mg CC01 in combination with a buffered salivary diluent, 1000 mg CC01 in combination with the buffered salivary diluent could not reduce the digestion rate of olive oil.

The data presented above suggested that that the reduction shown in the digestion of olive oil is caused by buffering the salivary diluent and not by alginate, and that can be supported by the digestion rate of olive oil alone treated with buffered diluent which was significantly lower than that of olive oil alone treated with normal olive oil (Figure 4.15). Buffering the salivary diluent may cause changes in the pH which in turn affect the activity pancreatic lipase. Therefore, the effect of buffering on the pH will be investigated later in this chapter.

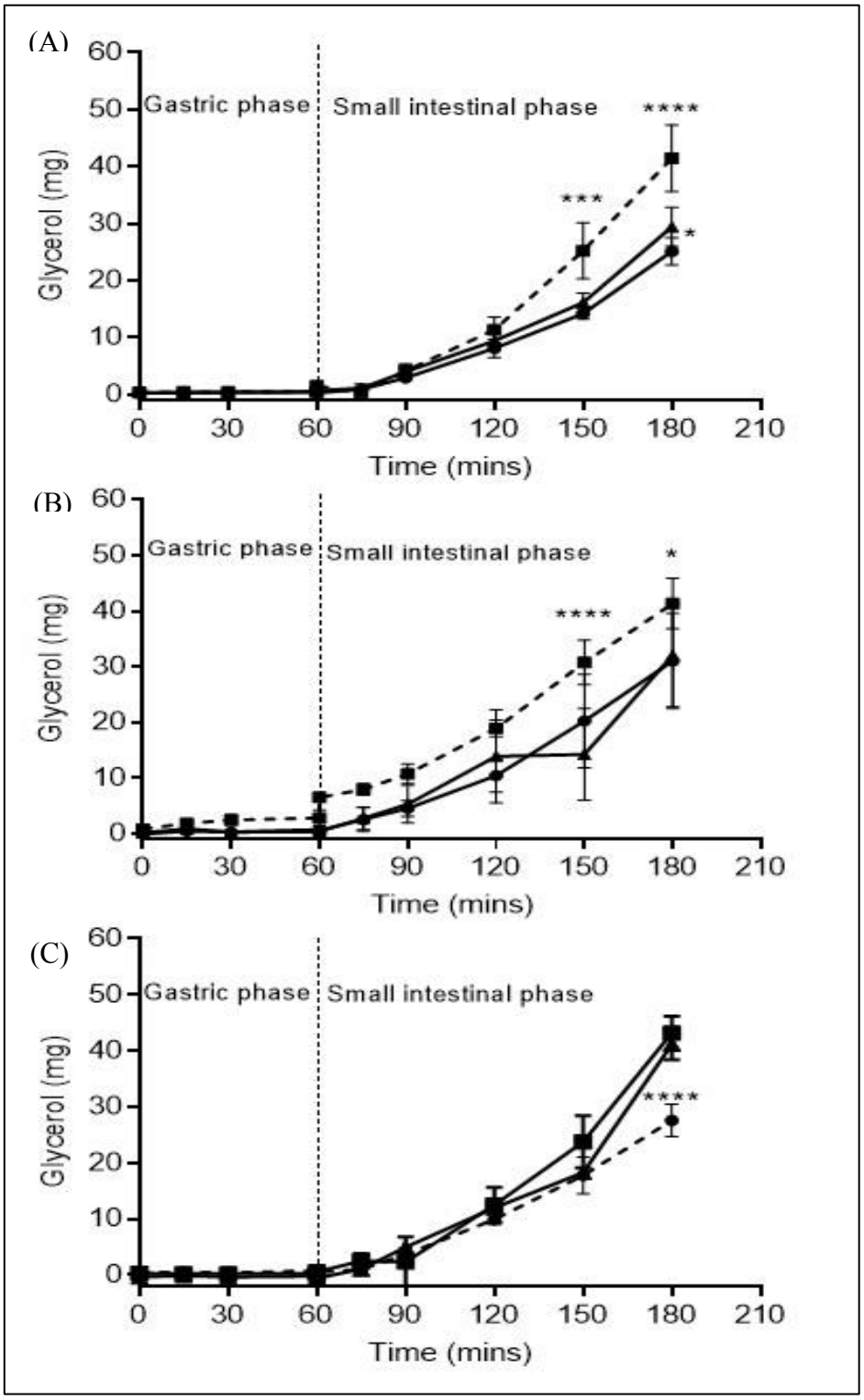

Figure 4.16. Glycerol liberation during the simulated digestion of olive oil alone using a buffered salivary diluent (●), olive oil treated with different amounts of CC01 using a normal (■) or buffered salivary diluent (▲) in the synthetic model gut. (A) 250, (B) 500 and (C) 1000 mg of CC01 were added the salivary phase of the model gut procedure. Data are shown as mean ±SD (n=3). P values <0.05 are represented by * < 0.001 are represented by ***, and < 0.0005 are represented by ****. The dotted line indicates the gastric (0-60 minutes) and small intestinal phases (60-180 minutes).

4.5.10 pH measurements during simulated digestion of fat in the model gut system

4.5.10.1 Olive oil alone and in combination with CC01 alginate added at the salivary phase

It has been reported that pancreatic lipase must remain stable over a broad pH range during the small intestinal phase of digestion to avoid irreversible denaturation [163]. The same paper states that although pancreatic lipase is produced as a component of pancreatic secretions at pH 8, it is exposed within the small intestine to pH ranging from approximately 6.5 in the duodenum to over 7 in the distal ileum. Furthermore, based on figure 1 from Brownlee et al. (2010) study, it has been shown that although the activity of pancreatic lipase is stable between the pH 6 and 7.5, there was a significant reduction in the pancreatic lipase activity when the pH is reduced below 6 or above 7.5. For example, changing pH from 5.5 to 6 increased the level of turbidity reduction from 0.15 to 0.45 (arbitrary units), indicating a significant increase in lipase activity by 200%. Also, there was an increase in the activity of pancreatic lipase by about 18% when pH was changed from 6 to 6.5. In contrast, there was a significant decrease by about 74% in the activity of pancreatic lipase when pH was altered from 7.5 to 8 [163]. To investigate if the effects of CC01 alginate on pancreatic lipase are due to pH changes resulting from its addition, the pH of olive oil alone or in combination with CC01, added at the salivary or small intestinal phase, across the range of concentrations was measured. Also, the effect of buffering the salivary diluent on the pH of pancreatic lipase was investigated.

Graphs A, B, and C in Figure 4.17 shows pH measurements at different time points for olive oil alone and olive oil in combination with 250, 500, and 1000 mg of CC01 alginate added at the salivary phase of the model gut system, respectively.

As seen in Figure 4.17 (graph A), during the gastric phase, the pH values for olive oil in combination with 250 mg CC01 alginate were higher than those for olive oil alone, but this difference was only significant ($P<0.05$) at 15 and 30 minutes, where the pH values for olive oil in combination with 250 mg of CC01 were 2.63 (±0.23) and 2.59 (±0.20), compared to 2.08 (±0.03) and 2.07 (± 0.06) for olive oil alone, respectively. However, during the small intestinal phase (60-180 minutes), there was no significant difference in the pH values between the olive oil alone and olive oil treated with 250 mg CC01.

During the gastric phase, the pH values for olive oil alone at 15, 30, and 60 minutes were 2.08 (±0.03), 2.07 (± 0.06), and 2.06 (± 0.04), respectively, and these values were significantly higher than those for olive oil in combination with 500mg CC01 which were 2.8 (±0.45) 2.9 (±0.46), 2.8 (±0.35), respectively (Figure 4.17, graph B). However, during the small intestinal phase, there was no significant difference at any time point between the pH values for the olive oil alone and olive oil in combination with 500 mg CC01 alginate.

There was a significant difference in pH values ($P<0.05$) for olive oil alone and those for the olive oil treated with 1000 mg CC01 alginate at all time points of the gastric phase. The pH values for the olive oil treated with 1000 mg CC01 alginate at 0, 15, 30, and 60 minutes of the gastric phase were 3.8 (±0.05), 3.7 (±0.1), 3.6 (±0.11), and 3.2 (±0.66), respectively, compared to 2.08 (±0.03), 2.076 (±0.03), 2.07 (± 0.06), and 2.06 (± 0.04) for olive oil alone. However, during the small intestinal phase (60-180 minutes), there was no significant difference ($P>0.05$) in the pH values between the olive oil alone and olive oil treated with 1000 mg CC01 (Figure 4.17, graph C).

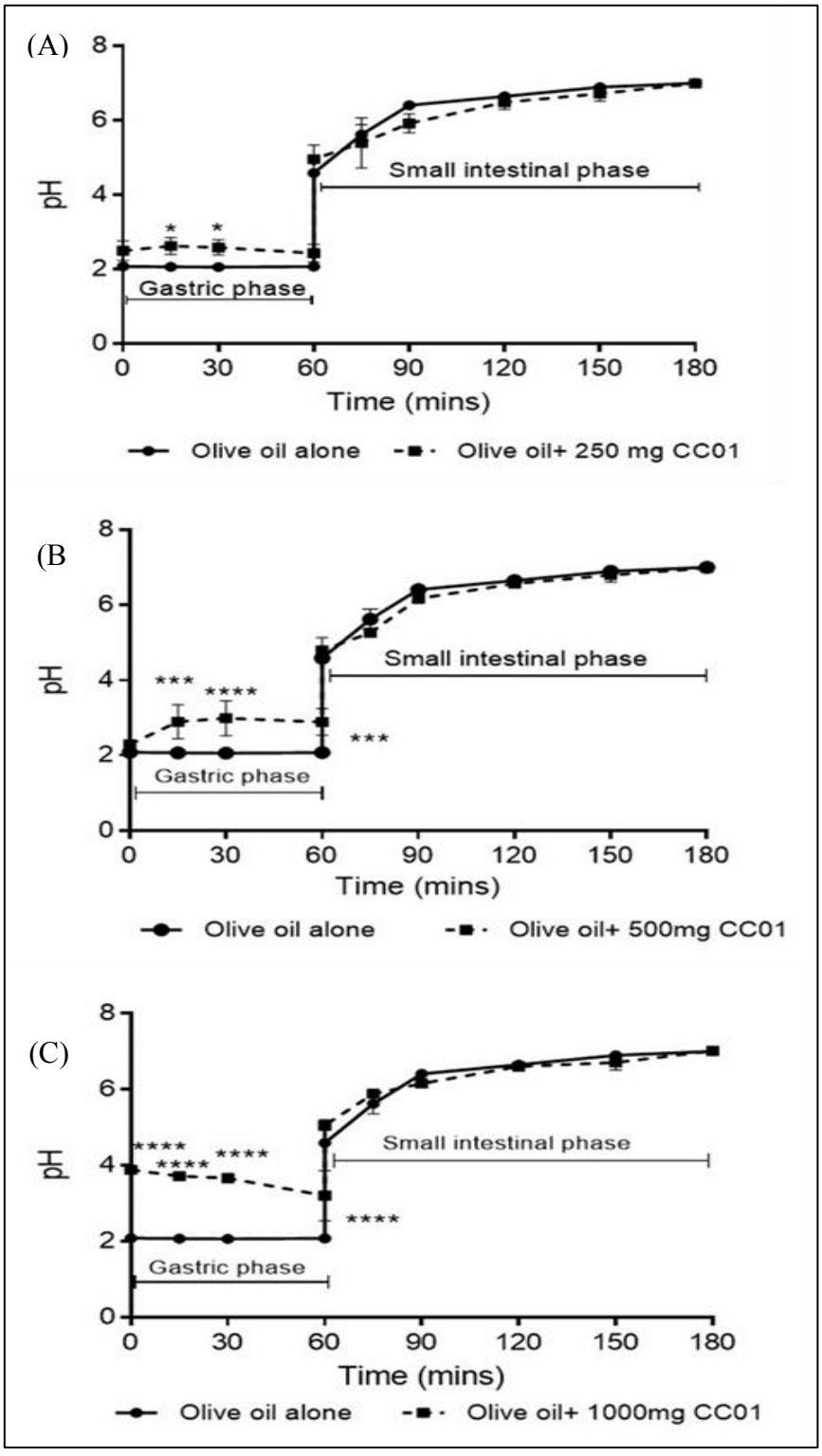

Figure 4.17. pH changes during simulated digestion of olive oil alone or in combination with different amounts of CC01 alginate. (A) 250, (B) 500, and (C) 1000 mg CC01 were added at the salivary phase of the synthetic model gut system. Data are shown as mean ±SD (n=3). P values <0.05 are represented by *, <0.001 are represented by ***, and <0.0005 are represented by ****.

4.5.10.2 Olive oil alone and in combination with CC01 alginate added at the small intestinal phase

Figure 4.18 demonstrates the pH measurements at different time points of the gastric and small intestinal phases within the synthetic model gut system for olive oil alone and olive oil in combination with 250, 500, and 1000 mg CC01 alginate added after 10 minutes of the small intestinal phase (at T_{70} of the model gut procedure). Expectedly, during the gastric phase (0-60 minutes) the pH values were highly acidic, ranging between 2 and 1.97 at the end of the gastric phase. Also, since the alginate was not yet added, the samples were identical to olive oil alone, therefore, the pH values were also identical. After 60 minutes, the bile was added to start the small intestinal phase, resulting in an increase in pH for all samples, reaching values of approximately 4.5. The pH increased further over time due to pumping of the pancreatic juice into the samples. At 70-minutes, when CC01 was added, no significant difference ($P>0.05$) was observed between the pH values for olive oil alone and those for the olive oil in combination with CC01 alginate (250, 500 or 1000 mg), indicating that the addition of alginate at the small intestinal phase did not affect the pH of the mixture, hence, the inhibition observed in olive oil digestion by 500 and 250 mg CC01 alginate, presented earlier in this chapter (Figure 4.10A and Figure 4.12, section 4.5.7), was independent of the small intestinal pH.

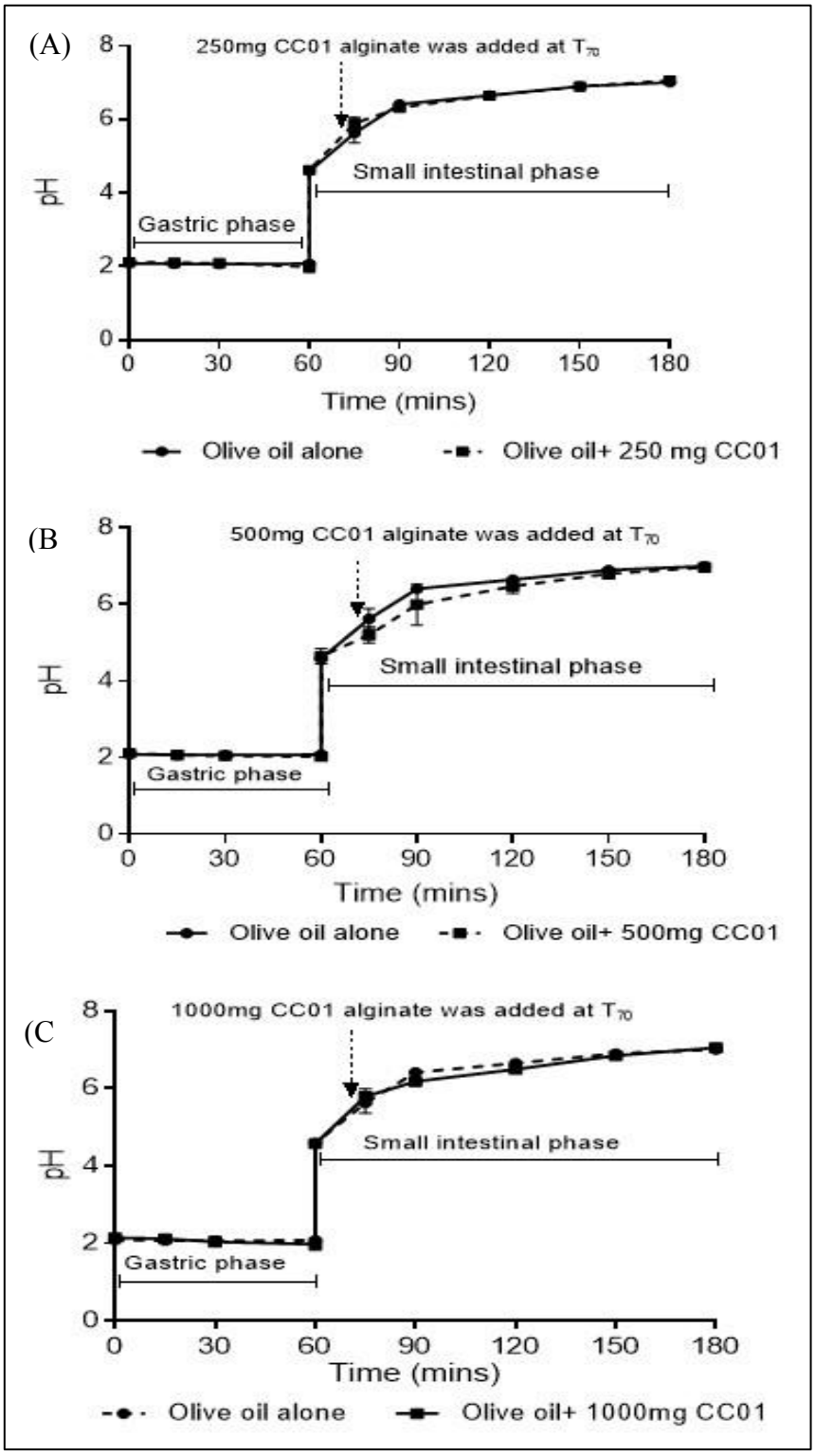

Figure 4.18. pH changes during simulated digestion of olive oil alone or in combination with different amounts of CC01 alginate. (A) 250, (B) 500, and (C) 1000 mg CC01 were added during the small intestinal phase of the synthetic model gut system. Values are shown as mean ± SD (n=3). The dotted arrow shows that alginate was added in the small intestinal phase at T_{70} of the model gut procedure.

pH data presented in Figures 4.17 and 4.18 of this chapter have been combined to allow comparison between the pH values of olive oil in combination with 250, 500, and 1000 mg of CC01 alginate added at the salivary phase and those for olive oil in combination with 250, 500, and 1000 mg of CC01 alginate added after 10 minutes of the small intestinal phase (Tables 4.5-4.7).

There was no significant difference ($P>0.05$) between the pH values for the olive oil treated with 250 mg CC01 added at the salivary phase and those for olive oil treated with 250 mg CC01 added at the small intestinal phase.

Comparison of the pH values for olive oil in combination with 500 mg of CC01 alginate added either at the salivary phase or small intestinal phase showed that at 15, 30, and 60 minutes of the gastric phase, the pH values for olive oil treated with 500 mg of CC01 alginate were significantly higher ($P<0.05$) than those for olive oil treated with 500 mg CC01 added at the small intestinal phase (Table 4.6). However, during the small intestinal phase (60T-180 minutes), there was no significant difference between the pH values for olive oil in combination with 500 mg CC01 added at the salivary phase and those for olive oil in combination with 500 mg CC01 added at the small intestinal phase.

The pH data presented in the Table 4.7 indicates that the pH values for olive oil treated with 1000 mg CC01 alginate added at the salivary phase were significantly higher ($P<0.05$) than those for olive oil in combination with 1000 mg of CC01 alginate added at the small intestinal phase at all time points of the gastric phase. However, during the small intestinal phase (60T-180 minutes), no significant difference ($P>0.05$) was observed between the pH values for olive oil in combination with 1000 mg CC01 added either at the salivary or small intestinal phases.

Adding alginate into the model gut system either at the start of the salivary phase or the small intestinal phase had no effect on the pH of samples removed from the model gut during the small intestinal phase. However, as shown in Figure 4.17, the presence of alginate during the salivary phase increased the pH of samples taken during the simulated gastric digestion.

Time (minute)	250mg CC01 alginate added at the salivary phase		250mg CC01 alginate added at the small intestinal phase		Signif.
	pH	± SD	pH	±SD	
0	2.50	± 0.26	2.11	± 0.04	ns
15	2.60	± 0.22	2.1	±0.03	ns
30	2.59	± 0.20	2.09	±0.03	ns
60	2.43	± 0.23	1.99	±0.14	ns
60T	4.96	± 0.37	4.62	±0.11	ns
75	5.40	± 0.67	5.88	±0.16	ns
90	5.92	± 0.25	6.31	±0.07	ns
120	6.48	± 0.18	6.64	±0.05	ns
150	6.72	± 0.20	6.88	±0.01	ns
180	6.99	± 0.03	7.05	±0.04	ns

Table 4.5. Comparison between the pH values for olive oil treated with 250 mg CC01 alginate added at the salivary phase and the pH values for olive oil with 250 mg CC01 added at the small intestinal phase. The gastric phase lasted for 1 hour (0-60 minutes) and the small intestinal phase lasted for 2 hours (60T-180 minutes). 60T indicates the zero time of small intestinal phase. Data are shown as mean ± SD, (n=3), P values >0.05 indicates non-significant difference (ns) in pH values between the samples.

Time (minute)	500 mg CC01 alginate added at the salivary phase		500 mg CC01 alginate added at the small intestinal phase		Signif.
	pH	± SD	pH	±SD	
0	2.30	± 0.03	2.11	± 0.04	ns
15	2.89	± 0.45	2.06	±0.05	*
30	2.99	± 0.46	2.04	±0.05	*
60	2.89	± 0.35	2.02	±0.05	*
60T	4.79	± 0.33	4.60	±0.02	ns
75	5.26	± 0.02	5.20	±0.21	ns
90	6.16	± 0.10	5.99	±0.53	ns
120	6.57	± 0.09	6.48	±0.19	ns
150	6.79	± 0.18	6.80	±0.12	ns
180	6.98	± 0.10	6.97	±0.04	ns

Table 4.6. Comparison between the pH values for olive oil treated with 500 mg CC01 alginate added at the salivary phase and the pH values for olive oil with 500 mg CC01 added at the small intestinal phase. The gastric phase lasted for 1 hour (0-60 minutes) and the small intestinal phase lasted for 2 hours (60T-180 minutes). 60T indicates the zero time of small intestinal phase. Data are shown as mean ± SD, (n=3). P value <0.05 was taken to detect the significant difference in pH values where P values < 0.05 are represented by *, and P values > 0.05 are represented by ns (non-significant difference).

Time (minute)	1000 mg CC01 alginate added at the salivary phase		1000 mg CC01 alginate added at the small intestinal phase		Signif.
	pH	± SD	pH	±SD	
0	3.88	± 0.05	2.14	± 0.06	****
15	3.71	± 0.10	2.12	±0.05	****
30	3.66	± 0.11	2.03	±0.13	****
60	3.20	± 0.66	1.97	±0.15	****
60T	5.05	± 0.14	5.79	±0.06	ns
75	5.88	± 0.07	6.18	±0.20	ns
90	6.15	± 0.60	6.49	±0.10	ns
120	6.60	± 0.05	6.48	±0.08	ns
150	6.70	± 0.20	6.84	±0.05	ns
180	7.01	± 0.08	7.05	±0.04	ns

Table 4.7. Comparison between the pH values for olive oil treated with 1000 mg CC01 alginate added at the salivary phase and the pH values for olive oil with 1000 mg CC01 added at the small intestinal phase. The gastric phase lasted for 1 hour (0-60 minutes) and the small intestinal phase lasted for 2 hours (60T-180 minutes). 60T indicates the zero time of small intestinal phase. Data are shown as mean ± SD, (n=3). P value <0.05 was taken to detect the significant difference in pH values where P values <0.0005 are represented by ****, whereas P values > 0.05 are represented by ns (non-significant difference).

4.5.10.3 Glyceryl trioctanoate alone and in combination with 500 mg CC01 added at the salivary phase and in the small intestinal phase

Table 4.8 shows the pH values for glyceryl trioctanoate alone (as a control) and glyceryl trioctanoate in combination with 500 mg CC01 added either at the salivary phase or 10 minutes after the start of the small intestinal phase (at T_{70} of the model gut procedure).

During the gastric phase, the pH values for glyceryl trioctanoate in combination with 500 mg CC01 added at the salivary phase were significantly higher than ($P<0.05$) those for glyceryl trioctanoate alone. However, during the small intestinal phase, no significant difference ($P>0.05$) was detected between the pH of glyceryl trioctanoate alone and those of glyceryl trioctanoate in combination with 500 mg CC01 added at the salivary phase.

Table 4.8 also shows the pH values for glyceryl trioctanoate alone and in combination with 500 mg of CC01 added 10 minutes after the start of the small intestinal phase. As expected, during the gastric phase where the alginate was not present, no significant difference ($P>0.05$) was seen in pH values between the samples. During the small intestinal phase, there was no significant difference between the pH values for glyceryl trioctanoate alone and those for glyceryl trioctanoate in combination with 500 mg CC01.

Data from Table 4.8 also shows that at 15, 30, and 60 minutes of the gastric phase (0-60 minutes), the pH values for glyceryl trioctanoate treated with 500 mg CC01 added at the salivary phase were significantly higher ($P<0.05$) than those for glyceryl trioctanoate where CC01 was not yet added to the sample. However, when 500 mg CC01 was added 10 minutes after the start of the small intestinal phase (60T-180 minutes), there was no significant difference ($P>0.05$) in the pH values for glyceryl trioctanoate in combination with 500 mg of CC01 added at the small intestinal phase and those for glyceryl trioctanoate in combination with 500 mg of CC01 added at the salivary phase.

During the small intestinal phase (60T-180 minutes) where the majority of triglyceride digestion occurs, the pH values for glyceryl trioctanote alone were not significantly different to the pH values for glyceryl trioctanoate in combination with 500 mg of CC01 added at the salivary phase nor the pH values for glyceryl trioctanoate added at the small intestinal phase (T_{70}). Also, no significant difference was observed between the pH values for glyceryl trioctanoate treated with 500 mg CC01

added at the salivary phase and those for glyceryl trioctanoate treated with 500 mg CC01 added at the small intestinal phase (T_{70}). Consequently, changes in pH could not account for any inhibition or activation of pancreatic lipase by alginate.

Time (minutes)	Glyceryl trioctanoate alone			500mg CC01 added at the salivary phase			500mg CC01 added at the small intestinal phase		
	pH	±SD	Signif	pH	±SD	Signif	pH	±SD	Signif
0	1.95	(±0.23)	ns	2.21	(±0.29)	ns	1.98	(±0.23)	ns
15	1.93	(±0.25)	c	2.50	(±0.48)	ab	1.97	(±0.22)	C
30	1.92	(±0.26)	c	2.54	(±0.56)	ab	1.96	(±0.25)	C
60	1.90	(±0.28)	c	2.47	(±0.50)	ab	1.93	(±0.24)	C
60T	4.47	(±0.33)	ns	4.45	(±0.15)	ns	4.45	(±0.16)	ns
75	5.35	(±0.50)	ns	5.11	(±0.46)	ns	5.41	(±0.34)	ns
90	5.69	(±0.09)	ns	5.81	(±0.13)	ns	5.55	(±0.33)	ns
120	6.08	(±0.12)	ns	6.03	(±0.14)	ns	5.98	(±0.07)	ns
150	6.21	(±0.01)	ns	6.20	(±0.02)	ns	6.22	(±0.04)	ns
180	6.51	(±0.06)	ns	6.46	(±0.05)	ns	6.46	(±0.03)	ns

Table 4.8. pH measurements for glyceryl trioctanoate alone and in combination with 500 mg CC01 alginate added either at the salivary phase or the small intestinal phase of the model gut system.Values are shown as mean ± SD, (n=3). P value < 0.05 was used for comparison between the pH values for glyceryl trioctanoate alone and those for the alginate samples to determine the significance difference (signif.). Letters a, b and c represent a significant difference ($P<0.05$) from the control, a significant difference ($P<0.05$) from the samples of alginate added at the small intestinal phase and a significant difference ($P<0.05$) from alginate added at the salivary phase, respectively. P values >0.05 are represented by ns (non-significant difference). 60T represents the zero-minute of the small intestinal phase. CC01 was added 10 minutes after the start of the small intestinal phase.

4.5.10.4 Olive oil alone and in combination with alginate added at the salivary phase using a buffered synthetic salivary diluent

Figure 4.19 illustrates the pH measurements within the synthetic model gut system for olive oil alone as a control and olive oil in combination with 250, 500, and 1000 mg CC01 alginate added at the salivary phase using buffered salivary diluent containing 372mM $NaHCO_3$.

The pH values for the olive oil in combination with 250 mg of CC01 at 0, 15, 30, and 60 minutes of the gastric phase were 5.39 (±0.16), 4.32 (±0.24), 3.59 (±0.15), and 3.03 (±0.11), and these values were significantly higher ($P<0.05$) than the pH values for olive oil alone at 0, 15, 30, and 60 minutes which were 4.89, 2.88, 2.32, and 1.97, respectively (Figure 4.19, graph A). However, during the small intestinal phase, there was no significant difference ($P>0.05$) between the pH values of the olive oil alone or in combination with 250 mg of CC01 at any time point.

The pH measurements for olive oil alone and in combination with 500 mg CC01 (Figure 4.19, graph A) shows that the pH of olive oil treated with 500 mg of CC01 at 0, 15, 30, and 60 minutes of the gastric phase was 5.25 (±0.08), 4.38 (±0.23), 3.85 (±0.13), and 3.44 (±0.15), respectively, compared to 5.3 (±0.19), 3.40 (±0.06), 2.75 (±0.07), and 2.29 (±0.10) for olive oil alone at 0, 15, 30, and 60 minutes, respectively. The pH values for olive oil in combination with 500 mg of CC01 were significantly higher ($P<0.05$) than those for olive oil alone at 15, 30, and 60 minutes, but not at 0-minute. During the small intestinal phase, no significant difference was observed between the pH values for olive oil alone and those for olive oil treated with 500 mg CC01.

The pH values for olive oil in combination with 1000 mg CC01 at 0, 15, 30, and 60 minutes of the gastric phase were 5.9 (±0.19), 5.14 (±0.58), 4.16 (±0.19), and 3.67 (±0.03), compared to 5.6 (±0.15), 3.06 (±0.12), 2.42 (±0.08), and 2.08 (±0.10) for olive oil alone, respectively (Figure 4.19, graph C). The difference in gastric pH values for olive oil alone and olive oil in combination with 1000 mg CC01 became significant ($P<0.05$) at 15, 30, and 60 minutes. During the small intestinal phase (60-180 minutes), there was no significant difference between the pH values of olive oil alone and the pH of olive oil in combination with 1000 mg CC01.

Based on the pH data from the graphs A, B, and C of Figure 4.19, all three concentrations (250, 500 and 1000 mg) of alginate could significantly increase the pH in the gastric phase. However, the pH values for olive oil in combination with 1000 mg CC01 at 0, 15, 30, and 60 minutes of the

gastric phase were the highest, indicating that the change in pH is a concentration dependent.

Although the gastric pH of olive oil treated with CC01 (250, 500 or 1000 mg) in the intestinal phase were significantly higher ($P<0.05$) than those for olive alone, the pH values for olive oil treated with CC01 in the small intestinal phase, where the majority of triglyceride digestion occurs, were not altered from those for olive oil alone, indicating that the shift in pH cannot explain the change in pancreatic lipase activity.

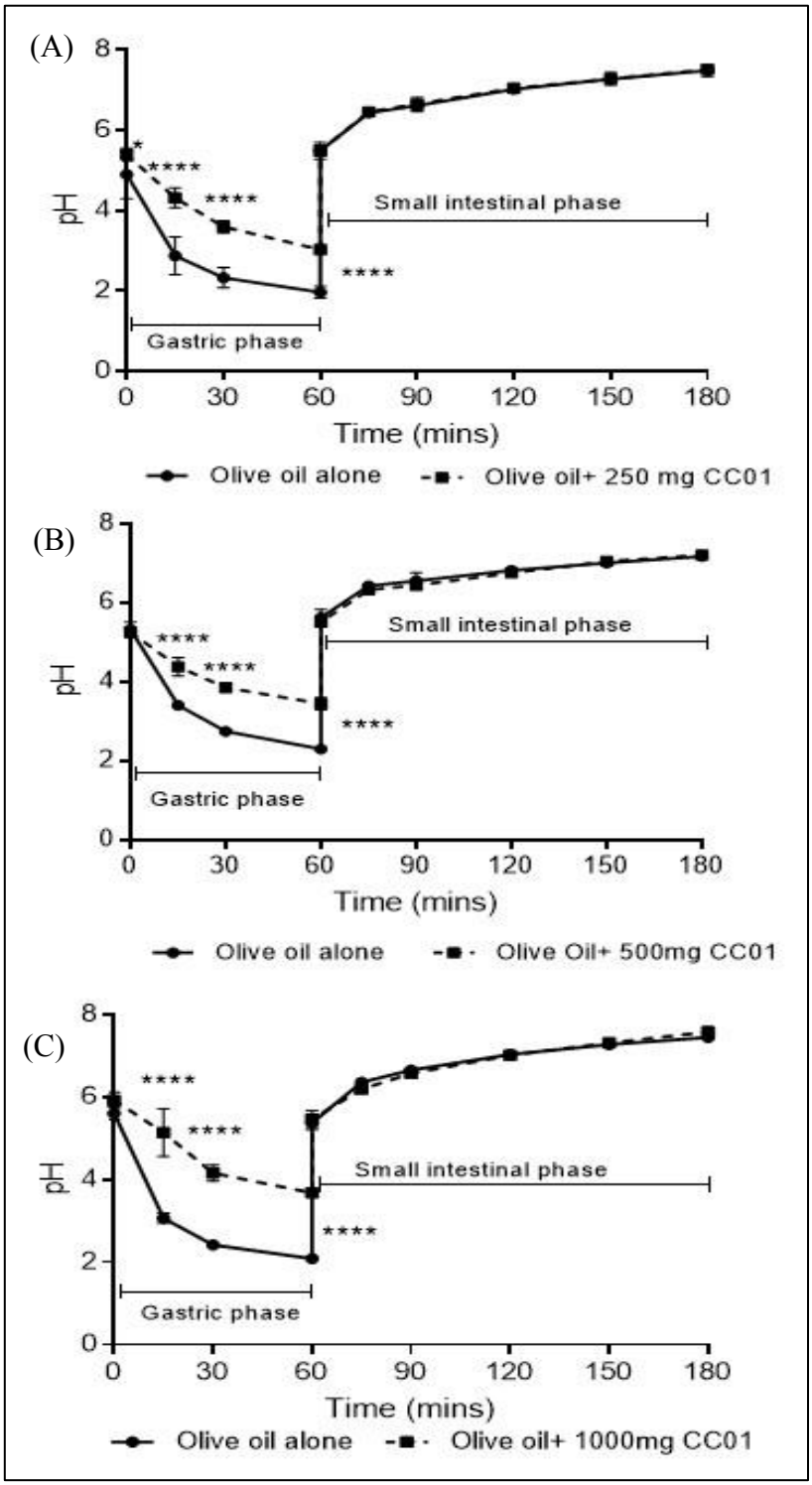

Figure 4.19. pH changes during the digestion of olive oil alone using buffered salivary diluent and olive oil in combination with different amounts of CC01 alginate using buffered salivary diluent. (A) 250, (B) 500 and (C) 1000 mg CC01 were added at the salivary phase within the model gut system. Data are shown as mean ± SD, (n=3). The significant difference was determined based on P value <0.05 where * represents P values < 0.05 and **** represent P <0.0005.

4.5.10.5 Olive oil in combination with CC01 using a buffered salivary diluent and olive oil in combination with CC01 using normal salivary diluent

Table 4.9 shows the pH measurements for olive oil alone using either normal saliva containing 62mM $NaHCO_3$ or buffered saliva containing 372mM $NaHCO_3$. During the gastric phase (0-60 minutes), the pH values for the olive oil treated with buffered saliva appeared higher than those for olive oil treated with normal saliva, but the difference in pH values was significant only at zero-minute of the gastric phase. However, during the small intestinal phase (60T-180 minutes), there was no difference between the pH values for olive oil treated with buffered saliva and those for olive oil treated with normal saliva, indicating that the reduction in the digestion rate of olive oil treated with buffered saliva compared with that of olive oil treated with normal saliva was independent of pH.

Tables 4.10, 4.11 and 4.12 demonstrate pH values for olive oil treated with 250, 500, and 1000 mg CC01 added at the salivary phase using either normal synthetic saliva containing 62mM $NaHCO_3$ or buffered synthetic saliva 372mM $NaHCO_3$, respectively.
It is obvious from Table 4.10 that during the gastric phase (0-60 minutes), the pH values for olive oil treated with 250 mg CC01 and buffered saliva were significantly higher than ($P<0.05$) those for olive oil treated with 250 mg CC01 and normal saliva at all time intervals. However, during the small intestinal phase (60T-180 minutes), although the pH values for olive oil treated with 250 mg CC01 and buffered saliva were higher than those for olive oil in combination with 250 mg CC01 and normal saliva at all time points, Bonferroni's test indicated a significant difference ($P<0.05$) only at 75 and 90 minutes.

Data in Table 4.11 show that during the gastric phase (0-60 minutes), the pH values for olive oil in combination with 500 mg CC01 and buffered saliva were significantly higher ($P<0.05$) than those for olive oil treated with 500 mg CC01 and normal saliva at 0, 15, and 30 minutes, but not at 60-minute. However, during the small intestinal phase (60T-180 minutes), although the pH values for olive oil treated with 500 mg CC01 and buffered saliva were higher than those for olive oil treated with 500 mg CC01 and normal saliva, Bonferroni's test showed a significant difference in pH values only at 60T and 75 minutes (Table 4.11).

The pH measurements in Table 4.12 demonstrate that during the gastric phase (0-60 minutes), the pH values for olive oil in combination with 1000 mg CC01 alginate and buffered saliva were higher than those for olive oil in combination with 1000 mg CC01 and normal saliva. However, Bonferroni's test indicates a significant difference between the gastric pH values only at 0 and 15 minutes. During the small intestinal phase (60T-180 minutes), however, the pH values for olive oil treated with buffered saliva and 1000 mg CC01 were higher than those for olive oil treated with normal saliva and 1000 mg CC01, but no significant difference ($P>0.05$) was observed between pH values at any time point of the small intestinal phase.

Unlike alginate added at the salivary phase with saliva containing 62mM $NaHCO_3$, when the alginate was added at the salivary phase in combination with salivary diluent containing 372mM $NaHCO_3$, less gel was formed in the samples and this could be because the buffered saliva produced a higher pH in the gastric phase which prevents or reduces acid gel formation.

It is obvious that the digestion rate of olive oil alone in the presence of buffered saliva was slower than its digestion rate in the presence of normal saliva, but no significant difference was detected between their pH values in the small intestinal phase, therefore that the reduction in the digestion of olive oil treated with buffered saliva was independent of the pH, suggesting that this reduction might be because of calcium binding with bicarbonate through cation exchange.

The pH changes in the gastric and pancreatic phases might account for the change in the levels of pancreatic lipase activity which might provide an explanation for the reduction in the digestion rate of olive oil treated with buffered saliva and CC01 alginate compared with the digestion rate of olive oil treated with normal saliva and CC01 alginate.

Time (minute)	Olive oil with normal salivary diluent		Olive oil with buffered salivary diluent		P value	Signif.
	pH	± SD	pH	±SD		
Zero	2.08	± 03	4.51	± 0.17	<0.0001	****
15	2.07	± 0.03	3.03	±0.38	>0.05	ns
30	2.06	± 0.06	2.59	±0.16	>0.05	ns
60	2.03	± 0.04	2.27	±0.17	>0.05	ns
60T	4.59	± 0.07	5.32	±0.33	>0.05	ns
75	5.62	± 0.26	6.06	±0.57	>0.05	ns
90	6.41	± 0.08	6.29	±0.52	>0.05	ns
120	6.65	± 0.07	6.78	±0.27	>0.05	ns
150	6.89	± 0.09	6.99	±0.27	>0.05	ns
180	7.00	± 0.09	7.20	±0.22	>0.05	ns

Table 4.9. pH changes during simulated digestion of olive oil alone using normal or buffered salivary diluent within the synthetic model gut system. The normal salivary diluent contained 62mM $NaHCO_3$, whereas the buffered salivary diluent contained 372mM $NaHCO_3$. Data are shown as mean ± SD, (n=3). P values <0.0001 are represented by ****, whereas P values >0.05 are represented by ns (non-significant difference). The gastric phase lasted for one hour (0-60 minute) whereas the small intestinal phase lasted for two hours (60T-180 minute). 60T represents the zero-minute of the small intestinal phase.

Time (minute)	Olive oil with 250 mg CC01 using normal salivary diluent		Olive oil with 250 mg CC01 using buffered salivary diluent		P value	Signif.
	pH	± SD	pH	±SD		
Zero	2.50	± 0.26	5.39	± 0.16	<0.0001	****
15	2.60	± 0.22	4.32	±0.25	<0.0001	****
30	2.59	± 0.20	3.59	±0.15	<0.005	***
60	2.43	± 0.23	3.03	±0.12	<0.05	*
60T	4.96	± 0.30	5.49	±0.21	>0.05	ns
75	5.40	± 0.67	6.46	±0.12	<0.005	***
90	5.83	± 0.24	6.65	±0.16	<0.005	***
120	6.48	± 0.18	7.04	±0.11	>0.05	ns
150	6.72	± 0.20	7.27	±0.17	>0.05	ns
180	6.99	± 0.03	7.50	±0.12	>0.05	ns

Table 4.10. pH changes during simulated digestion of olive oil in combination with 250 mg CC01 added at the salivary phase using normal or buffered salivary diluent within the model gut system.Data are shown as mean ± SD, (n=3). P values < 0.05 are represented by *, <0.0005 are represented by ***, and <0.0001 are represented by ****, whereas P values >0.05 are represented by ns (non-significant difference). The gastric phase lasted for one hour (0-60 minute) whereas the small intestinal phase lasted for two hours (60T-180 minute). 60T represents the zero-minute of the small intestinal phase.

Time (minute)	Olive oil with 500 mg CC01 using normal salivary diluent		Olive oil with 500 mg CC01 using buffered salivary diluent		P value	Signif.
	pH	± SD	pH	±SD		
Zero	2.30	± 0.03	5.26	± 0.08	<0.0001	****
15	2.89	± 0.45	4.38	±0.23	<0.0001	****
30	2.99	± 0.46	3.85	±0.12	<0.005	**
60	2.89	± 0.35	3.44	±0.16	>0.05	ns
60T	4.79	± 0.33	5.51	±0.12	<0.05	*
75	5.26	± 0.02	6.32	±0.06	<0.0005	***
90	6.16	± 0.10	6.43	±0.04	>0.05	ns
120	6.57	± 0.09	6.75	±0.03	>0.05	ns
150	6.79	± 0.18	7.04	±0.01	>0.05	ns
180	6.98	± 0.10	7.20	±0.02	>0.05	ns

Table 4.11. pH changes during simulated digestion of olive oil in combination with 500 mg CC01 added at the salivary phase using normal or buffered salivary diluent within the model gut system.Data are shown as mean ± SD, (n=3). P values < 0.05 are represented by *, <0.005 are represented by **, <0.0005 are represented by ***, and <0.0001 are represented by ****. P values >0.05 are represented by ns (non-significant difference). The gastric phase lasted for one hour (0-60 minute) whereas the small intestinal phase lasted for two hours (60T-180 minute). 60T represents the zero-minute of the small intestinal phase.

Time (minute)	Olive oil with 1000 mg of CC01 using normal salivary diluent		Olive oil with 1000 mg of CC01 using buffered salivary diluent		P value	Signif.
	pH	± SD	pH	±SD		
Zero	3.88	± 0.05	5.92	± 0.19	<0.0001	****
15	3.71	± 0.10	5.14	±0.58	<0.0001	****
30	3.66	± 0.11	4.16	±0.19	>0.05	ns
60	3.20	± 0.66	3.67	±0.03	>0.05	ns
60T	5.05	± 0.14	5.46	±0.21	>0.05	ns
75	5.88	± 0.07	6.19	±0.04	>0.05	ns
90	6.15	± 0.60	6.56	±0.07	>0.05	ns
120	6.60	± 0.05	7.00	±0.02	>0.05	ns
150	6.70	± 0.20	7.31	±0.04	>0.05	ns
180	7.01	± 0.08	7.57	±0.11	>0.05	ns

Table 4.12. pH changes during simulated digestion of olive oil in combination with 1000 mg CC01 added at the salivary phase using normal or buffered salivary diluent within the model gut system.Data are shown as mean ± SD, (n=3. P values <.0001 are represented by * and ****, respectively, whereas P values >0.05 are represented by ns (non-significant difference). The gastric phase lasted for one hour (0-60 minute) whereas the small intestinal phase lasted for two hours (60T-180 minute). 60T represents the zero-minute of the small intestinal phase.

4.6 Discussion

In this chapter, three different fat substrates, glyceryl trioctanoate, olive oil and sunflower oil, were run alone or in combination with alginates in a synthetic model gut system to investigate alginates as potential lipase inhibitors. The data presented here showed that all the fat substrates were digestible in the synthetic model gut with different rates of digestion, suggesting that the digestion rate of fat substrates is dependent on fatty acid chain length and their degree of saturation.

During the gastric phase of the model gut system, only trace amounts of glycerol were released from digestion of glyceryl trioctanoate, olive oil and sunflower oil, showing that little digestion of fat takes place in the gastric phase. These observations agree with earlier studies which reported that only 20% of triglyceride intake undergoes hydrolysis in the stomach by the action of gastric lipase which is resistant to denaturation by pepsin and thus can function even in an acidic environment [164]. Furthermore, it has been stated that approximately 10-30% of fat intake is digested in the stomach, releasing free fatty acids and 2-monoglycerides. The digestion process of fats in the stomach enables their full hydrolysis in the small intestine due to formation of these hydrolysis products which in turn promote triglyceride solubility and accelerate binding of colipase to the substrate interface [54, 165-167]. As hydrolysis is only partial in the stomach, then little glycerol will be released as this requires complete hydrolysis. This fatty acid release results in the activation of cholecystokinin (CCK), a hormone which sequentially stimulates the pancreas to produce digestive enzymes including pancreatic lipase and procolipase [165, 167]. Moreover, Mu & Høy (2004) reported that triglycerides are partially hydrolysed in the stomach by gastric or lingual lipase depending on the species considered, and both lipases tend to break down the *sn*3-ester bond, producing sn1, 2-diacylglycerides and fatty acids [110]. The lipases tendency to attack the ester bond at *sn*3 is two times higher than the *sn*1-ester bond. In addition, it has been stated that lingual and gastric lipases can hydrolyse short- and medium-chain triglycerides more effectively than long-chain triglycerides [64, 168]. Also, Borel et al (1994) demonstrated that in the rabbit, pure gastric lipase hydrolysed medium-chain triglycerides three times faster than long-chain triglycerides [169].

The data presented here based on glycerol release from glyceryl trioctanoate, olive oil and sunflower oil digestion at the end of small intestinal phase showed that higher amounts of glycerol were released during the small intestinal phase as opposed to the gastric phase of the model gut.

This is as expected as triglyceride hydrolysis occurs mainly in the small intestinal phase by the action of pancreatic lipase. Embleton, & Pouton (1997) and Mu & Høy (2004) reported that pancreatic lipase shows a high preference to attack the ester bonds at *sn*1 and *sn*3, but not the *sn*2 ester bond, producing 2-monoacylglyceride and free fatty acids as the main products of small intestinal hydrolysis [110, 170]. However, they stated that 2-monoacylglyceride may be rearranged to 1-monoacylglyceride via slow and non-enzymatic isomerisation under alkaline pH, resulting in complete hydrolysis for triglyceride into glycerol and free fatty acids [64, 110, 170]. It has been reported that the relative quantities of the various products arising from triglyceride hydrolysis in a normal human are mostly as follows: 22% glycerol, 72% 2-monoglycerides and 6% 1-monoglycerides [170] .

It is clear from the data presented in this chapter that the digestion rate of glyceryl trioctanoate was the highest among the three fat substrates, and that may occur because of the difference in length of the fatty acids and the degree of unsaturation. Glyceryl trioctanoate consists of pure saturated medium-chain triglycerides containing octanoic acids (C8:0) at the 1, 2 and 3 positions. Olive oil is a mixture of monounsaturated long- medium chain triglycerides consisting of monounsaturated oleic acids (C18:1) and saturated palmitic acids (C16: 0), while sunflower oils are long-chain triglycerides containing polyunsaturated linoleic acids (C18: 2) and monounsaturated oleic acids (C18: 1) at 1 and 3 positions. Olive oil triglycerides contain oleic (55-83%), palmitic (7.5-20%), linoleic (3.5-21) %, linolenic (0.01-1%), stearic (0.5-5%), and palmitoleic (0.3-3.5%) acids [171]. Although olive oil is composed of different fatty acids, oleic acid is the most abundant, forming up to 68-80% of the fatty acids present in olive oil, whereas palmitic acid forms 9-12% of olive oil fatty acids [172] . According to Orsavova et al (2015), sunflower oil triglycerides contain different fatty acids, however, oleic acid (28%) and linoleic acids (62%) are the predominant fatty acids in the oil [173].

All lipases responsible for triglyceride digestion attack the ester bonds of triglycerides specifically at the 1 and 3 positions, and these enzymes have tendency to hydrolyse short- and medium-chain triglycerides more than long-chain triglycerides [174]. Additionally, pancreatic lipase tends to hydrolyse medium-chain triglycerides more than long-chain triglycerides, and the intraluminal breakdown of these medium-chain triglycerides occurs very rapidly in the small intestine [175]. Another study on rats reported that the hydrolysis rate of medium-chain fatty acid triglycerides is more rapid than for long-chain fatty acid triglycerides [176]. In this current study, based on the

glycerol produced at T_{180}, the digestion of olive oil alone was quicker than the sunflower oil, and this might occur because triglycerides of olive oil includes saturated palmitic acid (C16:0) and monounsaturated fatty acids (oleic acid, C18:1), while sunflower oil triglycerides contain monounsaturated fatty acids (oleic acid, C18:1) and polyunsaturated fatty acids (linoleic acids, C18:2) at the 1 and 3 positions, respectively. Triglycerides containing polyunsaturated fatty acids are more rigid (less flexible) than those with saturated and monounsaturated fatty acids. Therefore, these two triglycerides may differ in the way that they insert to the active site of enzymes especially considering that the rotation around the double bond is restricted, while the rotation around the single bond is free.

The data obtained from digestion of fat substrates in combination with 500 mg alginate added at the salivary phase was unexpected. Glyceryl trioctanoate treated with either 500 mg CC01 or 1N80 showed a significant reduction in digestion ($P< 0.05$) compared with the relevant control (glyceryl trioctanoate alone), while 500 mg 1LF80 had no significant effect on glyceryl trioctanoate digestion. The ability of the alginates to inhibit digestion of octanoic acid (C8:0) containing triglycerides may relate to the fact that trioctanoate hydrolysis is more rapid than triglycerides containing palmitic acid (C16:0) and oleic acid (C18:1) or linoleic acid (C18:2). In addition, when the alginate was added to glyceryl trioctanoate at T_{70}, it did not inhibit digestion, suggesting for the alginate to be active, it must pass through the low gastric pH phase. It may be that some substrate/inhibitor interaction in the gastric phase is necessary to allow inhibition of pancreatic lipase.

There was no significant reduction in digestion rates of either olive oil or sunflower oil treated with 500 mg CC01, 1N80 or 1LF80. During the model gut experiments, it was noticed that once the alginate (CC01, 1N80 or 1LF80) had been added to glyceryl trioctanoate, olive oil or sunflower oil at the salivary phase, the pH ranged between 7 and 7.3, and once the synthetic gastric juice was added to start the gastric phase, some gelatinous precipitates were observed. However, at the end of the pancreatic phase, there were some gelatinous pieces in the olive oil and sunflower oil chambers beakers, but not in the glyceryl trioctanoate chamber.

The alginate may precipitate and form an acid gel due to the rapid decrease in pH to 2-2.5 when the gastric juice is added. Draget and his colleagues, in 2006, demonstrated that the rapid decrease in the pH of an alginate solution from pH 7 will result in the precipitation of alginate, however, they reported that an alginic acid gel may be formed when the pH of the alginate solution is

decreased slowly. Furthermore it has been reported that at low pH, -CCO^- ions of the alginate chain are protonated to -COOH, thus the electrostatic repulsion between alginate chains decreases and the chains become closer to each other, leading to formation of hydrogen bonds and increasing viscosity, and when a further decrease in the pH occurs, a gel will form at pHs between 3 and 4 [177]. However, Cuibal and his colleagues reported that alginates lack the ability to form gels and they tend to precipitate at pHs < 3.5 [178]. Imeson (2012) stated that at low pH, less than or around the pKa of alginic acid (3.5), foods and beverages containing alginates will be unaffected by the stability and thickening properties of alginates, and when a further decline in pH occurs, the alginate will undergo a partial protonation, losing its net negative charge and the alginic acid begins to precipitate [179]. Furthermore, the presence of calcium chloride in saliva and pancreatic juice may result in alginate precipitation and gel formation. Even though sodium alginate immediately precipitates or forms gel in the presence of $CaCl_2$, small amounts of sodium alginate are unable to form a homogenous gel (without any lumps) in the presence of calcium ions even with high-speed stirring because of the strong, quick and permanent formation of junctions in the gel and the high rate of gelation [103].

It has been reported that alginate usually forms hydrogels in the presence of cross-linking agents such as $CaCl_2$, where the calcium ions bind only to G-blocks of alginate chains because of their structural features, which provide a suitable distance between COO^- and OH^- groups, hence allowing a high level of coordination with calcium ions [100, 180]. The G-block of one polymer links with G-blocks of neighbouring polymer chains making a gel structure with a shape referred to as the egg-box structure (shown in Figure 2.10, Chapter 2 of this thesis) [100]. Additionally, it has been reported that G-block regions possess a pleated conformation due to the presence of diaxial linkages which restrict rotation around the glycosidic bonds, hence producing a stiff and extended chain while MG-blocks are softer and more flexible [181]. Furthermore, the mannuronate/guluronate (M/G) ratio has been reported by many studies as a crucial factor in determining the quality of an alginate gel where the alginate with a high content of G-block forms strong stiff gels, while alginate with high M-block content produces soft and flexible gels [159, 160].

A key difference in the model gut experiments with glyceryl trioctanoate was the pancreatic juice used contained a higher amount of sodium bicarbonate (322.8 mM) compared with the pancreatic juice used in olive oil and sunflower oil experiments (110 mM), to avoid the reduction in pH which

may arise from fatty acid release especially because glyceryl trioctanoate triglycerides produce fatty acids with a low pKa (4.9). The higher concentration of sodium bicarbonate may provide a more alkaline environment which could degrade the gel, thus releasing the alginate which then inhibited glyceryl trioctanoate digestion.

Experimental results from the model gut digestion of olive oil treated with alginate added after 10 minutes of the pancreatic small intestinal phase showed that both 250 and 500 mg CC01 significantly reduced olive oil digestion. Additionally, 500 mg 1N80 significantly decreased olive oil digestion at 150-minute, while 500 mg 1LF80 had no effect on olive oil digestion. It is apparent that unlike glyceryl trioctanoate where passage through the gastric phase is necessary for alginate inhibition, passage of alginate through the gastric phase prevents alginate inhibition of olive oil. This could be explained by a lack of alginate substrate interaction in the gastric phase which cannot then form in the more alkaline small intestinal phase.

The amount of glycerol released from the digestion of olive oil treated with 500 mg CC01 in the small intestinal phase was significantly lower than the amount of glycerol released from the digestion of olive oil treated with 250 mg CC01, showing that the inhibitory effect of alginate is dependent on concentration. This result is in agreement with the results obtained from the turbidity microplate assay presented in Chapter 2 of this thesis which showed that alginate potency as a pancreatic lipase inhibitor is influenced by concentration where the higher concentrations of alginate could inhibit pancreatic lipase activity *in vitro* to level much greater than the lower concentrations. Wilcox et al (2014) reported that there is a positive correlation between inhibition of pancreatic lipase activity and alginate concentration. They found that increasing LFR5/60 alginate concentration from 0.21 mg/ml to 0.86 mg/ml increased the reduction of pancreatic lipase activity by 75% and increasing alginate concentration from 0.86 to 3.43 mg/ml increased the reduction by a further 56% [72].

The data presented here showed that the digestion rates of glyceryl trioctanoate and olive oil treated with CC01 were slower than the digestion rates when they were treated with 1N80, and the variation in inhibition may relate to the structural features of the alginates. ^{1}H NMR data for the alginates, shown in Chapter 2, revealed that CC01 possesses the highest content of G-homopolymeric blocks (GG and GGG-blocks) compared to 1N80, hence CC01 had the ability to reduce fat digestion by reducing pancreatic lipase activity more than 1N80. However, 1LF80 had

no impact on fat digestion and that might be because of its high content of M- blocks, (MM, and MMM residues). These results are in agreement with the earlier results in Wilcox et al 2014 which demonstrated that alginates with high content of guluronic acid are considered to be strong inhibitors of lipase. In the presence of divalent cations such as calcium ions, alginate rich in G blocks produces a stiff and brittle hydrogel where the G blocks bind to each other through diaxial linkages, creating cavities where the ions can bind to these sites, producing the egg-box conformation [182].

The reduction in olive oil digestion achieved by CC01 (250 or 500 mg) and 500 mg 1N80 added at the small intestinal phase could also be explained by the relatively high pH in the small intestinal phase compared to the low pH in the gastric phase. At an acidic pH of less than the pKa of guluronic acid (3.5), alginate forms a highly viscus acid-gel due to protonation of carboxylic acids which accept protons and lose their net negative charge [179, 183]. However, the data obtained from experiments of alginate added at the small intestinal phase showed that pH after adding the bile and pancreatic juice ranged between 4.5 and 4.7. Therefore, an alginate gel will not form, allowing the alginate to be free in solution to inhibit the pancreatic lipase.

A confounding result is that addition of 1000 mg alginate at the salivary phase to olive oil containing free fatty acids and olive oil free from free fatty acids resulted in a significant increase ($P<0.05$) in the digestion rates of both. A possible explanation for the apparent increase in digestion rate might be that alginate gelling reduces the volume for reaction, increasing the relative enzyme-substrate concentration, and therefore, increasing activity.

Model gut experiments with alginate added at the small intestinal phase (T_{70}) showed that unlike 500 mg, using 1000 mg alginate unexpectedly increased olive oil digestion. Also, 1000 mg 1LF80 added at T_{70} caused a significant increase in olive oil digestion although 500 mg 1LF80 added at T_{70} did not affect olive oil digestion. Consequently, simple experiments with alginate and glycerol using the glycerol assay, which is described in the method sections of this chapter, were carried out to investigate whether there was any interference by alginate in the glycerol assay, causing an apparent increase in glycerol release. Alginate in DH_2O at three different concentrations, 8, 4, and 2 mg/ml, were prepared. These concentrations were chosen because they are almost identical to the used alginate concentrations (1000, 500 and 250 mg in volume 120 ml, respectively) at the zero time of small intestinal phase of the model gut where the majority of fat digestion occurs. The data

from the experiments indicated interference from alginate in the glycerol assay. The interference effect was corrected for the samples by subtracting the absorbance of alginate obtained from glycerol assay from the absorbance of the samples, however, the digestion rate of olive oil treated with 1000 mg of alginate still showed an increased rate, indicating that the interference effect could not explain all of the increase.

An additional possible explanation for the apparent increase in olive oil digestion by 1000 mg alginate might be found in solubility issues. Samples of olive oil treated with 500 mg alginates added at the small intestinal phase did not show any gelation or precipitation, however, some precipitation and formation of gel lumps were seen in the samples treated with 1000 mg alginate. Thus, it is possible that 500 mg alginate dissolves more efficiency than 1000 mg and becomes released into the solution, binds the pancreatic lipase and reduces its activity. Another possible explanation is when olive oil is present alone, lipases interact differently with triglycerides containing different fatty acid chain length and degree of saturation. In the presence of 1000 mg alginate, triglycerides containing long and unsaturated fatty acids could bind preferentially with the alginate, thus preventing reaction with lipases and allowing them to hydrolyse saturated triglycerides with shorter fatty acids, and thus increasing the reaction rate. Further investigation of these potential effects is required.

A previous study found that low methylic ester pectin (LM pectin) at a concentration 1.5 g/100 ml could reduce the activity of trypsin, lipase, and amylase *in vitro* by 86, 96, and 100% respectively through lowering the pH of duodenal juice from 5.7 to 3.9 [141]. Also, it has been reported that activity of pancreatic lipase is influenced by the intestinal pH. The approximate pH in the small intestine ranges from 6.5 in the duodenum to above 7 in the distal ileum (Brownlee et al., 2010). The data obtained from pH measurements for olive oil alone or in combination with alginate added either at the salivary phase or small intestinal phase (T_{70}) indicated that the pH values for olive oil in combination with alginate added at the salivary phase were significantly higher than those for fat substrate alone or in combination with alginate added at the small intestinal phase. As mentioned earlier, the salivary pH of alginate containing olive oil solution experienced a rapid sudden drop to below the pKa for uronic acids (3.5) when the gastric juice was added, producing gel and precipitation, and reducing the free release of alginate into the reaction mixture, thus, the inhibitory effect of alginate on triglyceride digestion would be affected. On the other hand, during the small intestinal phase where fat digestion mainly occurs, the data did not show any significant difference

in pH neither between the fat substrate alone or fat substrate in combination with alginate added at the salivary phase, nor between the pH values for fat substrate alone and those for fat substrate in combination with alginate added at the T_{70} of small intestinal phase, demonstrating that unlike the LM pectin which inhibited pancreatic lipase through reducing the pH of duodenal juice, adding alginate either at the salivary or small intestinal phase did not change the pH within the small intestinal phase. Therefore, it is likely that for the alginate added to olive oil, the regulatory affect (activation or no effect) was influenced by the gel formed at low pH in the gastric phase, but, for the reduction in olive oil digestion produced by alginate added at the small intestinal phase, the alginate effect on fat digestion seemed dependent on pH in term of the gelling effect. However, as was shown previously in this work, the gelling effect of alginate at low pH in the gastric phase was not observed when glyceryl trioctanoate in combination with alginate was passed through the gastric phase, also, no significant difference was observed between the small intestinal pH values for olive oil alone, olive oil with alginate added at the salivary phase, and olive oil with alginate added at the T_{70} of small intestinal phase, indicating that the regulatory effect of alginate is independent of pH. Obviously, unlike LM pectin, the inhibitory effect of alginate added either at the salivary phase or at the small intestinal phase to glyceryl trioctanote did not rely on a reduction of small intestinal pH.

A buffered synthetic salivary diluent containing 372mM $NaHCO_3$ was used to produce less acidic pH in the gastric phase, hence, avoiding or reducing the amount of gel and precipitation produced from alginate due to acidic pH in the gastric phase of model gut. The data obtained from the digestion of olive oil in combination with CC01 alginate added at the salivary phase using buffered saliva showed no change in the digestion rate of olive oil treated with CC01 alginate. However, in the small intestinal phase, where triglyceride digestion mainly takes place, no significant difference was shown between the pH levels for olive oil in combination with alginate and buffered saliva, and the pH levels for olive oil in buffered saliva without alginate. This indicates that the regulatory effect of alginate added at the salivary phase in combination with buffered saliva on olive oil digestion was independent of small intestinal pH.

Furthermore, the data presented here showed that the digestion rate of olive oil alone treated with buffered saliva containing 372mM $NaHCO_3$ was significantly lower than the digestion rate of olive oil treated with normal saliva containing 62mM $NaHCO_3$. The reduction in digestion rate of olive oil treated with buffered saliva compared to that of olive oil treated with normal saliva could be

explained by Ca^{++} ions binding bicarbonate through cation exchange, producing insoluble calcium bicarbonate which cannot dissociate. Therefore, lower concentration of calcium ions would be present in the reaction mixture, consequently, the activity of pancreatic lipase is affected. Previous studies showed that calcium ions are important for lipase activity. Armand et al, (1992) reported that calcium ions can modulate the activity of lipase until the enzyme reaches its maximum activity. It has been suggested that calcium ions may reduce the electrostatic repulsion, which takes place at the emulsion/water interface due to the binding of bile salts, allowing the penetration of lipase to the substrate interior, and reducing the duration of lag phase (i.e. the time required for activation of the pancreatic lipase) [55-57].

The digestion rate of olive oil treated with CC01 alginate and buffered saliva was significantly lower than that of olive oil in combination with 250 mg CC01 and normal saliva. Also, the amount of gel formed in samples of olive oil treated with alginate and buffered saliva was lower than that formed in samples of olive oil treated with alginate and normal saliva. As described above this could be because of the binding of calcium with bicarbonate through cation exchange, reducing the concentration of Ca^{2+} in the reaction mixture and therefore the interaction between Ca^{2+} and alginate.

The data presented here showed that the gastric pH values for alginate in combination with buffered saliva were significantly higher than those for alginate in combination with normal saliva. These high pH values in the gastric phase likely explain the lower amounts of gel, lumps and precipitate seen in the samples of alginate treated with the buffered saliva. This would allow more alginate to be present in the reaction mixture compared to the alginate present in the reaction mixture treated with normal saliva. This might explain the reduction in the digestion rate of olive oil treated with alginate and buffered saliva compared to the digestion rate of olive oil treated with alginate and normal saliva.

In this chapter, model gut experiments for CC01, 1N80 and 1LF80 alginates, as pancreatic lipase inhibitors, showed different results from those of the microplate assay for the same alginates, however, this variation in results between the microplate assay and model gut system may occur for many reasons. Lipase microplate assay experiments conducted by Wilcox et al were carried out in well-controlled conditions where a single enzyme (pancreatic lipase) was used, thus the inhibitory capacity of alginate as a pancreatic lipase inhibitor can be observed clearly. Conversely,

the synthetic model gut has been developed to imitate the human gastro-intestinal tract, therefore, the model gut system is more complicated than the lipase microplate assay since the model gut system involves several types of chemicals, digestive secretions and enzymes. Alginate may interact with other enzymes of the synthetic diluents within the model gut system such as pepsin instead of pancreatic lipase as previous studies reported that alginate could inhibit pepsin activity *in vitro* by 52% where the direct binding of alginate to pepsin has been suggested as one of the inhibition mechanisms [107]. Moreover, in the model gut system, bile and pancreatin from pig were used, where the bile is made up of bile salts, mucus, phospholipids, cholesterol, and bilirubin, and the pancreatin involves all the digestive enzymes present in pancreatic secretions. Previous studies have shown that dietary fibres such as alginate can interact with bile salts [184, 185]. Also, a further difference between the model gut and microplate assay is stirring. The stirring applied within the model gut system may change the possible interaction between alginate and the pancreatic lipase or fat substrate [162]. The synthetic model gut system was stirred at 0.05 Hz in an attempt to mimic the motion of the gastro-intestinal tract in human body. The motion of the model gut system does not exactly imitate shearing, mixing and stirring produced by gastric motility and peristaltic movement within the gastrointestinal tract of human body [162], hence it is obvious that the digestion within the model gut does not take place in the complete *in vivo* environment. Furthermore, lipase microplate assays were performed at a constant pH (7.3), while the model gut system was carried out at different pH conditions. During the gastric phase, the pH was acidic, and once the gastric phase ended and the small intestinal phase started, bile and pancreatin from pig were added, hence the pH increases gradually and becomes neutral or more alkaline. As mentioned earlier, pH affects alginate properties since alginate at acidic pH produces gel due to protonation of uronic acids and the gel formation may affect alginate's capacity as a pancreatic lipase inhibitor.

4.7 Conclusion

The data obtained from digestion of fat substrates within the synthetic model gut system revealed that tiny amounts of the fat substrate were digestible within the gastric phase, however, the majority of fat substrates were digestible in the small intestinal phase, confirming previous studies which reported that although triglyceride digestion starts in stomach, it occurs mostly in the small intestine, proving the capacity of the synthetic model gut in representing *in vivo* digestion from the mouth to small intestine. However, the digestion rate of fat substrate was dependent on length of fatty acids as well as saturation degree of these fatty acids. The model gut did not digest olive oil and sunflower oil to the same level. A possible explanation for the difference in olive oil and sunflower oil digestion is that in enzymatic reactions, the rate of end product production is governed by their concentrations where the accumulation of these products may slow the enzymatic reaction; however, under some circumstances of high product concentration, the reaction may be driven in reverse back toward reactants [186], meaning if there is high concentration of products then this will slow the rate of end product production (glycerol and free fatty acids). Since the synthetic model gut lacks absorption capability, the end products may accumulate and slow the rate of production, however, the product production rate is unaffected *in vivo* since the products of triglycerides digestion would be absorbed.

The regulatory effect of alginate added at the salivary phase in combination with normal saliva containing 62mM $NaHCO_3$ was influenced by the gastric pH within the synthetic model gut system where passage of alginate through the gastric phase produced a gel, some lumps and precipitation which might prevent solubility and free release of alginate in the small intestinal phase where triglyceride digestion occurs mainly. However, the regulatory effect of alginate added at the small intestinal phase was independent of pH. Moreover, the regulatory effect of alginate passed through the stomach phase in combination with buffered saliva containing 372mM $NaHCO_3$ was independent of small intestinal pH.

Chapter 5: Digestion of alginate bread in the synthetic model gut system

5.1 Aims

In this chapter, 4% (w/w wet dough) powdered CC01 alginate, which previously inhibited pancreatic lipase activity in the turbidity assay and reduced fat digestion in the synthetic model gut (data presented in Chapters 2 and 3 of this thesis), was incorporated into bread, known as alginate bread (AB). Alginate-free bread was used as a control bread (CB), glyceryl trioctanoate and olive oil were used as fat substrates. This chapter aims to:

- Investigate whether AB will be completely digestible within the synthetic model gut, and if the alginate released from bread digestion can be measured using an improved version of the Periodic Acid-Schiff (PAS) assay [187].
- Evaluate the efficiency of the PAS assay as a method in measuring alginate in model gut solutions (MG) taken from the gastric and small intestinal phase of the synthetic model gut system.
- Study effect of AB on digestion of both glyceryl trioctanoate and olive oil *in vitro* using the synthetic model gut to assess wither the AB can reduce *in vitro* fat digestion.

5.2 Introduction

Prospective studies have stated that diets rich in dietary fibres could reduce body weight and obesity development [28, 188]. Furthermore, human intervention studies in overweight subjects indicated that consuming dietary fibres or fibre-based supplement in combination with caloric-limited diets decreases body weight and reduces energy intake [189-191]. Moreover, Wilcox et al. (2014) and Houghton et al. (2015) showed that some alginates could reduce pancreatic lipase activity *in vitro* and the inhibition level depends on alginate content of G- and M-blocks and concentration [72, 192]. Further work conducted by Chater et al. (2015) demonstrated that alginate inhibits pepsin activity *in vitro*, and this finding was in agreement with earlier work of Sunderland et al. (2000) who presented that alginate diminishes pepsin activity [193]. Furthermore, incorporating dietary fibres into food could reduce obesity and its related metabolic diseases. Earlier studies have reported that taking moderate amounts of soluble NSP (non-starch

polysaccharide) fibres decreases fasting cholesterol level in blood and changes the ratio of HDL: LDL cholesterol in plasma [194-197].

Jenkins et al. 1980 reported that guar gum, which is unabsorbed polysaccharide, possesses beneficial effects in treating diabetes over about one year. Jenkins and his colleagues informed that a significant decrease (40-50%) in glucose level was found in 2h urine samples collected from diabetic subjects after consumption of bread, soup, and either fruit juice or mashed potatoes containing 25g guar/day [198]. Additionally, it has been found that incorporating guar gum into foods containing carbohydrates reduces hyperglycaemia and insulinaemia in normal and diabetic individuals [198, 199]. Furthermore, Shah et al. (1986) reported that water soluble polysaccharides, pectin and guar gum, reduce pepsin activity *in vivo* by 57 and 44%, respectively [200]. Shah and his colleagues reported that the reduction in pepsin activity is associated with the fibres capability to form viscous solutions in the stomach which in turn attenuates the stirring process in stomach, hence limiting binding of enzyme to substrate. Moreover, Seal and Mathers (2001) reported that NSP fibres alginate (SA) and guar gum (GG) may be used to reduce the risk of hypercholestrileamia since their study on male rats feeding with cholesterol-free diets containing SA alginate (50 or 100g/kg) for 21 days decreased the cholesterol level in plasma and increased the amounts of bile acids excreted in faeces, hence they suggested that alginate could be used as a dietary supplement to reduce the development of hypercholestrileamia [201].

Alginate can form both an acidic gel at low pH in stomach (pH<3.5), and an ionic gel in the presence of divalent cations [202], and its content of guluronate acid residues affects its gelling capability, gel strength, and viscosity [203]. Alginate viscosity/gel plays a crucial role in the gastrointestinal signals that moderate hunger, promote satiety and reduce caloric intake [82, 202]. Many studies have revealed that incorporating alginate into beverages or cereal bars reduces body weight, suggesting that alginate could be used in obesity treatment. The beneficial health effects stated in these studies include decreasing blood glucose and insulin [114], increasing excretion of fat and bile acids [106], promoting weight loss [83], enhancing satiety and reducing energy intake [202].

Bread is a very acceptable and popular basic food which is consumed regularly in all parts of the world [204]. It is a staple constituent in diets of many Western countries. Archeology and history indicate that bread has been consumed from early in the history of humans. In Egypt, where

civilization was significantly more developed, Greek, and Roman civilization, bread was a consistent component of diets consumed every day [205]. In the UK, bread is the most predominant basic food among starch foods. About 12 million loaves and packs are produced daily, also, bread is one of the major sectors in food industry in the UK (Federation of Bakers, 2005, cited in Burton & Lightowler, 2008 [206]). Furthermore, white bread constitutes over 70% of all sold breads in the UK ([206]). It has been reported that bread is an excellent source of macronutrients (carbohydrates, proteins and fats), and micronutrients (minerals and vitamins) important for human health [204].

Alginates, which are polysaccharides, can be quantified using many methods such as polyhexamethylenebiguandinium chloride (PHMBH+ Cl^-), 1,9-dimethyl methylene blue (DMMB), Safranin-O (S-O), Toludine Blue (T-B), and Periodic Acid-Schiff (PAS) assay [207-209]. However, Houghton et al's study (2014) indicated that the PAS assay was more sensitive in detecting low concentrations of alginate with a wide range of absorbance and an excellent linearity compared with the cationic dyes DMMB, S-O, and T-B.

PAS assay is a simple and sensitive staining technique used to detect polysaccharides which undergo oxidation on exposure to periodic acid. PAS assay technique involves preparing Schiff reagent following by linking the Schiff reagent with oxidised sugars which are already oxidised by periodic acid [187].

Many types of carbohydrates, including monosaccharides, polysaccharides, glycogen, and mucoproteins, are PAS positive substances [210]. Therefore, the polysaccharide content and position within constituents of plant and animal are frequently determined through PAS staining assay [211]. In Periodic Acid-Schiff reaction, periodic acid (HIO_4) is used as an oxidising agent to oxidise hydroxyl (-OH) groups on neighbouring carbon atoms where the C-C bond is cleaved, and aldehydes are produced. Then, the resulting aldehydes are detected using a colourless Schiff reagent which gives a colour ranged between magenta and purple at the sites of oxidisable carbohydrates where the aldehydes exist (Figure 5.1) [210].

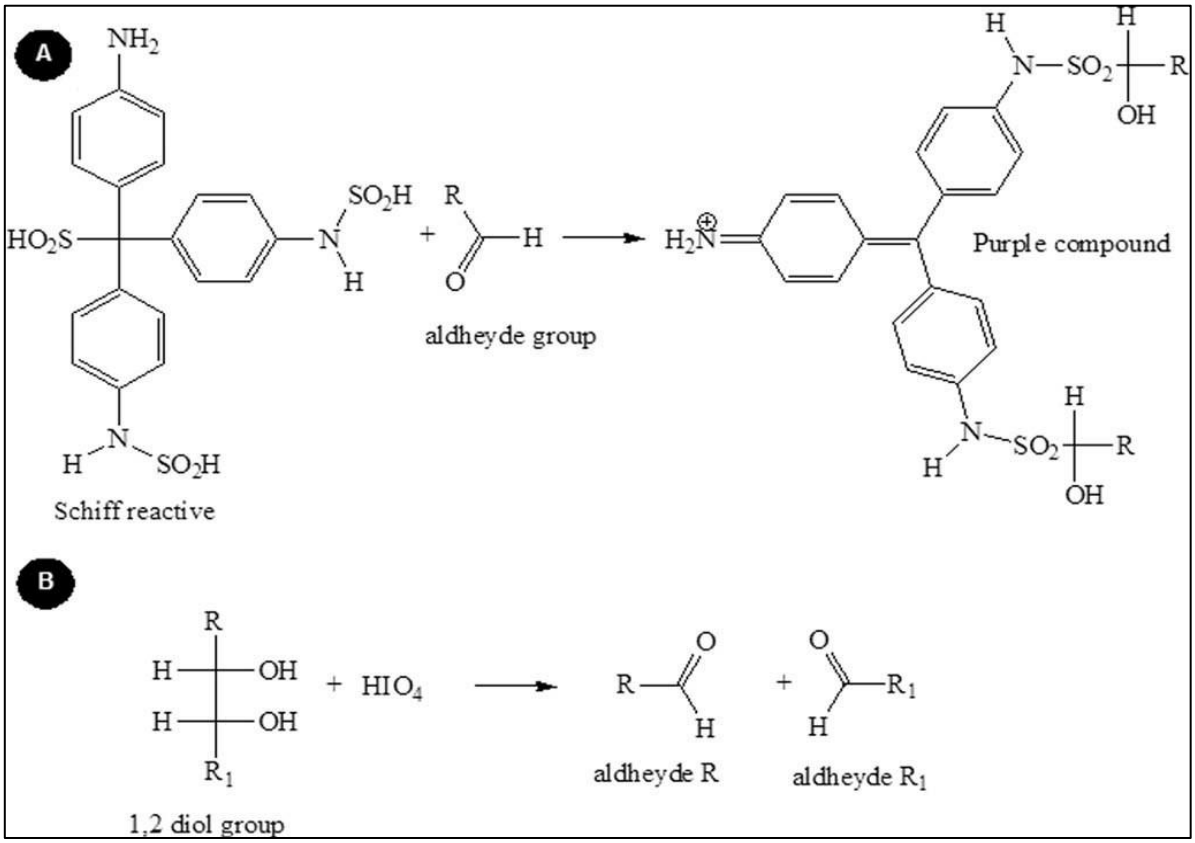

Figure 5.1. Mechanism of Periodic Acid-Schiff (PAS) reaction. A, Schiff reagent interacts with aldehydes producing a purple complex. The Schiff reagent may be used to distinguish polysaccharides following treatment with periodic acid (HIO_4). B, Periodic acid reacts with 1, 2-diol groups inside polysaccharides, and then oxidises them into a dialdehyde compound. Adapted from Fernandes et al., (2006) [211].

Data from the olive oil turbidity assay presented in Chapter 2 of this thesis revealed that CC01 significantly reduced *in vitro* pancreatic lipase activity by 69.8 (± 11.7) %. Also, ^{1}H NMR neighbour analysis (Chapter 2) showed that CC01 is rich in guluronic acid. These results agree with the Wilcox et al. study in 2014 which indicated that alginate rich in guluronate reduces pancreatic lipase activity more than alginate rich in mannuronic acid [72]. Moreover, the data from the model gut experiments presented in Chapter 4 of this thesis shows that free CC01, which was used as a powder in model gut experiments, reduced digestion of glyceryl trioctanoate and olive oil. Additionally, previous *in vivo* studies mentioned in the introduction of this chapter, reported that adding alginate into diets reduces energy intake, and ultimately controls body weight. Therefore, in this chapter, digestion of fat substrates was assessed using alginate bread containing CC01 in an attempt to reduce *in vitro* fat digestion.

5.3 Methods

5.3.1 Materials

All chemicals, materials and enzymes used in the current synthetic model gut experiments were identical to those used in Chapter 4**.** The alginate sample CC01 was provided by Coca-Cola. The fluids of synthetic model gut (saliva, gastric and pancreatic juices) were prepared as described in Chapter 4, and they were used as stock solutions, whereas the enzymes were added before passing the sample through the model gut.

For the PAS assay, periodic acid $HIO_4.2H_2O$, acetic acid CH_3COOH, sodium metabisulphate $Na_2S_2O_5$ and Schiff fusion-sulphite reagent were purchased from Sigma-Aldrich, UK.

For bread preparation, strong white bread flour, skimmed milk powder, rape seed oil, sugar, salt, and fast acting yeast were purchased from a local supermarket (Cooperative Food, UK)

5.3.2 Model gut equipment

Model gut equipment, procedure, sampling, and glycerol quantification were as described in Chapter 4.

5.3.3 Periodic Acid-Schiff (PAS) assay

The PAS assay used was a modified version of Mantle and Allen (1978) to be performed in 96-well microplate. In the assay, 10 µl of 50% (v/v) $HIO_4.2H_2O$ was added into 5 ml of 7% (w/v) CH_3COOH in DH_2O and mixed. Then, 20 µl of the mixture from the previous step was added into wells of a 96-well microplate containing 200µl of sample in duplicate. Next, 87.8 mM $Na_2S_2O_5$ in Schiff fusion-sulphite reagent was prepared and mixed. After that, both 96-well microplate and Schiff fusion-sulphite mixture were incubated at 37 $^{\circ}$C for one hour. Then, 20 µl of Schiff fusion-sulphite mixture was added to each well and the plate incubated for 30 minutes at room temperature with shaking to allow colour development. Finally, absorbance was measured at 550nm.

5.3.4 Standard curves for mucin and alginate

Standard curves for mucin and alginate were prepared using the modified version of the PAS assay (Mantle and Allen, 1978) described above. For a mucin standard curve, purified porcine gastric mucin was dissolved in DH_2O at a concentration of 1 mg/ml. Then, the mucin solution was diluted further in DH_2O to create a mucin standard curve over concentration range of 0-2 mg/ml. The mucin standard curve was used here as a positive control to assess the validity of the PAS assay in detecting the polysaccharides. For the standard curve of alginate released in the gastric phase of the model gut (0-60 minutes), the model gut (MG) solution from 60 minutes was titrated to pH 7 using 1M NaOH. Then, alginate was dissolved in the titrated MG solution at a concentration of 2 mg/ml which was then diluted further in DH_2O to produce a standard curve over concentration range of 0-0.25 mg/ml. For the standard curve of alginate released in small intestinal phase, 5 mg/ml alginate in MG solution taken at 180-minute was prepared. This was further diluted by 50% in methanol to produce 2.5 mg/ml alginate in methanol which was placed at -20 ºC for 30 minutes. After that, the alginate in methanol was centrifuged at 12,000 rpm for 30 minutes at 4 $^{\circ}$C, the supernatant removed, and the pellet freeze dried. The expected weight of isolated alginate following freeze drying should be 2.5 mg for each ml of alginate in methanol. Following freeze drying, the alginate sample was re-suspended in 5ml of DH_2O to give a concentration of 0.5 mg/ml. This was then diluted further in DH_2O to generate a standard curve over concentration range of 0-0.25 mg/ml. The colour of MG solution may affect the accuracy of PAS assay in quantifying alginate; therefore, the colour effect of MG solution was removed through precipitation and dilution processes as described above. MG solutions alone from 60 and 180 minutes of the model gut with the same dilution used to dilute alginate in the gastric and small intestinal phase were used as controls for measuring alginate released in gastric and small intestinal phase of model gut, respectively. Next, 200 µl of different concentrations of mucin in DH_2O, alginate in MG solutions from 60 and 180 minutes of the model gut, and their controls were added to 96 well plate in duplicate and the PAS assay was performed. The absorbance of DH_2O was subtracted from mucin, whereas the absorbance of controls for alginate in gastric and pancreatic phase was deducted from alginate samples to remove any interference from the samples.

5.3.5 Preparation of control and alginate bread

Control and alginate bread were prepared in a home bread making machine (Morphy Richards) following the manufacturer's instructions for a 2lb loaf. Control bread contained standard ingredients (Table 5.1). Alginate bread additionally contained 208 mg alginate and the preparation procedure was adjusted to accommodate this. Briefly, skimmed milk powder, rape seed oil, and sugar were added to a pan containing water. Salt was dissolved in an additional 150 ml water. The salt-water solution was added gently to the pan ingredients with continuous mixing using a fork to allow hydration of the dry ingredients. After that, half of the total quantity of flour (300g) and half of the alginate were added to the pan, followed by addition of half of the rest of the flour (150g) and the remaining alginate, and then the remaining amount of flour (150g). Finally, the yeast was placed on the top of flour and the programme started. Both AB and CB were baked at Newcastle University, and the baking process took three hours for each type of bread.

Ingredient	Control Bread (CB)	Alginate Bread (AB)
Water (Warm ~ 30 °C)	360ml	360ml
Skimmed Milk Powder	30g	30g
Rape Seed Oil	40g	40g
Sugar (Granulated)	20g	20g
Salt	10g	10g
Strong White Bread Flour	600g	600g
Fast Acting Yeast	7g	7g
Alginate (CC01)	-	50g
Additional Water	-	150ml
Total Weight	1067g	1267g
Weight after Baking	933g	1064g
Percent of Alginate (Wet Weight)	-	3.9% (w/w)
Percent of Alginate (Dry Weight)	-	4.7% (w/w)

Table 5.1. Quantity of ingredients involved in CB and AB preparation.

5.3.6 Isolation and quantification of alginate released from the alginate bread vehicle

To determine the amount of alginate released from alginate enriched bread, the bread was placed within the synthetic model gut system which mimics *in vivo* digestive process from the mouth to small intestine. Thus, the alginate bread was digested, allowing the release of alginate which was subsequently measured.

In this set of experiments, three samples AB, CB, and MG solution were placed in water bath 2 of

the model gut system, whereas the synthetic gastrointestinal fluids (gastric juice and pancreatic juice) and porcine bile were placed in water bath 1 (Figure 5.2). The bread was cut into small pieces ranging between 2 and 4 cm since this size of bread and conditions imitates that of bread masticated in human mouth. The AB sample contained 5.2 g of AB, 5 ml saliva, and 10 ml DH_2O, CB sample contained 5.2 g CB, 5 ml saliva, 10 ml DH_2O, while MG solution contained 5 ml saliva and 10 ml DH_2O. These three samples were passed through the gastric and small intestinal phases of synthetic model gut as described in Chapter 4. During the gastric phase of model gut digestion, 500 µl of MG solution alone and MG solution with either CB or AB was collected at different time points. Then, the samples taken from the gastric phase were titrated to pH 6-7 using 1M NaOH to stop enzymatic reactions. Following titration, the samples were centrifuged at 13,500 rpm for 10 minutes to remove insoluble materials. After that, 500µl of the supernatant was added to 500µl deionised water and mixed. During the small intestinal phase, 500µl of the three samples were added to Eppendorf tubes containing 500µl methanol and vortexed. Next, the samples were placed in a freezer at -20 ºC for 30 minutes, and then centrifuged at 4100 rpm for 30 minutes at 4 ºC. The supernatant was removed, and the pellet was re-suspended in 4ml of DH_2O. After that, 200µl of the samples was added to 96 well plates, and the PAS assay performed as described earlier. The absorbance of MG was subtracted from CB and AB absorbance. Then, the remaining CB absorbance was subtracted from the remaining AB absorbance. The amount and concentration of CC01 alginate that would be released from the complete digestion of 5.2g AB at the end of synthetic model gut was calculated as in equation 5.1.

5.2g AB contains 4% by weight of CC01 alginate powder

(5.2x4)/100= 0.208g x 1000= 208 mg at 180 minutes (the end of model gut)

Total volume of solution at 180 minutes= 180 ml

Concentration of alginate at 180 minutes = 208 mg/180ml = 1.16 mg/ml

Equation 5.1. Calculation of the maximum amount of alginate present in 5.2g AB.

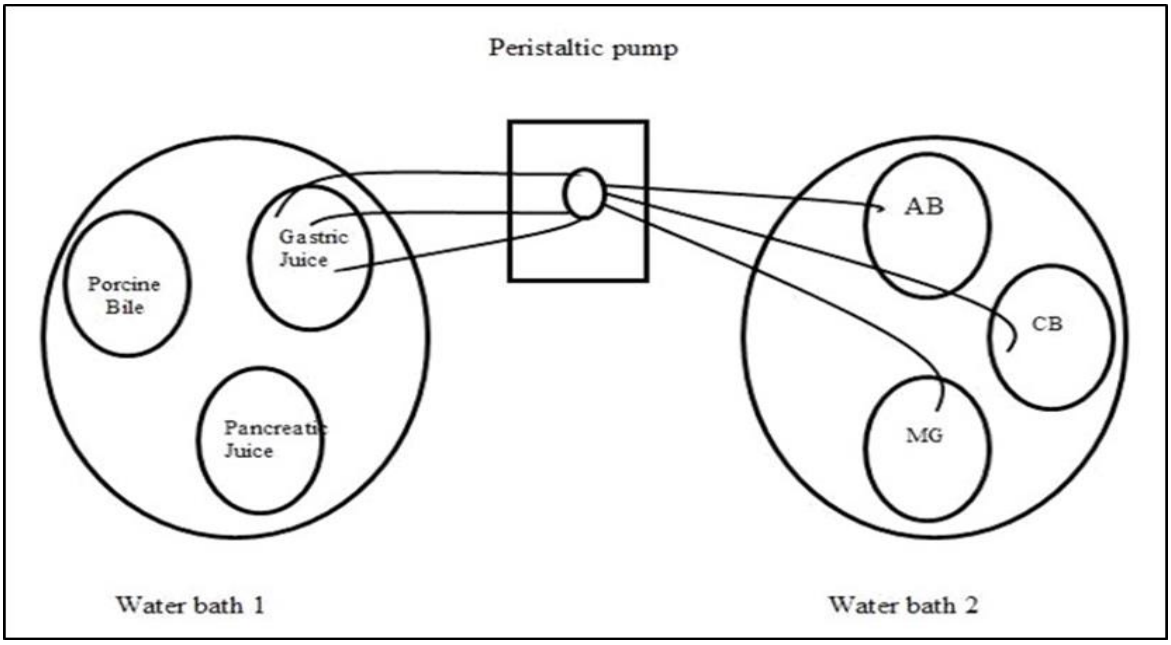

Figure 5.2. Bread digestion in the synthetic model gut system. Taken from Houghton, D., (2013)Water bath 1 contained gastric juice, porcine bile, and pancreatic juice. Water bath 2 contained three samples with saliva: alginate bread (AB), control bread CB, and model gut solution (MG). Gastric juice was added to each sample and then pumped into the samples via peristaltic pump for one hour. At the small intestinal phase, porcine bile was added to the samples, then the pancreatic juice was pumped into the samples for two hours.

5.3.7 Digestion of fat substrates in combination with CB and AB in the synthetic model gut

In this set of model gut experiments, two fat substrates (glyceryl trioctanoate and olive oil), and four samples (AB in combination with fat substrate, AB alone, CB in combination with fat substrate, and CB alone) were used. As described earlier in this chapter, the bread was cut into small pieces ranging between 2 and 4 cm, and the model gut samples were prepared as the following:

- AB in combination with fat substrate consisted of 5.2 g AB, 5 ml saliva, 5 ml DH_2O, and 5 ml fat substrate (glyceryl trioctanoate or olive oil).
- AB alone. It consisted of 5.2 g AB, 5 ml saliva, and 10 ml DH_2O.
- CB in combination with fat substrate consisted of 5.2 g CB, 5 ml saliva, 5 ml DH_2O, and 5 ml fat substrate (glyceryl trioctanoate or olive oil).
- CB alone. It consisted of 5.2 g CB, 5 ml saliva, and 10 ml DH_2O.

Briefly, the samples were passed through the model gut system for three hours as described in Chapter 4 of this thesis, and 500 µl of each sample was taken at different time points of the gastric (0-60 minutes) phase and small intestinal phase (60-180 minutes) and added into Eppendorf tubes containing 500 µl of 10% (w/v) TCA (trichloroacetic acid) to stop enzymatic reactions. Then, the samples were kept at 4 °C overnight. After that, the samples were centrifuged at 10,000 rpm for 10 minutes, and the supernatants analysed using the glycerol assay as described in Chapter 4 to assess the glycerol liberated from fat digestion. The experiment was repeated six times.

5.4 Statistical analysis

The effectiveness of alginate incorporated into bread (AB) on fat digestion in the model gut was assessed using Two-way Repeated ANOVA followed by a Post-Hoc Bonferroni test at a significance level (α) below 0.05 to compare between the alginate released from bread digestion at the gastric phase and small intestinal phase, to compare between the pH of the AB, CB and MG, and to compare between the amount of glycerol released from the digestion of fat substrates in combination with CB and the glycerol amount released from fat substrates in combination with AB. Data is shown as mean and standard deviation (SD), and the number of replicates is revealed in each figure legend

5.5 Results

5.5.1 Standard curve for mucin

The standard curve of mucin in DH_2O which was used as a positive control in the modified PAS assay is shown in Figure 5.3. The absorbance range was between 0-1.27 OD for 0-0.2 mg/ml mucin, with good linearity (R_2=0.99).

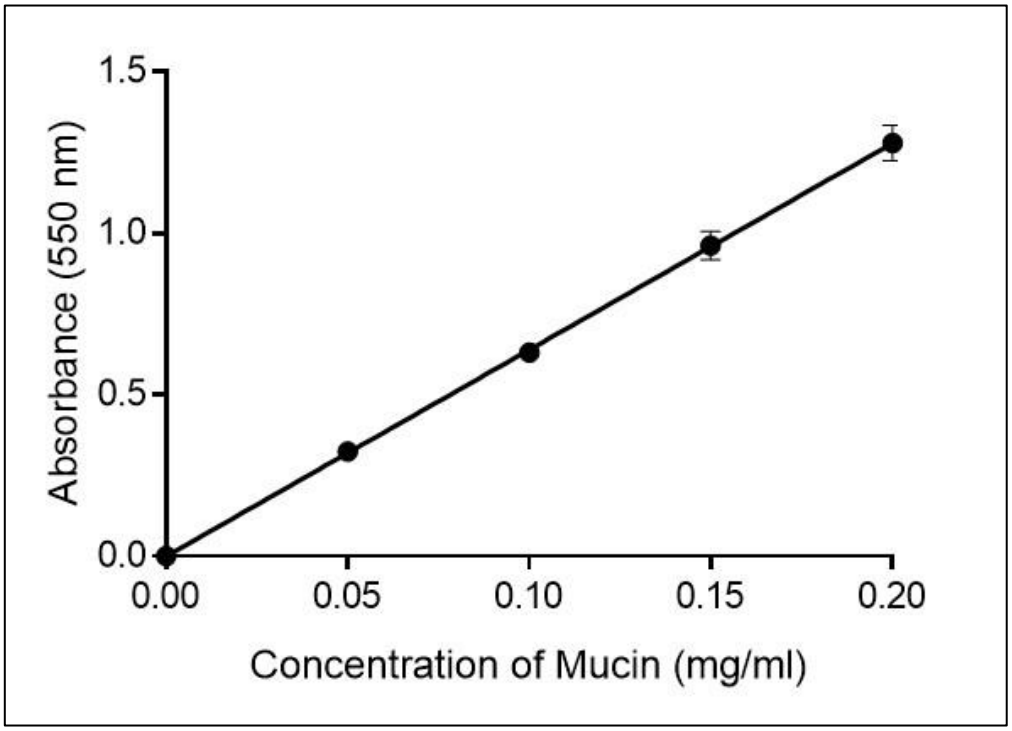

Figure 5.3. Standard curve for mucin in DH2O using the modified PAS assay. The values are mean ±SD (R2=0.99; n=6).

5.5.2 Standard curve for alginate released in stomach and small intestine

Graphs A and B of Figure 5.4 illustrate standard curves of alginate in MG solutions taken at 60 minutes and 180 minutes of the gastric and small intestinal phases, respectively. The absorbance range for alginate in MG solution of gastric phase was between 0 and 0.52 OD for 0-0.25 mg/ml alginate with good linearity (R_2=0.99), while the absorbance range for alginate in MG solution of small intestinal phase was between 0 and 0.23 OD for 0-0.25 mg/ml alginate with good linearity (R_2=0.99).

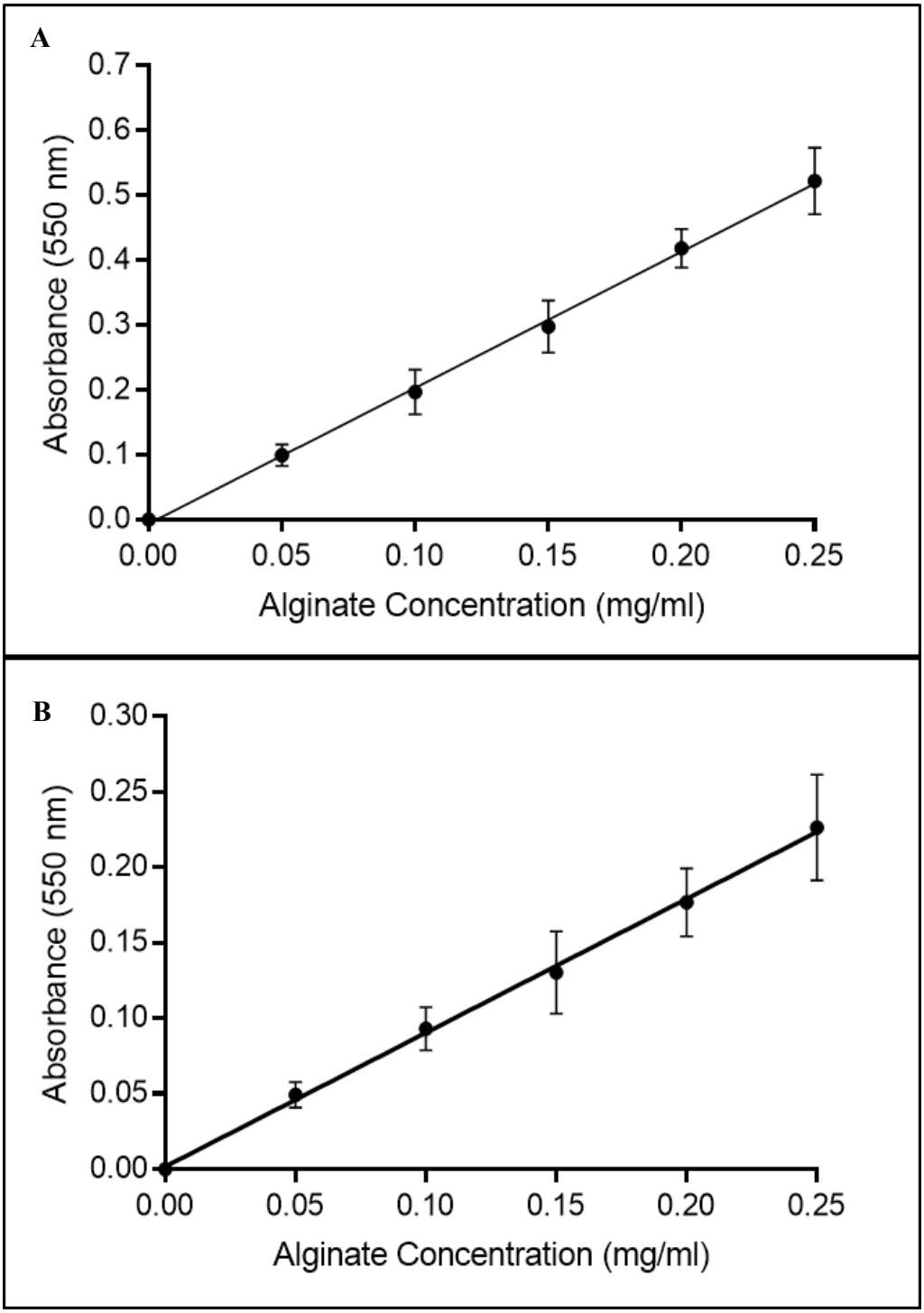

Figure 5.4. Standard curves for CC01 alginate in MG solution of (A) the gastric phase and (B) small intestinal phase using the PAS assay. The MG solutions were taken at 60 minutes (end of gastric phase) and 180 minutes (end of small intestinal phase) minutes of the model gut procedure to represent alginate released in the gastric phase and small intestinal phase, respectively. The values are mean ±SD (n=6).

5.5.3 Recovery of freeze-dried alginate in MG solution taken at the end of model gut

The predicted and measured weights of freeze-dried alginate isolated at the end of the model gut are shown in Table 5.2. To test the efficiency of alginate recovery during the freeze dry process, 5mg/ml alginate in MG solution taken at 180 minutes was prepared. This was diluted 1in 2 with methanol and freeze dried, following the procedure described in section 5.3.5, and the amount of recovered alginate weighed. For each ml of alginate solution, the expected yield after freeze drying would be 2.5 mg/ml if the process is 100% efficient. However, the mean measured weight of freeze-dried alginate was 3.6 mg, higher than the predicted weight by 1.1 mg, and suggesting that other materials could be precipitated with the alginate.

Replicate	Predicted weight (mg)	Measured weight (mg)	Difference in weight (mg)
First	2.5	3.1	+ 0.6
Second	2.5	3.7	+ 1.2
Third	2.5	4.0	+ 1.5
Mean	2.5	3.6	+ 1.1

Table 5.2. Predicted weight, measured weight, and the difference between predicted and measured weights for 5 mg/ml alginate in MG solution. The MG solution was taken at the end of small intestinal phase of model gut (at 180 minutes).

5.5.4 Alginate released from bread digestion in the synthetic model gut

Data from the digestion of AB within the synthetic model gut system is shown in Figure 5.5. It is obvious from the figure that the bread was digestible within the synthetic model gut, and the greater amount of alginate was released from digestion of bread in the small intestinal phase. According to the total amount of alginate (208 mg) that would be released if the AB was completely digested, 10.6% (22 mg), 12.6% (26.2 mg), and 73.1% (152 mg) of the total alginate was liberated at 0.5, 60, and 180 minutes, respectively. There was no significant difference between the amounts of alginate produced from AB digestion at 0.5 and 60 minutes of the gastric phase ($P>0.05$), however, the amount of alginate produced from AB digestion at 180 minutes was significantly different from

that produced at 0.5, 30 and 60 minutes (P<0.05).

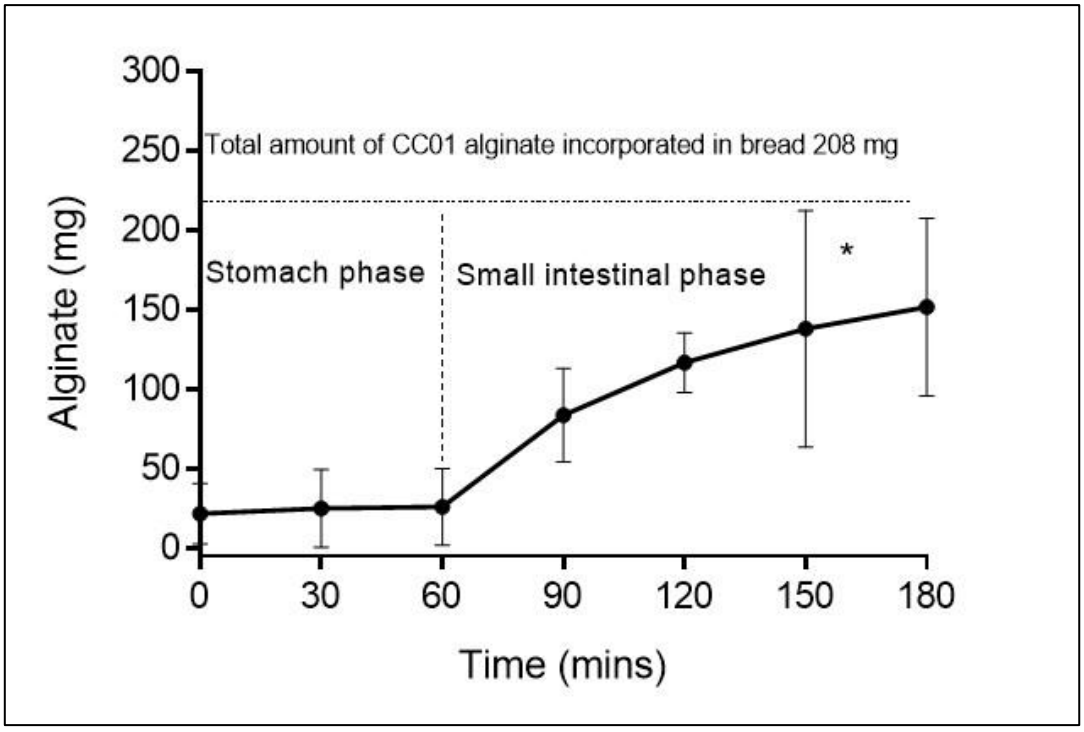

Figure 5.5. Alginate produced from AB digestion in the stomach and small intestinal phases of the synthetic model gut. Values are mean ± SD (n=3), * shows that there was a significant difference between mean alginate produced from AB digestion at 180 minutes of the small intestinal phase and those produced at 0.5, 30, and 60 minutes of the stomach phase, P<0.05. The horizontal dotted line at 208 mg shows total amount of CC01 alginate present within the bread, while vertical dotted line shows stomach and small intestinal phases within the model gut system.

5.5.5 pH measurements for CB, AB, and MG solution alone within the model gut system

Figure 5.6 demonstrates the pH for AB, CB, and MG alone within the synthetic model gut system. The pH in the mouth was 7.8 (±0.22), 7.2 (±0.21), and 8.3 (±0.09) for AB, CB, and MG, respectively. In the mouth, the pH for MG was significantly higher (P<0.05) than those for AB and CB, also, the pH for AB was significantly higher than that for CB. However, after adding the gastric juice to start the stomach phase, there was a significant reduction (P<0.05) in the pH for all the three samples compared to the pH in the mouth where the pH reached 2.9 (±0.3), 2.6 (±0.06), and 1.8 (±0.17) for AB, CB, and MG, respectively. During the first 15 minutes of stomach phase, there was an increase in pH of AB reaching to 3.2 (±0.12), whereas the pH for CB and MG decreased to

2.5 (±0.06) and 1.7 (±0.06) at 15 minutes, respectively. Then, the pH for the three samples decreased further for all samples reaching to 2.7 (±0.13), 2.2 (±0.09), and 1.6 (±0.07) at the end of the stomach phase (60-minute) for AB, CB, and MG, respectively. Also, Bonferroni's test showed a significant difference ($P<0.05$) in mean pH values between AB and MG, and between CB and MG at 0.5 minutes of the stomach phase. In addition, there were significant differences between AB and CB, between AB and MG, and between CB and MG at 15, 30, and 60 minutes of the stomach phase ($P<0.05$). During the small intestinal phase, there was a significant increase in pH levels for all the three samples, reaching to 7.8 (±0.11), 7.7 (±0.06), and 8 (±0.06) for AB, CB, and MG, respectively, at the end of small intestinal phase (180-minute). However, there were no significant differences ($P>0.05$) in pH between AB, CB, and MG at all time points of the small intestinal phase

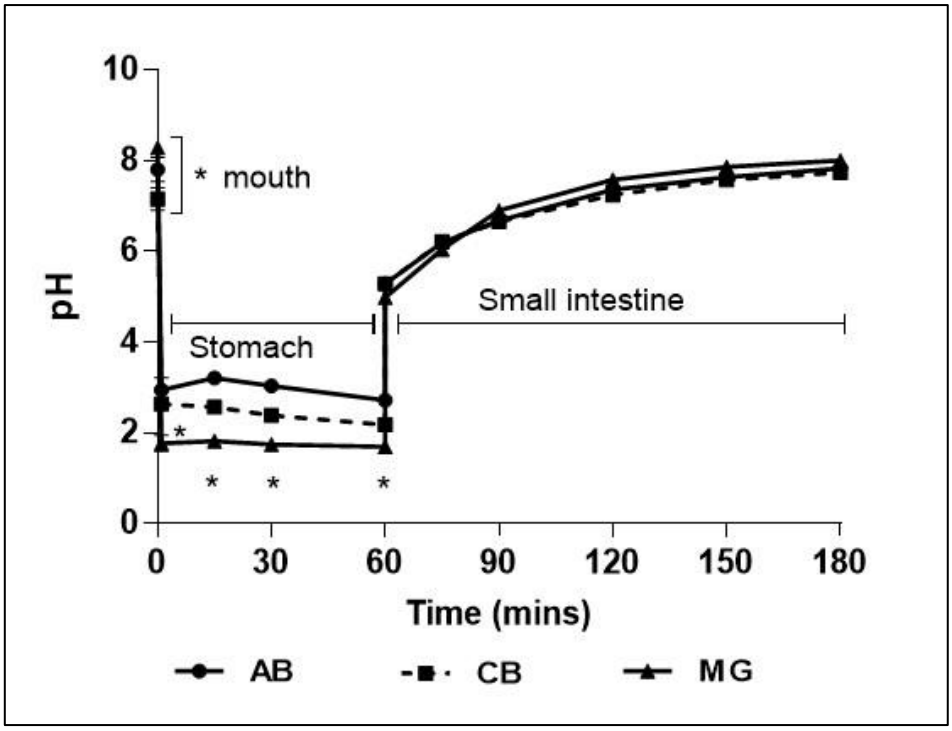

Figure 5.6. Mean pH for AB, CB, and MG throughout their digestion within the model gut system. The error bars are the standard deviation of three replicates (± SD; n=3), * indicates significant differences in pH. Horizontal lines show the stomach and small intestinal phases of the model gut system, $P<0.05$.

5.5.6 Digestion of glyceryl trioctanoate in the presence of control and alginate bread

Figure 5.7 shows the digestion of 5ml glyceryl trioctanoate with 5.2g of either CB or AB in the

synthetic model gut. During the gastric phase, only small quantities of glyceryl trioctanoate with either CB or AB were digestible. During the small intestinal phase, there was a gradual increase in the digestion of glyceryl trioctanoate with CB and AB reaching to 38.5 (±21.8) mg and 40 (±58) mg glycerol released at 180 minutes (the end of small intestinal phase), respectively. However, there was no significant difference (P>0.05) at any time points between the mean glycerol released from digestion of glyceryl trioctanaote with CB and that released from digestion of glyceryl trioctanoate with AB.

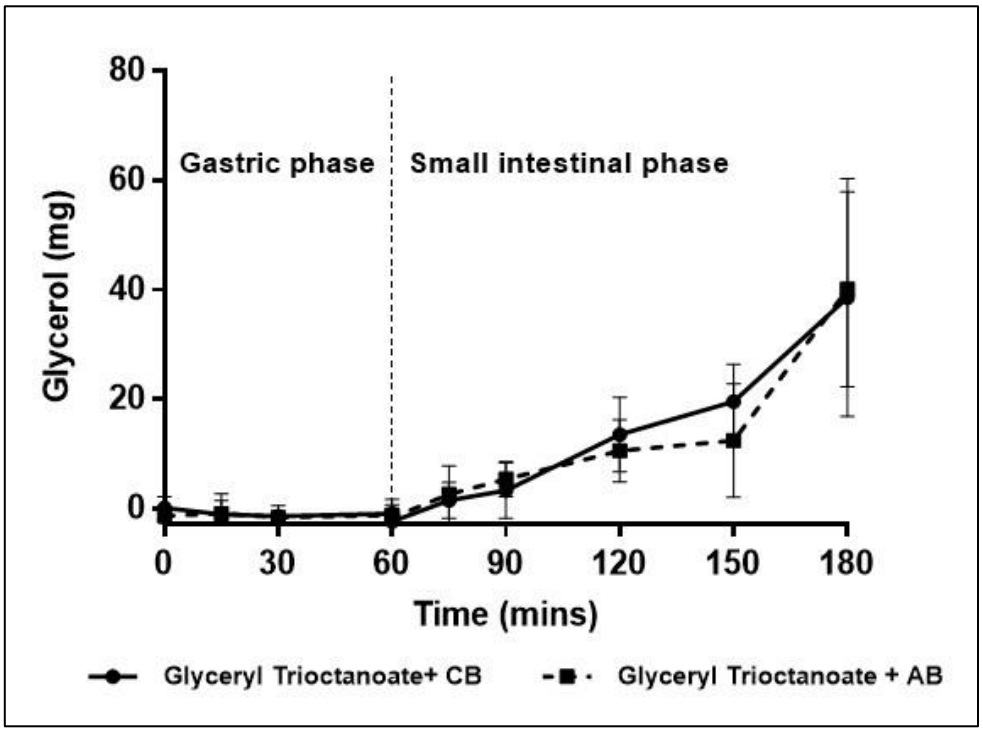

Figure 5.7. Glycerol liberated during the digestion of glyceryl trioctanoate with either CB or AB in the synthetic model gut system. For the digestion within the model gut system, 5.2g of either CB or AB was added to 5ml of glyceryl trioctanoate Values are mean ± SD (*n*=6), P>0.05.

5.5.7 Digestion of olive oil in the presence of control and alginate bread

Figure 5.8 demonstrates the digestion of olive oil with CB and AB in the synthetic model gut. During the gastric phase, the amount of glycerol released from digestion of olive oil with AB was higher than that released from olive oil with CB, however, no significant difference was seen at any time point. During the small intestinal phase, higher amounts of olive oil with either CB or AB were digestible compared with the gastric phase, however, there was no significant difference between the amount of glycerol released from digestion of olive oil with AB and olive oil with CB ($P>0.05$) at all time point, indicating that alginate incorporated into bread did not reduce olive oil digestion.

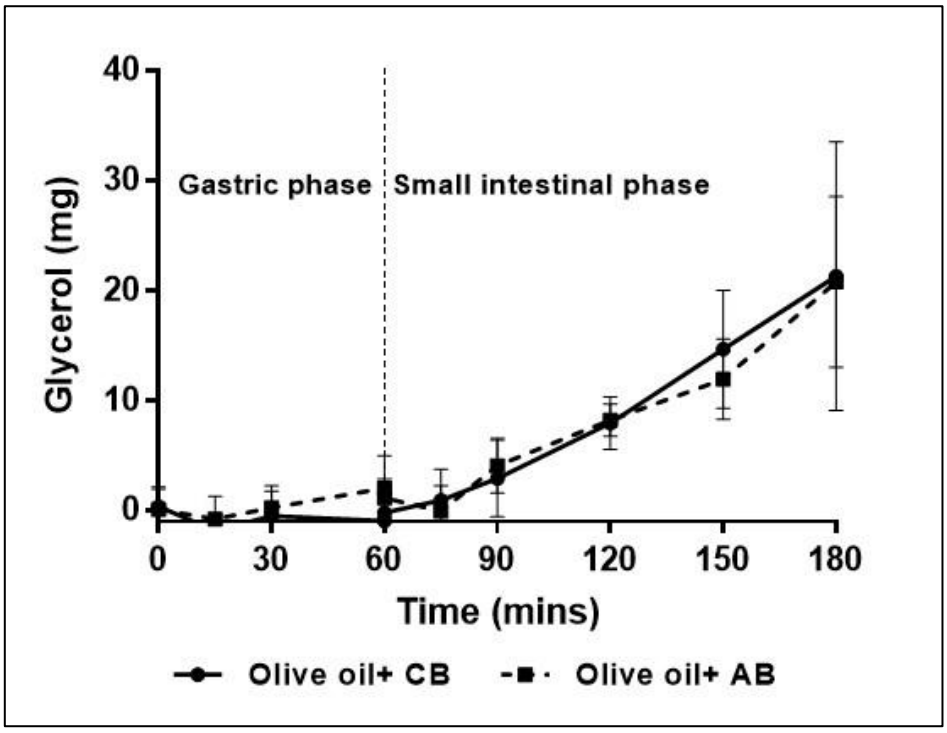

Figure 5.8. Glycerol liberation during the digestion of olive oil with either CB or AB in the synthetic model gut system. For the digestion within the model gut system, 5.2g of either CB or AB was added to 5ml of olive oil. Values are mean ± SD (n=6), $P>0.05$.

5.6 Discussion

The results of the olive oil turbidity assay presented in Chapter 2 of this thesis shows that alginate CC01 inhibited pancreatic lipase enzyme activity *in vitro* by 75.6% (± 10.6) suggesting that CC01 alginate could be used as a potential inhibitor for pancreatic lipase *in vivo* [122]. Additionally, the data from kinetic assay for pancreatic lipase presented in Chapter 3 showed that although all the tested alginates reduced the rate of lipase-catalysed reaction, showing these alginates as pancreatic lipase inhibitors, the highest inhibition was by CC01. Moreover, the data from model gut experiments of fat substrate digestion presented in Chapter 4 showed a significant reduction in digestion of fat substrates treated with CC01 alginate as compared with digestion of fat substrates alone. Additionally, earlier studies have reported that adding alginate into food showed beneficial effects (described in the introduction section of this chapter). Therefore, in this chapter, bread which is a very popular, acceptable and staple food consumed regularly in all parts of the world, was used as a delivery vehicle for alginate.

Bread containing CC01 (AB) was passed through the synthetic model gut and the amount of alginate released measured using a modified version of PAS assay [187]. Furthermore, the pH for AB (alginate bread), CB (control bread), and MG (model gut) solution were measured at the salivary phase and at different time points of the gastric and small intestinal phases of model gut system to determine if the addition of bread significantly altered the pH particularly in the small intestinal phase as a change in pH could modify lipase activity. The effect of AB on digestion of fats containing triglycerides with different fatty acid chain length using the synthetic model gut was also investigated.

Houghton et al. (2014) reported that quantifying alginate released *in vitro* using a synthetic model gut could be difficult due to the wide range of materials involved in the model gut system which may interfere with the technique used for alginate measuring and affect its efficiency in detecting alginate. Besides, it has been stated that alginate at pH less than pKa of the uronic acid residue (3.38 for mannuronic acid and 3.65 for guluronic acid) undergoes protonation and an acidic gel (alginic acid) could be formed [159, 212, 213]. The gel formation may affect coupling of alginate with any dye used, hence, reducing the amount of alginate bound to the dye [161]. In human, the pH ranges between 5-7 in mouth, while stomach pH ranges between 1 and 3. The gastric pH increases after consumption of food, but it declines gradually to pH ≈ 2 after one hour or so from

food ingestion. The pH in small intestine ranges between 6 and 7.5 [214]. Moreover, in the model gut, both porcine bile and pancreatic juice had been added at the small intestinal phase, thus, the colour of MG solution changed from transparent to a dark green/brown solution and that may influence the coloumertic assay used for alginate quantification [161].

In this chapter, AB was used as a delivery vehicle for alginate. AB has to be digested to release the alginate and reduce fat digestion; therefore, AB was passed through the model gut at 37 °C and at optimum pH conditions identical to pH conditions in human body to enable bread digestion and alginate release. Wickham et al. (2009) reported that validity of any model gut in studying *in vitro* digestion requires ability of this model to mimic *in vivo* conditions and processing present in the mouth, stomach (cumulative to the mouth), and the duodenum (cumulative of mouth and stomach) [215]. The predominant ingredient of ingested bread is carbohydrates, and most of ingested carbohydrates are in the form of starch [216]. Starch digestion starts in the mouth by the action of salivary amylase, however, the role of salivary amylase in starch digestion is limited due to its inactivation by the acidic pH of gastric contents. The complete digestion of starch occurs in the small intestine by the action of pancreatic α-amylase and brush-border enzymes. Pancreatic α-amylase cleaves interior 1-4 glycosidic bonds in starch, releasing three disaccharide molecules: α-limited dextrins, maltose, and maltotriose. These disaccharides undergo further hydrolysis by α-dextrinase, maltase, and sucrase to glucose (monosaccharides) which is then absorbed via epithelial cells of small intestine [217]. If the AB was digestible within the model gut, then, the alginate would be released, and an improved version of PAS assay [187] could be used here to measure it.

Data presented here showed that the standard curve of mucin in DH_2O, which was used as a positive control in PAS assay, was linear with an excellent linearity (R^2=0.99), confirming a previous study in which the PAS assay was suggested as a simple, repeatable and sensitive method for detecting mucin and polysaccharides (Mantle & Allen, 1978). In addition, the data presented here indicated that standard curves of alginate in MG solution taken from the end of either gastric phase or small intestinal phase of the model gut both had excellent linearity (R^2=0.99) with absorbance ranging between 0-0.52 OD and 0-0.23 OD for 0-25 mg/ml of alginate in MG solutions of gastric and small intestinal phases, respectively,

Mantle and Allen's study in 1987 used the PAS staining method on glycogen and glycoproteins extracted from mucus of either stomach or small intestine of pig and found that all these substances

were PAS-positive, however, they noticed that sensitivity per mg of these substances relied on the level of oxidation by periodic acid. Among the three tested substances, glycogen was the most positive substance for PAS since all residues within glycogen were oxidizable by periodic acid, whereas the gastric glycoprotein positivity for PAS was the lowest because most of the sugar residues within the gastric glycoprotein linked via 1-3 glycosidic bonds are not oxidizable via periodic acid due to the absence of adjacent –OH groups. For the sugars to be oxidizable by periodic acid, they require the presence of adjacent -OH groups within their structure. In the PAS assay, the intensity of the red- magenta colour, which appears at the oxidizable carbohydrate sites where aldehydes are present, following the addition of Schiff reagent, relies on the number of neighboring –OH groups. Therefore, the higher quantities of glycoproteins will produce higher absorbance values.

Alginate is a polysaccharide consisting of two uronate sugars residues (D-mannuronic (M) acid and L-guluronic (G) acid) which are linked together via 1-4 glycosidic bonds. These uronate sugar residues are relatively comparable to the sugar residues of glycoprotein where both sugar residues of glycoprotein and uronate sugars of alginate have adjacent -OH groups in their structure. Uronate sugars of alginate have adjacent –OH groups at C^1, C^2, C^3, and C^4, suggesting that the PAS techniques may be used to measure amount of alginate in solution within the synthetic model gut system.

The modified version of PAS assay (Mantle & Allen, 1978) was an accurate assay for alginate detection since the assay was able to measure alginate at relatively low concentrations [187]. Furthermore, data from the standard curves of alginate in MG solutions taken from the end of gastric and pancreatic phases presented in this chapter illustrated that the absorbance of alginate in MG solution of the gastric phase at any alginate concentration was higher than that of alginate in MG solution of the small intestinal phase. The lower absorbance of alginate in MG solution of small intestine could be because of alginate binding with other materials within the model gut system such as bile salts and acids which in turn reduces free release of alginate. Another reason for the low absorbance values for alginate in MG solution of small intestine compared to those for alginate in MG solution of gastric phase could be alginate degradability in acid condition, hence, the alginate in MG solution of gastric phase may become more PAS positive. The PAS results presented here confirmed data from a 2014 study by Houghton et al. which showed that the modified version of PAS assay (Mantle & Allen, 1978) is a simple, repeatable, sensitive, and high

throughput method for alginate quantification compared with other cationic dyes DMMB, T-B, and S-O. In the original work, standard curves for alginate in deionised water using different concentrations of DMMB, S-O, and T-B in DH_2O, and PAS assay were created to measure alginate [218] . It was found that only the PAS assay had the ability to measure alginate in DH_2O at relatively low concentrations (0.0-0.5mg/ml), with a varied range of absorbance (0-0.45 OD) within the linear absorbance scale (0-1), showing the efficiency of the PAS assay in detecting alginate despite the possibility of interference that may arise from some materials within the model gut. However, Houghton stated that despite the ability of DMMB, S-O, and T-B cationic dyes to measure alginate, using these methods for measuring free alginate released from bread digestion within the model gut would be inappropriate since the standard curves of these methods showed either poor linearity or absorbance outside linear absorbance scale (0-1) [161, 218].

The data presented here showed that the weight of recovered freeze dried alginate (3.6 mg) was higher than the predicted weight (2.5 mg) by 1.1 mg, indicating that even with the attempts to remove contaminating material by precipitation, centrifugation, and dilution processes as described in the method section of this chapter, some materials, possibly bile components (bile acids and salts), remain attached to the alginate. It has been reported that dietary fibres have high affinity to bind bile salts and acids [184, 185, 219]. Moreover, a study by Wang et al. in 2001 investigated the binding capability of soluble and insoluble dietary fibres from seaweeds with bile salts and found that although both types of dietary fibres had the ability to bind bile salts, the binding affinity of soluble dietary fibres with bile salts was higher than that of insoluble dietary fibres. Therefore, if the binding between alginate (soluble dietary fibre) and bile acids happened here, then this could be responsible for the lower absorbance of alginate in MG solution of small intestinal phase compared with absorbance of alginate in MG solution of stomach phase and could be also responsible for the excess weight of freeze-dried alginate.

Furthermore, the data presented here showed a significant difference ($P<0.05$) in the amount of alginate released at 180 minutes (152 mg) and that released at 0.5 (22 mg) and 60 (26.2 mg) minutes, demonstrating that the AB was digestible within the synthetic model gut, and greater amounts of CC01 alginate were released from bread matrix in the small intestinal phase compared with the gastric phase. It is well-known that the digestion of carbohydrate, namely starch, which is the major form of carbohydrate, predominantly occurs in the small intestine by the action of pancreatic amylase which may provide a reasonable explanation for higher release of alginate in the small

intestinal phase (73.1%) compared to the gastric phase (10.6%). The alginate incorporated into bread was 208 mg, however, only 73.1% of the alginate was released from AB digestion. The partial release of alginate could be because of alginate degradation and fragmentation due to high temperature during the cooking process. These alginate fragments might not be precipitated by methanol which was used here to precipitate the alginate as methanol has the ability to precipitate large polymers such as alginate. As a result, these small molecules (fragments) might not precipitate and therefore would be lost when the supernatant was removed.

The effect of AB containing 4% of powdered alginate by weight (208 mg) on the digestion of fat substrates containing medium- and long- chain triglyceride was investigated in attempt to reduce triglyceride digestion. The amount of glycerol released here from fat digestion was assessed using the glycerol assay described in Chapter 4.

The data presented here from glyceryl trioctanoate and olive oil in combination with either CB or AB showed that the amounts of glycerol released from digestion of glyceryl trioctanoate and olive oil in combination with CB during the gastric phase (0-60 minute) were negligible, however, during the small intestinal phase, higher amounts of glycerol were released, suggesting that triglyceride digestion predominantly takes place in the small intestine. This observation agrees with Carey et al. (1983) who reported that although triglyceride digestion starts in the stomach, 80-90% of its digestion takes place in the small intestine [220]. Also, Klein et al., (2006) stated that only 20% of triglyceride hydrolysis occurs in the stomach [164] . Moreover, Mu & Hoy (2004) reported that triglycerides are partially hydrolysed in the stomach by the action of gastric or lingual lipases which tend to breakdown ester bond at *sn-3* producing 1, 2-diacylglycerides and fatty acids [110]. In addition, it has been reported that although triglyceride hydrolysis occurs predominantly in the lumen of the small intestine, triglycerides undergo partial hydrolysis in stomach [221] , however, this would not be detected in the model gut system as it does not generate the free glycerol which is detected by the assay used here.

As expected, digestion of glyceryl trioctanoate containing pure saturated medium-chain triglycerides was quicker than the digestion of olive oil containing a mixture of long to medium chain triglycerides with saturated and unsaturated fatty acids, a result that is consistent with previous studies showing that the digestion rate of fat substrates is dependent on fatty acid chain length and degree of saturation. The impact of fatty acid chain length and degrees of unsaturation

on triglyceride digestion rates were discussed in detail in Chapter 4 of this thesis.

The data presented here also showed that amounts of glycerol released from digestion of glyceryl trioctanoate (38.5 mg) and olive oil (17.1 mg) in combination with CB bread at the end of the small intestinal phase were lower than those released from digestion of glyceryl trioctanoate (59.6 mg) and olive oil (35.4 mg) alone (data presented in Chapter 4). The reduction in digestion of glyceryl trioctanoate and olive oil in combination with CB could be due to interaction of pancreatic lipase with some ingredients of bread, preventing substrate binding to the enzyme, or interaction of the substrate with the bread, preventing enzyme access to oil/water interface. Both interactions would slow enzyme-substrate binding and reduce triglyceride digestion rate.

Additionally, the data available here indicated that AB did not reduce either glyceryl trioctanote or olive oil digestion. However, it was shown in Chapter 4 of this thesis that the dry powder CC01 alginate (250 and 500 mg) added at the small intestinal phase, could significantly reduce olive oil digestion, and 500 mg of dry powder CC01 alginate added at the salivary phase could significantly decrease glyceryl trioctanoate digestion. Failure of alginate incorporated into bread in reducing fat digestion here could be due to alginate degradation, alginate concentration, or alginate binding with other substances within the model gut system.

Triglyceride digestion occurs mainly in the small intestine by the action of pancreatic lipase. The expected volume of MG solution at the beginning of small intestinal phase (T_{60}) is 120 ml, and the amount of alginate incorporated into bread was 208 mg. Therefore, if the AB was completely digestible within the model gut and all the alginate incorporated into bread would be released, the predicted concentration of alginate released at the beginning of small intestinal phase would be 1.73 mg/ml. However, this concentration is lower than the concentrations achieved with 250 and 500 mg of dry powder alginate added to olive oil and glyceryl trioctanoate which correspond to 2.08 and 4.16 mg/ml alginate, respectively. However, data available here from quantification of alginate released from the digestion of AB using PAS assay showed that about 73.1% of alginate incorporated into the bread was released in the small intestinal phase, suggesting that the AB was not completely digestible within the model gut system. Alginate could interact with other substance within the model gut such as bile salts and acids, and this binding might be revealed from the excess weight of isolated free dried alginate here as shown earlier, and this could reduce free alginate concentration in the reaction mixture.

Furthermore, alginate incorporated into bread may experience degradation for many reasons. Degradation of alginate may affect the essential properties of alginate such as viscosity and molecular size; subsequently, the effect of alginate as a pancreatic lipase inhibitor would be affected. One possible reason for alginate degradation could be pH. Haug and his colleagues investigated the degradation of alginate extracted from *Laminaria digitata* at diverse pHs and reported that alginate remains stable at pH 5 to 10. The same authors reported that at pH less than 5, alginate undergoes degradation via proton-catalysed hydrolysis, while at pH more than 10, alginate undergoes degradation through β-alkoxy-elimination [222]. Lee & Mooney (2012) showed a negative correlation between alginate viscosity and pH where alginate viscosity increases as pH decreases, and the alginate solution becomes highly viscous at pH between 3 and 3.5. However, at pH below 3, the carboxyl groups in the alginate backbone undergo protonation and hydrogen bonds are formed [100]. The data presented here showed that the pH for AB at the salivary phase was 7.8, however, the pH rapidly declined to 2.9 following the addition of gastric juice, and 2.7 at the end of the gastric phase, suggesting that alginate may undergo proton-catalysed hydrolysis. Subsequently, the glycosidic bond linking alginate sugar monomers together would be broken down, hence, the viscosity of alginate will be reduced. Houghton and his colleagues (2015) reported that exposing alginate in DH_2O to the alterations in pH values over the same time course as the model gut system caused a 70% drop in viscosity where the specific viscosity decreased from 9.9 to 2.8 [223]. However, the possibility of alginate degradation because of low pH is not thought to be reasonable here, as only a slight amount of alginate was released in the gastric phase. This observation was expected since the digestion of bread occurs predominantly in the small intestine. The pH measurements for AB within the model gut showed that the pH for AB at the beginning of the small intestinal phase was greater than 5, indicating the possibility of fragmentation of alginate incorporated into bread here due to low pH was not likely to occur.

Commercially available alginates usually contain trace quantities of phenolic compounds which can stimulate oxidative-reductive reactions. Therefore, alginates may experience depolymerisation and fragmentation at neutral pH due to the effect of these phenolic compounds [181]. However, while this is a possibility, it is unlikely to be the explanation in these experiments because the ^{1}H NMR spectra of CC01 alginate within the shaded region show that there is no evidence for the presence of polyphenolic compounds within the alginate sample (Appendix B, Figure 2, p. 265).

The chemical shift in ppm for polyphenol peaks is in the regions from 7.8 to 6 and 4 to 3 [224], and the peaks which are used for alginate determination are in the regions between 5.2 and 4.3. Therefore, no polyphenolic compounds were detected within the alginate sample.

Alginate and other polymers can undergo fragmentation by reactive oxygen species (ROS) such as the hydroxyl radical (·OH), which can be formed from oxygen or water molecules. Glycosidic bonds linking uronate monomers of alginate polymer can be cleaved by this radical ROS through an oxidative-reductive depolymerisation reaction, producing smaller fragments of alginate. Metal ions such as Cu^{++} and Fe^{++}/Fe^{+++} have great affinity to alginate and may accumulate during the production and processing of alginate. These ions can catalyse the formation of ROS through the Fenton reaction, therefore, they must be removed from alginate to produce highly pure alginate [225]. Alginate incorporated into bread may undergo fragmentation through this type of reaction due to the presence of iron (Fe) in the bread flour or alginate itself. Based on the current UK bread and flour regulations, iron must be added to several foods including flour where each 100 g must have up to 1.65 mg of iron added as powdered iron, ferric ammonium citrate or ferrous sulphate [226]. The presence of such catalytic metal in bread flour can stimulate oxidative-reductive depolymerisation.

Another possible explanation for alginate degradation could be the high temperature during the baking process. AB is exposed to temperature up to 120 ºC for 65 minutes during baking process, and this may result in degradation of alginate. Hasatani and his colleagues (1991) studied the influence of different methods of bread baking and could determine the temperature of different parts of bread [227]. They reported that the temperature at the central part of the loaf may only range between 70 to 80 ºC, while the temperature of crust may range between 180 to 200 ºC. However, the accurate temperature of whole loaf of bread in the present study was not measured here. Breaking down alginate polymers into smaller fragments will affect the viscosity of alginate.

The viscosity of alginate has been suggested as the mechanism by which alginates reduce digestive enzyme activity. This viscosity is influenced by many physical factors such as temperature, alginate concentration, polymer size, shear rate, the existence of water miscible solvents, and chemical factors such as pH, sequestrants, polyvalent cations and monovalent salts [228]. Lacík (2004) reported that the viscosity of a polymeric solution can be increased by increasing polymer concentration or polymer molecular weight [229].

Houghton et al's study (2015) indicated that the viscosity of free alginate (0.91, ±0.41)[1] added as a powder at time zero of the model gut, at the same concentration which would be expected to be liberated from alginate bread (AB) at the end of digestion in the model gut, was higher than the actualviscosity of AB (0.42, ±0.01) after passing through the model gut system, suggesting that the bread process decreased the capacity of alginate to form a viscous solution [223]. Moreover, Houghton et al compared viscosities of model gut solutions and CB where alginate was added either at the start or the end of model gut process. When the alginate was added at the end of the process, viscosity was greater in both model gut solution and CB than when it was added at the start of the process (viscosity of model gut solution with alginate added at end= 2.96 ±0.71, viscosity of model gut solution with alginate added at the start= 0.91 ±0.41; viscosity of CB with alginate added at the end= 2.88 ± 0.57, viscosity of CB with alginate added at the end= 0.42 ±0.01. Indicating that passing alginate through the model gut system either as free alginate (powder) or incorporating into bread attenuates alginate's ability to form a viscous solution.

Additionally, the Houghton et al's study (2015) on the impact of different temperatures on alginate viscosity revealed that the viscosity of alginates LFR 5/60, and DM SF200 after heating at 37, 50, or 100 °C for 30 minutes was constant [223]. However, the viscosity of alginate solution significantly decreased after heating at 150°C for 30 minutes and approached zero after heating at 200 °C for 30 minutes, demonstrating that alginate chains experienced extensive fragmentation.

1. The viscosity is expressed in a unitless form as it is viscosity (ηsp) of sample divided by the viscosity (ηsp) of buffer, therefore the units cancel out.

McDowell (1961) and Leo et al. (1990) have demonstrated that alginate may undergo depolymerisation when exposed to temperatures more than 100 ºC. McDowell (1961) showed alginate exposed to a temperature around 200°C, will be extensively degraded and CO2 will be rapidly produced from the uronic acids [230, 231]. Blackburn (2005) stated that viscosity of alginate decreases as the temperature increases, and high temperature may result in depolymerisation of alginate [232]. Also, Qin (2018) reported that exposing alginate to temperatures of more than 50 ºC for many hours may result in depolymerisation of polymer causing a permeant reduction in viscosity and molecular weight [233].

Alginate forms acidic gels at pH below the pKa of uronic acid [159, 213], and forms ionic gels in the presence of multi-valent cations such as Ca^{2+} due to the interaction between Ca^{2+} and guluronate in the alginate backbone, producing the egg-box model. Alginate with a high content of G-blocks can form stronger gels than that produced by alginate low in G-block, and the gel strength plays a crucial role in gastric emptying, gel breakdown and transport of nutrients to small intestine [202, 234, 235]. Alginate has been used in industry, pharmacology and medicine, and these applications are reviewed elsewhere [236]. Although large amounts of seaweeds are eaten in South East Asia, alginate and other algal phycocolloids (carrageenan and agar) are used mostly as emulsifying, stabilising and thickening agents in the food industry in the Western world (Brownlee et al., 2005). It has been reported that consuming meals rich in alginate slows macronutrient digestion and decreases appetite due to the high viscosity of alginate produced from its gelation at the acidic pH in stomach [10, 85, 103, 201, 237]. Jensen et al's study in 2012 stated that there is a reduction by 6.78 (±3.67) kg in body weight of obese subjects following drinking a strong-gelling sodium alginate beverage, which is rich in guluronate, in combination with calorie-limited diet before main meals compared with a reduction of 5.04 (±3.40) kg in obese subjects who consumed placebo beverage in combination with calorie-limited diet [238]. Paxman and her colleagues (2008) and Kristensen & Jensen (2011) reported that the mechanisms for the influence of sodium alginate fibres in conjunction with calcium involved alterations in critical physical characteristics such as viscosity, gel production, and alterations of stomach contents, hence these alterations may decrease gastric clearance and attenuate absorption of nutrients in the small intestine, reduce postprandial glucose and insulin responses, which ultimately enhance the sense of fullness [10, 85]. The same authors stated that capability of alginate to produce both acidic and ionic gels may account for a poor mixing of gastric and small intestinal contents, hence enzyme-substrate binding will be slowed,

and subsequently, nutrients digestion and absorption will be reduced [85, 238]. It has been stated that solid meals may have a considerable influence on satiety more than liquid meals of the same size and number of calories because the solid meals can attenuate gastric emptying and expand the antrum which will send signal of increased satiety through tension receptors [202]. However, high-viscosity beverages or beverages containing unbreakable solids (lumps) have an unpleasant taste and became unpalatable, therefore, it has been suggested to use a meal which has the capability to form a viscous/gel solution immediately in the presence of gastric acid in the stomach [202].

Even though viscosity has been suggested as the mechanism by which alginate may reduce gastric emptying, reduce hunger, increase the sense of satiety, and slow macronutrient digestion and absorption, the viscosity may pose a problem for alginate in term of poor acceptability [238]. It has been shown that highly viscous meals containing strong-gelling alginate or guar are less acceptable since such high molecular weight biopolymers form a viscous solution on hydration which may be slimy in the mouth, hence their products become undesirable [202]. It has also been reported that consumption of diets containing alginate may cause abdominal pain, nausea, mild diarrhea, and unpleasant taste [238], and it has been indicated that adding large amounts of alginate to food may slow absorption of some beneficial minerals and nutrients such as calcium, iron, cobalt, chromium, and β-carotene [236, 239-241]. Additionally, a study by Jensen, Kristensen, & and Astrup (2012) indicated that subjects who ingested diets containing sodium alginate experienced an increase in blood pressure compared with the control group [238].

Although viscosity has been suggested to be the mechanism by which dietary fibres reduce digestive enzyme activity *in vitro* [200, 201], the Wilcox et al. (2014) and Houghton et al. (2015) studies reported that viscosity was not responsible for the reduction in pancreatic lipase activity in a turbidity assay. Houghton and his colleagues reported that alginate may inhibit pancreatic lipase in a similar way to that pectin inhibits pancreatic lipase, in which serine and histidine residues at the enzyme active site are protonated, preventing enzyme binding with substrate [144]. In the original work, Houghton investigated the effect of temperature and concentration on the inhibitory effect of alginate (DM) isolated from alginate bread using a turbidity assay and olive oil as a substrate. They observed that despite the significant reduction in viscosity (78%) of isolated alginate upon heating at 150°C, this alginate at concentrations 3 and 2 mg/ml was still able to decrease pancreatic lipase activity *in vitro* by 35% and 18%, respectively, compared with 33 and 18 % achieved by 3 and 2 mg/ml of alginate following heating at 37 °C. By contrast, there was a

significant reduction by 88% in the inhibitory properties of the isolated alginate following heating at 200 ˚C, showing that such high temperature (200˚C) seems to induce a significant change in alginate structure which is crucial for gel formation and inhibitory effects [218, 223]. Houghton et al also showed that freeze-dried alginate isolated from alginate bread was able to reduce pancreatic lipase activity *in vitro*, indicating that the cooking and baking processes did not affect the inhibitory properties of alginate as a pancreatic lipase inhibitor. In contrast, the AB used in this study did not inhibit pancreatic lipase activity. The AB used here was cooked using an alternative method of baking in which the AB was cooked for 65 minutes. However, the AB used in Houghton et al. study was made by Greggs, a commercial baker, using the Chorleywood bread process in which the AB was cooked for a shorter time (17-25 minutes), Therefore, less breakdown of the alginate would be expected. This was an unexpected result. It was not anticipated that changing the production method would alter the inhibitory properties of alginate and the mechanism requires investigation. For alginate to be a useful additive to foods, how it is altered by food production processes needs to be known.

Alginate rich in G-blocks reduces pancreatic lipase activity *in vitro* more than alginate rich in M-block [72, 223]. In addition, alginate with a high content of G-block forms stronger gel than alginate with low content of G-blocks, and the gel strength is essential in gastric clearance, gel breakdown, and food transport into small intestine [202, 234, 242].

Another potential explanation for the failure of alginate incorporated into bread in reducing triglyceride digestion could be that alginate degradation reduces the steric hindrance effect which in turn affects the inhibitory effect of alginate. Large alginate polymers may bind to the substrate binding site of the enzyme or to the oil/water surface of the substrate, blocking the substrate access to the enzyme or the enzyme entry to the substrate, preventing the formation of the E-S complex, subsequently, inhibiting triglyceride digestion (Figure 5.9A). However, if the alginate undergoes degradation, smaller fragments of alginate would be produced which in turn reduces the steric hindrance, where these small fragments can easily diffuse in and out of the active site of the enzyme, hence, the substrate can bind to the enzyme forming the E-S complex. Also, the binding of these fragments to the oil/water surface of the substrate will not affect the access of the enzyme to the substrate, hence, the E-S complex will be formed (Figure 5.9B).

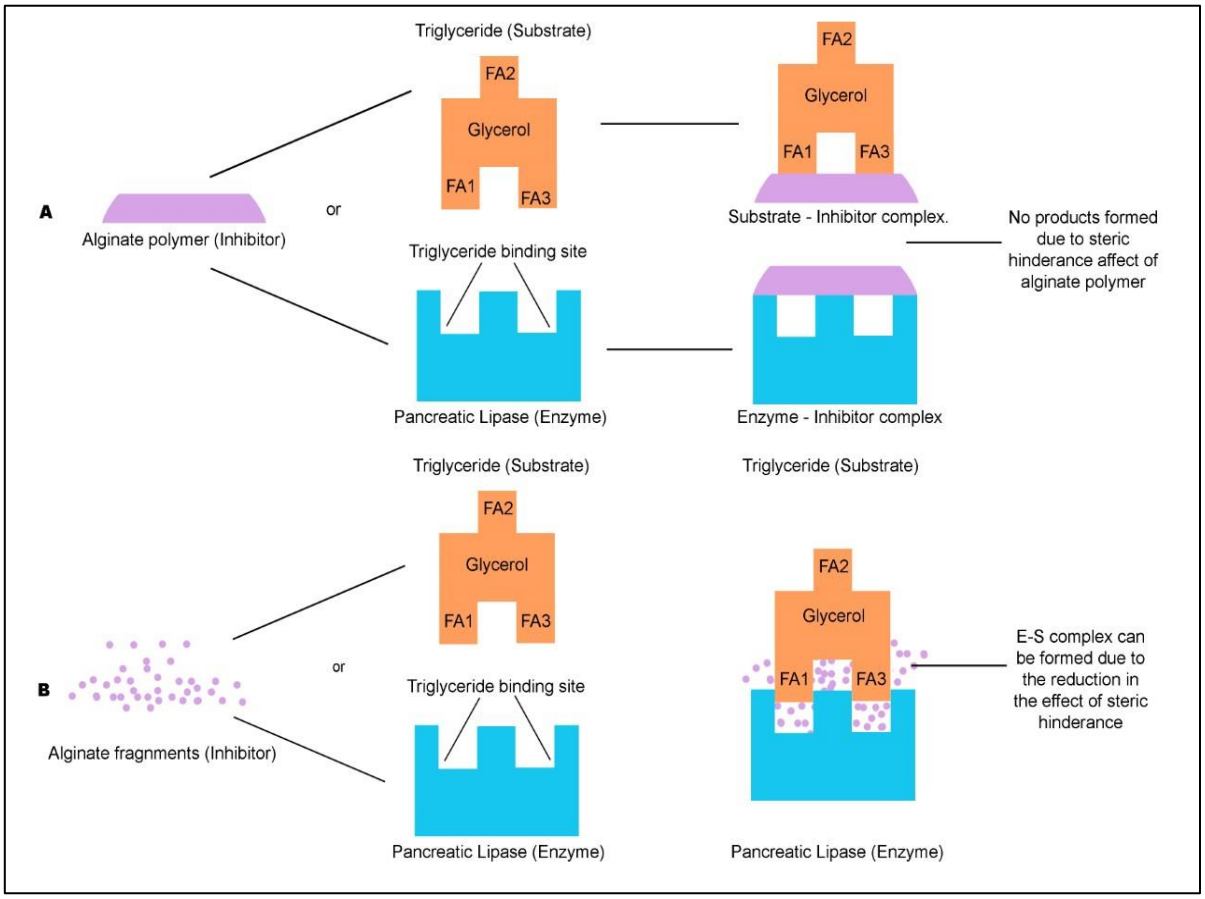

Figure 5.9. Schematic diagram showing the effects of size on the inhibitory properties of alginate as a pancreatic lipase inhibitor. Triglycerides substrate consists of glycerol and three fatty acids (FA1, FA2, and FA3). A. Alginate as a large polymer can bind to both the enzyme and substrate. Alginate can bind to the substrate binding site of the enzyme, blocking the access of the substrate to the enzyme. Alginate can also bind to the substrate interface (oil/water interface), preventing the access of the enzyme to the substrate interface due to the steric hindrance of alginate. Subsequently, the E-S complex will be inhibited, and the products will not be formed. B. Alginate fragments can bind to the enzyme or substrate; however, the steric hindrance effect of these small molecules is much less. Thus, the substrate can bind to the enzyme and E-S complex can be formed. Also, the binding of these fragments to the substrate interface will not prevent the formation of E-S complex.

Even though there is limited data on fibres incorporated into food and their capability to reduce pancreatic lipase activity [223], other fibres could significantly reduce pancreatic lipase activity *in vitro* such as pectin [141] and chitosan [150]. The exact mechanism by which alginate can inhibit pancreatic lipase activity is still unknown, however, several mechanisms have been suggested and some of them involve substrate-enzyme binding [72, 243]. These mechanisms were described in detail in Chapter **2** of this thesis.

5.7 Conclusion

The data described in this chapter showed that the modified version of the PAS assay [187] could be used to detect alginate produced from AB digestion in the model gut system. Standard curve data for alginate in MG solution of stomach phase and alginate in MG solution of small intestinal phase confirmed that PAS is an efficient and sensitive protocol in quantifying alginate since the linearity for both curves was excellent, and the protocol succeed in measuring alginate at relatively lower concentrations, and this finding is in agreement with previous findings [187, 223]. Furthermore, the AB used here was digestible within the model gut, supporting the ability of the synthetic model gut to mimic the digestive processes in the human body from mouth to small intestine. Also, the measured pHs at the salivary, stomach, and small intestinal phases of the synthetic model gut were similar to *in vivo* pHs.

The majority of alginate released from AB digestion was in the small intestine, however, the alginate released from bread digestion did not reduce fat digestion through the synthetic model gut, and that could be due to alginate degradation, alginate concentration used, or alginate interacting with other materials such as bile. Alginate degradation may result from proton-catalysed hydrolysis (pH<3), thermal degradation (high temperature during baking process), or fragmentation due to the presence of phenolic compounds in alginate which stimulate oxidative-reductive reactions. Also, binding between alginate and other substances within the model gut such as bile may affect the amount of alginate available in the solution. In addition, failure of alginate in reducing fat digestion could be associated with the presence of bread in the model gut system. Alginate degradation may even induce some alterations in alginate structure which in turn impact alginate capability in gel formation and inhibiting digestive enzymes activity *in vitro*. All these factors may affect regulatory effects of alginate as a pancreatic lipase inhibitor.

Chapter 6: General Discussion

Obesity has become a serious and common problem which potentially threatens public health and increases health care expenditure in the developed and developing countries. Some chronic diseases such as heart disease, type 2 diabetes, hypertension, non-alcoholic fatty liver disease (NFLD), and some types of cancer may develop from obesity [244]. Obesity is due to accumulation of body fat in adipose tissue, where individuals with BMI above 30 kg/m^2 can be considered as obese and that can be confirmed by an increase in the waist circumference [245]. Factors such as consumption of large amounts of food, lack of physical activity and some inherited diseases can be associated with obesity development.

It has been reported that the majority of excess caloric intake comes from the digestion and absorption of dietary lipids. Therefore, pancreatic lipase which is the main enzyme responsible for dietary lipid digestion and absorption becomes a potential target for obesity treatment where many anti-obesity drugs that aim to reduce lipid digestion and absorption have been developed to inhibit its activity [77].

Marine seaweeds have numerous beneficial effects on health since they are rich in dietary fibres which are indigestible in the upper gut. Marine seaweeds have been considered to form a prospective source of bioactive compounds with anti-obesity properties (Hu et al., 2016). The majority of these bioactive compounds are extracted from marine algae, mainly brown seaweeds [246]. Algal bioactive alginate is an indigestible polysaccharide which exists in the cell wall and intercellular space of brown algae (*Phyophyceae),* also, some bacterial species such as *Azotobacter* and *Pseudomonas genii* can produce alginate as a constituent of their extracellular matrix [115, 116].

Beside the various applications of alginate in medicine and pharmacology as prebiotics, antibacterial agents, antiviral agents and non-toxic antioxidants, and in industry as stabilising, thickening, and emulsifying agents [94], earlier studies showed that some alginates could be used as inhibitors for digestive enzymes responsible for macromolecule digestion such as pepsin [107, 108, 243] and pancreatic lipase [72, 192, 209]. This suggests a use for alginate as an inhibitor for pepsin and pancreatic lipase *in vivo* to reduce protein and fat digestion and absorption, subsequently, reducing the amount of calories absorbed from diets.

In this study, the regulatory effect of alginate on pancreatic lipase and fat digestion were investigated using three methods: a turbidimetric assay, a kinetic assay, and a synthetic model gut system.

6.1 Lipase regulation by alginate

In this study, data obtained from the turbidimetric lipase activity assay in which olive oil was used as a substrate showed that all the alginates used here could inhibit the activity of pancreatic lipase *in vitro* and the inhibition in lipase activity caused by different alginates was dependent on the structure and concentration of these polymers. Data obtained from the turbidimetric assay and ^{1}HNMR analysis for CC01, 1N80 and 1LF80 alginates showed that CC01, which contained the highest number of G blocks, could reduce the activity of pancreatic lipase to the greatest extent (75.6%) compared with other alginates, indicating that alginates with high content of G blocks could potentially reduce the activity of pancreatic lipase more than alginate with high content of M block. Also, higher concentrations of alginate caused a significant reduction in lipase activity compared to lower concentrations of alginate. These results are compatible with earlier results from Wilcox et al. (2014) who reported that the alginate could reduce activity of pancreatic lipase *in vitro* by 72.2% with DGGR (a synthetic substrate) and by 58% with olive oil (a natural substrate), and the extent of inhibition of lipase activity relied on the concentration and chemical structure of the alginate [72]. Wilcox and his colleagues found that alginate rich in G blocks could significantly inhibit the activity of pancreatic lipase more than alginate rich in M residues. Also, they found that the level of inhibition of lipase produced by alginate was dose dependent, where increasing the alginate concentration increased the inhibition level of lipase [72]. However, in the same study, Wilcox and his colleagues found that inhibitory effect of alginate was unaffected by the viscosity and molecular weight of the alginate. The results described herein in addition to previous results from the Wilcox et al. study (2014) suggested that alginates could be used as pancreatic lipase inhibitors *in vivo* to reduce triglyceride digestion and absorption, thus, reduce caloric intake and manage body weight. Therefore, the activity of pancreatic lipase might be modulated to a variable level based on the alginate used.

6.2 Kinetic assay of lipase activity

Kinetic parameters from the Michaelis-Menten plots presented in Chapter 3 of this study indicated that the presence of alginate in the reaction mixture allowed the lipase-catalysed reaction to approach the V_{max} at lower value compared to the V_{max} of control reaction in which alginate was not present. Also, the reduction in reaction velocity was dependent on the alginate structure, where alginate rich in G blocks could significantly decrease the velocity of lipase-catalysed reaction more than alginate rich in M blocks, showing that alginate had anti-pancreatic lipase activity which was dependent on the chemical structure of alginate.

In addition, the kinetic information produced from Lineweaver-Burk plots showed all three tested alginates acted as mixed inhibitors where they could bind to both the free enzyme and the enzyme-substrate complex with different binding affinities

Several mechanisms have been suggested for lipase inhibition by alginate, however, the exact mechanism by which alginate can inhibit pancreatic lipase is still unknown. Alginate can interact with the free enzyme and the substrate. Alginate has been shown to interact with the protein segment of a glycoprotein namely mucin and the presence of G residue is very important factor for this interaction where alginate rich in M residue would not interact with the mucin [139]. Alginate also may inhibit pancreatic lipase through protonation of hydroxyl (-OH) group of serine residues at the active site of the enzyme by the carboxyl (-COOH) group of the G blocks of alginate, reducing or stopping the proton shuttle mechanism which is a very important mechanism for the catalytic action of pancreatic lipase as described in Chapter 1 (Figure 1.6). This is believed to be the mechanism by which pectin inhibits the pancreatic lipase activity. It is therefore important to note that the carboxyl groups of pectin are at positions similar to the carboxyl groups of G residues of alginate (Figure 2.10 in Chapter 2 of this thesis) [72, 144]. Moreover, alginate could interact with the water/oil interface of the substrate, reducing the enzyme access to the substrate and decreasing formation of enzyme-substrate complex which in turn decreases the formation of product. This is reported to be the mechanism by which other anti-pancreatic lipase inhibitors such as chitosan, DEAE-sephadex and DEAE-polydextrose act [91, 150].

6.3 Fat digestion within the synthetic model gut system

Three different fat substrates (glyceryl trioctanoate, olive oil, and sunflower oil) were passed through the synthetic model gut system, and the amount of glycerol, which is a product released from fat digestion, was quantified. The data obtained from the digestion of the fat substrate showed that all the substrates were digestible within the synthetic model gut, however, the majority of substrate digestion occurred in the small intestinal phase by the action of pancreatic lipase. This finding is supported by previous finding [110, 164, 165, 167]. The digestion of fat substrates showed that the synthetic model gut used here was able to mimic *in vivo* gastrointestinal digestion of fat.

However, the digestion rates of fat substrates varied depending on the chain length of fatty acids of the triglyceride components of the fat substrates as well as the degree of saturation of these fatty acids. It has been reported that lipases preferentially hydrolyse short and medium chain triglycerides more than long-chain triglycerides [134, 175, 176]. The digestion rate of glyceryl trioctanoate containing saturated medium-chain triglycerides (octanoic acid) was the quickest. However, digestion of olive oil containing a mixture of triglycerides with medium- and long-chain triglycerides containing mostly palmitic acid (C16:0, saturated fatty acid,) and oleic acid (C18:1, monounsaturated fatty acid) was quicker than the digestion rate of sunflower oil consisting mainly of triglycerides containing long-chain polyunsaturated fatty acids (linoleic acids, C18:2). Consequently, these triglycerides may bind differently to the active site of enzyme because unlike the free rotation around the single bond, the rotation around the double bond is hindered.

Furthermore, 500 mg of alginate passed through the gastric phase of model gut was able to reduce glyceryl trioctanoate digestion with different levels of inhibition depending on the alginate content of G blocks. However, alginate passed through the gastric phase had no effect on olive oil or sunflower oil digestion and this appears to be due to alginate gelling caused by acidic pH during the gastric phase or because of $CaCl_2$ present in the synthetic saliva, hence, creating an ionic gel (calcium-alginate gel). Alginate can produce an acidic gel at low pH [103, 177, 202]. Additionally, it has been reported that alginate produces highly viscous acid-gels at pH less than the pKa of its uronic acids (3.5) [179, 183]. Besides, alginate produces an ionic gel in the presence of cationic ions such Ca^{2+} [100, 103, 180]. Alginate containing a high fraction of G blocks produces strong and stiff gels, but, alginate with a high fraction of M blocks produces soft and flexible gels [159,

160]. Gel formation might affect inhibitory properties of alginate since it will reduce the amount of free alginate within the reaction mixture, subsequently, the potency of alginate as a pancreatic lipase inhibitor will be reduced because the inhibition of pancreatic lipase by alginate is concentration-dependent.

However, alginates added after 10 minutes of the small intestinal phase could inhibit olive oil digestion, and that might be because the pH values within the small intestinal phase, which ranged between 4.5 and 4.7, was higher than the pKa of uronic acids (3.5) of alginate, hence, no gel was formed, allowing the free release of alginate within the reaction mixture to reduce fat digestion. In addition, it was found that 500 mg CC01 added at the small intestinal phase could reduce the digestion rate of olive oil to level much greater than that caused by 250 mg CC01, showing that inhibition effects of alginate are affected by alginate concentration. Wilcox et al. (2014) reported that specific alginates could inhibit pancreatic lipase activity *in vitro*, and the inhibition level of lipase caused by alginates were dependent on alginate concentrations [72].

Higher amounts of alginate (1000 mg) added either at the salivary phase or added after 10 minutes of the small intestinal phase appears to activate lipase, increasing the digestion of olive oil. The apparent activation in the digestion rate of olive oil treated with 1000 mg of alginate could be due to gel formation caused by low pH in the gastric phase (acidic gel) or the presence of Ca^{2+} ions in the saliva (ionic gel). The gel will bind a lot of water which will mean that the remaining solution will have less volume, thus, the enzyme-substrate concentrations in solution will be higher, leading to activation of triglyceride digestion. The gel produced from 1000 mg of alginate was larger than that produced from lower amounts of alginate (500 or 250 mg), thus, the larger the gel, the higher potential to bind higher amounts of water, causing more increases in the enzyme-substrate concentrations. This could explain the apparent activation in the digestion rate of triglycerides treated with 1000 mg alginate added at the salivary phase. Another possible explanation for the apparent increase in the digestion rate of olive oil treated with 1000 mg alginate added either at the salivary or small intestinal phase could be the effect of different affinity of alginate to triglycerides containing fatty acids with different degrees of saturation. Olive oil consists of a mixture of saturated and monounsaturated medium- and long- chain triglycerides, and as mentioned early, lipases show different binding affinity for different triglycerides containing different fatty acids with different chain length and different degrees of saturation. Thus, during the digestion of olive oil in the model gut, lipases would have different binding affinities for different triglycerides.

Therefore, the digestion rate of olive oil treated with 1000 mg of alginate might be accelerated because alginate may prefer binding to triglycerides containing long and unsaturated fatty acids, preventing these triglycerides binding with lipases, allowing hydrolysis of saturated triglycerides with shorter fatty acids by lipases, and accelerating the reaction rate. Further investigation of this hypothesis is needed.

In other studies, a synthetic saliva containing higher concentration of $NaHCO_3$ (372 mM) instead of normal saliva (62 mM) was used in an attempt to buffer the gastric pH in the model gut and prevent or reduce the gelling of alginate through the gastric phase. The data showed that the digestion rate of olive oil treated with buffered saliva was significantly less than the digestion rate of olive oil treated with normal saliva. Also, the pH measurements for olive oil treated with buffered and normal saliva showed that the gastric pH values for olive oil treated with buffered saliva were significantly higher than the gastric pH for olive oil treated with normal saliva, however, no significant difference was detected between the pH values for olive oil treated with buffered saliva and the pH for olive oil treated with normal saliva in the small intestinal phase, indicating that reduction in the digestion of olive oil treated with buffered saliva was not caused by a pH change. A possible reason for the reduction in the digestion of olive oil treated with buffered saliva could be the binding of calcium to bicarbonate through a cation exchange. As a result, the concentration of calcium ions in the reaction mixture will be reduced, hence, the activity of pancreatic lipase will be affected. Previous studies showed that the presence of calcium ions is essential for the activity of pancreatic lipase. Calcium ions could decrease the lag phase by reducing the electrostatic repulsion between the lipase and the surface of emulsion, facilitating the penetration of the enzyme to the emulsion interface [55]. Also, calcium ions can precipitate with free fatty acids, which are the products of triglycerides hydrolysis, removing them from the substrate surface and preventing the inhibition of pancreatic lipase caused by their accumulation at the substrate surface [56, 59].

The amount of glycerol released during olive oil digestion treated with alginate in combination with buffered saliva containing 372mM $NaHCO_3$ passed through the gastric phase was lower than that released from olive oil treated with alginate in combination with normal saliva containing 62mM $NaHCO_3$. The reduction in digestion of olive oil treated with alginate and buffered saliva could be because the buffered saliva provided pH values in the gastric phase higher than the pKa of uornic acids (3.5), hence, the gelling effect of alginate caused by acidic pH was reduced. Another possible reason could be the cation exchange between $CaCl_2$ and $NaHCO_3$, leading to formation of

insoluble calcium bicarbonate, consequently, the amount of free calcium ions in the reaction mixture would be reduced, resulting in less binding between the calcium ions and the alginate, thus, less gel would be formed.

6.4 Digestion of alginate bread in the synthetic model gut system

Several *in vivo* studies indicated that adding alginate into beverages or cereals resulted in valuable effects on health such as reducing the levels of glucose and insulin the in blood [114, 247], increased excretion of fat and bile acids [106], promoting weight loss [238], increasing satiety and reducing caloric intake [202, 238] and decreasing hunger [247]. Alginate can produce both an acidic and ionic gel [202, 203]. The ability of alginate to produce a viscous/gel solution is an important factor in the gastrointestinal signals that reduces hunger, increases feeling of satiety and reduce energy consumption [82, 202]. However, the ability of alginate to form a gel could be responsible for the poor acceptability of products containing alginate due the slimy feel in the mouth which makes it difficult to consume alginate-contained products every day. However, a previous ileostomy study in this lab showed that individuals involved in the study favoured the bread rich in alginate (4%) more than the alginate-free bread (control bread), showing that bread rich in alginate could abolish the issue of poor acceptability, and suggesting alginate bread as a palatable product which may be consumed every day [248] . Due to the worldwide acceptability and popularity of bread as a basic food which is consumed on a daily basis [204], bread was chosen in this study as a vehicle to deliver the CC01 alginate bioactive, which had the highest inhibitory effect based on the data obtained from both turbidimetric and kinetic assays for pancreatic lipase in this study, in an attempt to reduce pancreatic lipase activity, and thus triglyceride digestion and absorption. Alginate bread used here had to be passed through the synthetic model gut system and the alginate released had to be measured to investigate whether the alginate bread was digestible allowing the alginate to be released and reduce triglyceride digestion.

In this study, the standard curves for both alginate in MG solution taken from the end of the gastric phase (0-0.25 mg/ml) and alginate in MG solution taken from the end of the small intestinal phase (0-0.25 mg/ml) showed the accuracy of the modified PAS assay in measuring alginate in samples taken from the model gut even at relatively low concentrations. These results agree with previous studies which suggested the PAS assay as an accurate and sensitive method for measuring

glycoprotein and alginate [187, 223]. Also, alginate bread (AB) used here was shown to be digestible within the synthetic model gut and the bread digestion took place mainly in the small intestinal phase where the data from PAS assay showed that 73% of alginate was released in the small intestinal phase compared to 11% of alginate released in the gastric phase, demonstrating that the synthetic model gut used here could imitate digestive process of the upper part of the gastrointestinal tract *in vivo*. However, the data showed that about 16% of alginate incorporated into the bread was not measurable, suggesting that alginate might bind to other materials within the model gut system such as bile salts. Previous studies reported that alginates have high binding affinity to bile salts and acids [184, 185]. Although 73% of alginate incorporated to bread was released in the small intestinal phase where triglyceride digestion mainly occurs, the digestion of triglyceride in combination with AB was not reduced, showing that alginate incorporated into bread could not reduce the activity of pancreatic lipase. This could be because of alginate fragmentation caused by high temperature during the cooking process where the alginate was exposed to a temperature around 120 °C for 65 minutes. McDowell (1961) and Leo et al. (1990) reported that alginate polymers will experience an intensive fragmentation accompanied with the rapid release of CO_2 from the uronic acids constituents of alginate when the polymer is subjected to a temperature greater than 100°C [230, 231]. Also, the alginate might contain some phenolic compounds which could cause degradation and fragmentation of alginate polymer. It has been stated that some phenolic compounds could be present in the commercial alginate, and these compounds enhance oxidative-reductive reactions which results in alginate fragmentation [181].

In addition, alginate might undergo fragmentation via proton-catalysed reactions due to low pH in the stomach phase. Haug et al., (1963) reported that at pH below 5 alginate polymer experiences degradation by proton-catalysed hydrolysis, however, at pH above 10, β-alkoxy-elimination reaction occurs, resulting in depolymerisation of alginate polymer [222]. However, the possibility of alginate degradation due to low pH in the gastric phase is not accountable for the alginate incorporated into bread as little alginate was released from bread digestion in the gastric phase. Alginate fragmentation and degradation could reduce the size of alginate, hence, the efficiency of alginate as a pancreatic lipase inhibitor would be affected.

Although the results obtained here which revealed that AB did not reduce the activity of pancreatic lipase, the Houghton et al study (2015) showed that alginate incorporated into bread could reduce the activity of pancreatic lipase. This discrepancy could be because the bread used in the Houghton et al. study was made by Greggs, an industrial baker, using the Chorleywood process which only

cooks for 17-25 minutes, therefore, less breakdown of the alginate is likely to have occurred. However, the bread used in this study was cooked for a longer time (about 65 minutes), thus, more fragmentation of the alginate could be expected. Future studies could determine if this is the cause of the difference between this study and that of Houghton et al (2015).

6.5 Future work

This work has raised many interesting possibilities for future investigations not yet completed due to time constraints. In this study, data from both the turbidimetric assay and the synthetic model gut system have shown that alginates can potentially inhibit pancreatic lipase activity *in vitro*. The data also indicate that the level of lipase inhibition caused by alginate is affected by alginate concentration and structure. The capacity of alginates to inhibit the pancreatic lipase activity *in vitro* supports the future use of alginate, for example as a capsule, *in vivo* as a pancreatic lipase inhibitor to reduce fat digestion and absorption and hence, to treat obesity. The effect of alginate on pancreatic lipase activity *in vivo* could be evaluated by measuring the triglyceride level in the plasma. Moreover, this current study has focused on studying the effect of alginate on the fat digesting enzyme pancreatic lipase. It would, therefore, be interesting to study the effect of alginate on carbohydrate digestive enzymes such as α-amylase, α-glucosidase as well as protein digestive enzymes such as pepsin *in vitro* through α-amylase assay, α-glucosidase assays, pepsin assay and trypsin assay, respectively. Also, the regulatory effect of alginate on the activity of these enzymes in *vivo* could be investigated either through measuring the level of carbohydrate digestive enzymes (α-amylase and α-glucosidase) and the level of protein digestive enzymes (pepsin and trypsin) in saliva and gastric juice samples respectively, or through measuring the level of the end products of carbohydrate digestion (glucose) and the end products of protein digestion (amino acids, dipeptides, and tripeptides) in the blood after a test meal.

Regardless of the several mechanisms which have been suggested for pancreatic lipase inhibition by alginate, the exact inhibition mechanism is still unknown. Therefore, it would be worthwhile to investigate the specific mechanism by which alginate inhibits the pancreatic lipase activity in future studies through the use of an x-ray crystallography techniques. In such techniques, a mixture of enzyme and inhibitor is crystallised, then the molecular structure of enzyme-inhibitor complex can be determined by x-ray.

The synthetic data from model gut experiments show that a high amount (1000mg) of alginate activates olive oil digestion. This activation could be due to gel formation resulting from either low pH in the gastric phase or the presence of Ca^{2+} ions in the saliva. The gel binds a lot of water, decreasing the volume of reaction solution, consequently, the enzyme-substrate concentrations in solution becomes higher, leading to activation of triglyceride digestion. Therefore, it would be sensible to do further binding studies on samples containing alginate and olive oil to investigate the level of enzyme-substrate interaction increases in the presence of high amount of alginate.

The synthetic model gut data presented in this study also indicate that incorporating alginate into bread results in the loss of the inhibitory effect of alginate on pancreatic lipase activity and this might occur due to fragmentation of alginate as a result of the high temperatures during the cooking process. Alginate fragmentation affects its inhibition properties and reduces alginate capacity as a potent pancreatic lipase inhibitor. Therefore, a further study is still required to investigate the effect of high temperature on alginate polymer. This might be performed by heating alginate at different temperatures ranging from 50 to 200 ^{0}C, then the molecular size of alginate can be assessed using different techniques such as mass spectrometry, light scattering, analytical ultracentrifugation and viscosity.

Bibliography

1. Sabán-Ruíz, J., et al., An Approach to Obesity as Cardiometabolic Disease: Potential Implications for Clinical Practice in Anti-Obesity Drug Discovery and Development, J. Aaseth, Editor. 2014, Bentham Books. p. 4, chapter 1.
2. Mason, P., Dietary Foods, in Handbook of Nutraceuticals Volume I: Ingredients, Formulations, and Applications, Y.V. Pathak, Editor. 2009, CRC Press. p. 322, chapter 19
3. Weisberg, S.P., et al., *Obesity is associated with macrophage accumulation in adipose tissue.* Journal of Clinical Investigation, 2003. **112**(12): p. 1796-1808.
4. Birari, R.B. and K.K. Bhutani, *Pancreatic lipase inhibitors from natural sources: unexplored potential.* Drug Discovery Today, 2007. **12**(19-20): p. 879-889.
5. Xiao, J. and W. Yang, Weight Loss Is Still an Essential Intervention in Obesity and its Implications: A Review. Journal of Obesity, 2012. **2012**: p. 1-6.
6. Ng, M., et al., Global, regional, and national prevalence of overweight and obesity in children and adults during 1980-2013: a systematic analysis for the Global Burden of Disease Study 2013. Lancet, 2014. **384**(9945): p. 766-781.
7. Stevens, G.A., et al., National, regional, and global trends in adult overweight and obesity prevalences. Popul Health Metr, 2012. **10**(1): p. 22.
8. Kelly, T., et al., *Global burden of obesity in 2005 and projections to 2030.* Int J Obes (Lond), 2008. **32**(9): p. 1431-7.
9. Collaboration, N.C.D.R.F., Trends in adult body-mass index in 200 countries from 1975 to 2014: a pooled analysis of 1698 population-based measurement studies with 19.2 million participants. Lancet, 2016. **387**(10026): p. 1377-1396.
10. Paxman, J.R., et al., Daily ingestion of alginate reduces energy intake in free-living subjects. Appetite, 2008. **51**(3): p. 713-9.
11. Campbell, J., *Campbell's Physiology Notes For Nurses*. 2006, John Wiley & Sons. p. 149-174, chapter 8.
12. Ireland, K.A., *Visualizing Human Biology*. 2010, John Wiley & Sons. p. 411-429, chapter 15.
13. Sreekumar, S., *Basic Physiology, 1/e*. 2010, Prentice-Hall Of India Pvt Limited. p. 87, 88, chapter 6
14. Brown, J., *Nutrition Now*. 2007, Cengage Learning. p. 7.4, chapter 7.
15. Rosenblum, J.L., C.L. Irwin, and D.H. Alpers, *Starch and glucose oligosaccharides protect salivary-type amylase activity at acid pH.* AJP - Gastrointestinal and Liver Physiology, 1988 **254**: p. 775-780.
16. Goodman, B.E., *Insights into digestion and absorption of major nutrients in humans.* Advances in Physiology Education, 2010. **34**(2): p. 44-53.
17. Fink, H., L. Burgoon, and A. Mikesky, *Practical Applications in Sports Nutrition*. 2009, Jones & Bartlett Learning. p. 35-42, chapter 2.
18. Khurana, I., *Textbook of Human Physiology for Dental Students*. 2014, Elsevier Health Sciences. p. 351, 352, chapter 77
19. Pearson, J.P., et al., *Pepsin* in *Effects, Diagnosis and Management of Extra-Esophageal Reflux*. 2010, Nova Science Publishers. p. 29-41, chapter 4
20. Powers, J.C., A.D. Harley, and D.V. Myers, *Subsite specificity of porcine pepsin.* Adv Exp Med Biol, 1977. **95**: p. 141-57.
21. Premkumar, K., *The Massage Connection: Anatomy and Physiology*. 2004, Lippincott Williams and Wilkins. p. 594, 595, chapter 11.

22. Steel, A. and M.A. Hediger, The Molecular Physiology of Sodium- and Proton-Coupled Solute Transporters. News Physiol Sci, 1998. **13**: p. 123-131.
23. Eljamil, A.S., *Lipid Biochemistry: for Medical Science.* . 2015, iUniverse. p. Introduction section, chapter 2
24. Iqbal, J. and M.M. Hussain, *Intestinal lipid absorption.* Am J Physiol Endocrinol Metab 2009. **296**(6): p. E1183-94.
25. Brody, T., *Nutritional Biochemistry*. 1999, Academic Press. p. 94, chapter 2.
26. Lowe, M.E., *The triglyceride lipases of the pancreas.* J Lipid Res, 2002. **43**(12): p. 2007-16.
27. Armand, M., *Lipases and lipolysis in the human digestive tract: where do we stand?* Curr Opin Clin Nutr Metab Care, 2007. **10**(2): p. 156-64.
28. Buisson, C., et al., Three dimentional structure of porcine pancreatic α-amylase at 2.9 resolution Å. Role of calcium in structure ans activity. The EMBO Journal, 1987. **6**(13): p. 3909-3916.
29. Rosenthal, M.D. and R.H. Glew, *Medical Biochemistry: Human Metabolism in Health and Disease*. 2011, John Wiley & Son. p. section 3.2.2, chapter 3.
30. Bishu, S. and E.M.M. Quigley, *Nutrien digestion, absorption and sensing*, in *Textbook of Gasroenterolog*, D.K. Podolsky, et al., Editors. 2015, John Wiley & Sons. p. 538, chapter 29.
31. Harvey, R.A. and D.R. Ferrier, *Biochemistry*. 5 ed. 2011: Lippincott Williams & Wilkins.
32. Sky-Peck, H.H. and P. Thuvasethakul, Human pancreatic alpha-amylase. II. Effects of pH, substrate and ions on the activity of the enzyme. Ann Clin Lab Sci, 1977. **7**(4): p. 310-7.
33. Vallee, B.L., et al., *Metal content of alpha-amylases of various origins.* J. Biol. Chem. , 1959. **234**: p. 2901-2905.
34. Wong, D.W.S., *Food Enzymes: Structure and Mechanism*. 2013, Springer Science and Business Media. p. 45, chapter 3.
35. Pinto, G.P., et al., Establishing the catalytic mechanism of human pancreatic alpha-amylase with QM/MM methods. J Chem Theory Comput, 2015. **11**(6): p. 2508-16.
36. Palashoff, M.H., Determining the specificity of pepsin for proteolytic digestion, in The Department of Chemistry and Chemical Biology in partial fulfillment of the requirements for the degree of Master of Science in the field of Chemistry. 2008, Northeastern University, Boston, Massachusetts. Chapter 1 (pp.20, 21).
37. Sielecki, A.R., et al., Molecular and crystal structures of monoclinic porcine pepsin refined at 1.8 A resolution. J Mol Biol, 1990. **214**(1): p. 143-70.
38. Sielecki, A.R., et al., *Refined Structure of Porcine Pepsinogen at 1.8-a Resolution.* Journal of Molecular Biology, 1991. **219**(4): p. 671-692.
39. Fujinaga, M., et al., Crystal structure of human pepsin and its complex with pepstatin. Protein Sci., 1995 **4**(5): p. 960-972.
40. Cooper, J.B., et al., X-ray analyses of aspartic proteinases. II. Three-dimensional structure of the hexagonal crystal form of porcine pepsin at 2.3 A resolution. J Mol Biol, 1990. **214**(1): p. 199-222.
41. Fusek, M. and V. Vėtvička, *Aspartic ProteinasesPhysiology and Pathology*. 1995 CRC Press. p. 22, chapter 2.
42. Prasad, B.V. and K. Suguna, *Role of water molecules in the structure and function of aspartic proteinases.* Acta Crystallogr D Biol Crystallogr, 2002. **58**(Pt 2): p. 250-9.
43. Simon, L.M., et al., The effects of organic solvent/water mixtures on the structure and catalytic activity of porcine pepsin. Process Biochemistry, 2007. **42**(5): p. 909-912.
44. Hunkapiller, M.W. and J.H. Richards, *Studies on the catalytic mechanism of pepsin using a*

new synthetic substrate. Biochemistry, 1972. **11**(15): p. 2829-39.
45. Chatterjea, M.N. and R. Shinde, *Textbook of Medical Biochemistry*. 2011, Jaypee Brothers,Medical Publishers Pvt. Limited. p. 393, 439, 464, chapters: 24-26
46. Tasker, A., et al., Is gastric reflux a cause of otitis media with effusion in children? Laryngoscope, 2002. **112**(11): p. 1930-1934.
47. Bauer, E., S. Jakob, and R. Mosenthin, *Principles of physiology of lipid digestion.* Asian-Australasian Journal of Animal Sciences, 2005. **18**(2): p. 282-295.
48. Winkler, F.K., A. D'Arcy, and W. Hunziker, *Structure of human pancreatic lipase.* Nature, 1990. **343**(6260): p. 771-4.
49. van Tilbeurgh, H., et al., *Structure of the pancreatic lipase-procolipase complex.* Nature, 1992. **359**(6391): p. 159-62.
50. van Tilbeurgh, H., et al., Interfacial activation of the lipase-procolipase complex by mixed micelles revealed by X-ray crystallography. Nature, 1993. **362**(6423): p. 814-20.
51. Aoubala, M., et al., Human pancreatic lipase. Importance of the hinge region between the two domains, as revealed by monoclonal antibodies. J Biol Chem, 1995. **270**(8): p. 3932-7.
52. Sembulingam, K. and P. Sembulingam, *Essential of Medical Physiology*. 2012, JP Medical Ltd. p. 244, chapter 39
53. Sitrin, M.D., Digestion and Absorption of Dietary Triglycerides, in The Gastrointestinal System: Gastrointestinal, Nutrional and Hepatobiliary Physiology, P.S. Leung, Editor. 2014, Springer Science & Business-Medical. p. 162, chapter 7
54. Borgstrom, B., Importance of phospholipids, pancreatic phospholipase A2, and fatty acid for the digestion of dietary fat: in vitro experiments with the porcine enzymes. Gastroenterology, 1980. **78**(5 Pt 1): p. 954-62.
55. Armand, M., et al., Effects of Droplet Size, Triacylglycerol Composition, and Calcium on the Hydrolysis of Complex Emulsions by Pancreatic Lipase - an Invitro Study. Journal of Nutritional Biochemistry, 1992. **3**(7): p. 333-341.
56. Alvarez, F.J. and V.J. Stella, Pancreatic lipase-catalyzed hydrolysis of esters of hydroxymethyl phenytoin dissolved in various metabolizable vehicles, dispersed in micellar systems, and in aqueous suspensions. Pharm Res, 1989. **6**(7): p. 555-63.
57. Brown, W.J., A.A. Belmonte, and P. Melius, Effects of divalent cations and sodium taurocholate on pancreatic lipase activity with gum arabic-emulsified tributyrylglycerol substrates. Biochim Biophys Acta, 1977. **486**(2): p. 313-21.
58. Scow, R.O., Effect of sodium taurodeoxycholate, CaCl2 and albumin on the action of pancreatic lipase on droplets of trioleoylglycerol and the release of lipolytic products into aqueous media. Biochimie, 1988. **70**(9): p. 1251-61.
59. Thomas, N., et al., Characterising Lipid Lipolysis and Its Implication in Lipid-Based Formulation Development. Aaps Journal, 2012. **14**(4): p. 860-871.
60. Zangenberg, N.H., et al., A dynamic in vitro lipolysis model. I. Controlling the rate of lipolysis by continuous addition of calcium. Eur J Pharm Sci, 2001. **14**(2): p. 115-122.
61. Wickham, M., et al., Modification of a phospholipid stabilized emulsion interface by bile salt: effect on pancreatic lipase activity. J Lipid Res, 1998. **39**(3): p. 623-32.
62. Yang, J., et al., In vitro analysis of roles of a disulfide bridge and a calcium binding site in activation of Pseudomonas sp. strain KWI-56 lipase. J Bacteriol, 2000. **182**(2): p. 295-302.
63. Wicker-Pianquart, C. and A. Puigserver, *Regulation of gastrointestinal Lipase Gene Expression by Dietary Lipids*, in *Nutrition and Gene Expression*, C.D. Berdanier and J.L. Hargrove, Editors. 2018, CRC Press. p. section B: Pancreatic lipse, chapter 3
64. Gropper, S.S. and J.L. Smith, *Advanced Nutrition and Human Metabolism*. 2012, Cangage

Learning. p. 146, 147, chapter 5.
65. Jegannathan, K.R., et al., *Production of biodiesel using immobilized lipase--a critical review.* Crit Rev Biotechnol, 2008. **28**(4): p. 253-64.
66. Fabricatore, A.N. and T.A. Wadden, *Treatment of Obesity: An Overview.* Clinical Diabetes, 2003. **21**(2): p. 67-72.
67. Ayyad, C. and T. Andersen, Long-term efficacy of dietary treatment of obesity: a systematic review of studies published between 1931 and 1999. Obes Rev, 2000. **1**(2): p. 113-9.
68. Blackburn, G.L., *Obesity and Diabetes*, in *Diet, Exercise, and Behavioural Treatment of Obesity*, C.S. Mantzoros, Editor. 2007, Springer Science & Business Media. p. 448, chapter 25.
69. Terre, L., W.S.C. Poston, and J.P. Foreyt, *Overview and the Future of Obesity Treatment*, in *The Management of Eating Disorders and Obesity*, D.J. Goldstein, Editor. 2007, Springer Science & Business Media. p. 167, chapter 12
70. Östman, J., M. Britton, and E. Jonsson, *Treating and Preventing Obesity: An Evidence Based Review*. 2006, John Wiley & Sons. p. 272, chapter 6
71. Clifton, P.M., *Dietary treatment for obesity.* Nature Clinical Practice Gastroenterology & Hepatology, 2008. **5**(12): p. 672-681.
72. Wilcox, M.D., et al., *The modulation of pancreatic lipase activity by alginates.* Food Chem, 2014. **146**: p. 479-84.
73. Tucci, S.A., E.J. Boyland, and J.C.G. Halford, The role of lipid and carbohydrate digestive enzyme inhibitors in the management of obesity: a review of current and emerging therapeutic agents. Diabetes, Metabolic Syndrome and Obesity: Targets and Therapy, 2010. **3**: p. 125-143.
74. Dewick, P.M., *Medicinal Natural Products: A Biosynthetic Approach* 2011, John Wiley & Sons. p. Box 3.2, chapter 3.
75. Kang, J.G. and C.Y. Park, *Anti-Obesity Drugs: A Review about Their Effects and Safety* Diabetes and Metabolism Journal, 2012. **36**(1): p. 13-25.
76. Sabán-Ruíz J, et al., An Approach to Obesity as a Cardiometabolic Disease: Potential Implications for Clinical Practice. , in Anti-Obesity Drug Discovery and Development, Atta-ur-Rahman and I.M. Choudhary, Editors. 2014, Bentham Ebooks. p. 4, chapter 1.
77. Lunagariya, N.A., et al., Inhibitors of pancreatic lipase: state of the art and clinical perspectives. EXCLI J, 2014. **13**: p. 897-921.
78. Borgstrom, B., Mode of action of tetrahydrolipstatin: a derivative of the naturally occurring lipase inhibitor lipstatin. Biochim Biophys Acta, 1988. **962**(3): p. 308-16.
79. Benarouche, A., et al., An interfacial and comparative in vitro study of gastrointestinal lipases and Yarrowia lipolytica LIP2 lipase, a candidate for enzyme replacement therapy. Biochimie, 2014. **102**: p. 145-53.
80. Atta-ur-Rahman, M.I. Choudhary, and N.T. Khan, *Changing paradigm for drug development: A case study of natural products.* Pure and Applied Chemistry, 2011. **83**(9): p. 1643-1650.
81. Aronne, L.J., K.K. Isoldi, and D.T. Roarke, *Therapeutic options for modifying obesity and cardiometabolic risk factors*, in *The John Hopkins Textbook of Dyslipidemia*, P.O. Kwiterovich, Editor. 2012, Lippincott Williams & Wilkins. p. 287, chapter 24.
82. Solah, V.A., et al., Differences in satiety effects of alginate- and whey protein-based foods. Appetite, 2010. **54**(3): p. 485-491.
83. Georg Jensen, M., M. Kristensen, and A. Astrup, Effect of alginate supplementation on weight loss in obese subjects completing a 12-wk energy-restricted diet: a randomized controlled trial. Am J Clin Nutr, 2012. **96**(1): p. 5-13.
84. Papathanasopoulos, A., et al., A preliminary candidate genotype-intermediate phenotype

study of satiation and gastric motor function in obesity. Obesity (Silver Spring), 2010. **18**(6): p. 1201-11.
85. Kristensen, M. and M.G. Jensen, Dietary fibres in the regulation of appetite and food intake. Importance of viscosity. Appetite, 2011. **56**(1): p. 65-70.
86. Burton-Freeman, B., *Dietary fiber and energy regulation.* Journal of Nutrition, 2000. **130**(2): p. 272s-275s.
87. Fernandes, J., et al., Adiposity, gut microbiota and faecal short chain fatty acids are linked in adult humans. Nutrition & Diabetes, 2014. **4**.
88. Howarth, N.C., E. Saltzman, and S.B. Roberts, *Dietary fiber and weight regulation.* Nutrition Reviews, 2001. **59**(5): p. 129-139.
89. Ikeda, K. and T. Kusano, In Vitro Inhibition of Digestive Enzymes by Indigestible Polysaccharides Cereal Chem 1983. **60**(4): p. 260-263.
90. Vanbergehenegouwen, G.P., et al., *Effect of Standardized Wheat Bran Preparation on Serum-Lipids in Young Healthy-Males.* American Journal of Clinical Nutrition, 1979. **32**(4): p. 794-798.
91. Tsujita, T., et al., *Inhibition of lipase activities by basic polysaccharide.* J Lipid Res, 2007. **48**(2): p. 358-65.
92. Lordan, S., R.P. Ross, and C. Stanton, Marine Bioactives as Functional Food Ingredients: Potential to Reduce the Incidence of Chronic Diseases. Marine Drugs, 2011. **9**(6): p. 1056-1100.
93. Kraan, S., Algal Polysccharides, Novel Applications and Outlook, Carbohydrates - Comprehensive Studies on Glycobiology and Glycotechnology, in Carbohydrates: Comprehensive Studies on Glycobiology and Glycotechnology, C.F. Chang, Editor. 2012, IntechOpen. p. 495, 496, chapter 22
94. Chojnacka, K., et al., *Biologically Active Compounds in Seaweeds Extracts- the Prospects for the Application.* The Open Conference Proceedings Journal, 2012. **3**: p. pp: 20-28.
95. Eom, S.H., et al., Pancreatic Lipase Inhibitory Activity of Phlorotannins Isolated from Eisenia bicyclis. Phytotherapy Research, 2013. **27**(1): p. 148-151.
96. Matsumoto, M., et al., Suppressive effects of the marine carotenoids, fucoxanthin and fucoxanthinol on triglyceride absorption in lymph duct-cannulated rats. European Journal of Nutrition, 2010. **49**(4): p. 243-249.
97. Chater, P.I., et al., *Inhibitory activity of extracts of Hebridean brown seaweeds on lipase activity.* Journal of Applied Phycology, 2016. **28**(2): p. 1303-1313.
98. Nussinovitch, A., *Hydrocolloid Applications: Gum Technology in the food and other Industries*. 1997, Springer Science & Business Media. p. 20, 21, chapter 2
99. Venugopal, V., *Marine Polysaccharides: Food Applications*. 2016, CRC Press, Taylor & Francis Group-Technology & Engineering. p. 104, 107, chapter 4
100. Lee, K.Y. and D.J. Mooney, *Alginate: Properties and biomedical applications.* Progress in Polymer Science, 2012. **37**(1): p. 106-126.
101. Lencina, M.M.S., et al., *Recent Studies on Alginates Based Blends, Composites, and Nanocomposites*, in *Advances in Natural Polymers*, S. Thomas, P.M. Visakh, and A.P. Mathew, Editors. 2012, Springer Science & Business Media: Berlin. p. 194-197, chapter 7
102. Pawar, S.N. and K.J. Edgar, Alginate derivatization: A review of chemistry, properties and applications. Biomaterials, 2012. **33**(11): p. 3279-3305.
103. Draget, K.I., G. Skjak-Braek, and B.T. Stokke, *Similarities and differences between alginic acid gels and ionically crosslinked alginate gels.* Food Hydrocolloids, 2006. **20**(2-3): p. 170-175.
104. Donati, I. and P. Sergio, *Material Properties of Alginates*, in *Alginates: Biology and Applications* B.H. Rehm, Editor. 2009, Springer Berlin Heidelberg. p. 3, chapter 2.

105. Williams, J.A., et al., Inclusion of guar gum and alginate into a crispy bar improves postprandial glycemia in humans. Journal of Nutrition, 2004. **134**(4): p. 886-889.
106. Sandberg, A.S., et al., *Alginate, Small-Bowel Sterol Excretion, and Absorption of Nutrients in Ileostomy Subjects.* American Journal of Clinical Nutrition, 1994. **60**(5): p. 751-756.
107. Sunderland, A.M., P.W. Dettmar, and J.P. Pearson, Alginates inhibit pepsin activity in vitro; A justification for their use in gastro-oesophageal reflux disease (gord). Gastroenterology, 2000. **118**(4): p. A21.
108. Chater, P.I., et al., Alginate as a protease inhibitor in vitro and in a model gut system; selective inhibition of pepsin but not trypsin. Carbohydrate Polymers, 2015. **131**: p. 142-151.
109. Strugala, V., et al., The role of an alginate suspension on pepsin and bile acids - key aggressors in the gastric refluxate. Does this have implications for the treatment of gastro-oesophageal reflux disease? J Pharm Pharmacol, 2009. **61**(8): p. 1021-8.
110. Mu, H. and C.E. Høy, *The digestion of dietary triacylglycerols.* Progress in Lipid Research, 2004. **43**(2): p. 105-33.
111. Rolls, B.J., *The relationship between dietary energy density and energy intake.* Physiology & Behavior, 2009. **97**(5): p. 609-615.
112. Sebban-Kreuzer, C., et al., Inhibitory effect of the pancreatic lipase C-terminal domain on intestinal lipolysis in rats fed a high-fat diet: chronic study. Int J Obes Relat Metab Disord, 2003. **27**(3): p. 319-25.
113. Cavaliere, H., I. Floriano, and G. Medeiros-Neto, Gastrointestinal side effects of orlistat may be prevented by concomitant prescription of natural fibers (psyllium mucilloid). Int J Obes Relat Metab Disord, 2001. **25**(7): p. 1095-9.
114. Torsdottir, I., et al., A small dose of soluble alginate-fiber affects postprandial glycemia and gastric emptying in humans with diabetes. J Nutr, 1991. **121**(6): p. 795-9.
115. Boyd, A. and A. Chakrabarty, *Role of alginate lyase in cell detachment of Pseudomonas aeruginosa.* Appl Environ Microbiol, 1994. **60**(7): p. 2355-9.
116. Ertesvag, H., et al., Mannuronan C-5-epimerases and their application for in vitro and in vivo design of new alginates useful in biotechnology. Metab Eng, 1999. **1**(3): p. 262-9.
117. Rowley, J.A., G. Madlambayan, and D.J. Mooney, *Alginate hydrogels as synthetic extracellular matrix materials.* Biomaterials, 1999. **20**(1): p. 45-53.
118. Grasdalen, H., High-Field, H-1-Nmr Spectroscopy of Alginate - Sequential Structure and Linkage Conformations. Carbohydrate Research, 1983. **118**(Jul): p. 255-260.
119. Grasdalen, H., B. Larsen, and O. Smidsrod, *C-13-Nmr Studies of Monomeric Composition and Sequence in Alginate.* Carbohydrate Research, 1981. **89**(2): p. 179-191.
120. Grasdalen, H., B. Larsen, and O. Smidsrod, *Pmr Study of the Composition and Sequence of Uronate Residues in Alginates.* Carbohydrate Research, 1979. **68**(1): p. 23-31.
121. Draget, K.I. and C. Taylor, Chemical, physical and biological properties of alginates and their biomedical implications. Food Hydrocolloids, 2011. **25**(2): p. 251-256.
122. Vogel, W.C. and L. Zieve, A rapid and sensitive turbidimetric method for serum lipase based upon difference between the lipases of normal and pancreatitis serum. Clinical Chemistry, 1963. **9**(2): p. 168-181.
123. Barrett, K. and H. Raybould, in *Berne & Levy Physiology, Updated Edition E-Book*, B.M. Koeppen and B.A. Stanton, Editors. 2009, Elsevier Health Sciences. p. 527, chapter 29.
124. Lindberg, G., Basic Physiology of Motility, Absorption and Secretion, in Intestinal Failure: Diagnosis, Management and Transplantation A.N. Langnas, et al., Editors. 2009, John Wiley & Sons. p. 28, chapter 3.
125. Kumar, P. and K.K. Dubey, Current trends and future prospects of lipstatin: a lipase inhibitor

and pro-drug for obesity. Rsc Advances, 2015. **5**(106): p. 86954-86966.
126. Karupaiah, T. and K. Sundram, Effects of stereospecific positioning of fatty acids in triacylglycerol structures in native and randomized fats: a review of their nutritional implications. Nutrition & Metabolism, 2007. **4**: p. 16.
127. Alfieri, A., et al., *Effect of Plant Oil Interesterified Triacylglycerols on Lipemia and Human Health.* International Journal of Molecular Science, 2018. **19**(104): p. 1-11.
128. Whitney, E. and S. Rolfes, *Understanding Nutrition*. 2018, Cengage Learning. p. 129-132, chapter 5
129. King, I.B., *Lipids in Foods: Chemistry and Nomenclature*, in *Handbook of Lipids in Human Nutrition*, G.A. Spiller, Editor. 1995, CRC Press: Washington. p. 3, chapter 1.1.
130. Kent, M., *Advanced Biology*. 2000, Oxford University Press: Oxford. p. 30, 31, chapter 2
131. Myers, R., *The Basics of Chemistry*. 2003, Greenwood Press: Westport. p. 228, chapter 16
132. Ramirez, M., L. Amate, and A. Gil, *Absorption and distribution of dietary fatty acids from different sources.* Early Hum Dev, 2001. **65 Suppl**: p. S95-S101.
133. Shah, N.D. and B.N. Limketkai, *The Use of Medium-Chain Triglycerides in Gastrointestinal Disorders.* Practical Gastroenterology, 2017. **41**(2): p. 20-28.
134. You, Y.Q.N., et al., Effects of medium-chain triglycerides, long-chain triglycerides, or 2-monododecanoin on fatty acid composition in the portal vein, intestinal lymph, and systemic circulation in rats. Journal of Parenteral and Enteral Nutrition, 2008. **32**(2): p. 169-175.
135. Christensen, M.S., et al., Intestinal-Absorption and Lymphatic Transport of Eicosapentaenoic (Epa), Docosahexaenoic (Dha), and Decanoic Acids - Dependence on Intramolecular Triacylglycerol Structure. American Journal of Clinical Nutrition, 1995. **61**(1): p. 56-61.
136. Decker, E.A., The role of stereospecific saturated fatty acid positions on lipid nutrition. Nutr Rev, 1996. **54**(4 Pt 1): p. 108-10.
137. Symersky, T., et al., The effect of equicaloric medium-chain and long-chain triglycerides on pancreas enzyme secretion. Clin Physiol Funct Imaging, 2002. **22**(5): p. 307-11.
138. Isaacs, P.E., et al., Comparison of effects of ingested medium- and long-chain triglyceride on gallbladder volume and release of cholecystokinin and other gut peptides. Dig Dis Sci, 1987. **32**(5): p. 481-6.
139. Taylor, C., et al., Mucous systems show a novel mechanical response to applied deformation. Biomacromolecules, 2005. **6**(3): p. 1524-1530.
140. Wilcox, M.D., *Bioactive Alginates.* 2010, PhD Thesis, Newcastle University. Chapter 5 (p. 185): Newcastle Upon Tyne.
141. Isaksson, G., I. Lundquist, and I. Ihse, *In vitro inhibition of pancreatic enzyme activities by dietary fiber.* Digestion, 1982. **24**(1): p. 54-9.
142. Isaksson, G., et al., Influence of dietary fiber on exocrine pancreatic function in the rat. Digestion, 1983. **27**(2): p. 57-62.
143. Haugstad, K.E., et al., Direct Determination of Chitosan-Mucin Interactions Using a Single-Molecule Strategy: Comparison to Alginate-Mucin Interactions. Polymers, 2015. **7**(2): p. 161-185.
144. Kumar, A. and G.S. Chauhan, Extraction and characterisation of pectin from apple pomace and its evaluation as lipase (steapsin) inhibitor. Carbohydrate Polymers, 2010. **82**(2): p. 454-459.
145. Braccini, I. and S. Perez, Molecular basis of C(2+)-induced gelation in alginates and pectins: the egg-box model revisited. Biomacromolecules, 2001. **2**(4): p. 1089-96.
146. Braccini, I., R.P. Grasso, and S. Perez, Conformational and configurational features of acidic polysaccharides and their interactions with calcium ions: a molecular modeling investigation. Carbohydr Res, 1999. **317**(1-4): p. 119-30.

147. Wellner, N., et al., *FT-IR study of pectate and pectinate gels formed by divalent cations.* Carbohydrate Research, 1998. **308**(1-2): p. 123-131.
148. Axelos, M.A.V., Ion Complexation of Biopolymers - Macromolecular Structure and Viscoelastic Properties of Gels. Makromolekulare Chemie-Macromolecular Symposia, 1990. **39**: p. 323-328.
149. Leick, S., et al., Deformation of liquid-filled calcium alginate capsules in a spinning drop apparatus. Phys Chem Chem Phys, 2010. **12**(12): p. 2950-8.
150. Han, L.K., Y. Kimura, and H. Okuda, *Reduction in fat storage during chitin-chitosan treatment in mice fed a high-fat diet.* Int J Obes Relat Metab Disord, 1999. **23**(2): p. 174-9.
151. Harvey, R.A. and D.R. Ferrier, *Enzymes*, in *Lippincott's Illustrated Reviews: Biochemistry*, R.A. Harvey, Editor. 2011: Lippincott Williams & Wilkinson-Medical. p. 54-56, chapter 5.
152. Robinson, P.K., *Enzymes: principles and biotechnological applications.* Essays Biochem, 2015. **59**: p. 1-41

153. Schnell, S., Validity of the Michaelis–Menten equation–steady-state or reactant stationary assumption: that is the question. The FEBS Journal, 2014. **281** (2): p. 464-472.
154. Kenakin, T.P., Enzymes as Drug Targets, in Pharmacology in Drug Discovery: Understanding Drug Response. 2012, Academic Press. p. 105-124, chapter 6.
155. Burtis, C.A. and D.E. Bruns, *Tietz Fundamentals of Clinical Chemistry and Molecular Diagnostics - E-Book*. 2014, Elsevier Health Sciences- Medical. p. 227, 228, chapter 14.
156. Hames, D. and N. Hooper, *Instant Notes in Biochemistry*, in *Taylor & Francis-Science*. 2000. p. 87, 88, section C4
157. Ogilvie, B., E. Usuki, and A. Parkinson, In Vitro Approaches for Studying the Inhibition of Drug-Metabolizing Enzymes and Identifying the Drug-Metabolizing Enzymes Responsible for the Metabolism of Drugs (Reaction Phenotyping) with Emphasis on Cytochrome P450, in Drug-Drug Interactions, A.D. Rodrigues, Editor. 2019, CRC Press. p. 251, chapter 7.
158. Garrett, R.H. and C.M. Grisham, *Biochemistry*. 2008, Cengage Learning. p. 398, chapter 13.
159. Draget, K.I., G. Braek, and O. Smidsrod, *Alginic acid gels: the effect of alginate chemical composition and molecular weight.* Carbohydrate Polymers, 1994. **25**: p. 31-38.
160. Smidsrod, O., *Molecular-Basis for Some Physical-Properties of Alginates in Gel State.* Faraday Discussions of the Chemical Society, 1974. **57**: p. 263-274.
161. Houghton, D., et al., Method for quantifying alginate and determining release from a food vehicle in gastrointestinal digesta. Food Chemistry, 2014. **151**: p. 352-357.
162. Chater, P.I., *Bioactive alginates and macronutrient digestion.* 2014, PhD Thesis, Newcastle University. Chapter 6 (pp. 242, 277, 278): Newcastle Upon Tyne
163. Brownlee, I.A., et al., *Physiological parameters governing the action of pancreatic lipase.* Nutr Res Rev, 2010. **23**(1): p. 146-54.
164. Klein, S., S.M. Cohn, and D.H. Alpers, *Alimentary Tract in Nutrition* in *Modern Nutrition in Health and Disease*, M.E. Shils and M. Shike, Editors. 2006, Lippincott Williams & Wilkins. p. 1134, chapter 70
165. Hamosh, M. and R.O. Scow, *Lingual Lipase and Its Role in the Digestion of Dietary Lipid.* J Clin Invest, 1973 **52**(1): p. 88-95.
166. Hamosh, M., et al., *Pharyngeal lipase and digestion of dietary triglyceride in man.* J Clin Invest, 1975. **55**(5): p. 908-13.
167. Hamosh, M., A review. Fat digestion in the newborn: role of lingual lipase and preduodenal digestion. Pediatr Res, 1979. **13**(5 Pt 1): p. 615-22.

168. Wahbeh, G.T. and D.L. Christie, *Basic Aspects of Digestion and Absorption*, in *Pediatric Gastrointestinal and Liver Disease*, R. Wyllie, J. Hyams, and M. Kay, Editors. 2015, Elsevier Health Sciences. p. 16, chapter 2
169. Borel, P., et al., Hydrolysis of Emulsions with Different Triglycerides and Droplet Sizes by Gastric Lipase in-Vitro - Effect on Pancreatic Lipase Activity. Journal of Nutritional Biochemistry, 1994. **5**(3): p. 124-133.
170. Embleton, J.K. and C.W. Pouton, *Structure and function of gastro-intestinal lipases Advanced Drug Delivery Reviews*. Advanced Drug Delivery Reviews, 1997. **25**(1): p. 15-32.
171. D., B., G. Blekas, and M. Tsimidou, *Olive Oil Composition*, in *Olive Oil: Chemistry and Technology*, G. Blekas, Editor. 2015, Elsevier Science. p. 42, chapter 4.
172. Ramirez-Tortosa, M.C., S. Granados, and J.L. Quiles, *Chemical Compsition, Types and Chracteristics of Olive Oil*, in *Olive Oil and Health*, J.L. Quiles, M.C. Ramírez-Tortosa, and P. Yaqoob, Editors. 2006, CABI Pub. p. 51, chapter 2
173. Orsavova, J., et al., Fatty Acids Composition of Vegetable Oils and Its Contribution to Dietary Energy Intake and Dependence of Cardiovascular Mortality on Dietary Intake of Fatty Acids. Int J Mol Sci, 2015. **16**(6): p. 12871-90.
174. Wang, T.Y., et al., *New insights into the molecular mechanism of intestinal fatty acid absorption.* European Journal of Clinical Investigation, 2013. **43**(11): p. 1203-1223.
175. Bach, A.C. and V.K. Babayan, *Medium-Chain Triglycerides - an Update.* American Journal of Clinical Nutrition, 1982. **36**(5): p. 950-962.
176. Jandacek, R.J., et al., The Rapid Hydrolysis and Efficient Absorption of Triglycerides with Octanoic-Acid in the 1-Position and 3-Position and Long-Chain Fatty-Acid in the 2-Position. American Journal of Clinical Nutrition, 1987. **45**(5): p. 940-945.
177. King, A.H., *Brown seaweed extracts (alginates)* in *Food hydrocolloids*, M. Glicksman, Editor. 2019, CRC Press. p. section C. Viscosity, chapter 6
178. Guibal, E., T. Vincent, and F.B. Blondet, Biopolymers as Supports for Heterogeneous Catalysis: Focus on Chitosa, a Promising Aminopolysaccharide, in Ion Exchange and Solvent Extraction: A Series of Advances, A.K. SenGupta, Editor. 2007, CRC Press. p. 159, chapter 4.
179. Onsoyen, I., *Alginates*, in *Thickening and Gelling Agents for Food*, A.P. Imeson, Editor. 2012, Springer Science & Media Business-Technology & Engineering. p. 21, chapter 1
180. Pandey, J. and G.K. Khuller, *Alginate as a Drug Delivery Carrier*, in *Handbook of Carbohydrate Engineering*, K.J. Yarema, Editor. 2005, CRC Press. p. 802, chapter 27
181. Draget, K.I., *Alginates*, in *Handbook of Hydrocolloids*, P.G.O. Phillips and P.A. Williams, Editors. 2009, Elsevier Science. p. 815, chapter 29
182. Smidsrod, O. and G. Skjakbraek, *Alginate as Immobilization Matrix for Cells.* Trends in Biotechnology, 1990. **8**(3): p. 71-78.
183. Machluf, M., Protein Therapeutic Delivery Using Encapsulated Cell Platform, in Applications of Cell Immobilisation Biotechnology. , V. Nedovic and R. Willaert, Editors. 2006, Springer Netherlands. p. 200, section 5.
184. Eastwood, M.A. and G.S. Boyd, *The distribution of bile salts along the small intestine of rats.* Biochim Biophys Acta, 1967. **137**(2): p. 393-6.
185. Adiotomre, J., et al., *Dietary Fiber - Invitro Methods That Anticipate Nutrition and Metabolic-Activity in Humans.* American Journal of Clinical Nutrition, 1990. **52**(1): p. 128-134.
186. Starr, C., C. Evers, and L. Starr, *Biology Today and Tomorrow Without Physiology*. 2020, Cengage Learning. p. 81, chapter 4
187. Mantle, M. and A. Allen, Isolation of the Major Water-Soluble Glycoprotein from Pig Small-Intestine Mucus and Evidence for Relatively Simple Carbohydrate Side Chains.

Biochemical Society Transactions, 1979. **7**: p. 393-395.
188. Koh-Banerjee, P., et al., Changes in whole-grain, bran, and cereal fiber consumption in relation to 8-y weight gain among men. American Journal of Clinical Nutrition, 2004. **80**(5): p. 1237-1245.
189. Ryttig, K.R., et al., A Dietary Fiber Supplement and Weight Maintenance after Weight-Reduction - a Randomized, Double-Blind, Placebo-Controlled Long-Term Trial. International Journal of Obesity, 1989. **13**(2): p. 165-171.
190. Rigaud, D., et al., Overweight Treated with Energy Restriction and a Dietary Fiber Supplement - a 6-Month Randomized, Double-Blind, Placebo-Controlled Trial. International Journal of Obesity, 1990. **14**(9): p. 763-769.
191. Birketvedt, G.S., et al., Long-term effect of fibre supplement and reduced energy intake on body weight and blood lipids in overweight subjects. Acta Medica (Hradec Kralove), 2000. **43**(4): p. 129-32.
192. Houghton, D., et al., Biological activity of alginate and its effect on pancreatic lipase inhibition as a potential treatment for obesity. Food Hydrocolloids, 2015. **49**: p. 18-24.
193. Chater, P.I., et al., *A synthetic model gut system to study macronutrient digestion in vitro.* Proceedings of the Nutrition Society, 2015. **74**(Oce1): p. E6-E6.
194. Tredger, J.A., et al., The Effects of Guar Gum, Sugar-Beet Fiber and Wheat Bran Supplementation on Serum-Lipoprotein Levels in Normocholesterolemic Volunteers. Journal of Human Nutrition and Dietetics, 1991. **4**(6): p. 375-384.
195. Frape, D.L. and A.M. Jones, Chronic and Postprandial Responses of Plasma-Insulin, Glucose and Lipids in Volunteers Given Dietary Fiber Supplements. British Journal of Nutrition, 1995. **73**(5): p. 733-751.
196. Truswell, A.S., *Dietary Fiber and Plasma-Lipids.* European Journal of Clinical Nutrition, 1995. **49**: p. S105-S109.
197. Brown, L., et al., *Cholesterol-lowering effects of dietary fiber: a meta-analysis.* American Journal of Clinical Nutrition, 1999. **69**(1): p. 30-42.
198. Jenkins, D.J.A., et al., Treatment of Diabetes with Guar Gum - Reduction of Urinary Glucose Loss in Diabetics. Lancet, 1977. **2**(8042): p. 779-780.
199. Jenkins, D.J., et al., Unabsorbable carbohydrates and diabetes: Decreased post-prandial hyperglycaemia Lancet, 1976. **2**(7978): p. 172-4.
200. Shah, N., R.R. Mahoney, and P.L. Pellett, Effect of Guar Gum, Lignin and Pectin on Proteolytic-Enzyme Levels in the Gastrointestinal-Tract of the Rat - a Time-Based Study. Journal of Nutrition, 1986. **116**(5): p. 786-794.
201. Seal, C.J. and J.C. Mathers, Comparative gastrointestinal and plasma cholesterol responses of rats fed on cholesterol-free diets supplemented with guar gum and sodium alginate. British Journal of Nutrition, 2001. **85**(3): p. 317-324.
202. Hoad, C.L., et al., In vivo imaging of intragastric gelation and its effect on satiety in humans. Journal of Nutrition, 2004. **134**(9): p. 2293-2300.
203. Draget, K.I., G. Skjak-Braek, and O. Smidsrod, *Alginate based new materials.* Int J Biol Macromol, 1997. **21**(1-2): p. 47-55.
204. Ijah, U.J., et al., Microbiological, Nutritional, and Sensory Quality of Bread Produced from Wheat and Potato Flour Blends. Int J Food Sci, 2014. **2014**: p. 671701.
205. Ayerza, R. and W.E. Coates, Chia Seeds and the Columbus Concept: Bakery and Animal Products, in Wild-type Food in Health Promotion and Disease Prevention: The Columbus Concept, F. DeMeester, Editor. 2008, Humana Press. p. 384, chapter 26.
206. Burton, P. and H.J. Lightowler, *The impact of freezing and toasting on the glycaemic*

response of white bread. European Journal of Clinical Nutrition, 2008. **62**(5): p. 594-599.
207. Kennedy, J.F. and I.J. Bradshaw, A Rapid Method for the Assay of Alginates in Solution Using Polyhexamethylenebiguanidinium Chloride. British Polymer Journal, 1984. **16**(2): p. 95-101.
208. Halle, J.P., et al., *Method for the Quantification of Alginate in Microcapsules.* Cell Transplantation, 1993. **2**(5): p. 429-436.
209. Richardson, J.C., et al., A simple, high throughput method for the quantification of sodium alginates on oesophageal mucosa. Eur J Pharm Biopharm, 2004. **57**(2): p. 299-305.
210. Turgeon, M.L., *Clinical Hematology: Theory and Procedures*. 2005, Lippincott Williams & Wilkins. p. 262, chapter 19
211. Fernandes, R., et al., Human salivary α-amylase (EC.3.2.1.1) activity and periodic acid and schiff reactive (PAS) staining: A useful tool to study polysaccharides at an undergraduate level. Biochemistry and Molecular Biology Education, 2006. **34**(4): p. 294-299.
212. Melia, C.D. and P. Timmins, *Natural Polysaccharides in Hydrophilic Matrices*, in *Hydrophilic Matrix Tablets for Oral Controlled Release*, P. Timmins, S.R. Pygall, and C.D. Melia, Editors. 2014, Springer New York. p. 100, chapter 4
213. Draget, K.I., et al., Swelling and partial solubilization of alginic acid gel beads in acidic buffer Carbohydrate Polymers, 1996. **29**(3): p. 209-215.
214. McClements, D.J., et al., Designing food structure to control stability, digestion, release and absorption of lipophilic food components. Food Biophysics, 2008. **3**(2): p. 219-228.
215. Wickham, M., R. Faulks, and C. Mills, In vitro digestion methods for assessing the effect of food structure on allergen breakdown. Mol Nutr Food Res., 2009 **53**(8): p. 952-958.
216. Ellis, P.R., et al., Guar Bread - Acceptability and Efficacy Combined - Studies on Blood-Glucose, Serum-Insulin and Satiety in Normal Subjects. British Journal of Nutrition, 1981. **46**(2): p. 267-276.
217. Costanzo, L.S., *Physiology E-Book*. 2017, Elsevier Health Sciences. p. 376, chapter 8.
218. Houghton, D., *Modulation of fat digestion using bioactive alginates.* 2014, PhD Thesis, Newcastle University. Chapter 2 (pp. 20-42): Newcastle Upon Tyne.
219. Selvendran, R.R., B.J. Stevens, and M.S. Du Pont, *Dietary fiber: chemistry, analysis, and properties.* Adv Food Res, 1987. **31**: p. 117-209.
220. Carey, M.C., D.M. Small, and C.M. Bliss, *Lipid Digestion and Absorption.* Annual Review of Physiology, 1983. **45**: p. 651-677.
221. Ehlers, S.J., H.E. Rasmussen, and J.Y. Lee, *Lipids*, in *Nutrition and Exercise Concerns of Middle Age*, J.A. Driskell, Editor. 2009, CRC Press. p. 59, chapter 3.
222. Haug, A., B. Larsen, and O. Smidsrød, *The degradation of alginate at different pH values.* Acta. Chem. Scand., , 1963. **17**(5): p. 1466-1468.
223. Houghton, D., et al., Alginate Enriched Bread Attenuates Circulating Lipids and Non-Alcoholic Fatty Liver Disease. Journal of Hepatology, 2015. **62**: p. S742-S743.
224. Savage, A.K., et al., Enhanced NMR-based profiling of polyphenols in commercially available grape juices using solid-phase extraction. Magn Reson Chem, 2011. **49 Suppl 1**: p. S27-36.
225. Andersen, T., et al., *Alginate as biomaterials in tissue engineering*, in *Carbohydrate Chemistry: Chemical and Biological Approaches*, A.P. Rauter and T.K. Lindhorst, Editors. 2011, Royal Society of Chemistry: Cambridge. p. 236, chapter 10.
226. Reilly, C., *The Nutritional Trace Metals*. 2008, John Wiley & Sons, Medical. p. 61, chapter 2.
227. Hasatani, M., et al., Heat and Mass-Transfer in Bread during Baking in an Electric Oven.

Drying 91, 1991: p. 385-393.
228. Day, D.F., *Alginates*, in *Biopolymers from Renewable Resources* D.L. Kaplan, Editor. 2013, Springer Science & Business Media-Technology & Engineering. p. 131, chapter 5
229. Lacík, I., *Polyelectrolyte Complexes for Microcapsule Formation*, in *Fundamentals of Cell Immobilisation Biotechnology*, V. Nedovic and R. Willaert, Editors. 2004, Springer Netherlands. p. 115, chapter 6.
230. McDowell, R.H., *Properties of alginates* 1961, Alginate Industries Ltd.: London. p. 5, 6.
231. Leo, W.J., A.J. Mcloughlin, and D.M. Malone, *Effects of Sterilization Treatments on Some Properties of Alginate Solutions and Gels.* Biotechnology Progress, 1990. **6**(1): p. 51-53.
232. Muri, J.M. and P.J. Brown, *Biodegradable and Sustainable Fibres.*, R. Blackburn, Editor. 2005, Elsevier-Technology & Engineering. p. 95, chapter 3
233. Qin, Y., Seaweed Hydrocolloids as Thickening, Gelling and Emulsifying Agents in Functional Food Products, in Bioactive Seaweeds for Food Applications: Natural Ingredients for Healthy Diets, Y. Qin, Editor. 2018, Academic Press. p. 138, chapter 7.
234. Grant, G.T., et al., Biological interactions between polysaccharides and divalent cations: the eggbox model. FEBS Lett 1973. **32**(1): p. 195–198.
235. Smidsrod, O. and K.L. Draget, *Chemistry and physical properties of alginates.* Carbohydrate European, 1996. **14**: p. 6-13.
236. Brownlee, I.A., et al., *Alginate as a source of dietary fiber.* Crit Rev Food Sci Nutr, 2005. **45**(6): p. 497-510.
237. Wolf, B.W., et al., Glycemic and insulinemic responses of nondiabetic healthy adult subjects to an experimental acid-induced viscosity complex incorporated into a glucose beverage. Nutrition, 2002. **18**(7-8): p. 621-626.
238. Georg Jensen, M., M. Kristensen, and A. Astrup, Effect of alginate supplementation on weight loss in obese subjects completing a 12-wk energy-restricted diet: a randomized controlled trial. American Journal of Clinical Nutrition, 2012. **96**(1): p. 5-13.
239. Bosscher, D., M. Van Caillie-Bertrand, and H. Deelstra, Effect of thickening agents, based on soluble dietary fiber, on the availability of calcium, iron, and zinc from infant formulas. Nutrition, 2001. **17**(7-8): p. 614-8.
240. Harmuth-Hoene, A.E. and R. Schelenz, *Effect of dietary fiber on mineral absorption in growing rats.* J Nutr, 1980. **110**(9): p. 1774-84.
241. Riedl, J., et al., Some dietary fibers reduce the absorption of carotenoids in women. J. Nutr. , 1999. **129**(12): p. 2170-2176.
242. Smidsrod, O. and K.I. Draget, *Chemistry and physical properties of alginates.* Carbohydrates in Europe, 1996. **14**: p. 7-13.
243. Strugala, V., et al., Inhibition of pepsin activity by alginates in vitro and the effect of epimerization. Int J Pharm, 2005. **304**(1-2): p. 40-50.
244. Eckel, R.H., S.M. Grundy, and P.Z. Zimmet, *The metabolic syndrome.* Lancet, 2005. **365**(9468): p. 1415-1428.
245. Haslam, D., N. Sattar, and M. Lean, *Obesity—time to wake up* BMJ, 2006. **333**: p. 640-642.
246. Lange, K.W., et al., *Dietary seaweeds and obesity.* Food Science and Human Wellness, 2015. **4**(3): p. 87-96.
247. El Khoury, D., et al., Effect of sodium alginate addition to chocolate milk on glycemia, insulin, appetite and food intake in healthy adult men. European Journal of Clinical Nutrition, 2014. **68**(5): p. 613-618.
248. Houghton, D., et al., Acceptability of alginate enriched bread and its effect on fat digestion in humans. Food hydrocolloids, 2019. **93**: p. 395-401.

Appendices

Appendix A- Concentration dependent inhibition of lipase by different alginates.

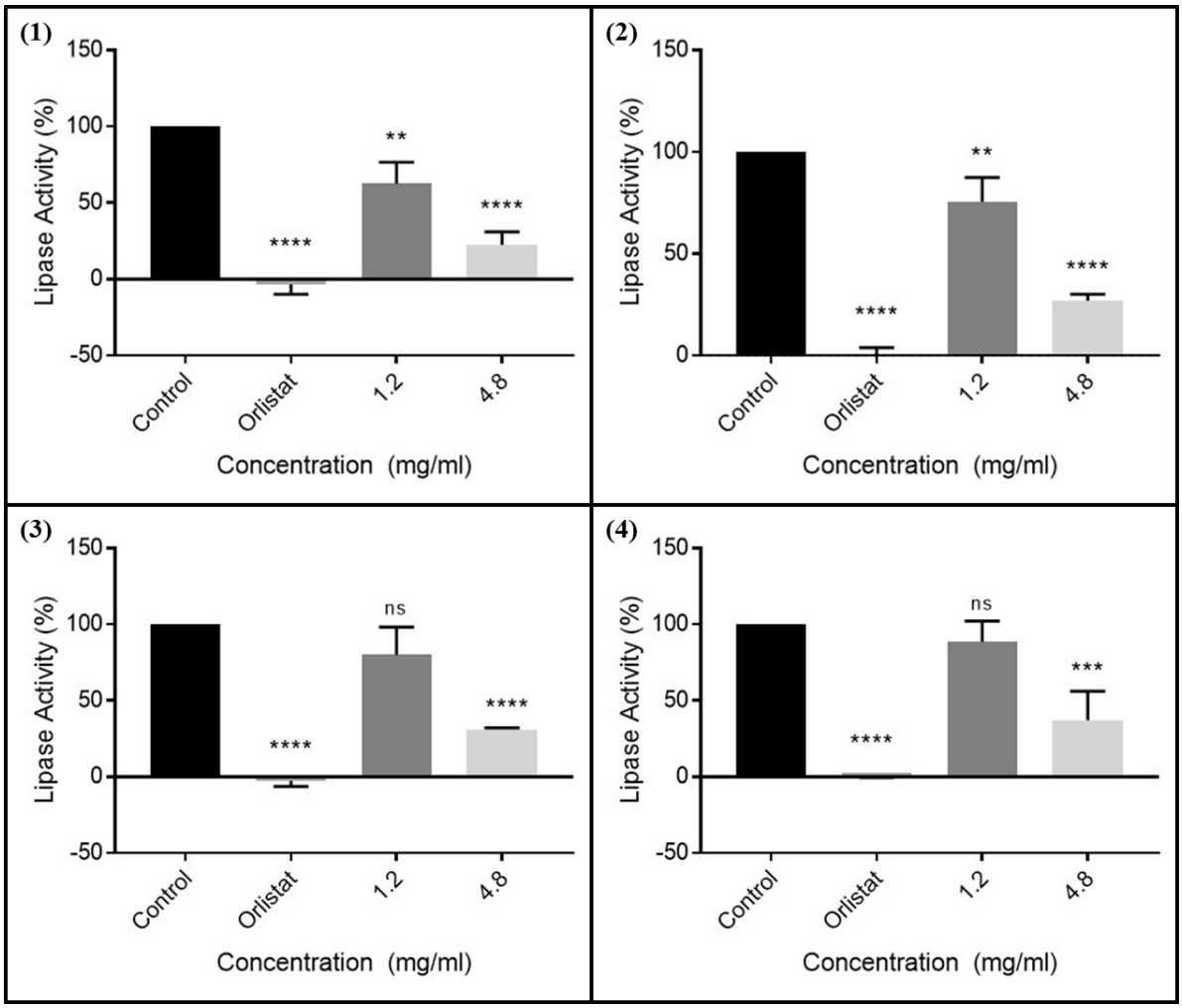

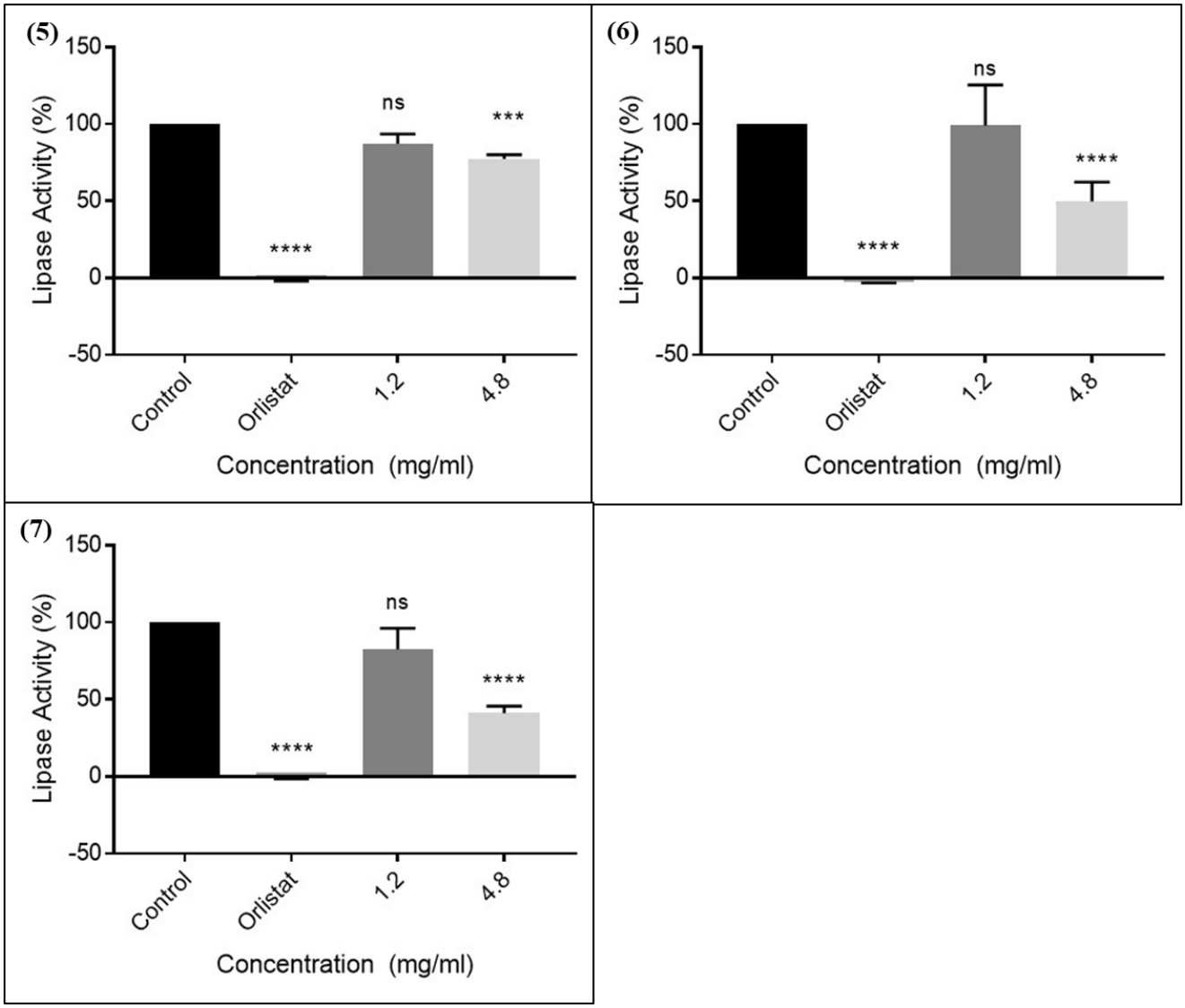

Graphs 1-7 - Concentration dependent inhibition of lipase caused by different alginates. Lipase activity (%) for olive oil alone (control), olive oil with Orlistat, and olive oil with1.2 and 4.8 mg/ml of (1) CC01, (2) 1N80, (3) 1LF80, (4) BG3600, (5) BG3610, (6) BG3700 and (7) BG3900 alginates. Values are mean percentage lipase activity and the error bars are the standard deviation of three replicates (± SD, n=3), P values <0.0005 are represented by ****, whereas P vale >0.05 is represented by ns (non-significant difference). Buffer diluent included 0.033 M C6H8O7, 0.033 M H3PO4, 0.343 M KOH, 0.033 M H3BO3, and 0.35% sodium taurodeoxycholate (pH 7.0 ± 0.3, at 25˚C). The substrate was prepared by diluting 1% (vol/vol) purified olive oil in acetone with buffer diluent to 0.04% (vol/vol).

Appendix B- **^{1}H NMR Spectrum of alginates using 700 and 500 MHz NMR machines.**

The method for preperation of alginates samples for ^{1}H NMR analysis as well as the calculation of alginate content of guluronate (G) and mannuronate (M) residues are described in chapter 2 (section 2.4.3, Figure 2.4 and Table 2.2, pp. 53-54) of this thesis. ^{1}H NMR Data was generated by Dr Corrine Wills, NMR Officer, SAGE Technical Services, Newcastle University.

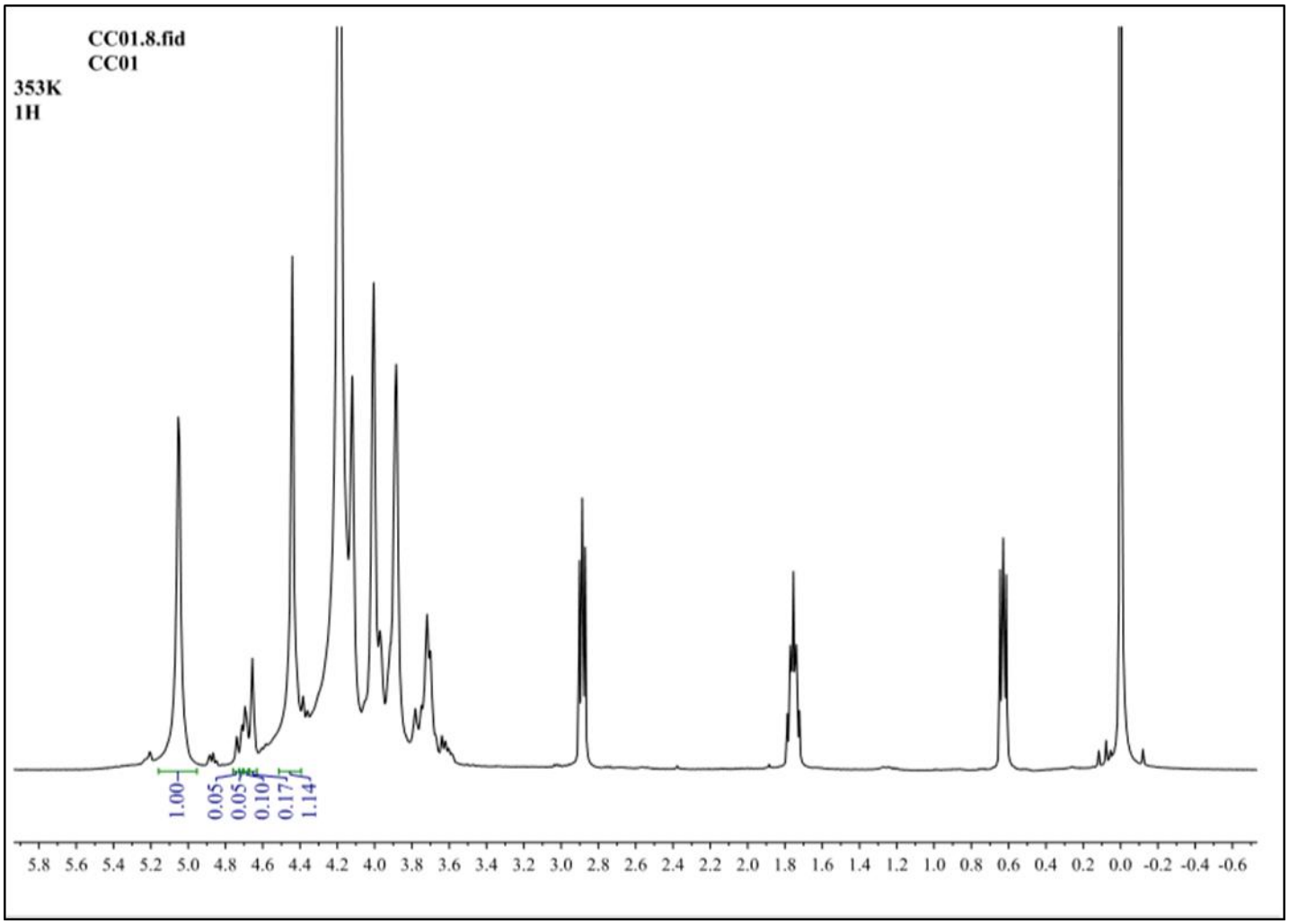

Graph 1: ^{1}H NMR Spectrum of CC01 alginate using 700 MHz NMR machine. The spectra were run at 353K. Data was generated by Dr Corrine Wills, NMR Officer, SAGE Technical Services, Newcastle University.

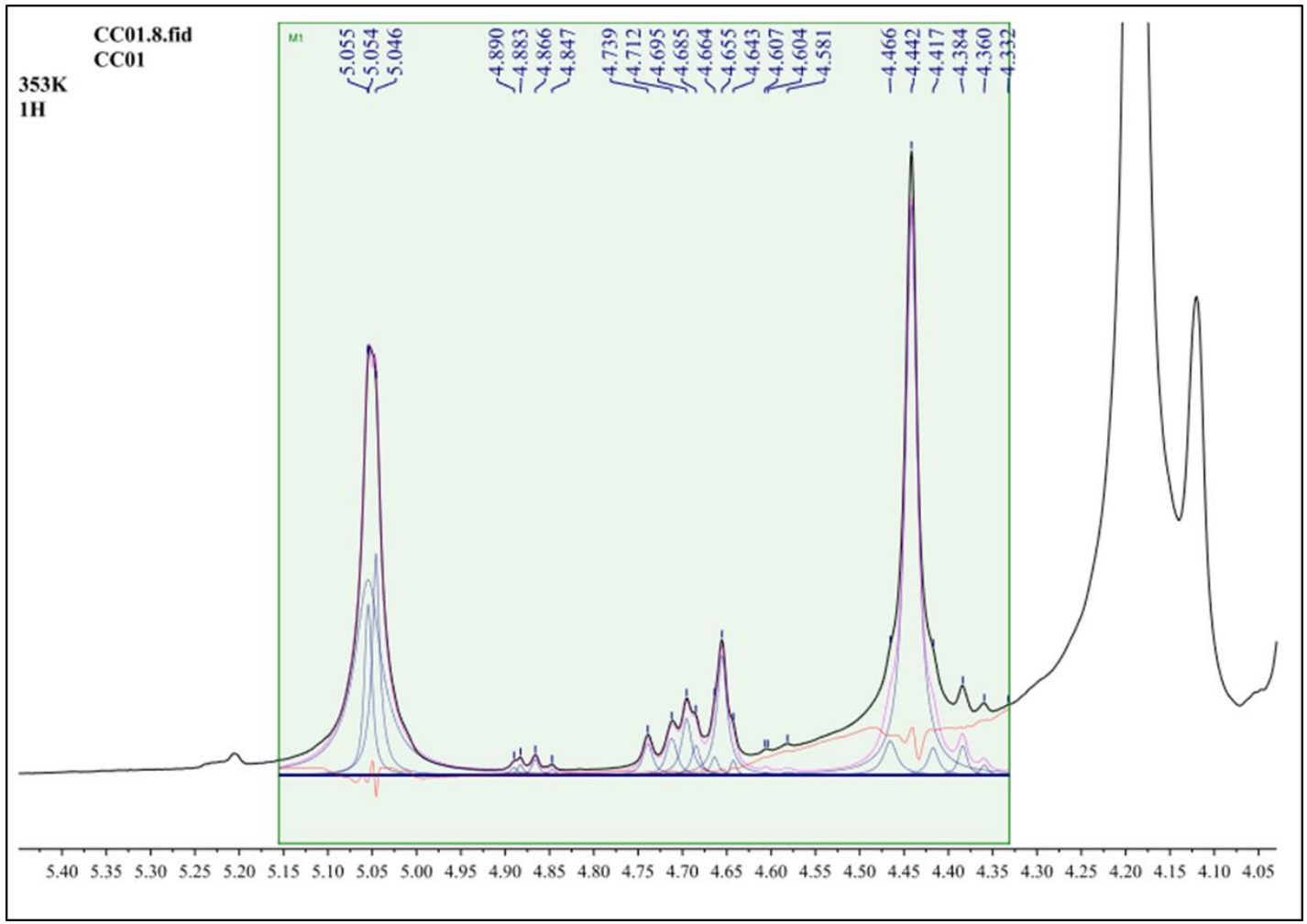

Graph 2: ^{1}H NMR Spectrum of CC01 alginate using 500 MHz NMR machine. The spectra were run at 353K. Data was generated by Dr Corrine Wills, NMR Officer, SAGE Technical Services, Newcastle University. Peaks in shaded region are relevant peaks to calculate signals A (G, proton1), B1 (GGM, proton 5), B2 (MGM, proton 5), B3 (MG, proton 1), B4 (MM, proton 1) and C (GG, proton 5) in order to determine alginate content and sequence of guluronate G) and mannuronate (M) residues (Chapter 2, Figure 2.4 and Table 2.2, pp. 53-54).

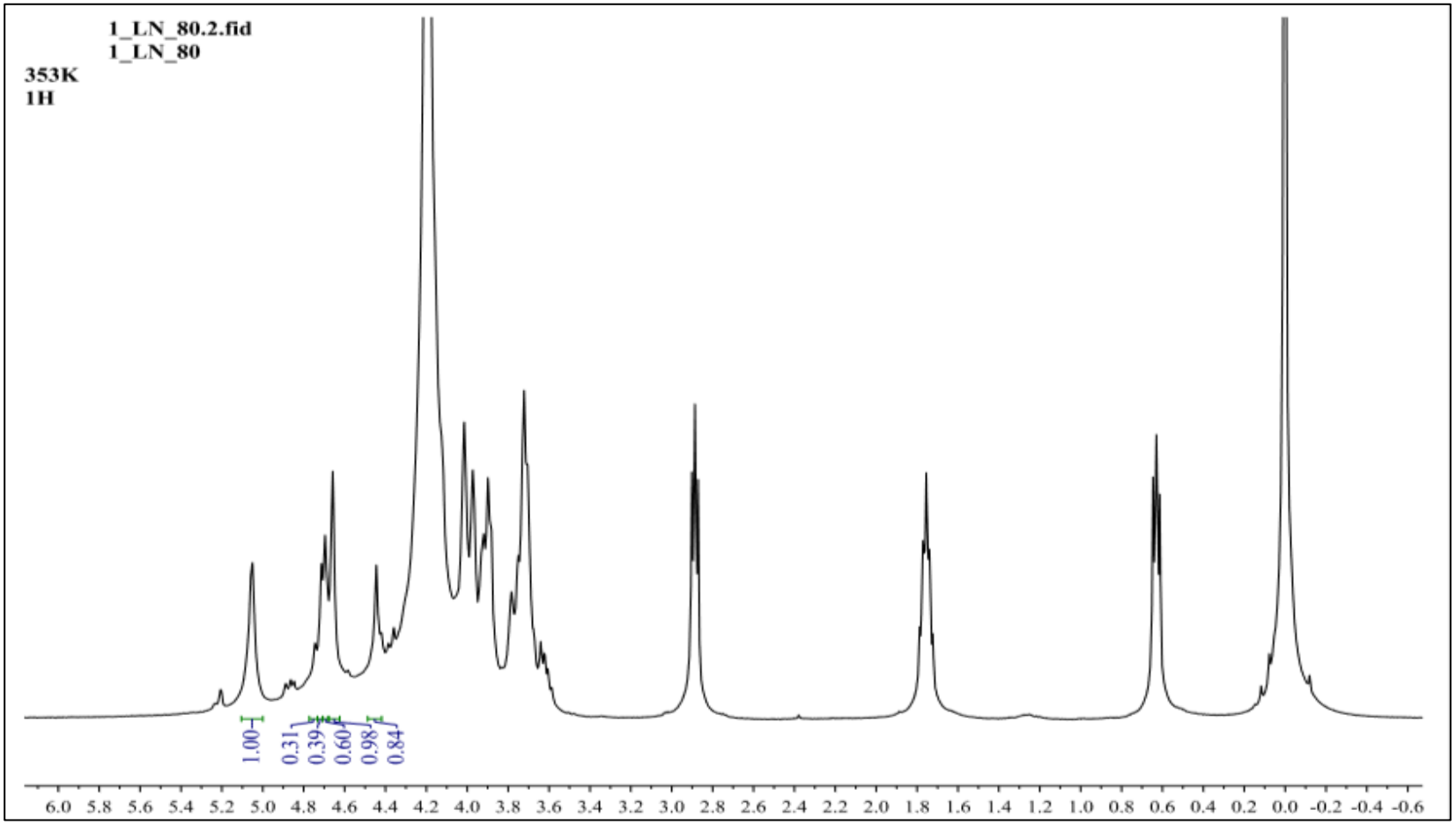

Graph 3: ^{1}H NMR Spectrum of 1N80 alginate using 700 MHz NMR machine. The spectra were run at 353K. Data was generated by Dr Corrine Wills, NMR Officer, SAGE Technical Services, Newcastle University.

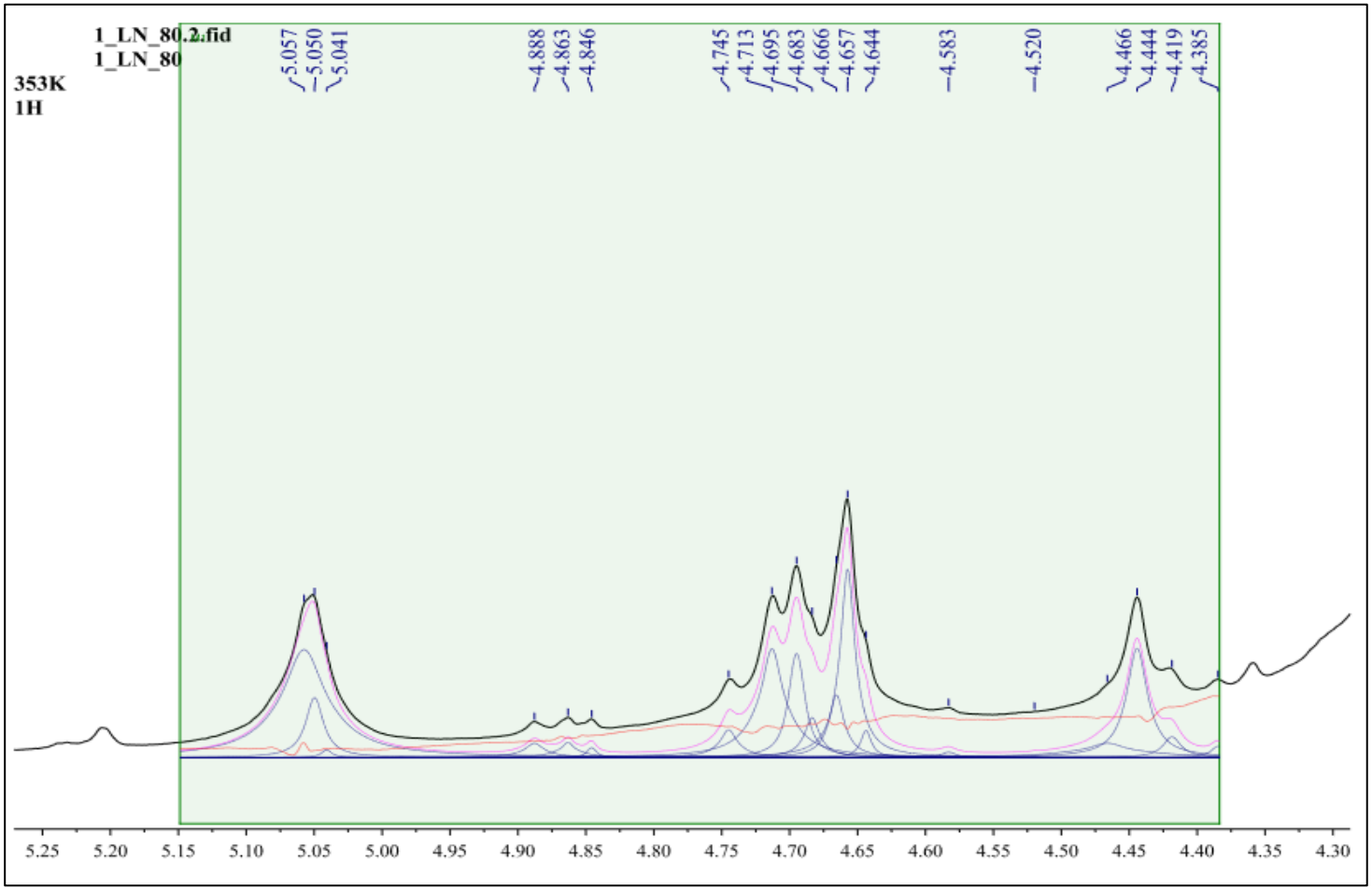

Graph 4: [1]H NMR Spectrum of 1N80 alginate using 500 MHz NMR machine. The spectra were run at 353K. (Carried out by NMR officer, Chemistry Department, Newcastle University). Data was generated by Dr Corrine Wills, NMR Officer, SAGE Technical Services, Newcastle University. Peaks in shaded region are relevant peaks to calculate signals A (G, proton1), B1 (GGM, proton 5), B2 (MGM, proton 5), B3 (MG, proton 1), B4 (MM, proton 1) and C (GG, proton 5) in order to determine alginate content and sequence of guluronate G) and mannuronate (M) residues (Chapter 2, Figure 2.4 and Table 2.2, pp. 53-54).

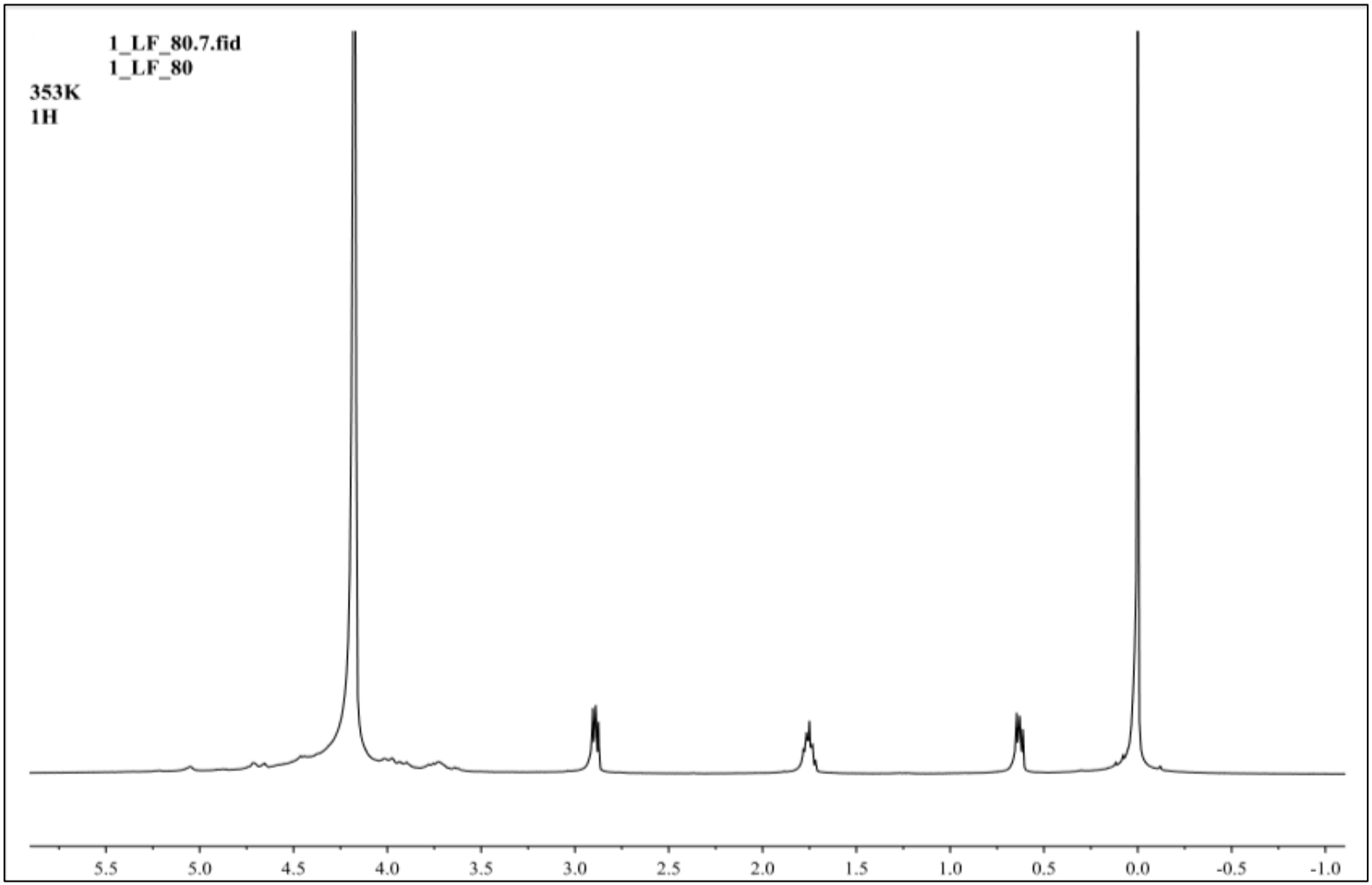

Graph 5: ^{1}H NMR Spectrum of 1LF80 alginate using 700 MHz NMR machine. The spectra were run at 353K. Data was generated by Dr Corrine Wills, NMR Officer, SAGE Technical Services, Newcastle University.

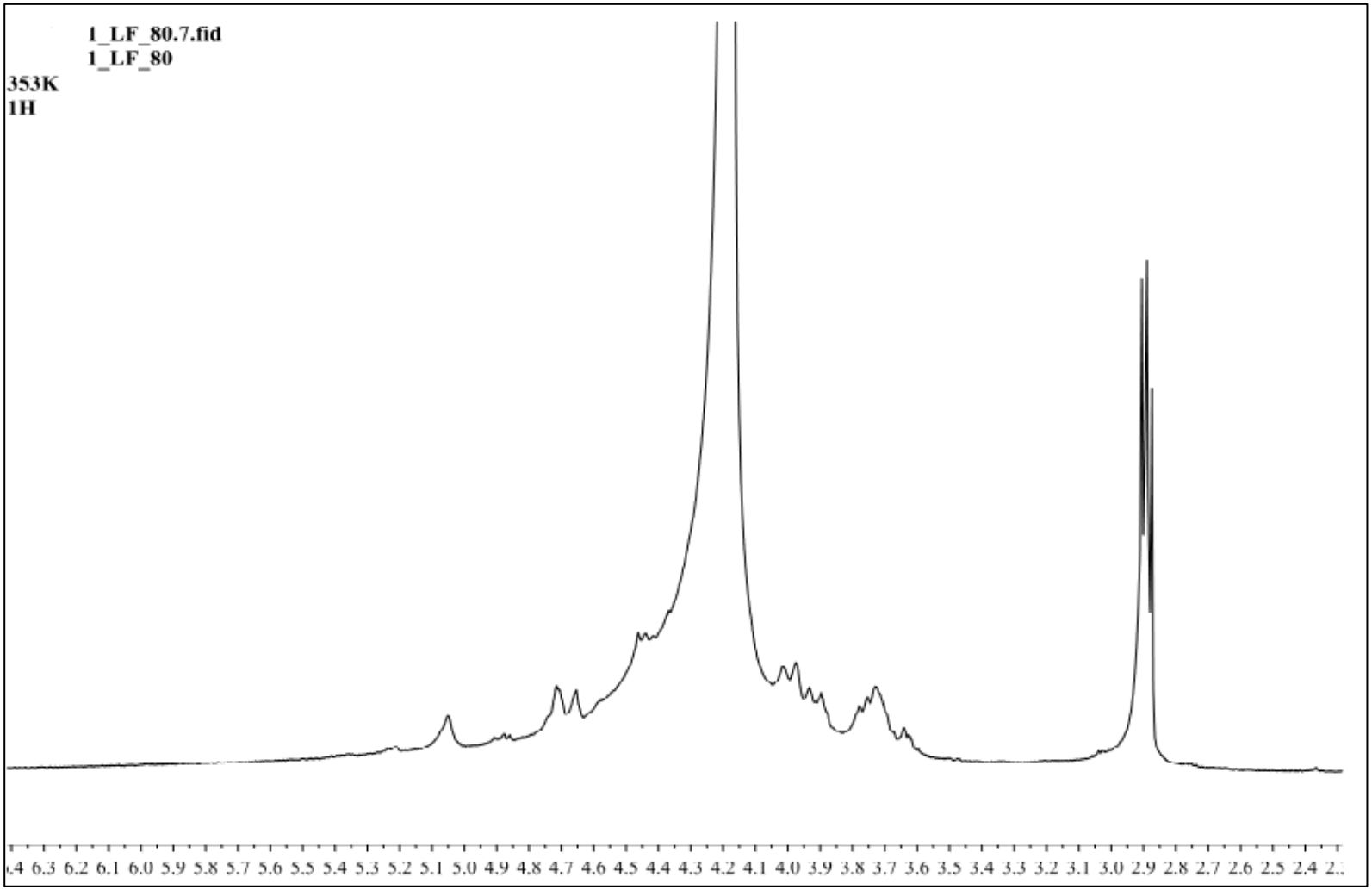

Graph 6: [1]H NMR Spectrum of 1LF80 alginate using 500 MHz NMR machine. The spectra were run at 353K. Data was generated by Dr Corrine Wills, NMR Officer, SAGE Technical Services, Newcastle University.

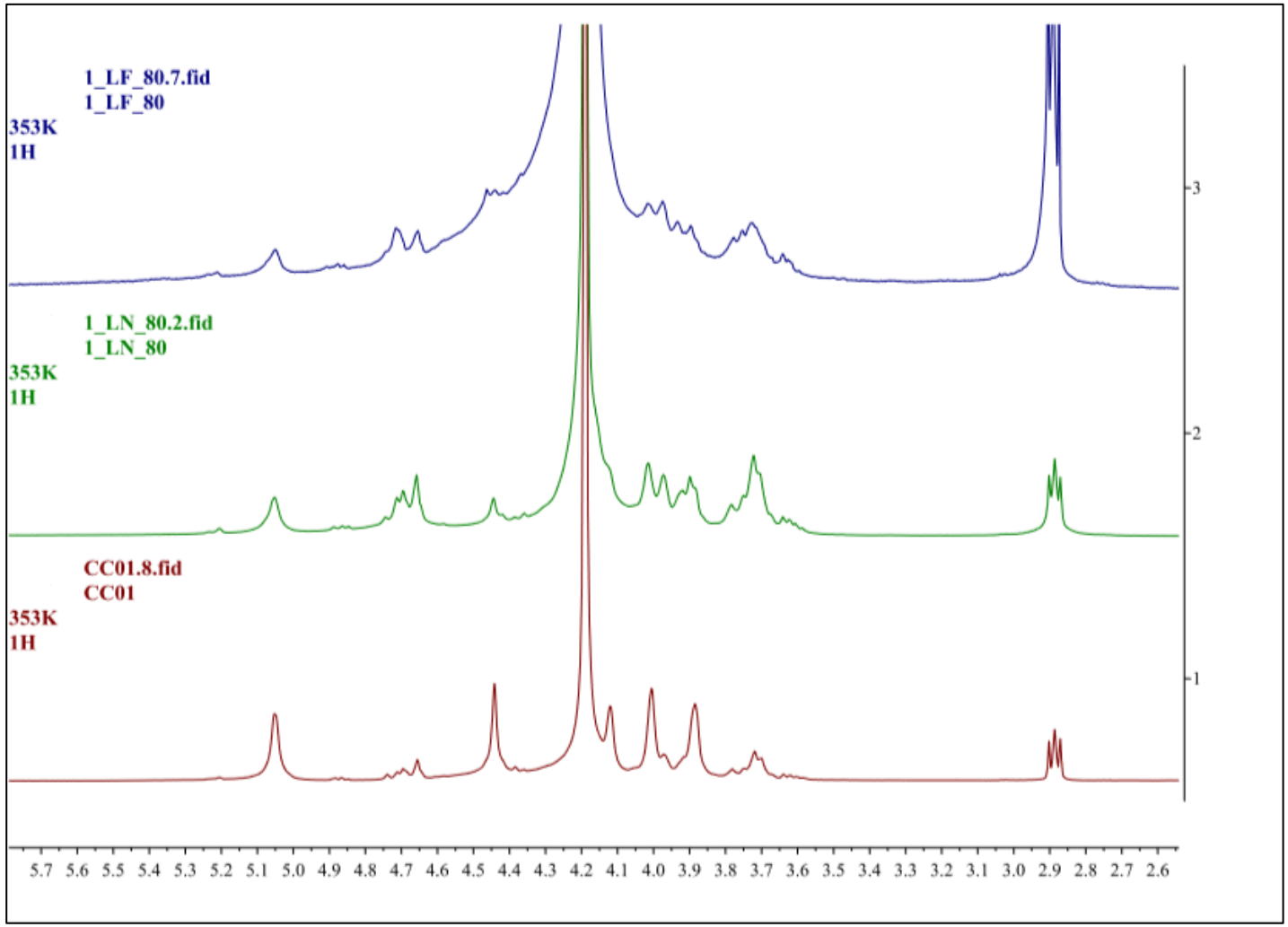

Graph 7: ^{1}H NMR Spectrum of CC01, 1N80, and 1LF80 alginates using 500 MHz NMR machine. The spectra were run at 353K. Data was generated by Dr Corrine Wills, NMR Officer, SAGE Technical Services, Newcastle University.